Journal of Advanced Transportation

Recent Advances in Intelligent Transportation Systems for Cloud-Enabled Smart Cities

Lead Guest Editor: Sang-Bing Tsai
Guest Editors: B. B. Gupta, Dharma P. Agrawal, Wenqing Wu, and Aijun Liu

Recent Advances in Intelligent Transportation Systems for Cloud-Enabled Smart Cities

Journal of Advanced Transportation

Recent Advances in Intelligent Transportation Systems for Cloud-Enabled Smart Cities

Lead Guest Editor: Sang-Bing Tsai
Guest Editors: B. B. Gupta, Dharma P. Agrawal, Wenqing Wu, and Aijun Liu

Copyright © 2021 Hindawi Limited. All rights reserved.

This is a special issue published in "Journal of Advanced Transportation." All articles are open access articles distributed under the Creative Commons Attribution License, which permits unrestricted use, distribution, and reproduction in any medium, provided the original work is properly cited.

Chief Editor

Gonçalo Homem de Almeida Correia, The Netherlands

Editorial Board

Kun An, China
Shriniwas Arkatkar, India
José M. Armingol, Spain
Vittorio Astarita, Italy
Socrates Basbas, Greece
Francesco Bella, Italy
Abdelaziz Bensrhair, France
María Calderon, Spain
Tiziana Campisi, Italy
Juan-Carlos Cano, Spain
Giulio E. Cantarella, Italy
Maria Castro, Spain
Mei Chen, USA
Nicolas Chiabaut, France
Steven I. Chien, USA
Pierluigi Coppola, Italy
Maria Vittoria Corazza, Italy
Luca D'Acierno, Italy
Andrea D'Ariano, Italy
Alexandre De Barros, Canada
Stefano de Luca, Italy
Rocío de Oña, Spain
Luigi Dell'Olio, Spain
Cédric Demonceaux, France
Sunder Lall Dhingra, India
Roberta Di Pace, Italy
Dilum Dissanayake, United Kingdom
Jing Dong, USA
Yuchuan Du, China
Juan-Antonio Escareno, France
Saber Fallah, United Kingdom
Zhixiang Fang, China
Haneen Farah, The Netherlands
Francesco Galante, Italy
Yuan Gao, China
Indrajit Ghosh, India
Ricardo Giesen, Chile
Ren-Yong Guo, China
Yanyong Guo, China
Md. Mazharul Haque, Australia
Jérôme Ha#rri, France
Evelien van der Hurk, Denmark
Hocine Imine, France
Umar Iqbal, Canada
Erik Jenelius, Sweden
Rui Jiang, China
Peter J. Jin, USA
Sheng Jin, China
Mehmet Karaköse, Turkey
Lina Kattan, Canada
Mehdi Keyvan-Ekbatani, New Zealand
Victor L. Knoop, The Netherlands
Alexandra Kondyli, USA
Alain Lambert, France
Michela Le Pira, Italy
Ludovic Leclercq, France
Jaeyoung Lee, USA
Seungjae Lee, Republic of Korea
Ruimin Li, China
Zhi-Chun Li, China
Keping Li, China
Christian Liebchen, Germany
Dung-Ying Lin, Taiwan
Yue Liu, USA
Chung-Cheng Lu, Taiwan
Tom Hao Luan, China
Filomena Mauriello, Italy
Luis Miranda-Moreno, Canada
Rakesh Mishra, United Kingdom
Tomio Miwa, Japan
Andrea Monteriù, Italy
Sara Moridpour, Australia
Giuseppe Musolino, Italy
Jose E. Naranjo, Spain
Mehdi Nourinejad, Canada
Eneko Osaba, Spain
Eleonora Papadimitriou, The Netherlands
Dongjoo Park, Republic of Korea
Paola Pellegrini, France
Luca Pugi, Italy
Hesham Rakha, USA
David Rey, Australia
Meaad Saberi, Australia
Nirajan Shiwakoti, Australia
Michele D. Simoni, Sweden
Ziqi Song, USA

Amanda Stathopoulos, USA
Lijun Sun, Canada
Richard S. Tay, Australia
Daxin Tian, China
Alejandro Tirachini, Chile
Long Truong, Australia
Avinash Unnikrishnan, USA
Pascal Vasseur, France
Nagendra R Velaga, India
Antonino Vitetta, Italy
Francesco Viti, Luxembourg
S. Travis Waller, Australia
Jianjun Wu, China
Hongtai Yang, China
Zhihong Yao, China
Shamsunnahar Yasmin, Australia
Vincent F. Yu, Taiwan
Jacek Zak, Poland
Guohui Zhang, USA
Jing Zhao, China
Zuduo Zheng, Australia
Ming Zhong, China
Yajie Zou, China

Contents

Hindawi
Journal of Advanced Transportation
Volume 2021, Article ID 9792543, 2 pages
https://doi.org/10.1155/2021/9792543

Editorial

Recent Advances in Intelligent Transportation Systems for Cloud-Enabled Smart Cities

Sang-Bing Tsai,[1] **B. B. Gupta**,[2,3] **Dharma P. Agrawal**,[4] **Wenqing Wu**,[5] **and Aijun Liu**[6]

[1]*Regional Green Economy Development Research Center, School of Business, Wuyi University, Wuyishan 354300, China*
[2]*National Institute of Technology, Kurukshetra 136119, Haryana, India*
[3]*Asia University, Taichung, Taiwan*
[4]*University of Cincinnati, Cincinnati, OH, USA*
[5]*Tianjin University, Tianjin, China*
[6]*Xidian University, Xi'an, China*

Correspondence should be addressed to Sang-Bing Tsai; sangbing@hotmail.com and Wenqing Wu; wenqingw@tju.edu.cn

Received 28 July 2021; Accepted 28 July 2021; Published 15 August 2021

Copyright © 2021 Sang-Bing Tsai et al. This is an open access article distributed under the Creative Commons Attribution License, which permits unrestricted use, distribution, and reproduction in any medium, provided the original work is properly cited.

The vision of a Smart City involves enriching the quality of life by gaining insights from data collected from interconnected sensors, devices, and people. Perpetual urban issues such as security, waste management, transportation, and traffic can be addressed by utilizing data to improve efficiency; however, to do this, all data needs to be stored in a location in which it can be easily accessed and used by all stakeholders, both private and governmental. The cloud service will help break down intergovernmental silos wherein different departments have no clear channel to communicate and understand data-based priorities of other departments—a factor seen as a major impediment to Smart City adoption. Security is also a major aspect of the new product, as the continued perpetuation of the "Internet of Things" has (and will) created demonstrable security concerns.

The concept of a Smart City focuses on cloud interoperability and connectivity scenarios, based on the Software-as-a-Service (SaaS) delivery model. This approach holds the promise of reducing capital and infrastructure costs, while improving the efficiency of service provision within the Smart City framework. SaaS delivers software over the Internet, eliminating the need to install and run the application on private servers, simplifying maintenance, and enabling customers to use applications remotely through the IoT from anywhere in the world. Intelligent transportation systems are designed to support the Smart City vision, and the IoT can be applied both in intelligent transportation systems and in Smart Cities to form an advanced platform for novel applications; however, there are various issues and challenges that arise.

Therefore, this Special Issue mainly focuses on recent advances in intelligent and smart transportation systems for IoT-enabled Smart Cities, which addresses both the original algorithmic development and new applications. This collection spans a body of work that represents the efforts of 9 original research papers.

X. Du et al. developed a sustainable GCU application system for intelligent transportation under blockchain. The results show that (1) solving social problems is the primary link, (2) economic tasks are mainly focused on smart contracts and affected by the social problems, (3) the continuous improvement of environmental issues requires a solution to social problems, and (4) the application system of blockchain in intelligent transportation needs to be built from three levels including the government layer, the company layer, and the user layer.

L.-L. Zhang et al. presented a traffic cyber physical system for urban road traffic signal control. With this proposed system, managers and researchers can realize the construction and simulation of various types of traffic scenarios, the rapid development, and optimization of new control strategies and can apply effective control strategies to actual traffic management. By carrying out a one-year practical test in Weifang City, Shandong Province, China, the system has been proved in terms of stability, security, scalability, practicability, and rapid practice, and verification of the new control strategy.

In the context of smart finance, taking into account the economic conditions, social benefits, industry characteristics, and other indicators related to the measurement of supply chain financial risk, K. Wang et al. established a relatively comprehensive index system for the evaluation of supply chain financial risk, which provides a reliable reference for the objective completion of multiobjective measurements.

D. Zhao et al. combined the concept of blockchain with the shared bicycle system, and they creatively constructed a deposit management system for shared bicycles based on the blockchain technology. The results show that the outstanding advantages of the proposed deposit management mode, which include improving deposit supervision and guaranteeing user deposit security, are also conducted.

Y. Chen et al. analyzed the sustainable development capability of the port logistics system for outbreak emergency supplies from overseas and formulated response strategies and robust collaborative optimization methods. The optimized and robust system is obtained through formula derivation and analysis, which realizes the coordinated optimization of emergency logistics infrastructure positioning and emergency rescue vehicle path positioning and minimizes the economic loss caused by the outbreak. Research data show that the shortest path can be planned between each material supply location.

D. Xiao et al. used the BP neural network data fusion method based on the multisource data fusion method to build a model to monitor the slope construction of the expressway. This study used a multisource data fusion method to invert the soil parameters to establish a monitoring point-slope model, analyze and calculate the displacement values at different depths at the monitoring points, and compare them with the measured displacement values.

Considering that the charging behaviors of users of electric vehicles (EVs) (including charging time and charging location) are random and uncertain and that the disorderly charging of EVs brings new challenges to the power grid, X. Xu et al. proposed optimal electricity pricing strategy for EVs based on region division and time division.

K. Lu and X. Wang built a concept model to investigate the effect of related factors on travelers' behavioral intentions of ride-hailing services adoption. In the concept model, the perceived value consists of two parts, i.e., perceived benefit and perceived sacrifice. Based on a survey in Nanjing, China, an empirical analysis was put forward to investigate the relationships between related factors and travelers' behavioral intention to adopt ride-hailing services. The results demonstrate that perceived value is positively related to behavioral intention. And, the factors of perceived benefit are related to perceived value positively, while the factors of perceived sacrifice have a negative effect on perceived value.

D. Li and X. Lin divided the high-speed rail industry chain into infrastructure construction market and manufacturing market of mobile equipment and used the empirical method of new experience industry organization to measure the market power premium of the high-speed rail upstream market. It is found in the study that the upstream market of the high-speed rail industry has a tendency of insufficient enterprise entry and the total social welfare increases with the increase in the number of upstream enterprise entries. Furthermore, the profit of enterprises in the upstream market of the high-speed rail decreases with the increase in the number of enterprises in the upstream.

In conclusion, we believe that this research topic presents a conceptual and practical broad work and that the papers included in this collection clearly contribute to our understanding of the recent advances of intelligent transportation systems for cloud-enabled Smart Cities.

Conflicts of Interest

The Guest Editors declare no conflicts of interest.

Sang-Bing Tsai
B. B. Gupta
Dharma P. Agrawal
Wenqing Wu
Aijun Liu

Hindawi
Journal of Advanced Transportation
Volume 2021, Article ID 8894563, 12 pages
https://doi.org/10.1155/2021/8894563

Research Article

A Decision-Making Model for Autonomous Vehicles at Urban Intersections Based on Conflict Resolution

Zi-jia Wang,[1] Xue-mei Chen ,[1,2] Pin Wang,[3] Meng-xi Li,[1] Yang-jia-xin Ou,[1] and Han Zhang[4]

[1]*Beijing Institute of Technology, School of Mechanical Engineering, Intelligent Vehicle Research Institute, 5 South Zhong Guan Cun Street, Haidian District, Beijing 100081, China*
[2]*Advanced Technology Research Institute, Beijing Institute of Technology, Jinan 250001, Shandong, China*
[3]*University of California, Berkeley, 1357 South 46th Street, Richmond, CA 94804, USA*
[4]*Shandong Hi-Speed Construction Management Group Co., Ltd., Jinan 250001, Shandong, China*

Correspondence should be addressed to Xue-mei Chen; chenxue781@126.com

Received 26 March 2020; Revised 6 November 2020; Accepted 19 November 2020; Published 13 February 2021

Academic Editor: Wenqing Wu

Copyright © 2021 Zi-jia Wang et al. This is an open access article distributed under the Creative Commons Attribution License, which permits unrestricted use, distribution, and reproduction in any medium, provided the original work is properly cited.

The decision-making models that are able to deal with complex and dynamic urban intersections are critical for the development of autonomous vehicles. A key challenge in operating autonomous vehicles robustly is to accurately detect the trajectories of other participants and to consider safety and efficiency concurrently into interactions between vehicles. In this work, we propose an approach for developing a tactical decision-making model for vehicles which is capable of predicting the trajectories of incoming vehicles and employs the conflict resolution theory to model vehicle interactions. The proposed algorithm can help autonomous vehicles cross intersections safely. Firstly, Gaussian process regression models were trained with the data collected at intersections using subgrade sensors and a retrofit autonomous vehicle to predict the trajectories of incoming vehicles. Then, we proposed a multiobjective optimization problem (MOP) decision-making model based on efficient conflict resolution theory at intersections. After that, a nondominated sorting genetic algorithm (NSGA-II) and deep deterministic policy gradient (DDPG) are employed to select the optimal motions in comparison with each other. Finally, a simulation and verification platform was built based on Matlab/Simulink and PreScan. The reliability and effectiveness of the tactical decision-making model was verified by simulations. The results indicate that DDPG is more reliable and effective than NSGA-II to solve the MOP model, which provides a theoretical basis for the in-depth study of decision-making in a complex and uncertain intersection environment.

1. Introduction

Today's driving-assistance systems have made traffic more efficient and safer and show considerable improvements towards the availability of autonomous driving. To develop the next generation of driver assistance systems or even self-driving systems, the algorithms that are capable of handling complex situations are required. Many researchers have proposed some approaches about perception [1], path planning [2], and control [3]. However, the decision-making of autonomous driving at intersections is still one of the major bottlenecks. The primary reason for the difficulty in analyzing crossing behavior is that most models may only work when given long-term, accurate predictions of the trajectories of other participants. To address this problem, this paper will focus on developing a tactical decision-making model for autonomous vehicles in intersection crossing scenarios.

The problems of robust tactical decision-making for autonomous vehicles in a complex and dynamic urban environment have been investigated quite extensively by many organizations and researchers, such as Google [4], Carnegie Mellon University [5], Berkeley [6], and Baidu [7]. The UCB utilized a minimal future distance and a two-level dynamic threshold to perform collision prediction tasks at urban intersections [8]. BMW and the University of Munich came up with a decision-making model based on partially observable Markov decision processes [9]. NVIDIA used a deep convolutional neural network (DCNN) to establish an end-to-end driving model [10].

In recent years, more and more researchers have begun studying decision-making behavior. Chen [11] established a vehicle decision model in an urban environment using a hierarchical finite state machine method for different drivers and road environment characteristics. Liu et al. [12] adopted the control prediction theory and the reinforcement learning theory to obtain a decision model. However, these models cannot be adapted to urban intersections. Ma et al. [13] proposed a decision-making framework titled "Plan-Decision-Action" for autonomous vehicles at complex urban intersections. Zhong et al. [14] proposed a model-learning-based actor-critic algorithm with the Gaussian process approximator to solve the problems with continuous state and action spaces. Xiong et al. [15] used a Hidden Markov model to predict other vehicles' intentions and built a decision-making model for vehicles at intersections. Lv et al. [16] combined offline and online machine learning methods to establish a personalized decision model that could simulate the characteristics of driver behavior. Chen et al. [17] used the rough-set theory to extract different drivers' decision rules. Chen et al. [18] used a novel RSAN (rough-set artificial neural network) method to learn decisions made by excellent human drivers. Chen et al. [19] proposed a merging strategy based on the least squares policy iteration (LSPI) algorithm and selected a basis function that included the reciprocal of TTC, relative distance, and relative velocity to represent the state space and discretize the action space. However, these studies did not take the overall interaction scenarios into consideration and can only be adopted for short-term trajectory prediction.

This paper focuses on the decision-making process of autonomous vehicles in an urban environment and develops a vehicle trajectory prediction model based on Gaussian process regression (GPR) [20], which can generate long-term predictions of incoming vehicles. The problem of conflict resolution among vehicles at intersections is modeled as a multiobjective optimization problem (MOP), in which the acceleration, as the only decision variable, is used to control the vehicles. The main contributions of this work are the presentations of two solutions of intersection multiobjective optimization problems. First, the noninferior genetic algorithm (NSGA-II) is applied to maximize the overall driving benefit of system; the other one considers the deep deterministic policy gradient (DDPG) algorithm of reinforcement learning with continuous actions. Its expected gradient of the action-value function means that DDPG can be estimated much more stable than the usual stochastic policy gradient. A simulation and verification platform was built to validate the results based on Matlab/Simulink and PreScan, and the proposed MOP decision-making method and calculation algorithms were verified in several typical scenarios.

The remainder of this paper is organized as follows: Section 2 elaborates upon the methodology used in this study, which includes an introduction of Gaussian process regression, nondominated sorting genetic algorithm (NSGA-II), and deep deterministic policy gradient algorithm of reinforcement learning. Section 3 describes data acquisition and data processing. Section 4 proposes the GPR models for trajectory prediction and the MOP decision-making model based on efficient conflict resolution at intersections, which is solved by NSGA-II and DDPG. The simulation verification platform to evaluate the effectiveness and reliability of the proposed model and performance between two algorithms is introduced in Section 5. In Section 6, conclusions and future work are presented.

2. Methodology

2.1. Gaussian Process Regression Model. Gaussian process regression (GPR) is a statistical method that can make full use of raw data by considering its temporal trends and periodic changes to establish a suitable predictive model. This model has been used to predict the trajectories of vehicles and has been proven to be efficient. Compared with LSTM, its main advantage is that it is more robust when dealing with data with noise, making it more suitable for urban intersections.

The log likelihood function of the sample data is shown as follows:

$$\log p(\mathbf{y}|\mathbf{X}) = -\frac{1}{2}\mathbf{y}^T\mathbf{C}^{-1}\mathbf{y} - \frac{1}{2}\log|\mathbf{C}| - \frac{N}{2}\log(2\pi). \quad (1)$$

The joint distribution of the model's observations and training data is shown as follows:

$$\begin{bmatrix} \mathbf{y} \\ y_* \end{bmatrix} \sim N\left(0, \begin{bmatrix} \mathbf{C} & \mathbf{K}_* \\ \mathbf{K}_*^T & \mathbf{C}(\mathbf{x}_*, \mathbf{x}_*) \end{bmatrix}\right), \quad (2)$$

where $\mathbf{K}_* = [\mathbf{C}(\mathbf{x}_*, \mathbf{x}_1), \mathbf{C}(\mathbf{x}_*, \mathbf{x}_2), \ldots, \mathbf{C}(\mathbf{x}_*, \mathbf{x}_n)]^T$ is the covariance matrix between the test data $\mathbf{x}_*$ and the training data and $\mathbf{C}(\mathbf{x}_*, \mathbf{x}_*)$ is the covariance matrix of the test data itself.

Therefore, the output of the model can be found with (3). By calculating the mean and variance of the output y_* of the model, the predicted mean $\widehat{y_*}$ and predictive confidence σ_*^2 of the model can be obtained separately:

$$\begin{cases} \widehat{y_*} = E(y_*) = \mathbf{K}_*^T\mathbf{C}^{-1}\mathbf{y}, \\ \sigma_*^2 = \mathrm{Var}(y_*) = \mathbf{C}(\mathbf{x}_*, \mathbf{x}_*) - \mathbf{K}_*^T\mathbf{C}^{-1}\mathbf{K}_*. \end{cases} \quad (3)$$

2.2. Nondominated Sorting Genetic Algorithm. In 2000, a new nondominated sorting genetic algorithm (NSGA-II) was proposed by Srinivas and Deb on the basis of the NSGA, which is a theory and method of handling the Pareto optima in multiobjective optimization problems. It is one of the most popular multiobjective genetic algorithms (GAs) in studying complex system analysis, and diversity results discovery. The structure of the algorithm is as shown in Figure 1.

The step-by-step procedure shows that NSGA-II algorithm is simple and straightforward. First, a combined population $Rt = Pt \cup Qt$ is formed. The population Rt is of size 2 N. Then, the population Rt is sorted according to nondomination. Since all previous and current population

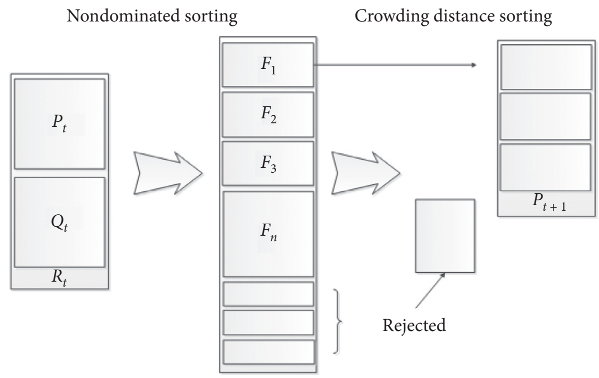

Figure 1: Structure of NSGA-II.

members are included in *Rt*, elitism is ensured. Now, solutions belonging to the best nondominated set F1 are of best solutions in the combined population and must be emphasized more than any other solution in the combined population. If the size of F1 is smaller than N, we definitely choose all members of the set F1 for the new population $Pt+1$. The remaining members of the population $Pt+1$ are chosen from subsequent nondominated fronts in the order of their ranking. Thus, solutions from the set F2 are chosen next, followed by solutions from the set F3, and so on. This procedure is continued until no more sets can be accommodated. Say that the set is the last nondominated set beyond which no other set can be accommodated [21].

2.3. Deep Deterministic Policy Gradient. The interactive learning process of reinforcement learning is similar to human learning, which can be represented as a Markov decision process consist of (s, a, P, r). In 2013, the DQN [22] algorithm was proposed by DeepMind, opening a new era of deep reinforcement learning. The core improvement of the algorithm is to use experience replay and build a second target network [23], which eliminate the correlation between the training samples and improve stability of training. Some algorithms evolved by DQN have made great progress in discrete action control problem, but it is difficult to learn continuous strategy control problem. In 2015, DeepMind proposed the DDPG algorithm based on the DPG and DQN algorithms [24], importing the normalization mechanism in deep learning [25]. Experiments show that the proposed algorithm performs well on multiple kinds of continuous control problems.

The DDPG algorithm is an improved actor-critic method. In the actor-critic algorithm, the actor function $\pi(s|\phi)$ generates an action given the current state. The critic evaluates an action-value function $Q(s, a|\theta)$ based on the output from actor, as well as the current state. The TD (temporal-difference) errors produced from the critic drive the learning in the critic network, and then actor network is updated based on policy gradient.

The DDPG algorithm combines the advantages of the actor-critic and DQN algorithms so that the converge becomes easier. In other words, DDPG introduces some concepts from DQN, which are employing the target network and estimate network for both of the actor and critic. Moreover, the policy of the DDPG algorithm is no longer stochastic but deterministic. It means the only real action is outputted from the actor network instead of telling probability of different actions. The critic network is updated based on

$$L = \frac{1}{N}\sum_{i}^{N}\left(Q\left(s_t, a_t|\theta^Q\right) - y_i\right)^2, \tag{4}$$

where $y_i = r_i + \gamma Q'(s_{t+1}, a_t|\theta^{Q'})$ is the Q value estimated by target network and N indicates the total number of minibatch size. The actor network is updated by means of the gradient term

$$\nabla_{\theta^\mu} J \approx \frac{1}{N}\sum_{i}^{N}\nabla_a Q\left(s, a|\theta^Q\right)|_{s=s_i, a=\mu(s_i)}\nabla_{\theta^\mu}\mu\left(s|\theta^\mu\right)|_{s=s_i}, \tag{5}$$

where $Q(s, a|\theta^Q)$ is from critic estimate network. Furthermore, the DDPG algorithm solves continuous action space problem by means of experience replay and asynchronous updating. The updates of the target critic and target actor networks are as follows:

$$\theta^{Q'} \longleftarrow \tau\theta^Q + (1-\tau)\theta^{Q'}. \tag{6}$$

3. Data

The data were collected from the intersections of Wei Gong Cun Road using subgrade sensors and a retrofit autonomous vehicle as the training and testing samples of the trajectory prediction model. The details are discussed in the following section.

3.1. Subgrade Data Acquisition. The camera for subgrade data acquisition was installed on the BIT Science and Technology Building. The vehicles' locations (x, y, z), velocities (v), and accelerations (a) were extracted. The symmetric exponential moving average (SEMA) method [26] was adopted to smooth out the training data.

3.2. Vehicle Data Acquisition. The vehicle data were collected with a BYD line-controlled autonomous vehicle which was retrofitted by the BIT Intelligent Vehicle Research Institute. The retrofit autonomous vehicle "Surui" [27] was equipped with several kinds of sensors, as shown in Figure 2(b).

The camera and LIDAR sensor were able to detect, track, and localize dynamic objects. The outputs of the fusion algorithm are the positions of vehicles.

4. Model

4.1. Analysis of Driving Behavior at Intersections. Due to the different driving directions and routes of vehicles at intersections, a collision may occur. As shown in Figure 3(a), a blue unmanned vehicle (unmanned vehicle, UV) may collide with a yellow manned vehicle (manned vehicle, MV) that

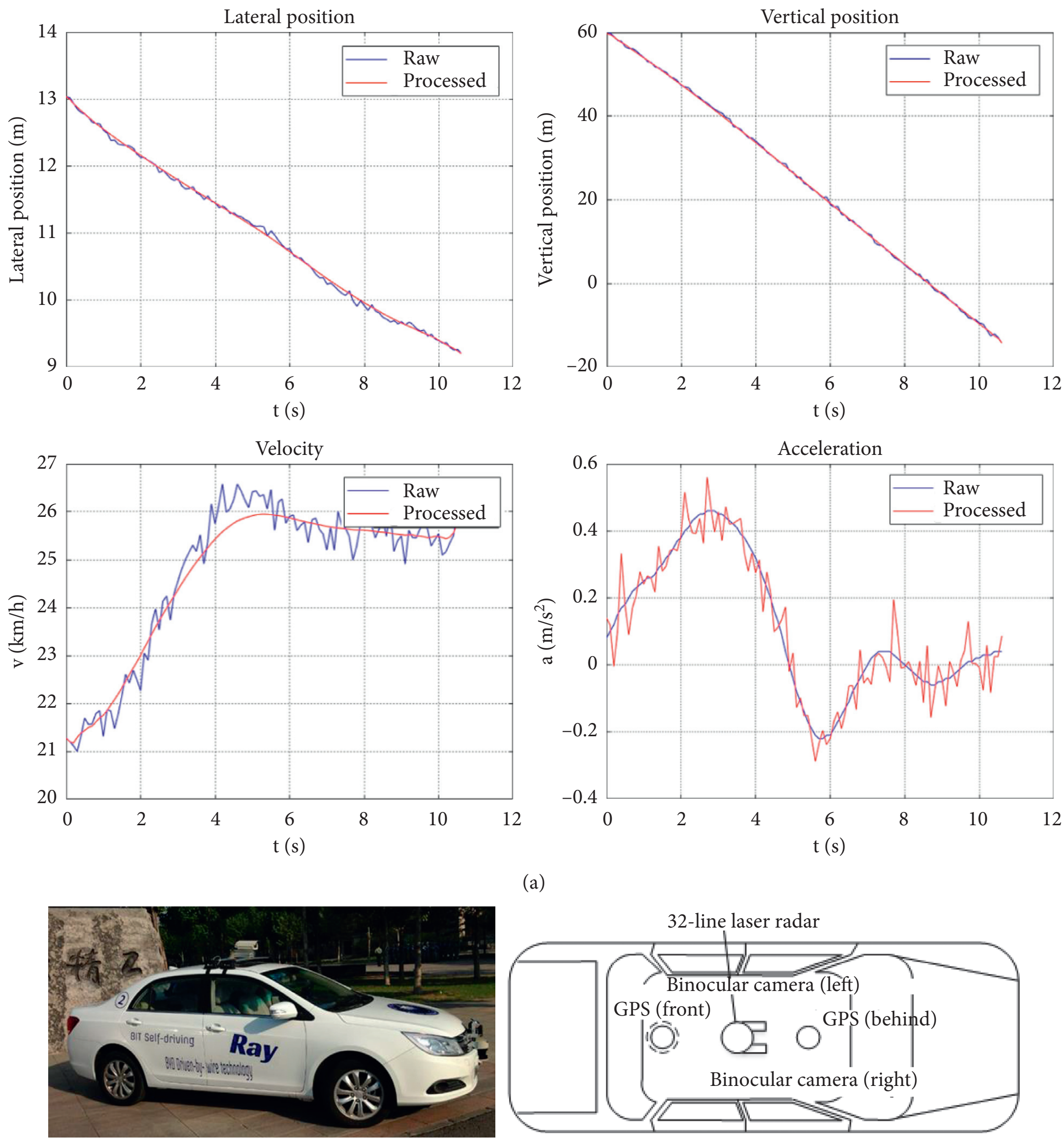

FIGURE 2: (a) The raw and processed data. (b) The layout of sensors on the BYD retrofit vehicle.

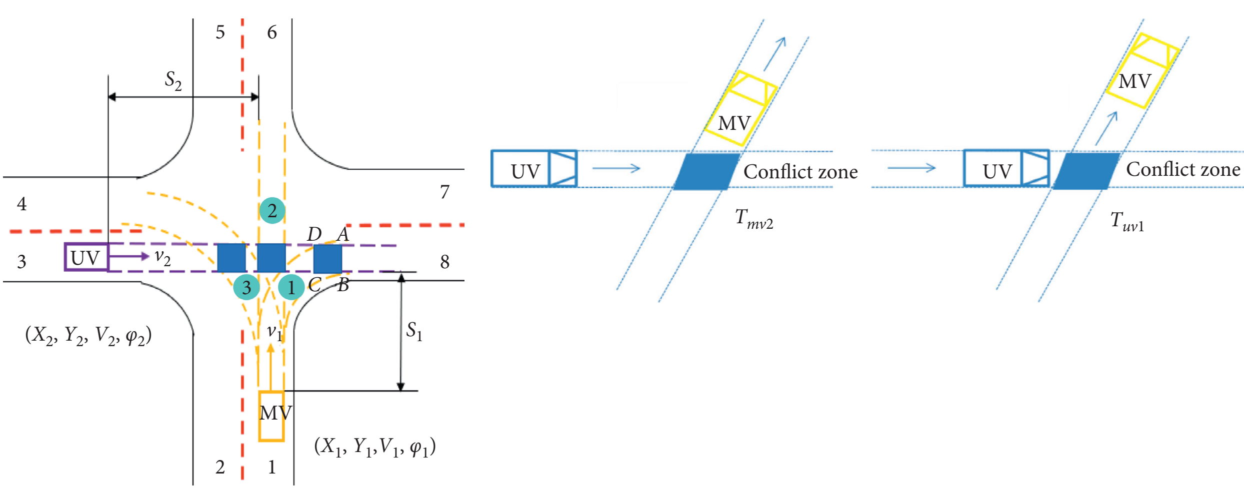

FIGURE 3: Scenes on crossing intersection with no signal.

may go straight and turn right or turn left at blue areas which called conflict zones. Therefore, a decision-making model was established to avoid collisions in these spaces based on vehicles crossing the intersection at different times. This paper only focused on the impacts of motor.

4.2. Research on Vehicle Trajectory Prediction

4.2.1. Feature Motion Parameter Extraction. Vehicle course angle and azimuth were extracted to distinguish if a vehicle turned or not, because these two parameters change linearly with time when vehicles turn. By utilizing vehicles' motion parameters to recognize driving patterns, incoming vehicles' trajectories were predicted effectively. Real-time acceleration was used to distinguish if a vehicle kept driving or gave way to incoming vehicles because vehicles' real-time accelerations for the two patterns are distributed across different ranges.

4.2.2. Trajectory Prediction Model. A trajectory prediction model based on the GPR model was used to predict the trajectories of MVs. The training process of GPR models [28] is shown in Figure 4(a).

In this paper, the data collected from the subgrade sensors were used for training the GPR models and optimizing its hyper parameters. $-(x(t), y(t), v_s(t), v_y(t))$ were the inputs, while $a_x(t)$ was the output. A square exponential covariance function (SE) was adopted as the kernel function, because it can accurately describe the nonlinear relationships between the inputs and outputs. A conjugate gradient optimization algorithm was then adopted to search for optimal parameters. When the error fell below 0.001, the results were regarded as convergent.

After training the prediction model, as this paper paid more attention to straight driving MVs, the CA (constant acceleration) [29] kinematic formula is utilized to calculate the follow-up trajectories more accurately, as shown in Figure 4(b).

4.3. A Decision-Making Model Based on Efficient Conflict Resolution. An appropriate parameter should be selected to analyze the traffic conflict. TTC (time to collision) is a widely used parameter in traffic conflict research, but it is generally used for scenes such as highway and is improper to evaluate the danger degree of vehicles collision at intersections. We use EPET (estimating postencroachment time) as the safety indicator which describes the time difference between vehicles passing through the center of conflict zone and can effectively evaluate collision danger between vehicles at any angles, as shown in Figure 3(b):

$$\text{EPET} = \left|T_{uv} - T_{mv_i}\right|, \quad (7)$$

where T_{uv} and T_{mv_i} are, respectively, the time when UV and MV(i) arrive the conflict zone. EPET is expected a larger value which means smaller risk of collision.

While ensuring safety, an appropriate speed is expected, which stands for efficiency during crossing the intersection. Using these criteria, we define the following measure combining safety and efficiency:

$$\begin{aligned} U &= U_{\text{safe}}(\text{EPET}) + U_{\text{efficiency}}(V) \\ &= -\exp(-\text{EPET}) - \frac{(V_{\text{MV}} - V_{\text{cri}})^2}{V_{\text{cri}}^2}, \end{aligned} \quad (8)$$

where U is the profit function, and we expect a larger U that represents more ideal motions during the crossing for vehicles. V_{cri} is the expected speed for MV, which is set to 40 km/h according to the driving rules at the intersections. The reason for defining the U negative is ensuring efficiency in the following model, e.g., deep reinforcement learning.

As the states and actions of vehicles are continuous, we use acceleration a as a parameter to control target. A constrained model of multiobjective optimization problem (MOP) is proposed based on conflict resolution at intersection, and the goal of which is to maximize profit of the system. The interaction between vehicles is quantized by importing a variable parameter P, and vehicles will cross the intersection in competition when P is zero. When P is 1, vehicles will be in cooperation completely.

The mathematical model of MOP is usually expressed as follows:

$$\begin{cases} \min f(X), \\ h_i(X) = 0, \quad i = 1, 2, \ldots, m, \\ g_j(X) \geq 0, \quad j = 1, 2, \ldots, l, \end{cases} \quad (9)$$

where $f(X)$ is object function and $h_i(X) = 0$ and $g_j(X) \geq 0$ are constraint conditions. For solving the maximum of U, it can be transformed into finding the minimum of negative function. Therefore, we can then establish

$$\begin{aligned} &\max \quad U = U_1 + p \cdot U_2, \\ &\text{s.t.} \quad a_{\min} \leq a_i \leq a_{\max}, i = 1, 2, \\ &0 \leq v_i \leq v_{\max}, i = 1, 2. \end{aligned} \quad (10)$$

v_{max} depends on the speed limit at the intersections, and a_{max} and a_{min} represent comfort requirement during driving, which are defined as $\pm 2m/s^2$ in this paper.

4.4. The Calculation Method Based on NSGA-II

4.4.1. Constraint Condition. To ensure safety, a simplified circle model for vehicles is established, as shown in Figure 5.

We set a safety constraint for no overlap between the excircles of vehicles:

$$\sqrt{\left((x_1(t) - x_2(t))^2 + (y_1(t) - y_2(t))^2\right)} \neq R_1 + R_2, \quad (11)$$

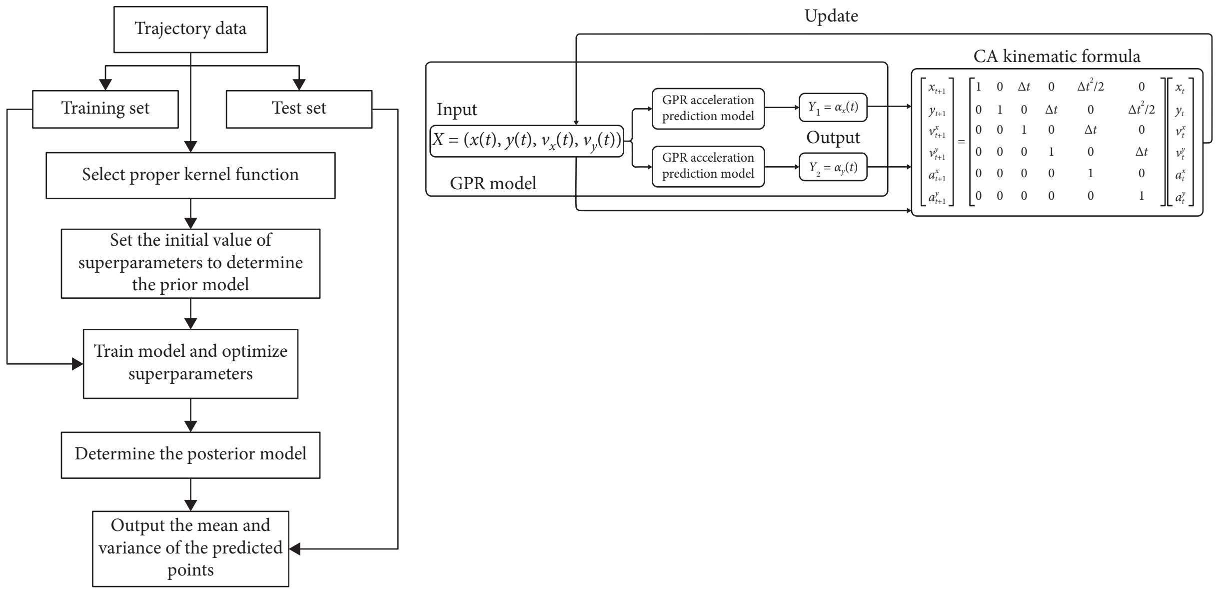

FIGURE 4: (a) The training process of the GPR model. (b) The trajectory prediction model.

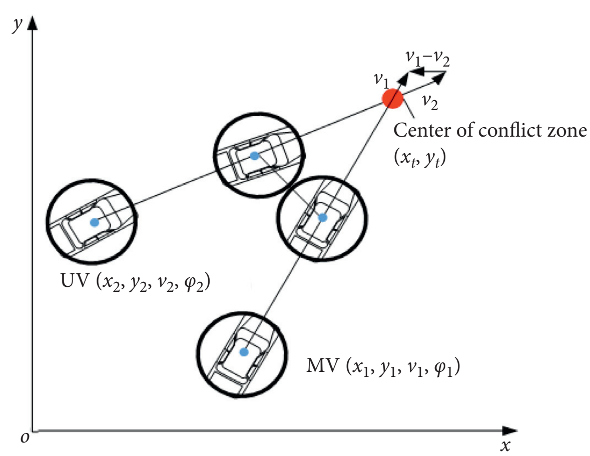

FIGURE 5: Simplified circle model.

where $R_i = \sqrt{L_i^2 + W_i^2}/2$, where L and W are, respectively, the length and width of vehicles.

The formula for the motion state of vehicles is as follows:

$$\begin{cases} x_i(t) = x_i(0) - \left[v_i(0)t + \frac{1}{2}a_i(0)t^2\right]\cos\varphi_i, \\ \qquad\qquad\qquad\qquad\qquad\qquad 0 \le t \le T, \\ y_i(t) = y_i(0) - \left[v_i(0)t + \frac{1}{2}a_i(0)t^2\right]\sin\varphi_i, \end{cases} \tag{12}$$

where $(x_i(0), y_i(0))$ is initial position and φ_1 is orientation.

4.4.2. Process of Decision Making. For the model of MOP, we perform an optimal solution based on NSGA-II, and the process is shown in Figure 6.

There are two stages in the solution process: the first phase is decision making at the initial moment and performing the action with the known information, and the second phase is to update the position and velocity of vehicles with dynamic information and then regenerate optimal motions.

4.5. The Calculation Method Based on Deep Reinforcement Learning. If we assume that the process of crossing intersections is a Markov decision process (MDP), it is practical to apply deep reinforcement learning for continuous action spaces. The input state is the speed of vehicles and distance from the center of vehicles to the center of conflict zone, i.e., $S = (V_{MV}, D_{MV}, V_{UV}, D_{UV})$; if there are more than one UV on the scene, all the speed and distance of UVs are appended into observation state. The output action is the acceleration a

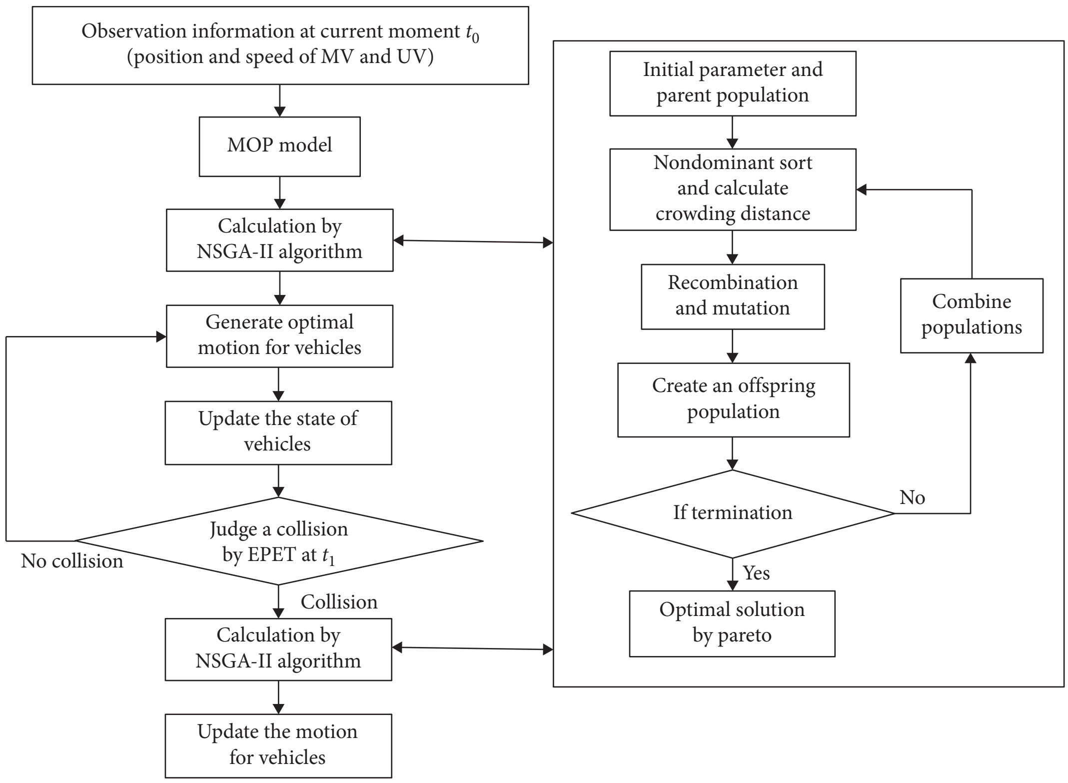

Figure 6: Process of the MOP model at intersections by the NSGA-II algorithm.

of MV. In this study, the reward function is built in the same way as (8), $R = U$, which is with consideration of safety and efficiency. We expect a larger total reward that means the sum of the rewards for each step and converge it through training based on policy gradient, which is the reason why we set the reward is negative. As for a positive reward function, a larger total reward may result from more step, which means more time to cross intersections by an inefficient policy. However, for a negative reward function, a larger total reward means a safe and efficient policy.

5. Discussion and Evaluation

In this section, we trained DDPG on OpenAI Gym and then tested the algorithms on PreScan to compare. This allowed us to verify the effectiveness and reliability of the proposed algorithms.

Simulation parameters are set as follows: we test the algorithms in single or multiple-vehicle scenes where there is one or more MVs driving straight from north to south, and a UV is excepted to cross the intersection controlled by algorithms with no collision. The length and width of vehicle MV and UV are 4800 mm and 2178 mm, respectively, communication distance range is less than 200 m apart from each other, and speed limit at intersection is 60 km/h.

5.1. Simulation and Verification Platform. PreScan is a simulation environment for developing advanced driving assistant systems (ADASs) and intelligent vehicle (IV) systems. It is a platform that can be used to build 3D virtual traffic scenes, generate vehicles, pedestrians, traffic lights, and other control modules, as shown in Figure 7(a). PreScan comes with a powerful graphics preprocessor, a high-end 3D visualization viewer, and a connection to standard MATLAB/Simulink. It is composed of various main modules. Some of these main modules represent a specific world. Multiple sensor readings were simulated and captured in the Sensor World.

We build a new task about intersection with multiple vehicles on OpenAI Gym, as shown in Figure 7(b). The deterministic actor policy network and critic policy network have the same architectures, which are multilayer perceptions with two hidden layers (64-64). For the metaexploration policy, we implemented a stochastic Gaussian policy with a mean network or variance network represented with a MLP with two hidden layers (64-64).

5.2. Analysis of Experimental Results

5.2.1. Results of Prediction Model. In this paper, the predictions of steering-vehicle trajectories and the straight vehicle trajectories are verified separately. These trajectories are divided into several different pieces to evaluate the prediction performance. The prediction lengths of the straight vehicle are 3 s, 4 s, 5 s, and 6 s. The prediction lengths of steering-vehicle are 3 s, 4 s, and 5 s. There are 80 trajectories in each group.

Figure 8(a) shows the prediction error of the straight vehicle trajectories. It can be found that the GPR model has better performance than the commonly used model in

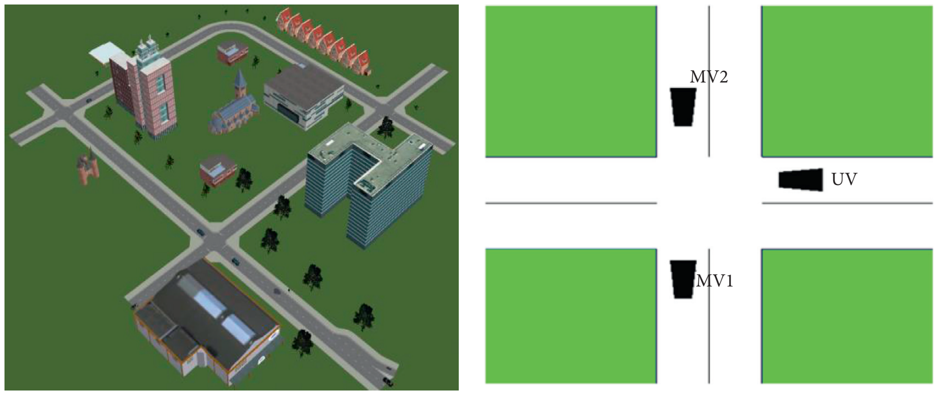

(a) (b)

Figure 7: Simulation platform. (a) PreScan. (b) OpenAI Gym.

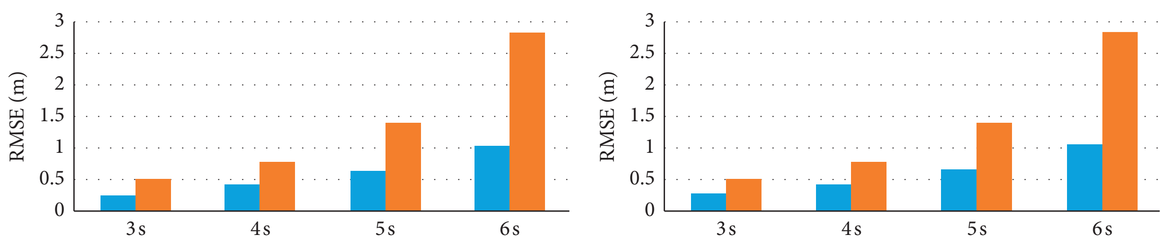

	3 s	4 s	5 s	6 s
GPR	0.2685	0.4257	0.6816	1.0579
CA	0.4896	0.7874	1.4217	2.8518

(a)

	3 s	4 s	5 s	6 s
GPR	0.2685	0.4257	0.6816	1.0579
CA	0.4896	0.7874	1.4217	2.8518

(b)

Figure 8: The trajectory prediction error of straight vehicle and left-turn vehicle. (a) Straight vehicle. (b) Left-turn vehicle.

prediction of straight vehicle trajectories. Figure 8(b) shows the prediction error of the steering-vehicle trajectories. It can be found that the GPR model is more accurate than the constant-rate steering motion model (CTRV).

5.2.2. Effect of MOP Model. Scenario 1: single-vehicle scenario

Figure 9(a) depicts the interaction between a UV and an incoming MV. Two experiments were carried out in the simulation platform. The difference between the two experiments was whether the UV was controlled by the tactical decision-making algorithm or not. In the first experiment, without the proposed algorithm, a collision between the MV and UV happened at $t = 5.8$ s. In the other experiment, the main vehicle was controlled by the proposed algorithm. When the two vehicles met at the intersection, the main vehicle predicted the trajectory of the other vehicle, which is shown in Figure 9(b). In this experiment, deceleration was the optimal choice. The desired velocities given by the decision-making algorithm and the actual velocity changes are shown in Figure 9(c). There was no collision because the algorithm chose to yield to the incoming vehicle.

Figure 9(c) shows that with the decision-making algorithm, the main vehicle decelerates before entering conflict zone, thus slowing down to give way to the incoming vehicle. Figures 9(d) and 9(e) show the distances and TTCs of the two vehicles. Before the algorithm is executed, both the distance and the TTC curves of the two vehicles pass through $x = 0$, indicating that a collision occurs at this time. After the algorithm is executed, the distance and the TTC remain within the safe range, indicating that no collision occurred.

5.2.3. Comparison of NSGA-II and DDPG Algorithm. Scenario 2: multiple-vehicle scenario

To compare the performances of the DDPG and NSGA-II algorithms, we conducted two groups of experiments on the same scene, in which D_{MV1} and D_{MV2} were, respectively, 10 m and 32 m, and the initial position of the UV, i.e., D_{UV}, was 30 m. We set MV1 and MV2 to drive with a constant speed of 40 km/h. Subsequently, we trained the DDPG algorithm based on the MOP model, tested the performance in group B, and compared it with that of NSGA-II in group A, as shown in Figure 10.

For group A, the UV adopts a yield strategy wherein it slows down before $t = 3$ s to wait for MV1 and MV2 to cross the intersection and then accelerates after the MVs move away. As shown in Figure 10(a), as the speed becomes

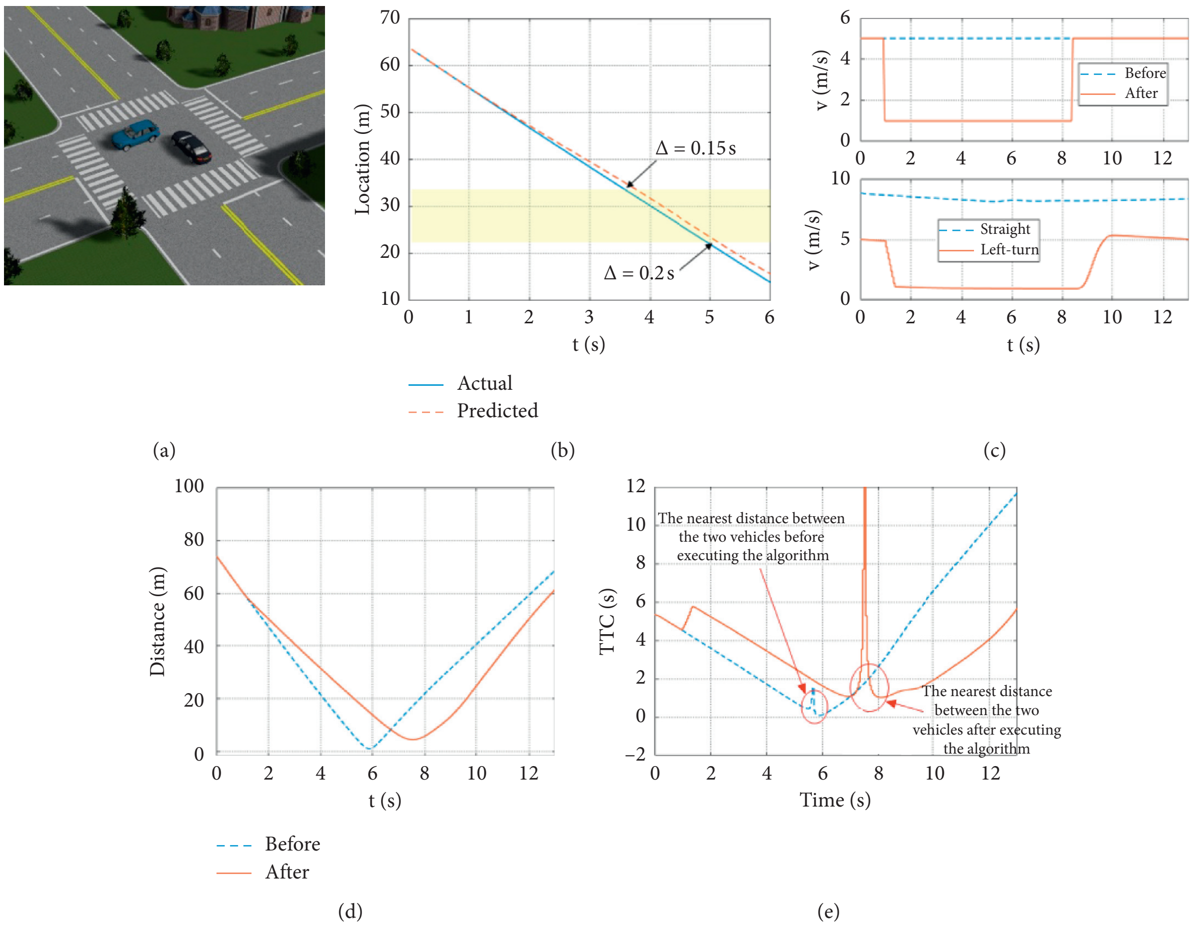

Figure 9: (a) Scenario 1. (b) Predicted trajectory. (c) Velocity. (d) Distance. (e) TTC.

increasingly lower than the expected speed, the reward appears to decline until $t = 3$ s and increases thereafter. A higher crossing time means a higher accumulation of the negative reward, which leads to a lower total reward of −44.184.

Figure 10(b) shows that the UV passes through the intersection between the two MVs with an efficient strategy in group B; as shown in the bottom image in Figure 10(b), the UV reaches the conflict zone at $t = 2$ s, approximately 0.5 s earlier than MV2. In the image, the shaded area represents the conflict zone in consideration of the size of the vehicles. With the efficient strategy of the DDPG, the UV maintains an acceleration of 2 m/s^2 during the entire process of passing through the intersection, thus achieving a much higher total reward than that in group A.

The comparison data in Table 1 show that the passing through time for the UV of group B is approximately 1.5 s lower than that of group A, which means that the DDPG algorithm reduces the traffic delay and improves the efficiency with which the UV passes through the intersection. Moreover, the rate of change in the acceleration of the UV is lower in group B, which implies a lower energy consumption. In general, the DDPG algorithm is more efficient than NSGA-II.

The stability of the DDPG and NSGA-II algorithms was studied by performing a new task wherein the initial speed of the UV was varied from 30 km/h to 55 km/h.

We built a single-vehicle scene, where there is only one UV, and imported the trained actor policy of the DDPG to output the motions of the UV. We then imported the NSGA-II algorithm as a compared group to observe the performance on the same task 10 times. As shown in Figure 11, because the NSGA-II algorithm was recalculated each time, the total reward is quite different at the same initial speed of the UV. On the other hand, the DDPG gives a more stable and efficient result, and the average of the total rewards of the DDPG is higher than that of NSGA-II. Furthermore, the averages of the total

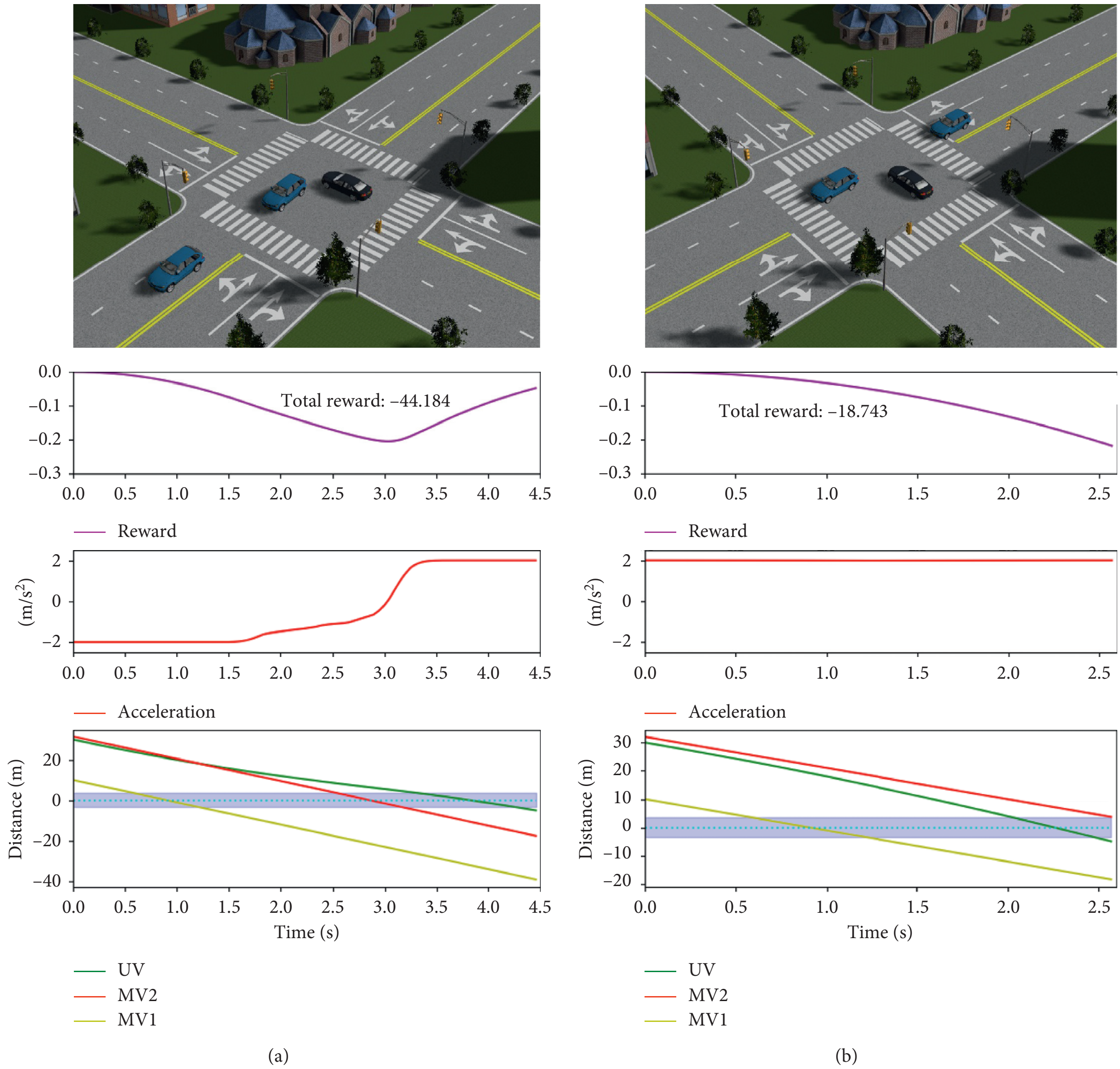

FIGURE 10: Comparison of the performance of the two algorithms. (a) NSGA-II. (b) DDPG.

TABLE 1: Comparison data of two algorithms.

Algorithm	Time to cross the conflict zone for UV (s)	Total reward	$\dot{a}_{max}$(m/s^3)
NSGA-II	3.75	−44.184	5
DDPG	2.25	−18.743	0

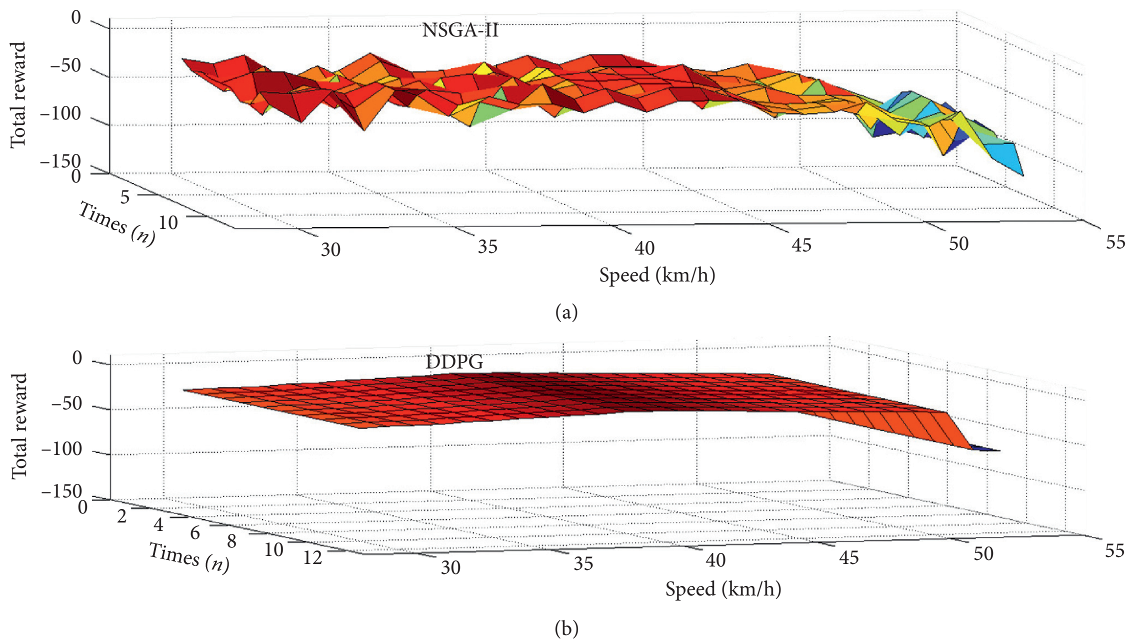

Figure 11: Stability and robustness of two algorithms.

rewards of the two algorithms decrease when the initial speed is greater than 50 km/h, which indicates the possibility of a collision.

6. Conclusion and Future Work

To improve the safety and efficiency of autonomous vehicles, this paper proposed a MOP decision-making model based on efficient conflict resolution for autonomous vehicles at urban intersections, which considers the complexity of urban intersections and the uncertainties of vehicle behavior. The prediction algorithm for incoming vehicles was studied, and we compare the performance for UV at intersections based on the decision-making model by NSGA-II and DDPG. The main conclusions are listed as follows:

(1) The trajectory prediction model fits the predicted trajectory by learning the probability distribution of a large amount of trajectory data, and the accuracy of the model depends on the quantity and quality of the training data. The incoming vehicle trajectory data collected in this paper was limited and was unable to cover all the incoming vehicle motion patterns.

(2) The MOP decision-making model performs well, which can avoid a collision for vehicles happened at intersections. Compared to a traditional machine learning algorithm, NSGA-II, the performance of DDPG algorithm is more stable and effective to solve the MOP model at intersections, and UVs perform the more appropriate and efficient motions by DDPG.

The decision making of autonomous vehicles is influenced by human-vehicle-road (environmental) factors. Due to limits on the length of this article, the impacts of pedestrians, non-motor vehicles, road structure types, and traffic flow density on decision-making were not considered in this study. In the future, the impacts of these factors will be studied and discussed. The interactions between people and vehicles will be considered to further improve the decision-making model of driving behavior under real road conditions.

Data Availability

The data used to support the findings of this study are provided in the Supplementary Materials section.

Conflicts of Interest

The authors declare that they have no conflicts of interest.

Acknowledgments

This work was supported in part by the Youth Science Fund (no. 51705021), Automobile Industry Joint Fund (no. U1764261) of the National Natural Science Foundation of China, Beijing Municipal Science and Technology Project (no.Z191100007419010), and Key Laboratory for New Technology Application of Road Conveyance of Jiangsu Province (no. BM20082061706).

Supplementary Materials

The data collected from the intersections of Wei Gong Cun Road in Beijing using subgrade sensors and a retrofit autonomous vehicle were as the training and testing samples of trajectory prediction model. And the data were divided into three categories: left-turn vehicles, right-turn vehicles, and straight vehicles. Every category included the vehicles, information like location, speed, acceleration, and so on. (*Supplementary Materials*)

References

[1] M. Paul Mureşan, I. Giosan, and S. Nedevschi, "Stabilization and validation of 3D object position using multimodal sensor fusion and semantic segmentation," *Sensors*, vol. 20, no. 4, 2020.

[2] H. Kim, J. Cho, D. Kim et al., "Intervention minimized semi-autonomous control using decoupled model predictive control," in *Proceedings of the Intelligent Vehicles Symposium. IEEE*, Las Vegas, NV, USA, July 2017.

[3] M. R. Boukhari, A. Chaibet, M. Boukhnifer et al., "Exteroceptive fault-tolerant control for autonomous and safe driving," in *Automation Challenges of Socio-technical Systems*Wiley Online Library, New Jersey, NY, USA, 2019.

[4] S. Gibbs, *Google Sibling Waymo Launches Fully Autonomous Ride-Hailing Service*, The Guardian, London, UK, 2017.

[5] S. Zelinski, T. Koo, and S. Sastry, "Optimization-based formation reconfiguration planning for autonomous vehicles," in *Proceedings of the 2003 IEEE International Conference on Robotics and Automation*, September 2003.

[6] C. Urmson, J. C. Baker, B. P. Salesky Rybski, W. Whittaker, D. Ferguson, and M. Darms, "Autonomous driving in traffic: boss and the urban challenge," *AI Magazine*, vol. 30, no. 2, pp. 17–28, 2009.

[7] H. Whittaker, Z. Fan, C. Liu et al., "Baidu apollo em motion planner," 2018, http://arxiv.org/abs/1807.08048.

[8] P. Wang and C.-Y. Chan, "Vehicle collision prediction at intersections based on comparison of minimal distance between vehicles and dynamic thresholds," *Iet Intelligent Transport Systems*, vol. 11, no. 10, pp. 676–684, 2017.

[9] C. Hubmann, M. Becker, D. Althoff et al., "Decision making for autonomous driving considering interaction and uncertain prediction of surrounding vehicles," in *Proceedings of the 2017 IEEE Intelligent Vehicles Symposium (IV)*, June 2017.

[10] M. Bojarski, D. Del Testa, D. Dworakowski et al., "End to end learning for self-driving cars," 2016, http://arxiv.org/abs/1604.07316.

[11] J. Chen, *Research on Decision Making System of Autonomous Vehicle in Urban Environments*, University of Science and Technology of China, Hefei, China, 2014.

[12] C. Liu, R. Zheng, and Q. Guo, "A decision-making method for autonomous vehicles based on simulation and reinforcement learning," in *Proceedings of the International Conference on Machine Learning & Cybernetics*, Tianjin, China, July 2013.

[13] Z. Ma, J. Sun, and Y. Wang, "A two-dimensional simulation model for modelling turning vehicles at mixed-flow intersections," *Transportation Research Part C: Emerging Technologies*, vol. 75, pp. 103–119, 2017.

[14] S. Zhong, J. Tan, H. Dong et al., "Modeling-learning-based actor-critic algorithm with Gaussian process approximator," *Journal of Grid Computing*, vol. 18, pp. 181–195, 2020.

[15] G. Xiong, Y. Li, S. Wang, X. Li, and P. Liu, "HMM and HSS based social behavior of intelligent vehicles for freeway entrance ramp," *International Journal of Control and Automation*, vol. 7, no. 10, pp. 79–90, 2014.

[16] C. Lv, C. Li, Y. Xing, C. Lu et al., "Hybrid-learning-based classification and quantitative inference of driver braking intensity of an electrified vehicle," *IEEE Transactions on Vehicular Technology*, vol. 99, no. 1, 2018.

[17] X. Chen, G. Tian, C.-Y. Chan, Y. Miao, J. Gong, and Y. Jiang, "Bionic lane driving of autonomous vehicles in complex urban environments: decision-making analysis," *Transportation Research Record: Journal of the Transportation Research Board*, vol. 2559, no. 1, pp. 120–130, 2016.

[18] X. Chen, M. Jin, M. Yi-song, and Q. Zhang, "Driving decision-making analysis of car-following for autonomous vehicle under complex urban environment," *Journal of Central South University*, vol. 24, pp. 1476–1482, 2017.

[19] X.-m. Chen, Q. Zhang, Z.-h. Zhang, G.-m. Liu et al., "Research on intelligent merging decision-making of unmanned vehicles based on reinforcement learning," in *2018 IEEE Intelligent Vehicles Symposium (IV)*, pp. 91–96, Changshu, Suzhou, China, July 2018.

[20] M. Chen, C. Pan, B. Yin et al., "Ship navigation trajectory prediction based on Gaussian process regression," *Technology Innovation and Application*, vol. 31, pp. 28-29, 2017.

[21] K. Deb, A. Pratap, S. Agarwal, and T. Meyarivan, "A fast and elitist multiobjective genetic algorithm: NSGA-II," *IEEE Transactions on Evolutionary Computation*, vol. 6, no. 2, 2002.

[22] V. Mnih, K. Kavukcuoglu, D. Silver et al., "Playing Atari with deep reinforcement learning," 2013, http://arxiv.org/abs/1312.5602.

[23] L. J. Lin, *Reinforcement Learning for Robots Using Neural Networks*, Carnegie-Mellon University, Pittsburgh, PA, USA, 1993.

[24] T. P. Lillicrap, J. J. Hunt, A. Pritzel et al., "Continuous control with deep reinforcement learning," 2015, http://arxiv.org/abs/1509.02971.

[25] S. Ioffe and C. Szegedy, "Batch normalization:accelerating deep network training by reducing internal covariate shift," 2015, http://arxiv.org/abs/1502.03167.

[26] M. Stuart, "FSM design and verification," *Electronic Engineering*, vol. 71, pp. 17-18, 1999.

[27] Y. Gu, Y. Hashimoto, L. T. Hsu et al., "Motion planning based on learning models of pedestrian and driver behaviors," in *2016 IEEE 19th International Conference on Intelligent Transportation Systems (ITSC)*, Rio de Janeiro, Brazil, November 2016.

[28] M. Du, *Trajectory Prediction Method of Surrounding Vehicles at Urban Intersections Based on Motion Modes Recognition*, Beijng Institute of Technology, Beijing, China, 2019.

[29] N. Zhao, W. Chen, Y. Xuan et al., "Focus and shift of visual attention in driving scenes," *Ergonomics*, vol. 17, no. 4, pp. 85–88, 2011.

Hindawi
Journal of Advanced Transportation
Volume 2020, Article ID 8891449, 10 pages
https://doi.org/10.1155/2020/8891449

Research Article

Intelligent Video Surveillance Technology in Intelligent Transportation

Fangcheng He

School of Foreign Languages, Chongqing University of Education, Chongqing, China

Correspondence should be addressed to Fangcheng He; gxwpc@cque.edu.cn

Received 26 March 2020; Revised 29 July 2020; Accepted 3 September 2020; Published 16 November 2020

Academic Editor: Wenqing Wu

Copyright © 2020 Fangcheng He. This is an open access article distributed under the Creative Commons Attribution License, which permits unrestricted use, distribution, and reproduction in any medium, provided the original work is properly cited.

Along with the strength of the country's overall strength, the people's pockets have become more and more popular, and there have been significant improvements in all aspects of life, especially in terms of travel methods. This reflects the increase in residents' income, but it also brings huge traffic pressure. In the long run, traffic congestion is not only detrimental to urban development, but frequent traffic accidents threaten residents' travel safety. Effective monitoring methods are essential to solving these problems, so it is necessary to carry out research on intelligent video monitoring technology in intelligent transportation. The purpose of this article is to solve the current situation of excessive traffic pressure in the city. Through the study of intelligent video surveillance technology in intelligent traffic, the use of constrained least squares algorithm to remove motion blur and apply Kalan filtering to the sharpening process is used to eliminate noise ambiguity and make a brief introduction to various classic moving target detection methods to realize real-time monitoring of intelligent traffic conditions and continuously adjust and verify the monitoring situation, and then establish intelligent video in intelligent traffic monitoring technology research system. The research results show that this kind of intelligent video surveillance technology research in intelligent transportation can effectively increase the awareness of intelligent video surveillance technology and improve the level of intelligent video surveillance technology. The data measurement time has been shortened by one hour, the aggregation time has been changed from three hours to two hours, and the analysis time has been shortened by half. Eased urban traffic road pressure and greatly reduced the incidence of traffic accidents, which is conducive to socialist harmony social construction.

1. Introduction

Since ancient times, transportation has been the basic industry of the national economy, an important factor determining national economic development and a basic condition for social development and the improvement of people's living standards [1, 2]. Since the founding of the People's Republic of China, China has realized a great transition from standing up to becoming rich to becoming strong [3]. With the overall strength of the country, people's pockets are getting bigger and bigger, and they have improved significantly in all aspects of life, especially in the way they travel. From bicycles in the 1980s and 1990s to today's buses, subways, and private cars, both in number and type, have undergone qualitative changes [4–6]. But at the same time, the rapid increase in the number of vehicles has brought great pressure to urban traffic roads. This is not only reflected in the poor effect of coordinating reasonable road flow but also reflects a large amount of material resources and manpower spent in maintaining road order. More distressing is the rapid rise in the incidence of traffic accidents caused by too many vehicles [7, 8]. These pressures pose a huge test to urban traffic, restrict the efficiency of various urban development work, and bring safety risks to residents' safe travel [9]. In the face of more and more severe traffic pressure, the traditional method has been unable to deal with a good deal. Some cities have adopted the method of limiting the number of orders to solve traffic problems. In fact, this method is essentially to reduce the number of traveling vehicles, thus reducing the traffic pressure [10]. But after all, this method is at the expense of some people's interests and cannot be used for a long time. Another phenomenon is the widespread construction of roads to accommodate the increasing number of vehicles. But its problem is also obvious: road design is often not reasonable enough to harm the long-term development of the city [11]. Even more unrealistic is the hope that civilized traffic awareness propaganda will change this situation [12]. Admittedly, the moral quality of Chinese residents has been improved obviously, but this kind of spiritual propaganda is too individual and has little effect. So, we still need a solution to adapt to advanced traffic to solve the huge traffic pressure.

The predecessor of intelligent video surveillance technology research is the intelligent vehicle road system. Intelligent transportation systems effectively integrate advanced information technology, data communication technology, sensor technology, electronic control technology, and computer technology into the entire transportation management system [13]. As a result, a comprehensive, real-time, accurate, and efficient comprehensive transportation and management system has been established that functions in a wide range and in all directions [14]. An intelligent transportation system is a complex and comprehensive system. From the perspective of system composition, it can be divided into the following subsystems: advanced traffic management system, advanced traffic information service system, advanced vehicle control system, freight management system, electronic toll collection system [15], and emergency rescue system [16]. In the expected design of the intelligent traffic detection system, it can greatly improve the efficiency of infrastructure use, thereby reducing government investment in infrastructure facilities; it can also effectively alleviate urban congestion and reduce the incidence of traffic accidents; it is also applied to solve the vehicle exhaust emissions and large vehicle energy consumption [17]. As the advantages of the intelligent transportation system have been well known to the public, speeding up the improvement of the system has been included in the top priority of the current research in the field of transportation, and it has become the trend of this era [18]. But after all, the intelligent transportation system is a discipline created by the convergence of electronic information technology, Internet of Things technology, automatic control theory, communication technology, and traditional traffic engineering theory, which means that its establishment must rely on a wealth of theoretical foundations [19, 20]. Then, a lot of infrastructure construction is added to form a large-scale and comprehensive transportation system, so that it can give full play to its role [21].

In order to better alleviate the pressure of urban traffic, this paper conducts research on intelligent video surveillance technology in intelligent traffic. Among them, Chan made a detailed introduction to intelligent video surveillance and believed that the application of dynamic target detection methods is of great significance [22, 23]. Khatri proposed in his paper the application of intelligent transportation systems in contemporary transportation systems and explained the characteristics of smart video surveillance technology and its main development prospects [24]. Cain et al. have a solution for smart video surveillance technology, detailed the feasibility of establishing an intelligent transportation system in the article, applied it to actual engineering, and obtained a large amount of data analysis [25]. Song et al. put forward some common problems in the technology required for system building and proposed the problems that may be encountered in building a corresponding intelligent transportation system [26]. Song et al. proposed a rough classification of dynamic target detection methods in the system and proposed the application of intelligent traffic video monitoring methods in real life and the solution of common problems [27]. Kumar et al. proposed the advantages and disadvantages of intelligent video monitoring technology, which is of great significance to fully solve the urban traffic pressure and believed that this is of great significance for building a harmonious society [28, 29].

To put it simply, this article takes intelligent traffic intelligent video monitoring technology as the main research content, that is, understanding and analyzing the causes and sources of urban traffic pressure, to identify the main directions that need to be resolved, and then to study intelligent traffic intelligent video monitoring technology. Specifically, the main research content of this article is roughly divided into five parts: the first part is the introduction part, which aims to systematically review the main research content of this article from the research background, research purpose, research ideas, and methods; the second part is the theoretical basis, a detailed and systematic summary of the current theories and methods of urban transportation and the current research status of intelligent transportation systems, and it also introduces the current level of convergence of technologies such as the Internet of Things and communication technologies. The third part is related research, which starts with the research of intelligent traffic intelligent video monitoring technology from the aspects of overall and function through specific survey data and detection results. The fourth part is to make a clear summary of the advantages and disadvantages of intelligent video monitoring technology by comparing the effectiveness of intelligent video monitoring technology in real life. The fifth part is the summary and suggestion part of this article. It is a summary of the results of this article and a prospect for the widespread application of intelligent video monitoring technology in intelligent transportation systems.

2. Proposed Method

2.1. Intelligent Video Detection Technology. In order to study and realize video tracking in intelligent traffic, objects (vehicles or people) moving in traffic must be determined first, which requires the use of target detection technology. Object detection technology is different from static image analysis but has some similarities [30]. The detection of the target is to divide the picture into the motion interval and the static interval, then analyze the continuous image transformation, extract the structural features of the moving target, and analyze and judge the state of the dynamic target. The image analysis of the moving target is to consider the sequence of the moving image to make up for the feature that the single frame image cannot detect the dynamic target. The commonly used dynamic target detection methods include optical flow method, interframe difference method, background difference method, morphology, and so on. The interface difference method is mainly to shoot video segmentation, each frame of the video segmentation, the adjacent two or a few frames in video sequences do bad, and the difference image threshold; the pixel gray level change is greater than the threshold value of points awarded for future, pixel gray sentenced to less than the threshold as the background, so as to detect the target contour [31]. The method has the following formula:

$$D_k(x, y) = f_k(x, y) - f_{k-1}(x, y). \tag{1}$$

The difference image is obtained by the pixel gray level of the position $f_{(k)}$ of frame k and the position $f_{(k-1)}$ of frame kitchen; threshold judgment is made on the difference image to distinguish foreground and background points, and banalization image is obtained, namely:

$$\begin{aligned} R_k(x, y) &= 0, \\ D_k(x, y) &< T, \\ R_k(x, y) &= 1, \\ D_k(x, y) &> T. \end{aligned} \tag{2}$$

Compared with other methods of target detection, the principle of interface difference method and operation is very simple, able to quickly detect the moving targets and to the actual monitoring scene has good adaptability, but in practical application, it is difficult to determine the definition of a threshold; the threshold is too small; it is hard to ignore the reality environment such as wind, instruments, and equipment, etc. The threshold is too large. It is easy to the omission of moving target detection and the image cannot detect the complete movement [32]. Therefore, this method is only applicable to the case where the camera is fixed and the environment is less affected.

The main idea of the background subtraction method is as follows: first, select a background image that does not contain the target and then make the difference between the current frame and the background image so as to obtain the target region in the current frame and achieve the goal of target detection [33]. The difference image is obtained by making a difference between frame k image $f_{(k)}$ and background image B:

$$D_k(x, y) = f_k(x, y) - B(x, y). \tag{3}$$

The selection of background image is very important for the background subtraction method [34]. In order to improve the reliability and accuracy of the background subtraction method, the background should timely select the appropriate background image according to the changes in the environment. In practice, it is very difficult to obtain an accurate objective background due to the influence of light changes, the movement of objects in the background, the changes of background itself, and the noise of image sensor equipment [35].

The concept of optical flow method was proposed by Gibson and Wallach in 1950. When the target in the real world of three-dimensional movement occurs, its corresponding projection point in the two-dimensional plane will change as an image of a light flow refers to the instantaneous velocity in grayscale mode. Based on the optical flow field of each pixel, movements can deduce the target movement in reality. The optical flow field contains the motion information of the actual three-dimensional world target [36]. The optical flow method is mainly used to detect the moving target according to the optical flow property of the moving target with the change of the pixel intensity in the video image sequence [37].

Assuming the pixel $p(x, y)$ in the image, the gray value at time t is $I(x, y, t)$; after a very short time interval Δt, we can consider that the intensity values of the two remain unchanged, as shown in the following formula:

$$I(x, y, t) = I(x + \Delta x, y + \Delta y, t + \Delta t). \tag{4}$$

Assuming that the change trend of gray value I is smooth, it can be obtained as follows:

$$I(x, y, t) + \frac{\partial I}{\partial x}\Delta x + \frac{\partial I}{\partial y}\Delta y + \frac{\partial I}{\partial t}\Delta t + e = I(x, y, t). \tag{5}$$

E is the higher order term. Its value is infinitesimal. Dividing both sides by Δt, the following can be obtained:

$$\frac{\partial I}{\partial x}\Delta x + \frac{\partial I}{\partial y}\Delta y + \frac{\partial I}{\partial t}\Delta t = 0. \tag{6}$$

Let u and v represent the velocity vectors in the X and Y directions, respectively, and represent the optical flow of I:

$$I_x u + I_y v = -I_t. \tag{7}$$

This is the optical flow constraint equation. According to the global method proposed by Horn and Shuck, a global smoothing constraint is introduced. That is,

$$e_c = \iint \left(\frac{\partial p}{\partial x}u + \frac{\partial p}{\partial y} + \frac{\partial p}{\partial t}\right)^2 \mathrm{d}x\mathrm{d}y. \tag{8}$$

The optical flow error of the grayscale conservation hypothesis is as follows:

$$e_b = I_x u + I_y v + I_t. \tag{9}$$

To sum up, the optical flow method can detect moving objects, but the optical flow method is difficult to carry out in real time due to its large and complicated calculation. In addition, the constraint equation of optical flow cannot be satisfied under the condition that the object under test is occluded, multilight source, and multinoise.

With the rapid development of computer technology, we no longer rely on our own eyes for image acquisition but use visual computer-aided systems to process big data information [38]. The important means of the visual aid system is to rely on imaging technology. The information control and processing of the system are realized by the computer. These tasks and contents include the collection, transmission, storage, and processing of visual information. The application goal of the visual computer system in an intelligent traffic system is to realize computer-aided traffic guidance. The system has the function of relying on visual sensitive feedback information to realize some visual monitoring task [39]. Computer-aided vision software is composed of automatic control and spatial positioning system [40]. Through the target monitoring technology and computer vision systems, intelligent video monitoring technology for a dynamic target within the scope of visual image analysis, the video image filtering prevents interference light change and natural phenomenon; if the existence of a dynamic target is sensed, the system will immediately upload the dynamic target's license plate number, vehicle direction information, color information, moving speed, and other information to the monitoring and dispatching system for further processing.

2.2. Evaluation Index of Intelligent Video Monitoring Technology. The evaluation index can reflect the reliability and feasibility of a system. Different evaluation indexes represent different contents of dynamic target detection methods. The rationality of evaluation indexes is directly related to the authenticity of the final evaluation results. The selection of evaluation indicators should follow the principles of typicality, independence, hierarchy, reliability, and quantifiable.

(1) Typicality: the evaluation indicators should be clear and able to measure and reflect the characteristics of a certain aspect of the system.

(2) Independence: the dynamic target information reflected by different evaluation indicators should be different. If the evaluation indicators are compatible with each other, it should be considered to combine the indicators with the same meaning. "the evaluation of one indicator should not be affected by other indicators.

(3) Hierarchy: the evaluation of the dynamic target detection method is divided into several levels for consideration, and the lower evaluation indexes are reasonably determined according to specific diagnostic indexes to form a structural system.

(4) Reliability: the evaluation index must be able to truly reflect the status of the actual parameters of the dynamic target, and the dynamic target state identified by each evaluation index should be consistent with the actual situation.

(5) Quantifiable: in order to carry out objective analysis and evaluation of targets, quantitative methods must be adopted. Therefore, evaluation indicators should be those that can be quantified according to a certain principle. Dynamic target detection is a complicated system problem. The influencing factors of dynamic target detection are numerous, but when choosing the evaluation index is not possible to all factors into consideration, only in combination with the actual situation to choose the most telling indicator, the traffic problem is the most difficult in the dynamic process of detection of target recognition because the limitation of the current knowledge of the process is not very understanding; that is, the detection of dynamic targets is in a situation where there is limited understanding. Obviously, the fact detection data is the most intuitive information reflecting the parameters of moving targets. Therefore, from the perspective of typicality, reliability, and quantification, it is necessary to use a variety of dynamic target detection methods to test the current difficult dynamic target detection problems to obtain a comprehensive evaluation.

3. Experiments

3.1. Related Processing of Experimental Data. In the process of the experiment, a large number of production management data need to be processed, and these data will inevitably have errors. It is also very important to deal with these errors properly. Error processing and analysis of the original data are quite necessary. Otherwise it will affect the positive and negative analysis of the experimental data. Systematic error, random error, and gross error are the main forms of experimental data error. Among them, the errors caused by random factors are called random errors, which are characterized by irregular signs and absolute values but are normally distributed with the increasing number of experiments. Because in the statistical data, due to artificial carelessness, or changes in environmental conditions, instrument instability, and other factors, resulting in the observation error, do not conform to a certain rule of statistical distribution error which is called the measurement error. The systematic error is caused by the reason of measuring instrument, the change of measuring datum, and the influence of external conditions. At present, the test of systematic errors of observed values generally constitutes the corresponding statistics according to the statistical characteristics of observed values, and then the test hypothesis is made according to the probability distribution characteristics, and the discrimination is made by comparing the actual calculated values with the fractional values' test method, variance test method, t-test method, and so on are commonly used measurement methods. To get the data, the first thing to do is to remove the influence of gross error and systematic error and ensure the accuracy of the next step [41].

At home and abroad, the least square method is mainly used to process the monitoring data [42]. The least square method assumes that the observed value contains only accidental error, which is impossible in practice. Therefore, a new theory of systematic error and gross error is generated. At present, the more effective method to deal with the system error is the additional parameter method. There are two methods to deal with a gross error. One is the data detection method which still belongs to the category of least square method. The other is the robust estimation method or the robust estimation method which is different from the least square method. In addition, in the actual monitoring engineering, the measured body is in constant change, and the measuring system is also in motion. Therefore, it can be considered that security detection belongs to dynamic measurement, and the error contained in the detection data is necessarily dynamic and time-varying. The gross error in the detection data often makes the statistical distribution difficult to determine or even beyond the general statistical law, and the detection data at different stages are also quite different, so it is difficult to meet the requirements of data processing with traditional methods. Modern error theory holds that the measured truth value cannot be measured, and the existence of quantum effect excludes the existence of a unique truth value, so the error cannot be obtained accurately. The error used in past measurements is actually a deviation. The measured error is actually the uncertainty of the measurement. Uncertainty refers to the degree of uncertainty to the measured value due to the existence of measurement error, and it is the evaluation of the range of magnitude that represents the measured truth value. Considering the characteristics of dynamic target continuity, the reliability of measured value can be considered according to the continuity, progress, and rationality of measured value, that is, the degree of certainty of measured value. High reliability means low uncertainty of measurement value. Low reliability means high uncertainty of measurement. The theory of ascertain mathematics can be used to describe the reliability of data. The following is the method of ascertain mathematics for the analysis and error processing of original data.

3.2. The Establishment of the Experimental Model of Intelligent Video Monitoring. It is planned to build a video image sharpening prototype system based on the guidance of moving object detection, which includes the following functions: video file reading, moving object detection and extraction, moving object sharpening processing, and video file saving and display. Moreover, the results of the video image sharpening under the guidance of different motion signs are compared. Through this algorithm, traffic video can be analyzed, and moving objects in the video can be clarified, providing a basis and support for the research and development of an intelligent traffic monitoring system.

3.2.1. The System Implements the Hardware Device. PC: the CPU is Intel 4, the memory size is 4G, the hard disk size is 240G. One digital camera: it is used to shoot video files of moving vehicles in intelligent transportation [41]. The image size is 320 times 240, and the acquisition rate is 15 frames per second.

3.2.2. System Design. The module structure of the system is mainly composed of a video reading module, moving object detection module, clearness processing module, and video display module. Video reading module is mainly responsible for storing the video images input by video input devices such as cameras into the computer cache frame by frame, providing the system with a frame-by-frame image sequence for further processing. This system can process real-time video input from the camera. The moving object detection module uses the method of interface difference and optical flow to detect the moving object, then performs morphological filtering on the detected foreground binary image, marks the connected region, and finally extracts the moving object, which provides the basis for the video image sharpness processing [43]. The deburring processing module firstly deburrs the image, then clarifies the extracted moving target area, and adopts the method of specific area enhancement. In order to display the result of the final clarification processing, the system displays the results of video images in the form of RGB. In the case of the same degree of blurriness of the video image, the constrained least squares algorithm is better than the Wiener filter to restore the clearing effect, and as the noise increases, the image becomes blurred, and the clarity of the image recovered is worse. Therefore, the recovery effect is worse, so the constrained least squares algorithm is selected to remove the motion blur, and the specific image quality evaluation under different noises is shown in Table 1.

Table 1 data represent the image quality evaluation table under different noises. The target position signal obtained from the intelligent traffic scene by video analysis technology contains various noises. The filtering algorithm of thought is in the sequence by predicting, update two steps iterative update constantly, causing the error of the system noise and observation noise to decrease gradually in order to obtain the best state parameter, achieve the goal of eliminating noise, and effectively avoid the traditional image of the video data after due to noise operator to bring further the defect of fuzzy. Wiener filter algorithm and constrained least squares method are used finally to remove the motion blur with the constrained least squares method, using the fuzzy kalian filter to eliminate noise and filtering based on a specific area to enhance the motivation method; this method can be a more outstanding image of some important information, make the image clearer, can reduce the amount of calculation, and at the same time improve the real-time performance.

4. Discussion

4.1. Analysis of Intelligent Video Monitoring Technology. There are many reasons for unclear video images in traffic monitoring, and different methods are adopted for different reasons. For the specific application of intelligent traffic monitoring, the main considerations are motion blur, noise blur, and low contrast blur [44]. In view of this, wiener filtering and constrained least square algorithms are, respectively, used for restoration and clearness processing. The variation trend of the effect is shown in Table 2:

It can be seen from the data in Table 2 that the effect is best when the gain value is 0.5. However, when the gain value is greater than 0.5, the predicted value of pixel will be higher than the actual value, so the effect of processing will be decreased.

The system carries out experiments on a number of traffic road video files collected, deburring the relatively fuzzy video, and then sharpening the video images of specific areas based on the detection guidance. In order to evaluate

Table 1: Image quality evaluation table under different noises.

	MAE	MSE	SNR
ó = 2	47921	67498	19.645
Ó = 4	87042	85079	10.297

Table 2: Image quality evaluation table.

Gain value	ΔR	NMSE
Gains = 0.25	0.432	0.004034
Gains = 0.50	0.259	0.002534
Gains = 0.75	0.542	0.005132

the quality and degree of image sharpening after the system sharpening processing, this paper compares the images before the sharpening processing with the processed images and compares the improved detection algorithm in this paper with the images processed by other common detection methods, so as to highlight that the improved algorithm is better. In this paper, the average absolute error, mean square error, normalized homogenization error, SNR, and minimum correlation number error are used to evaluate the image quality, as shown in Figure 1:

To read in the traffic video file, read the image, respectively, using frame differential method and background subtraction method, optical flow method, and frame flow method to detect moving targets, and then to detect the binary motion area of the postprocessing, such as median filter and morphological filtering and extracting the movement area, and then to extract the motion area of the recovery process, based on regional enhanced image clearer processing, finally display video images. As can be seen from the data in Figure 1, in several image motivation based on the detection algorithm, the MAE, MSE, NMSE, and ΔR values of the improved algorithm proposed in this paper are smaller than those of other algorithms, and the resulting value is larger than that of other algorithms, which explains the processed image is clearer and the difference between the original image is very small; this means that the improved algorithm in video image processing effect is better than other algorithms. After the application of intelligent video monitoring technology, compared with the traditional traffic system, the images are more specific and clearer, more information is obtained from the images, and the feedback is faster. The data measurement time has been shortened by one hour, the aggregation time has been changed from three hours to two hours, and the analysis time has been shortened by half. In these fast-paced times, every second can be the difference between success and failure. With the application of intelligent video monitoring system, urban residents can get feedback more quickly when they travel, so as to adjust their travel routes to reduce the unnecessary time wasted in traffic jams, which also extends the time available to residents in a hidden way and provides a guarantee for meeting residents' other needs. For the transportation department, a large amount of redundant data processing time can be reduced, so that manpower and material resources can be arranged more rationally.

Traffic flow monitoring is an important component of intelligent traffic. To study the function of video tracking technology in intelligent traffic, it is necessary to realize the function of traffic flow monitoring. Designated in the video picture need to monitor the alert area when moving inside the vehicle; based on the intelligent video surveillance technology, analysis platform immediately sends alarm information to the terminal interface and the vehicle's trajectory according to target motion trajectory in the management of terminal monitoring screen on the basis of the realization of target detection; the detected vehicle enters can automatically detect the video traffic detection scope and can be the flow in the management of terminal display; observation data is shown in Figure 2:

As can be seen from Figure 2, the real-time traffic flow of the road can be clearly understood through intelligent video monitoring technology. Traffic flow in parking lots, highways, central roads, and suburban intersections was observed. This means that if there is a traffic jam at the central intersection during the rush hour, the intelligent video monitoring technology can be used to give timely feedback so that the majority of residents can stagger the traffic flow.

4.2. Analysis of Dynamic Target Detection Method. The basic principle of dynamic object detection is to input the image of a dynamic object through a video camera and complete the digitization. In the process of image acquisition, some noise signals that affect image quality are generated, so before processing these digital images, digital image filtering should be carried out first. For the preprocessed images, corresponding video detection procedures can be conducted to extract the specific parameters of dynamic targets. Robustness, accuracy, and processing speed are the main indexes in the performance analysis of a moving date detection algorithm. The robustness of the algorithm means that the algorithm can work automatically and continuously and is less sensitive to the influence of noise, light, and weather factors. The processing speed of the algorithm is the real-time performance of the algorithm, as shown in Table 3:

It can be seen from Table 3 that the traditional dynamic target detection method has a long cycle and can no longer

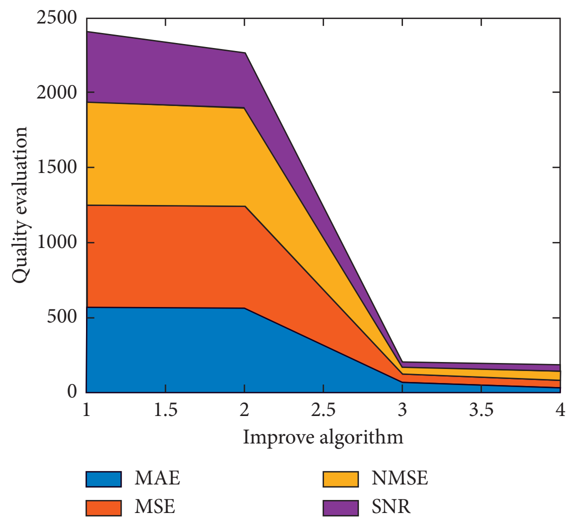

Figure 1: Quality evaluation of the improved algorithm.

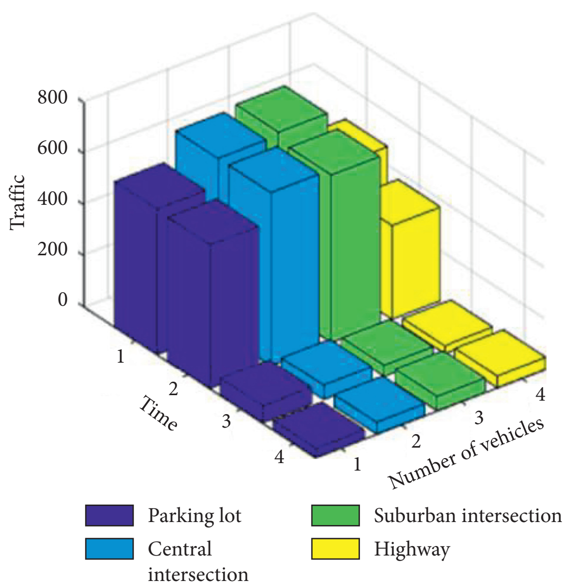

Figure 2: Traffic monitoring.

adapt to the current fast-paced era. It can be seen that the improved detection algorithm has good performance in robustness, accuracy, and processing speed. In the practical application, people often use the improved algorithm or a combination of several algorithms; then the performance will be different. Therefore, in the selection of algorithms, we should try to overcome the shortcomings of each algorithm in view of its advantages and disadvantages and give play to their respective advantages to improve the detection effect. Time is critical for dynamic target detection in intelligent transportation systems. So the development prospect of the improved algorithm is very good.

The improved algorithm integrates the multifeature extraction method to extract and analyze the dynamic target and integrates the classical algorithm to realize the dynamic target tracking of multifeature adaptive parameters, and proposes the traffic flow detection framework and process of dynamic target information, and expounds the traffic flow detection method based on video images. However, the field of transportation involves not only computer vision recognition, pattern recognition, and other information domain expertise but also a large part of factors that depend on the implementation of traffic rules of human factors and the natural environment. Therefore, in view of this concern, the dynamic target detection method is tested in a comprehensive environment to verify the correctness of the dynamic target. See Figure 3 for details.

As can be seen from Figure 3, the correctness test of the improved algorithm is much higher than that of the traditional method, which indicates that the improved algorithm has great potential. However, due to the limitation of the natural environment and the influence of human factors, the accuracy of the improved algorithm is not stable enough, which has some limitations on its application. If the improved algorithm is to be further introduced into the traffic field, its stability needs to be improved. If this problem can be completely solved, the pressure of urban traffic will be greatly relieved.

Video image sharpening processing is the core technology of all kinds of intelligent video monitoring systems. It is the cornerstone of various subsequent high-level processing and applications, such as target tracking, behavior recognition, target classification, and behavior analysis. To explore the ability to calmly cope with various changes in the complex environment, and accurately, quickly, and stably detect moving objects. According to relevant standards, the safety factor index standards are established, as shown in Figure 4:

As can be seen from Figure 4, the improved algorithm has the highest pixel and the best definition. The frame difference method has high robustness but slow accuracy and processing speed. Background differential flu robustness is low; accuracy and processing speed are fast. The robustness and processing speed of the optical flow method are slow and the accuracy is high.

Table 3: Algorithm performance comparison.

Detection algorithm	Frame difference method	Optical flow method	Improve algorithm
Robustness	High	Low	High
Accuracy	Low	Higher	High
Processing speed	Fast	Slow	General

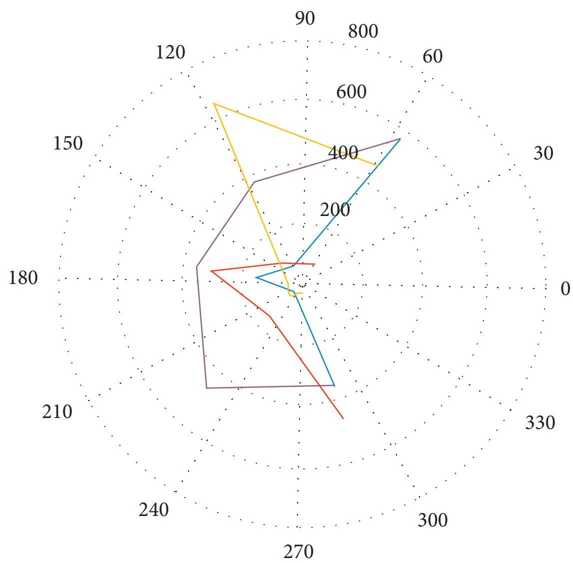

Figure 3: The correctness of different methods.

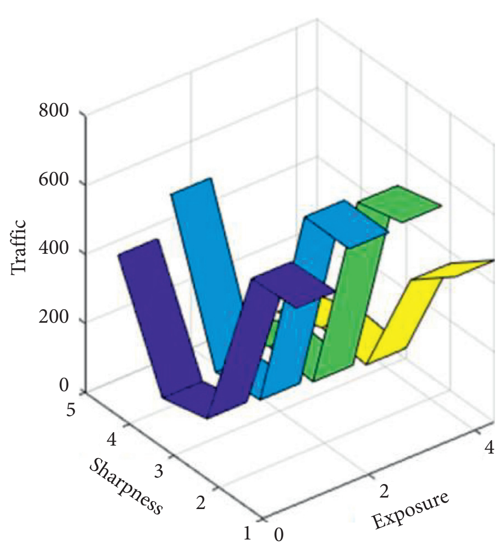

Figure 4: Pixel size comparison.

5. Conclusions

(1) This article analyzes the situation that with economic development, more and more residents are driving by car, which poses a great challenge to urban transportation to a certain extent. The main problem is that the speed of increasing vehicles is not consistent with the speed of road construction, resulting in the present problems such as traffic jams and long travel times in urban transportation which further affect the residents' life experience and are not conducive to the long-term development of the city. In the face of this increasingly severe traffic situation, the emergence of intelligent video monitoring systems provides a direction for solving such problems. Therefore, this article conducts research on intelligent video monitoring systems in order to deepen the understanding of emerging technologies and better apply them to go in real life.

(2) This article introduces the global positioning system, communication technology, and traditional transportation field theoretical technology. Based on the theory, it is clear that video surveillance technology is the product of multidisciplinary convergence and clarifies the definition and related characteristics of video surveillance technology. The classic moving target detection method is briefly introduced, and an improved target detection algorithm of the interframe difference optical flow method is proposed. It maintains the advantages of the fast and efficient extraction of moving targets by the interframe difference method. Moreover, the advantages of reliable optical target extraction and strong antinoise ability of optical flow method are maintained. The moving target detection method based on this can effectively extract the traffic target area from the surveillance video at the intersection.

(3) This paper made a certain analysis of the performance of the intelligent video monitoring technology and compared the improved algorithm with the interframe difference method, the background light method, and the optical flow method. X. It has improved by 20 percentage points in accuracy and has advantages unmatched by other target detection methods. It not only saves a lot of manpower and resources but also greatly improves efficiency. This study of intelligent video surveillance technology in intelligent traffic can effectively increase the awareness of intelligent video surveillance technology,

improve the level of intelligent video surveillance technology, and shorten the data measurement time by one hour and the aggregate time from three hours to two hours The reduction of analysis time is even more obvious, and the time spent is reduced by half. Relieving the pressure on urban traffic roads has also greatly reduced the incidence of traffic accidents, which is conducive to the construction of a harmonious socialist society.

Data Availability

All the data in this article are real and available.

Conflicts of Interest

There are no potential conflicts of interest in our paper. All authors have seen the manuscript and approved to submit it to the journal. The authors confirm that the content of the manuscript has not been published or submitted for publication elsewhere.

Acknowledgments

This work was supported by Chongqing Big Data Engineering Laboratory for Children, Chongqing Electronics Engineering Technology Research Center for Interactive Learning, Project of Science and Technology Research Program of Chongqing Education Commission of China (No. KJZDK201801601).

References

[1] T. Gaber, S. Abdelwahab, M. Elhoseny, and A. E. Hassanien, "Trust-based secure clustering in WSN-based intelligent transportation systems," *Computer Networks*, vol. 146, pp. 151–158, 2018.

[2] Z. Lv, S. Zhang, and W. Xiu, "Solving the security problem of intelligent transportation system with deep learning," *IEEE Transactions on Intelligent Transportation Systems*, pp. 1–10, 2020.

[3] X.-H. Zhang, S. Zhang, S. Fang, and X. Cao, "Clearing research on fog and dust images in coalmine intelligent video surveillance," *Journal of the China Coal Society*, vol. 9, no. 4, pp. 32-33, 2016.

[4] J. M. Huang, "Research on internet of vehicles and its application in intelligent transportation," *Applied Mechanics & Materials*, vol. 321–324, pp. 2818–2821, 2013.

[5] C.-H. Chen, "An arrival time prediction method for bus system," *IEEE Internet of Things Journal*, vol. 5, no. 5, pp. 4231-4232, 2018.

[6] L. Jinn, H. Goo, M. Liu, and J. Xiao, "Video event detection technology and its application in intelligent transportation," *Applied Mechanics & Materials*, vol. 20, no. 9, pp. 1-2, 2017.

[7] S. Wan, X. Li, Y. Xue, W. Lin, and X. Xu, "Efficient computation offloading for Internet of vehicles in edge computing-assisted 5G networks," *The Journal of Supercomputing*, vol. 76, no. 4, pp. 2518–2547, 2020.

[8] R.-H. Zhang, F. You, F. Chen, and W. Q. He, "Vehicle detection method for intelligent vehicle at night time based on video and laser information," *International Journal of Pattern Recognition & Artificial Intelligence*, vol. 32, no. 4, Article ID 1850009, 2018.

[9] C. Jinn, W. Dan, and K. Cain, "Research and implementation of image compression in intelligent video surveillance system based on SOPC," *IEEE Sensors Journal*, vol. 21, no. 1, pp. 10–20, 2016.

[10] J. Liu, H.-Q. Zhang, and Y. Liu, "Research on optimal selection of moving target defense policy based on dynamic game with incomplete information," *Act Electronica Sonica*, vol. 21, no. 15, pp. 110–120, 2018.

[11] Z. Lv, W. Kong, X. Zhang, D. Jiang, H. Lv, and X. Lu, "Intelligent security planning for regional distributed energy internet," *IEEE Transactions on Industrial Informatics*, vol. 16, no. 5, pp. 3540–3547, 2020.

[12] B. Cui, J. Cui, and D. Yong, "Intelligent security video surveillance system based on deviance technology," *Journal of Mechanical Strength*, vol. 42, no. 1, pp. 1–12, 2016.

[13] M.-G. Kim, H.-M. Moon, and Chung, "A survey and proposed framework on the soft biometrics technique for human identification in intelligent video surveillance system," *Journal of Biomedicine & Biotechnology*, vol. 42, no. 35, pp. 5-6, 2018.

[14] R. Parada, J. Melià-Seguí, and R. Pous, "Anomaly detection using RFID-based information management in an IoT context," *Journal of Organizational and End User Computing*, vol. 30, no. 3, pp. 1–23, 2018.

[15] N. Li, T. Zhao, and H. Jiang, "Research on dynamic coupling characteristic of rootless under actuated redundant robots," *Journal of Mechanical Engineering*, vol. 12, no. 21, pp. 12–16, 2016.

[16] W. Song, Y. Yang, M. Fu, Y. Li, and M. Yang, "Lane detection and classification for forward collision warning system based on stereo vision," *IEEE Sensors Journal*, vol. 18, no. 12, pp. 15-16, 2018.

[17] T. Yu, B. L. Hu, and Gao, "Research on dynamic tracking and compensation method for hyperspectral interference imaging," *Gangs Xebio/Act Photonic Sonica*, vol. 45, no. 7, pp. 25–36, 2016.

[18] I. Butun, P. Österberg, and H. Song, "Security of the Internet of things: vulnerabilities, attacks, and countermeasures," *IEEE Communications Surveys & Tutorials*, vol. 22, no. 1, pp. 616–644, 2020.

[19] Y. Zhang, H. Liu, J. Wu, J. He, and C. Zhang, "Statistical analysis for performance of detection and imaging of dynamic targets using the geostationary interferometric microwave sounder," *IEEE Journal of Selected Topics in Applied Earth Observations & Remote Sensing*, vol. 1, no. 1, pp. 3–11, 2018.

[20] Z. Lv and A. Kumar Singh, "Big data analysis of Internet of things system," *ACM Transactions on Internet Technology (TOIT)*, 2020.

[21] Y.-T. Chan, S.-J. Wang, and C.-H. Tsai, "Extracting foreground ensemble features to detect abnormal crowd behavior in intelligent video-surveillance systems," *Journal of Electronic Imaging*, vol. 64, no. 17, pp. 12–15, 2015.

[22] J. Lan, S. Li, and S. Wu, "Research on ensemble classification model of Trojan traffic detection," *Journal of Xian Tongan University*, vol. 49, no. 8, pp. 4–9, 2015.

[23] M. Elhoseny, "Multi-object detection and tracking (MODT) machine learning model for real-time video surveillance systems," *Circuits, Systems, and Signal Processing*, vol. 39, no. 2, pp. 611–630, 2019.

[24] V. Khatri, "Intelligent video surveillance using soft biometrics," *Xitsonga Lila You Shavian/System Engineering Theory and Practice*, vol. 35, no. 5, pp. 12-13, 2015.

[25] L. Cain, J. Xu, and L. Jinn, "Research on agricultural surveillance video of intelligent tracking," *Journal of Mechanical Engineering*, vol. 52, no. 4, pp. 13-14, 2016.

[26] G.-C. Song, Y.-X. Na, F.-Y. Yang, and S.-H. Cao, "Research on portable intelligent monitoring system based on video server," *Journal of Intelligent & Robotic Systems*, vol. 92, no. 3, pp. 1–12, 2017.

[27] W. Song, J. Zhang, W. Zhang, Y. Wang, Q. Zhuo, and W. Shi, "Research of intelligent video surveillance in substation based on ViBe," *Chinese Journal of Scientific Instrument*, vol. 99, no. 2, pp. 27-28, 2016.

[28] N. Kumar, J.-H. Lee, and J. Rodrigues, "Intelligent mobile video surveillance system as a bayesian coalition game in vehicular sensor networks: learning automata approach," *IEEE Transactions on Intelligent Transportation Systems*, vol. 39, no. 6, pp. 11-12, 2016.

[29] H. Elhoseny, M. Elhoseny, A. M. Riad, and A. E. Hassanien, "A framework for big data analysis in smart cities," *The International Conference on Advanced Machine Learning Technologies and Applications (AMLTA 2018)*, vol. 723, pp. 405–414, 2018.

[30] N. Babaguchi, A. Cavallaro, R. Chellappa, F. Dufaux, and L. Wang, "Special issue on intelligent video surveillance for public security and personal privacy," *IEEE Transactions on Information Forensics & Security*, vol. 16, no. 1, pp. 8–15, 2017.

[31] S. Wan, Y. Xia, L. Qi, Y.-H. Yang, and M. Atiquzzaman, "Automated colorization of a grayscale image with seed points propagation," *IEEE Transactions on Multimedia*, 2020.

[32] Z. You, G. Chen, and B. Wang, "Intelligent control based on a-support vector regression theory for regional traffic signal system," *Journal of Computer Applications*, vol. 37, no. 2, pp. 34–36, 2015.

[33] M. Chippewa, M. Trashy, and T. Moroccan, "Data fusion in a mufti agent system for person detection and tracking in an intelligent room," *Studies in Computational Intelligence*, vol. 57, no. 5, pp. 12–15, 2015.

[34] I. B. Guo, "Target detection method based on beam forming output DC response of coinsurance matrix," *Journal of Computer Applications*, vol. 45, no. 5, pp. 11–16, 2017.

[35] Y. Zhao and C. Yang, "Information fusion robust guaranteed cost Kalman estimators with uncertain noise variances and missing measurements," *International Journal of Systems Science*, vol. 50, no. 15, pp. 2853–2869, 2019.

[36] V. Agrawal, B. K. Panigrahi, and P. M. V. Subarea, "Intelligent decision support system for detection and root cause analysis of faults in coal mills," *IEEE Transactions on Fuzzy Systems*, vol. 32, no. 99, pp. 1–5, 2016.

[37] S. Ding, S. Qu, Y. Xi, and S. Wan, "A long video caption generation algorithm for big video data retrieval," *Future Generation Computer Systems*, vol. 93, pp. 583–595, 2019.

[38] Z. Li, R. A. Hassan, and Mohammad, "A hierarchical framework for intelligent traffic management in smart cities," *IEEE Transactions on Smart Grid*, vol. 45, no. 99, pp. 11–23, 2017.

[39] J. Yang, C. Wang, B. Jiang, H. Song, and Q. Meng, "Visual perception enabled industry intelligence: state of the art, challenges and prospects," *IEEE Transactions on Industrial Informatics*, p. 1, 2020.

[40] A. A. Rahmani Hosseinabadi, J. Vahidi, B. Saemi, A. Kumar Sangaiah, and M. Elhoseny, "Extended genetic algorithm for solving open-shop scheduling problem," *Soft Computing*, vol. 23, no. 13, pp. 5099–5116, 2019.

[41] M. R. Reddy, K. G. Srinivasa, and B. E. Reddy, "Smart vehicular system based on the Internet of things," *Journal of Organizational and End User Computing*, vol. 30, no. 3, pp. 45–62, 2018.

[42] X. Chen, Y. Xu, L. Meng et al., "Non-parametric partial least squares-discriminant analysis model based on sum of ranking difference algorithm for tea grade identification using electronic tongue data," *Sensors and Actuators B: Chemical*, vol. 311, Article ID 127924, 2020.

[43] H. Song and M. Brandt-Pearce, "A 2-D discrete-time model of physical impairments in wavelength-division multiplexing systems," *Journal of Lightwave Technology*, vol. 30, no. 5, pp. 713–726, 2012.

[44] B. Wang and L. L. Chen, "New results on fuzzy synchronization for a kind of disturbed memristive chaotic system," *Complexity*, vol. 2018, Article ID 3079108, 9 pages, 2018.

Hindawi
Journal of Advanced Transportation
Volume 2020, Article ID 4723687, 13 pages
https://doi.org/10.1155/2020/4723687

Research Article

Collision Avoidance of 3D Rectangular Planes by Multiple Cooperating Autonomous Agents

Jai Raj,[1] Krishna Raghuwaiya ,[2] and Jito Vanualailai[1]

[1]*School of Computing Information & Mathematical Sciences, The University of the South Pacific, Suva, Fiji*
[2]*School of Education, The University of the South Pacific, Suva, Fiji*

Correspondence should be addressed to Krishna Raghuwaiya; raghuwaiya_k@usp.ac.fj

Received 14 February 2020; Revised 23 September 2020; Accepted 8 October 2020; Published 28 October 2020

Academic Editor: Wenqing Wu

Copyright © 2020 Jai Raj et al. This is an open access article distributed under the Creative Commons Attribution License, which permits unrestricted use, distribution, and reproduction in any medium, provided the original work is properly cited.

We develop a set of novel autonomous controllers for multiple point-mass robots or agents in the presence of wall-like rectangular planes in three-dimensional space. To the authors' knowledge, this is the first time that such a set of controllers for the avoidance of rectangular planes has been derived from a single attractive and repulsive potential function that satisfies the conditions of the Direct Method of Lyapunov. The potential or Lyapunov function also proves the stability of the system of the first-order ordinary differential equations governing the motion of the multiple agents as they traverse the three-dimensional space from an initial position to a target that is the equilibrium point of the system. The avoidance of the walls is via an approach called the Minimum Distance Technique that enables a point-mass agent to avoid the wall from the shortest distance away at every unit time. Computer simulations of the proposed Lyapunov-based controllers for the multiple point-mass agents navigating in a common workspace are presented to illustrate the effectiveness of the controllers. Simulations include towers and walls of tunnels as obstacles. In the simulations, the point-mass agents also show typical swarming behaviors such as split-and-rejoin maneuvers when confronted with multiple tower-like structures. The successful illustration of the effectiveness of the controllers opens a fertile area of research in the development and implementation of such controllers for Unmanned Aerial Vehicles such as quadrotors.

1. Introduction

The motion planning and control (MPC) of mobile robots or agents is a challenging task and an interesting problem attracting considerable attention to the robotic community over the last couple of decades. The design of a particular robotic system and motion planning are usually treated independently [1]. Typically, MPC algorithms are applied to systems with fully fixed geometric and kinematic features, while the system design in robotics takes into account robustness, stiffness, workspace volume, obstacle avoidance schemes, and other performance features. The principle goal for any MPC problem is to find the most optimum design to optimise the motion between given configurations [2–7]. In an MPC problem, multiple robots are favoured as they are able to cooperate for faster and more efficient results [4, 5, 8–10], including other fields where multiagent operations are always preferred [11].

Path planning or MPC algorithms for mobile robots operating in an environment cluttered with obstacles are usually grouped according to the methodologies used to generate the geometric path, namely, the road map techniques, cell decomposition algorithms, and artificial potential field (APF) methods [4, 12]. These path planning algorithms have a common objective, which is to find the shortest and most optimal geometric path taking into account the moving objects and obstacles in the workspace [13–15]. While the calculation of a hindrance-free way may take care of numerous significant issues in industrial settings where the robot may move cautiously, it is inadequate and practically futile when the robot needs to move at sensibly high speeds, for example, multiple mobile robots navigating through dynamic cluttered situations and autonomous vehicles navigating in a highway traffic situation.

In this research article, we use the Lyapunov controllers, constructed via the Lyapunov-based Control Scheme

(LbCS), essentially an APF method, for the control and stability of a system point-mass mobile robots that, in theory, can take on reasonably high velocities. The LbCS has been employed to warrant point and posture stabilities in the sense of Lyapunov for MPC for various robotic systems, such as car-like mobile robotic systems [4], mobile manipulators [16], tractor-trailer systems [12, 17], and swarming [18]. We utilise the control scheme to derive and extract centralised velocity-based control laws for point-mass mobile robots.

1.1. Contributions. The novelty of this paper is the ease in developing autonomous controllers for the avoidance of three-dimensional wall-like rectangular planes by a mobile robot or agent while it is in motion using a technique known as the Minimum Distance Technique (MDT). The ability to do this opens up many possibilities. Walls can be used to model buildings and towers, windows, and doors. They can be used to model highways and tunnels. When we deal, for instance, with autonomous Unmanned Aerial Vehicles (UAVs), it is now possible to model a drone's performance in the face of such obstacles as buildings and tunnel walls, and its maneuverability inside buildings clustered with rectangular objects and exited. For disaster surveillance and in an urban war simulation and situation, this maneuverability is critical [19, 20].

The MDT was introduced by Sharma et al. [21] to create parking bays for the posture control problem of robotic systems and avoid the sides of a bay, modelled as straight lines. The MDT uses APF functions for the avoidance of the boundaries of the parking bay. In this paper, we extend the methodology to encompass rectangular planes. The MDT involves the computation of the minimum distance from the centre of the point-mass mobile robot to the surface of the rectangular plane and the avoidance of the resultant point on the s$t \geq 0$urface of the rectangular plane. The avoidance of the nearest point on the surface of the rectangular plane at any time $t \geq 0$ ensures that the point-mass mobile robot avoids the whole plane. As we shall see, this algorithm helps in simplifying the navigation laws. Surely, there are other methods of obstacle avoidance of polygons. The most recent one was proposed by Arantes et al. [22] who discussed path planning approaches for dynamic systems to handle non-convex constraints to be formulated as model-predictive control, which planned discrete time control and state sequences simultaneously through a constrained optimisation. The optimisation problem that needs to be solved in this case is the mixed-integer linear programming (MILP) when the dynamics are linear and the obstacles are represented by combinations of polytopes, with no uncertainty presence. The problem that lies in this particular approach is the *jumps* between the time steps, which could result in a trajectory cutting through the obstacle, given that the method is only concerned with satisfying the constraints at a discrete point in times, as shown in Figure 1(a). Arantes et al. devised a new approach to suppress this problem by imposing constraints that require every pair of adjacent states to be on the same side of an obstacle, as shown in Figure 1(b) [23].

Furthermore, comparing Arantes et al. approach to the MDT, the latter results in a smooth, continuous path for the avoidance of irregular shaped (rectangular plane) obstacles. An illustration of the MDT for the avoidance of a rectangular plane is shown in Figure 1(c).

The main contributions of this paper are summarised as follows:

(1) The design of the velocity algorithm for a point-mass mobile robot which is based on a Lyapunov function that acts as an energy function of the system. The velocity algorithm ensures safe, collision-free trajectories that converge to the intended target.

(2) The design of the velocity algorithm for the point-mass mobile robot which is based on the development of a Lyapunov function that acts as an energy function of the system. The velocity algorithm applied here is altogether not quite the same as the ones in the literature. Consistently enduring velocities are utilised; nonetheless, the robot needs to stop after it has accomplished its objective. This stop should not be unexpected by a truncation of speed; rather, the robot should slow down its motion and afterward come to rest. The velocity algorithm and the objective target intended for the robot guarantee a protected and safe stop at the goal objective and furthermore guarantee that the robot stays there.

(3) A three-dimensional rectangular-plane obstacle avoidance scheme using the MDT. While in motion, the distance between the point-mass robot and the closest point on the surface of the wall is computed and the point-mass robot avoids this point on the surface of the wall, resulting in the avoidance of the entire wall. In addition, we only consider the wall closest to the point-mass robot en route to its target. Subsequently, our obstacle avoidance scheme is more straightforward contrasted with, for instance, the avoidance schemes used in the artificial potential strategies where all of the obstacles are considered in parallel [4, 17].

(4) Stability analysis pertaining to the kinodynamic system. We use the Direct Method of Lyapunov to carry out the stability analysis, proving that the equilibrium point of the system, representing the target of a point mass, is stable.

The paper is organised as follows: In Section 2, we define the kinematic model of the point-mass robot; in Section 3, the APF functions are defined; in Section 4, the Lyapunov function is constructed and the robust nonlinear continuous control laws for the mobile robot are extracted; in Section 5, the stability of the system is discussed; in Section 6, the simulation results are presented to show the robustness and effectiveness of the proposed control inputs and followed by conclusion in Section 7.

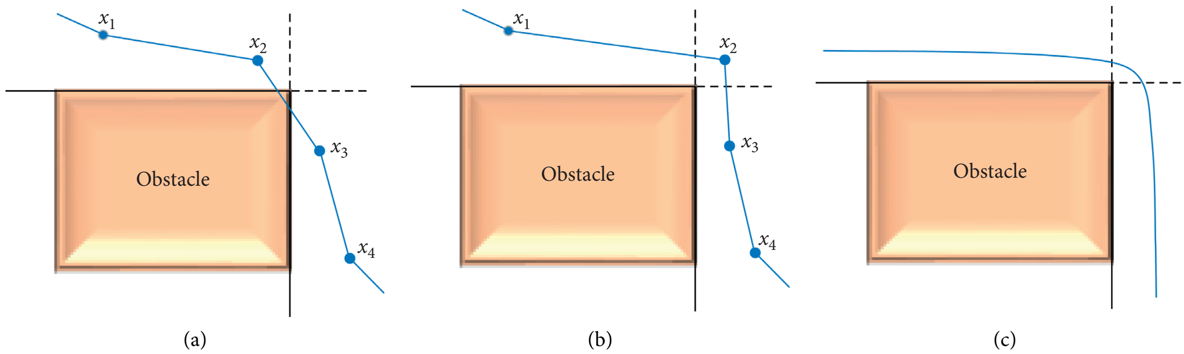

FIGURE 1: (a) Conventional model-predictive control-based path planning requires that states are outside of polygonal obstacles resulting in the path cutting through the obstacle. (b) The MILP approach of using a straight-line trajectory between waypoints [22]. (c) The smooth and continuous path for MDT demonstration of obstacle avoidance.

2. Modelling a Point-Mass Robot or Agent in 3D

The modelling process of a robotic system involves the conceptualisation of the problem, residing on the abstraction level. Simulation, however, mainly focuses on the implementation of the execution of the model to study the behavior and performance of an actual or theoretical system. This section proposes a simple kinematic model for the moving point-mass robot, an abstraction of a simple form of a robotic system. A two-dimensional schematic representation of a point-mass robot with and without rectangular obstacle avoidance is shown in Figure 2. We begin with the following definition.

Definition 1. A point mass, $\mathscr{P}_i$, is a sphere of radius rp_i and centred at $(x_i(t), y_i(t), z_i(t)) \in \mathbb{R}^3$ for $t \geq 0$. That is, it is the set

$$\mathscr{P}_i = \left\{(Z_1, Z_2, Z_3) \in \mathbb{R}^3 \colon\ (Z_1 - x_i)^2 + (Z_2 - y_i)^2 + (Z_3 - z_i) \leq \mathrm{rp}_i^2\right\}. \tag{1}$$

At time $t \geq 0$, the instantaneous velocity of the point mass will be given as $(v_i(t), w_i(t), u_i(t)) = (\dot{x}_i(t), \dot{y}_i(t), \dot{z}_i(t))$. Assuming the initial conditions, a system of the first-order ODEs governing $\mathscr{P}_i$ is

$$\left.\begin{aligned} &\dot{x}_i = v_i(t), \dot{y}_i = w_i(t), \dot{z}_i = u_i(t), \\ &x_{i0}\colon = x_i(t_0), y_{i0}\colon = y_i(t_0), z_{i0}\colon = z_i(t_0), \end{aligned}\right\} \tag{2}$$

for $i = 1, \ldots, n$. Let $\mathbf{x}_i\colon = (x_i, y_i, z_i) \in \mathbb{R}^3$ and $\mathbf{x}\colon = (\mathbf{x}_1, \ldots, \mathbf{x}_n) \in \mathbb{R}^{3n}$.

Next, we will formulate the components that form the Lyapunov function, essentially the attractive and repulsive potential field functions.

3. Construction of the APF Functions

In this section, we construct the components of the Lyapunov function. We assume that $\mathscr{P}_i$ has *a priori* knowledge of the entire workspace. The principle objective is to construct the Lyapunov function from which we derive the nonlinear velocity control inputs $v_i(t), w_i(t)$, and $u_i(t)$ for $i = 1, \ldots, n$ such that $\mathscr{P}_i$ navigates and reaches its target configuration, avoiding any obstacle, whether fixed, moving, or artificial, while it is in motion. The design of the nonlinear control inputs is captured in Figure 3, clearly illustrating the roles of the individual components in the design of the control scheme.

3.1. Attractive Potential Field Functions. We introduce basic mathematical notions to design and construct attractive functions for target attraction for $\mathscr{P}_i$.

3.1.1. Attraction to Target Function. To initiate movement and ensure convergence, we propose to have a target T_i for each of the point-mass mobile robots $\mathscr{P}_i$. The convergence of $\mathscr{P}_i$ to T_i will be guaranteed by the Lyapunov function.

Definition 2. The assigned target for the point-mass mobile robot of $\mathscr{P}_i$ is a sphere with centre $(\tau_{i1}, \tau_{i2}, \tau_{i3})$ and radius $r\tau_i$. That is, it is the set

$$T_i = \left\{(Z_1, Z_2, Z_3) \in \mathbb{R}^3 \colon\ (Z_1 - \tau_{i1})^2 + (Z_2 - \tau_{i2})^2 + (Z_3 - \tau_{i3})^2 \leq r\tau_i^2\right\}. \tag{3}$$

The next function will measure the Euclidean distance of $\mathscr{P}_i$ from its designated target T_i at time $t \geq 0$. It will be used as an attraction function:

$$V_i(\mathbf{x}) = \frac{1}{2}\left[(x_i - \tau_{i1})^2 + (y_i - \tau_{i2})^2 + (z_i - \tau_{i3})^2\right]. \tag{4}$$

An illustration of the total potentials for the target attraction function is shown in Figure 4(a), while Figure 4(b) shows the analogous contour plot generated over a workspace $0 < Z_1 < 100$ and $0 < Z_2 < 100$ for the point-mass mobile robot. For simplicity, we consider the target function in a 2-dimensional environment. The disk-shaped target for the point-mass mobile is fixed at $(\tau_{01}, \tau_{02}) = (50, 50)$ with a radius of $\mathrm{rp}_0 = 1$.

3.1.2. Auxiliary Function. In the MPC problem, $\mathscr{P}_i$ starts from an initial position and navigates towards its target. While navigating, the motion of $\mathscr{P}_i$ is such that it will avoid

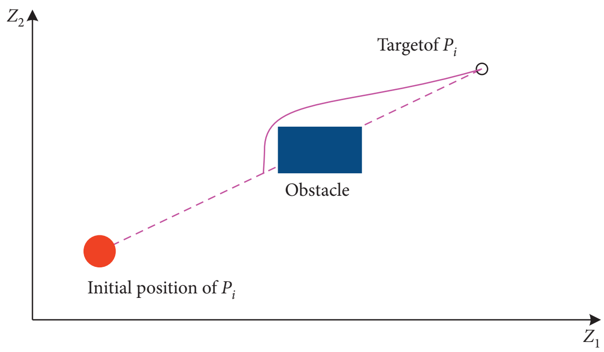

FIGURE 2: 2D schematic representation of $\mathscr{P}_i$ with planar obstacle in $Z_1 - Z_2$ plane.

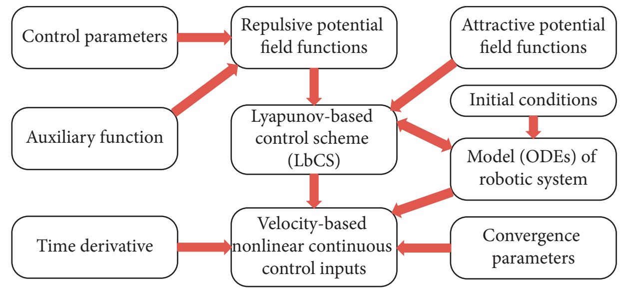

FIGURE 3: The block diagram outlining the LbCS design.

all obstacles, whether it is fixed or moving, with respect to the kinodynamic constraints that are tagged with the robotic system including the constraints on velocity and angles before reaching its objective target. Once it has reached the target, it essentially means that it has accomplished the task that was given to the robot, and hence it needs to stop at the target configuration. Intuitively, this means that the energy of the robotic system needs to be zero at the target configuration; that is, the nonlinear controllers need to vanish at the target. Hence, to achieve this and to ensure the convergence of $\mathscr{P}_i$ to its target configuration, we consider the auxiliary function of the form

$$G_i(\mathbf{x}) = V_i(\mathbf{x}). \tag{5}$$

3.2. Repulsive Potential Field Functions

3.2.1. Workspace Boundaries. We shall confine the motion of $\mathscr{P}_i$ in a cuboid constrained by the dimensions $\eta_1 \times \eta_2 \times \eta_3$. Since the motion is confined within these boundary walls, the walls are hence treated as fixed obstacles. Therefore, for the avoidance of these walls, the following functions are proposed:

$$\left.\begin{aligned} &\mathrm{WS}_{i1}(\mathbf{x}) = x_i - \mathrm{rp}_i, \mathrm{WS}_{i2}(\mathbf{x}) = \eta_2 - (y_i + \mathrm{rp}_i), \\ &\mathrm{WS}_{i3}(\mathbf{x}) = \eta_1 - (x_i + \mathrm{rp}_i), \mathrm{WS}_{i4}(\mathbf{x}) = y_i - \mathrm{rp}_i, \\ &\mathrm{WS}_{i5}(\mathbf{x}) = z_i - \mathrm{rp}_i, \mathrm{WS}_{i6}(\mathbf{x}) = \eta_3 - (z_i + \mathrm{rp}_i), \end{aligned}\right\} \tag{6}$$

for $i = 1, \ldots, n$, which are positive within the rectangular cuboid.

3.2.2. Rectangular-Plane Obstacle Avoidance. Disks in 2D and spheres in 3D are the simplest models of obstacles. However, they encompass extraspaces that are not needed for avoidance. For example, enclosing a rod-like structure within a sphere introduces spaces that need not be avoided. As an illustration, Figure 5(a) shows the contour plot of the total potentials and the corresponding collision-free path of a point mass over the workspace $0 < Z_1 < 40$ and $0 < Z_2 < 40$ encompassing a rod-shaped obstacle, while Figure 5(b) showcases the contour plot of the total potentials and the resulting path if the rod is replaced by a disk-shaped obstacle. The initial and final coordinates of the rod are $(10, 20)$ and $(30, 20)$, respectively. The disk portrayal of the rod has a diameter of 10, which matches the length of the rod, and is centred at $(20, 20)$. The path generated in the presence of the rod-shaped obstacle is optimal in terms of the distance traversed since the obstacle space is small in contrast to the disk portrayal of the rod. Therefore, in this article, we introduce rectangular obstacles.

To avoid the rectangular obstacles via the MDT, the surface wall of the rectangular plane is classified as a fixed obstacle. Let us fix $\ell = 1, \ldots, \bar{m}$, $\bar{m} \in \mathbb{N}$ rectangular-plane-shaped obstacles within the workspace. An illustration of a rectangular plane is showcased in Figure 6, which we shall use to derive the new mathematical equations for its avoidance. Three points are sufficient for deriving the saturation functions and hence designing the rectangular-plane avoidance functions. We begin with the following definition.

Definition 3. Assume that the three-dimensional ℓth planar obstacle has the three coordinates $(a_{\ell 1}, b_{\ell 1}, c_{\ell 1})$, $(a_{\ell 2}, b_{\ell 2}, c_{\ell 2})$, and $(a_{\ell 3}, b_{\ell 3}, c_{\ell 3})$, $\ell = 1, \ldots, \bar{m}$, $\bar{m} \in \mathbf{N}$ (see Figure 6). A single point in the plane is defined by

$$\mathrm{SP}_{i\ell} \colon = (Z_1, Z_2, Z_3) \colon = (Px_{i\ell}, Py_{i\ell}, Pz_{i\ell}) \in \mathbb{R}^3. \tag{7}$$

Then the plane can be precisely described by the set

$$P_\ell = (\mathrm{SP}_{1\ell}, \mathrm{SP}_{2\ell}, \ldots, \mathrm{SP}_{n\ell}) \in \mathbb{R}^{3n}. \tag{8}$$

Then the set of ℓ planes, $\ell \in \bar{m}$, is

$$\mathrm{CP} = \{P_1, P_2, \ldots, P_{\bar{m}}\} \in R^{3n\bar{m}}, \tag{9}$$

where $Px_{i\ell} = a_{\ell 1} + \lambda_{i\ell 1}(a_{\ell 2} - a_{\ell 1}) + \lambda_{i\ell 2}(a_{\ell 3} - a_{\ell 1})$, $Py_{i\ell} = b_{\ell 1} + \lambda_{i\ell 1}(b_{\ell 2} - b_{\ell 1}) + \lambda_{i\ell 2}(b_{\ell 3} - b_{\ell 1})$, and $Pz_{i\ell} = c_{\ell 1} + \lambda_{i\ell 1}(c_{\ell 2} - c_{\ell 1}) + \lambda_{i\ell 2}(c_{\ell 3} - c_{\ell 1})$ are the parametric representation for $0 \le \lambda_{i\ell 1,2} \le 1$, $\ell = 1, \ldots, \bar{m}$, and $i = 1, \ldots, n$.

The MDT necessitates that we identify the closest point on each of ℓ, the rectangular plane measured from the centre of $\mathscr{P}_i$. We compute the minimum Euclidian distance from the centre of $\mathscr{P}_i$ to the surface of the ℓth rectangular plane. The avoidance of the closest point of the surface of the rectangular plane at any time $t \ge 0$ results in the avoidance of the entire plane by $\mathscr{P}_i$. Minimising the Euclidean distance between the points (x_i, y_i, z_i), which is the centre of $\mathscr{P}_i$ and the ℓth rectangular plane, yields

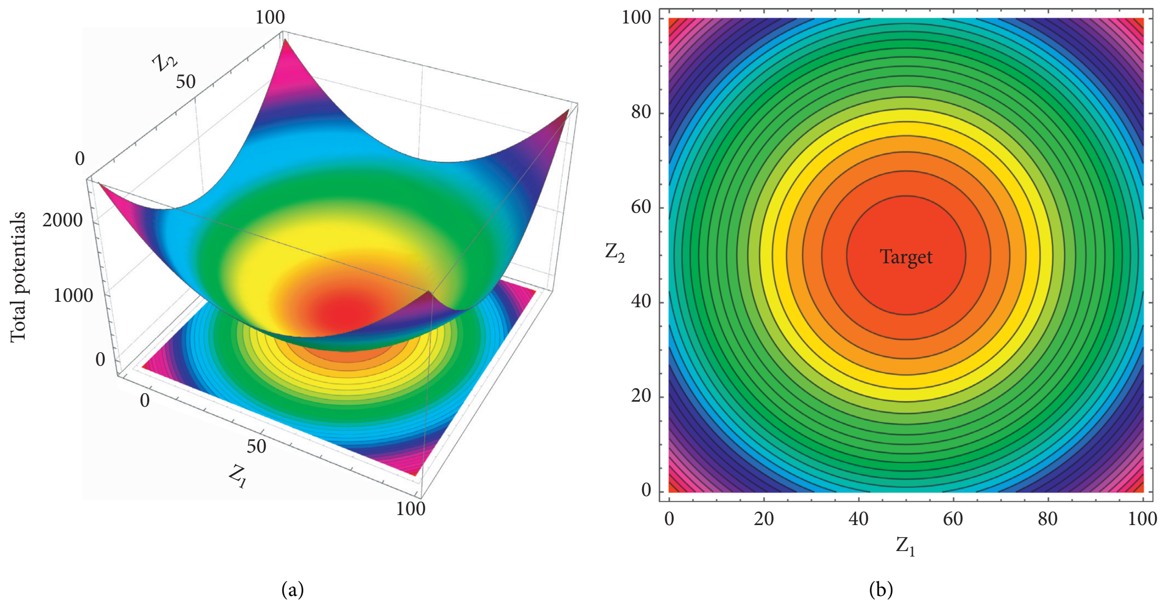

FIGURE 4: The 3D visualization of the attractive potential fields and the analogous contour plot (50 contours) generated using the target attractive function, equation (4). (a) 3D visualization. (b) Contour plot.

$$\lambda_{i\ell 1} = (x_i - a_{\ell 1})\bar{c}_{\ell 1} + (y_i - b_{\ell 1})\bar{d}_{\ell 1} + (z_i - c_{\ell 1})\bar{h}_{\ell 1},$$
$$\lambda_{i\ell 2} = (x_i - a_{\ell 1})\bar{c}_{\ell 2} + (y_i - b_{\ell 1})\bar{d}_{\ell 2} + (z_i - c_{\ell 1})\bar{h}_{\ell 2}, \quad (10)$$

where

$$\bar{c}_{\ell 1} = \frac{(a_{\ell 2} - a_{\ell 1})}{(a_{\ell 2} - a_{\ell 1})^2 + (b_{\ell 2} - b_{\ell 1})^2 + (c_{\ell 2} - c_{\ell 1})^2}, \bar{d}_{\ell 1} = \frac{(b_{\ell 2} - b_{\ell 1})}{(a_{\ell 2} - a_{\ell 1})^2 + (b_{\ell 2} - b_{\ell 1})^2 + (c_{\ell 2} - c_{\ell 1})^2},$$
$$\bar{h}_{\ell 1} = \frac{(c_{\ell 2} - c_{\ell 1})}{(a_{\ell 2} - a_{\ell 1})^2 + (b_{\ell 2} - b_{\ell 1})^2 + (c_{\ell 2} - c_{\ell 1})^2}, \bar{c}_{\ell 2} = \frac{(a_{\ell 3} - a_{\ell 1})}{(a_{\ell 3} - a_{\ell 1})^2 + (b_{\ell 3} - b_{\ell 1})^2 + (c_{\ell 3} - c_{\ell 1})^2}, \quad (11)$$
$$\bar{d}_{\ell 2} = \frac{(b_{\ell 3} - b_{\ell 1})}{(a_{\ell 3} - a_{\ell 1})^2 + (b_{\ell 3} - b_{\ell 1})^2 + (c_{\ell 3} - c_{\ell 1})^2}, \bar{h}_{\ell 2} = \frac{(c_{\ell 3} - c_{\ell 1})}{(a_{\ell 3} - a_{\ell 1})^2 + (b_{\ell 3} - b_{\ell 1})^2 + (c_{\ell 3} - c_{\ell 1})^2}.$$

The saturation functions are $\lambda_{i\ell 1,2}: \mathbb{R}^3 \longrightarrow [0,1] \in \mathbb{R}$, defined as

$$\lambda_{i\ell 1,2}(\bar{c}_{\ell 1,2}, \bar{d}_{\ell 1,2}, \bar{h}_{\ell 1,2}) = \begin{cases} 0, & \text{if } \lambda_{i\ell 1,2} < 0, \\ \lambda_{i\ell 1,2}, & \text{if } 0 \le \lambda_{i\ell 1,2} \le 1, \\ 1, & \text{if } \lambda_{i\ell 1,2} > 1. \end{cases} \quad (12)$$

The new obstacle avoidance functions are therefore of the form

$$\mathrm{RP}_{i\ell}(\mathbf{x}) = \frac{1}{2}\left[(x_i - Px_{i\ell})^2 + (y_i - Py_{i\ell})^2 + (z_i - Pz_{i\ell})^2 - (rp_i)^2\right], \quad (13)$$

for $i = 1, \ldots, n$ and $\ell = 1, \ldots, \bar{m}$. The function $\mathrm{RP}_{i\ell}(\mathbf{x})$ is the measure of the distance between the closest point on the surface of the ℓth rectangular-plane-shaped obstacle and the centre of $\mathcal{P}_i$.

3.2.3. Moving Obstacles. While in motion, each moving robot itself becomes a moving obstacle to every other mobile robot. For $\mathcal{P}_i$ to avoid $\mathcal{P}_j$, we consider the following function:

$$\mathrm{MO}_{ij}(\mathbf{x}) = \frac{1}{2}\left[(x_i - x_j)^2 + (y_i - y_j)^2 + (z_i - z_j)^2 - (\mathrm{rp}_i + \mathrm{rp}_j)^2\right], \quad (14)$$

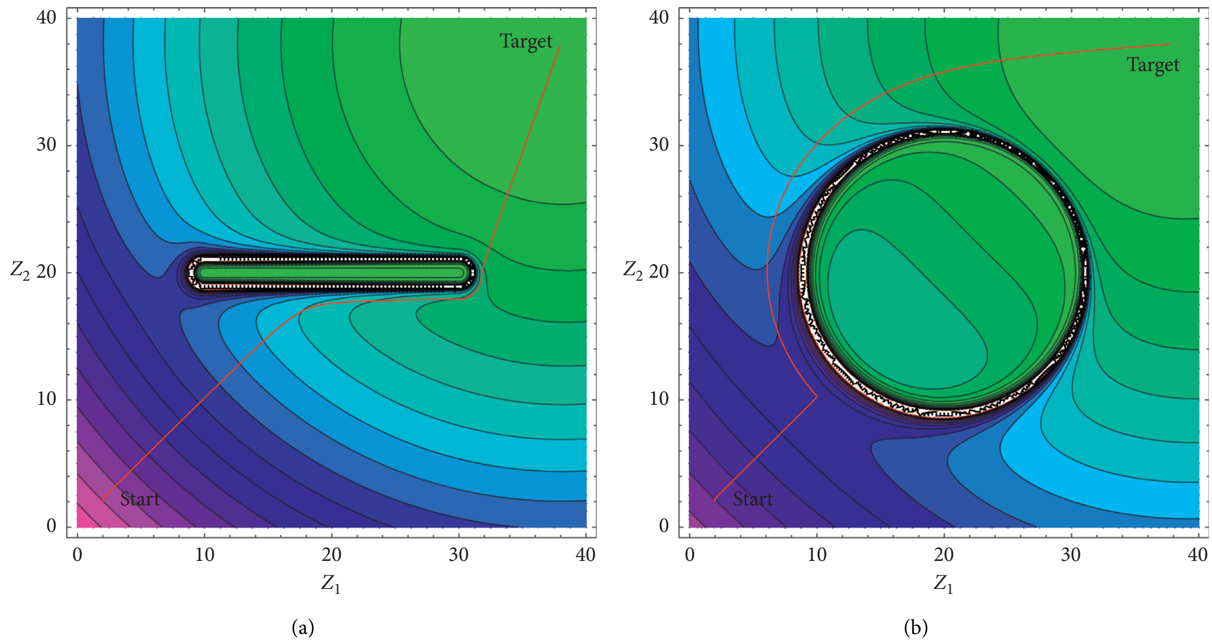

FIGURE 5: The contour plots of the total potential fields generated in the presence of a rod-shaped and a disk-shaped obstacle. (a) Rod-shaped obstacle. (b) Disk-shaped obstacle.

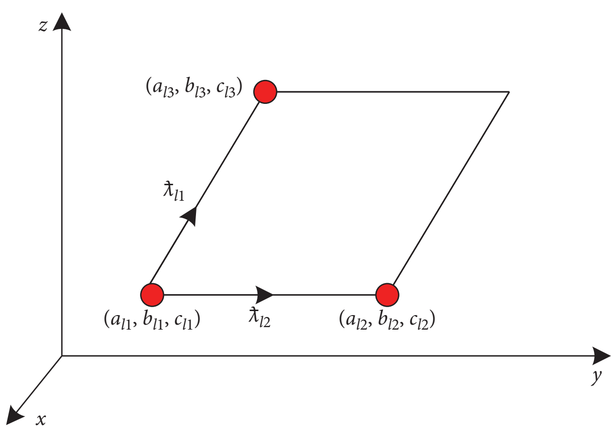

FIGURE 6: Schematic of a rectangular plane.

for $i, j = 1, \ldots, n$, $i \neq j$.

In a nutshell, all these components will now be incorporated to form a Lyapunov function, which will eventually lead to the design of the control inputs for the robotic system.

4. Design of the Control Inputs

In this section, we will first construct the Lyapunov function, followed by its time derivative from which we will ultimately extract the nonlinear control inputs for system (2).

4.1. Lyapunov Function. The Lyapunov function, the total potentials that guarantee target convergence and obstacle and collision avoidance, is the sum of the attractive and repulsive potential fields. We begin first by introducing the *control/tuning parameters*:

(i) $\wp_{i\bar{s}} > 0$ and $\bar{s} = 1, \ldots, 6$, for the avoidance of the $\bar{s}$th boundary of the workspace (see Section 3.2.1).

(ii) $\varsigma_{i\ell} > 0\varsigma_{i\ell} > 0$ and $\ell = 1, \ldots, \bar{m}$, for the avoidance of the surface wall of the ℓth rectangular plane (see Section 3.2.2).

(iii) $\beta_{ij} > 0$ and $i, j = 1, \ldots, n$, $i \neq j$, for the avoidance of the jth point-mass mobile robot (see Section 3.2.3).

Suitably combining all the attractive and repulsive potential filed functions using these tuning parameters, we define a Lyapunov function for system (2) as

$$L(\mathbf{x}) := \sum_{i=1}^{n} \left[V_i(\mathbf{x}) + G_i(\mathbf{x}) \left(\sum_{\bar{s}=1}^{6} \frac{\wp_{i\bar{s}}}{\mathrm{WS}_{i\bar{s}}(\mathbf{x})} + \sum_{\ell=1}^{\bar{m}} \frac{\varsigma_{i\ell}}{\mathrm{RP}_{i\ell}(\mathbf{x})} + \sum_{\substack{j=1 \\ j\neq i}}^{n} \frac{\beta_{ij}}{\mathrm{MO}_{ij}(\mathbf{x})} \right) \right], \tag{15}$$

which is positive over the domain $\mathbb{D}(L) = \{\mathbf{x} \in \mathbb{R}^{3n}\colon \mathrm{WS}_{i\bar{s}}\ (\mathbf{x}) > 0,\ \bar{s} = 1, \ldots, 6, \mathrm{RP}_{i\ell}\ (\mathbf{x}) > 0,\ \ell = 1, \ldots, \bar{m}$ and $\mathrm{MO}_{ij}\ (\mathbf{x}) > 0,\ j = 1, \ldots, n,\ i \neq j,\ i = 1, \ldots, n\}$.

4.2. Control Inputs. Next, we differentiate the various components of $L(\mathbf{x})$ separately with respect to t to obtain (on suppressing x) the control inputs for system (2):

$$
\begin{aligned}
f_{i1} = {} & \left(1 + \sum_{\bar{s}=1}^{6} \frac{\wp_{i\bar{s}}}{\mathrm{WS}_{i\bar{s}}} + \sum_{\ell=1}^{\bar{m}} \frac{\varsigma_{i\ell}}{\mathrm{RP}_{i\ell}} + \sum_{\substack{j=1\\ j\neq i}}^{n} \frac{\beta_{ij}}{\mathrm{MO}_{ij}}\right)(x_i - \tau_{i1}) - G_i \frac{\wp_{i1}}{(\mathrm{WS}_{i1})^2} + G_i \frac{\wp_{i3}}{(\mathrm{WS}_{i3})^2} \\
& - 2G_i \sum_{\substack{j=1\\ j\neq i}}^{n} \frac{\beta_{ij}}{\mathrm{MO}_{ij}}(x_i - x_j) - G_i \sum_{\ell=1}^{\bar{m}} \frac{\varsigma_{i\ell}}{\mathrm{RP}_{i\ell}} \begin{pmatrix} (x_i - Px_{i\ell})\left(1 - (a_{\ell 2} - a_{\ell 1})\bar{c}_{\ell 1} - (a_{\ell 3} - a_{\ell 1})\bar{c}_{\ell 2}\right) \\ -(y_i - Py_{i\ell})\left((b_{\ell 2} - b_{\ell 1})\bar{c}_{\ell 1} + (b_{\ell 3} - b_{\ell 1})\bar{c}_{\ell 2}\right) \\ -(z_i - Pz_{i\ell})\left((c_{\ell 2} - c_{k1})\bar{c}_{\ell 1} + (c_{\ell 3} - c_{\ell 1})\bar{c}_{\ell 2}\right) \end{pmatrix}, \\
f_{i2} = {} & \left(1 + \sum_{\bar{s}=1}^{6} \frac{\wp_{i\bar{s}}}{\mathrm{WS}_{i\bar{s}}} + \sum_{\ell=1}^{\bar{m}} \frac{\varsigma_{i\ell}}{\mathrm{RP}_{i\ell}} + \sum_{\substack{j=1\\ j\neq i}}^{n} \frac{\beta_{ij}}{\mathrm{MO}_{ij}}\right)(y_i - \tau_{i2}) + G_i \frac{\wp_{i2}}{(\mathrm{WS}_{i2})^2} - G_i \frac{\wp_{i4}}{(\mathrm{WS}_{i4})^2} \\
& -2G_i \sum_{\substack{j=1\\ j\neq i}}^{n} \frac{\beta_{ij}}{\mathrm{MO}_{ij}}(y_i - y_j) - G_i \sum_{\ell=1}^{\bar{m}} \frac{\varsigma_{i\ell}}{\mathrm{RP}_{i\ell}} \begin{pmatrix} -(x_i - Px_{i\ell})\left((a_{\ell 2} - a_{\ell 1})\bar{d}_{\ell 1} + (a_{\ell 3} - a_{\ell 1})\bar{d}_{\ell 2}\right) \\ +(y_i - Py_{i\ell})\left(1 - (b_{\ell 2} - b_{\ell 1})\bar{d}_{\ell 1} - (b_{\ell 3} - b_{\ell 1})\bar{d}_{\ell 2}\right) \\ -(z_i - Pz_{i\ell})\left((c_{\ell 2} - c_{\ell 1})\bar{d}_{\ell 1} + (c_{\ell 3} - c_{\ell 1})\bar{d}_{\ell 2}\right) \end{pmatrix}, \\
f_{i3} = {} & \left(1 + \sum_{\bar{s}=1}^{6} \frac{\wp_{i\bar{s}}}{\mathrm{WS}_{i\bar{s}}} + \sum_{\ell=1}^{\bar{m}} \frac{\varsigma_{i\ell}}{\mathrm{RP}_{i\ell}} + \sum_{\substack{j=1\\ j\neq i}}^{n} \frac{\beta_{ij}}{\mathrm{MO}_{ij}}\right)(z_i - \tau_{i3}) - G_i \frac{\wp_{i5}}{(\mathrm{WS}_{i5})^2} + G_i \frac{\wp_{i6}}{(\mathrm{WS}_{i6})^2} \\
& - 2G_i \sum_{\substack{j=1\\ j\neq i}}^{n} \frac{\beta_{ij}}{\mathrm{MO}_{ij}}(z_i - z_j) - G_i \sum_{\ell=1}^{\bar{m}} \frac{\varsigma_{i\ell}}{\mathrm{RP}_{i\ell}} \begin{pmatrix} -(x_i - Px_{i\ell})\left((a_{\ell 2} - a_{\ell 1})\bar{h}_{\ell 1} + (a_{\ell 3} - a_{\ell 1})\bar{h}_{\ell 2}\right) \\ -(y_i - Py_{i\ell})\left((b_{\ell 2} - b_{\ell 1})\bar{h}_{\ell 1} + (b_{\ell 3} - b_{\ell 1})\bar{h}_{\ell 2}\right) \\ +(z_i - Pz_{i\ell})\left(1 - (c_{\ell 2} - c_{\ell 1})\bar{h}_{\ell 1} - (c_{\ell 3} - c_{\ell 1})\bar{h}_{\ell 2}\right) \end{pmatrix},
\end{aligned} \tag{16}
$$

for $i = 1, \ldots, n$. In order to ensure stability in the sense of Lyapunov of system (2), we define the accompanying continuous velocity control laws as follows:

$$
\begin{aligned}
v_i &= -\frac{1}{\alpha_{i1}} f_{i1}, \\
w_i &= -\frac{1}{\alpha_{i2}} f_{i2}, \\
u_i &= -\frac{1}{\alpha_{i3}} f_{i3},
\end{aligned} \tag{17}
$$

for $i = 1, \ldots, n$. Our main theorem, given next, uses these laws to prove the stability of our system.

5. Stability Analysis

Using the notations $\mathbf{x}_{e_i}\colon = (\tau_{i1}, \tau_{i2}, \tau_{i3}) \in \mathbb{R}^3$ and $\mathbf{x}_e\colon = (\mathbf{x}_{e_1}, \ldots, \mathbf{x}_{e_n}) \in \mathbb{R}^{3n}$, we state the following theorem.

Theorem 1. *A stable equilibrium point of system (2) is* $\mathbf{x}_e \in \mathbb{D}(L(\mathbf{x}))$.

Proof. Since the Lyapunov function $L(\mathbf{x})$ of system (2) is defined, continuous and positive over the domain $\mathbb{D}(L) = \{\mathbf{x} \in \mathbb{R}^{3n}: \mathrm{WS}_{i\bar{s}}(\mathbf{x}) > 0, \bar{s} = 1, \ldots, 6, \mathrm{RP}_{i\ell}(\mathbf{x}), \ell = 1, \ldots, \bar{m}$ and $\mathrm{MO}_{ij}(\mathbf{x}) > 0, j = 1, \ldots, n, i \neq j, i = 1, \ldots, n\}$, it can easily be verified that $L(\mathbf{x})$ satisfies the following properties:

(1) $L(\mathbf{x})$ is continuous in the region $\mathbb{D}$ in the neighborhood of the point $\mathbf{x}_e$ of system (2)

(2) $L(\mathbf{x}_e) = 0$

(3) $L(\mathbf{x}) > 0$, $\forall \mathbf{x} \in \mathbb{D}((L(\mathbf{x}))/\mathbf{x}_e)$

Then, along a solution of system (2), we have

$$\dot{L}_{(1)}(\mathbf{x}) = \sum_{i=1}^{n} \left[f_{i1}\dot{x}_i + f_{i2}\dot{y}_i + f_{i3}\dot{z}_i \right]. \tag{18}$$

Using (17), we have the following time derivative of $L(\mathbf{x})$ seminegative definite function for system (2):

$$\dot{L}_{(1)}(\mathbf{x}) = -\sum_{i=1}^{n} \left[\alpha_{i1} v_i^2 + \alpha_{i2} w_i^2 + \alpha_{i3} u_i^2 \right] \leq 0. \tag{19}$$

Therefore, $\dot{L}_{(1)}(\mathbf{x}) \leq 0$, $\forall \mathbf{x} \in \mathbb{D}(L(\mathbf{x}))$ and $\dot{L}_{(1)}(\mathbf{x}_e) = 0$. Moreover $L(\mathbf{x}) \in C^1(\mathbb{D}(L(\mathbf{x})))$; hence, for system (2), $L(\mathbf{x})$ is classified as its Lyapunov function and $\mathbf{x}_e$ is a stable equilibrium point.

Furthermore, with the design of the new controllers and the stability analysed for the robotic system, the effectiveness of the control scheme is verified using computer simulations. □

6. Simulation Results

The three situations given in this section capture realistic situations to illustrate the adequacy, effectiveness, and robustness of the velocity-based controllers and the control scheme. In the following scenarios, the data use international units in the sense that parameters are unitless whereas the times can be treated consistently. For instance, the units of time can follow the international units like seconds or minutes and the distance can be in centimeters or meters.

6.1. Scenario 1. In this scenario, we consider a simple setup where $\mathscr{P}_i$ navigates itself from its initial position to its predefined target in the presence of a fixed rectangular-plane obstacle. There are 3 point-mass mobile robots and a rectangular-plane obstacle. Each of the point-mass mobile robots avoids each other as well as the rectangular-plane obstacle while en route to its target. It is very interesting to observe the proximity of the point-mass mobile robots to the wall as it tries to evade it, exerting just enough energy to move above the wall and converge to its targets. The behavior exhibited by $\mathscr{P}_i$ is quite intriguing as it mimics a similar behavior that a swarm of birds exhibits while the swarm approaches a wall. Figure 7(a) shows the default 3D view and Figure 7(b) shows the top 3D view while Figure 7(c) shows the front 3D view of the motion of the point-mass mobile robots. The obstacle has transparency to allow us to view the position and path of $\mathscr{P}_i$. The blue sphere represents the motion of $\mathscr{P}_i$ at $t = 0$ unit of time, red sphere at $t = 700$ units of time, green sphere at $t = 3500$ units of time, and purple sphere at $t = 15000$ units of time. Table 1 provides all the values of the initial conditions, constraints, and different parameters utilised in the simulation.

6.2. Scenario 2. Here we model rectangular towers, which could represent tall buildings in cities. These towers, constructed with 15 planes, block the path of a swarm of 5 point-mass mobile robots. The agents are observed to start from their initial positions and maneuver themselves to their predefined targets, while ensuring avoidance of the towers as well as interindividual collision avoidance. Each $\mathscr{P}_i$ computes the shortest and a collision-free path to its destination. Split maneuvers are observed while the robots are en route along their paths. Such an example with multiple towers can be used to model the obstacle avoidance capability of UAVs. Figure 8(a) shows the default 3D view and Figure 8(b) shows the top 3D view, while Figure 8(c) shows the front 3D view of the motion of the point-mass mobile robots. The blue sphere represents the motion of $\mathscr{P}_i$ at $t = 0$ unit of time, red sphere at $t = 700$ units of time, green sphere at $t = 3120$ units of time, and purple sphere at $t = 8000$ units of time. Table 2 provides all the values of the initial conditions, constraints, and different parameters utilised in the simulation, if different from the previous scenario. For the construction of the towers, the reader is referred to the figures for the extraction of the coordinates.

6.3. Scenario 3. An interesting research domain involves tunnel passing maneuvers. In this scenario, there are 3 point-mass mobile robots and we design tunnels using rectangular planes. We use 8 rectangular planes to construct the tunnel. In addition, the top and one of the side views have been strategically made transparent to show the trajectory and the position of $\mathscr{P}_i$ as it maneuvers through the tunnel. The snapshots show the way the point-mass robots strategize their motion to allow which robot will pass through the tunnel first and how they will converge to their respective predefined targets. Drones could be deployed in areas that are deemed to be "dull, dirty, and dangerous" as well as "difficult" such as that of collapsed tunnel passages to capture, store, check, and send data for analysis. Figure 8(a) shows the default 3D view and Figure 8(b) shows the top 3D view while Figure 8(c) shows the front 3D view of the motion of the point-mass mobile robots. The blue sphere represents the motion of $\mathscr{P}_i$ at $t = 0$ unit of time, red sphere at $t = 550$

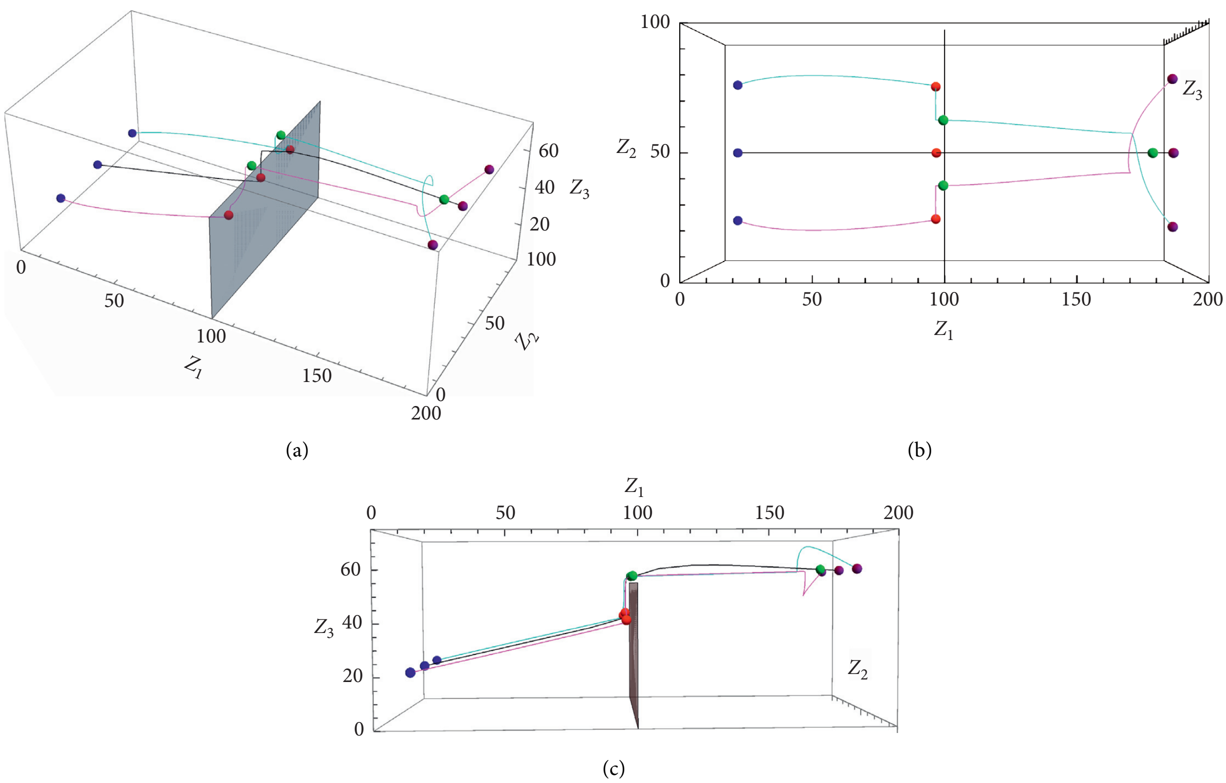

Figure 7: Scenario 1. The different viewpoints of $\mathscr{P}_i$ while it is in motion to its target with one rectangular-plane obstacle. (a) Default 3D motion view. (b) Top 3D motion view. (c) Front 3D motion view.

Table 1: Scenario 1. The parameters utilised in the numerical simulation. There are 3 point-mass mobile robots $(n = 3)$ and 1 rectangular-plane obstacle $(\overline{m} = t1)$.

Description	Value
Initial state of the point-mass mobile robots	
Workspace	$\eta_1 = 200, \eta_2 = 100, \eta_3 = 75$
Initial position, radius	$(x_1, y_1, z_1) = (10, 80, 20)$, $\mathrm{rp}_1 = 2$ $(x_2, y_2, z_2) = (10, 20, 20)$, $\mathrm{rp}_2 = 2$ $(x_3, y_3, z_3) = (20, 50, 20)$, $\mathrm{rp}_3 = 2$
Constraints	
Target centre, radius	$(\tau_{11}, \tau_{12}, \tau_{13}) = (190, 20, 60), r\tau_1 = 1$ $(\tau_{21}, \tau_{22}, \tau_{23}) = (190, 80, 60), r\tau_2 = 1$ $(\tau_{31}, \tau_{32}, \tau_{33}) = (190, 50, 60), r\tau_3 = 1$
Rectangular plane	$(a_{11}, b_{11}, c_{11}) = (100, 0, 0)$ $(a_{22}, b_{22}, c_{21}) = (100, 0, 55)$ $(a_{33}, b_{33}, c_{31}) = (100, 100, 0)$
Control and convergence parameters	
Avoidance of workspace	$\wp_{i\bar{s}} = 50$ for $i = 1, 2, 3$ and $\bar{s} = 1, \ldots, 6$
Avoidance of rectangular plane	$\varsigma_{i\ell} = 0.1$ for $i = 1, 2, 3i = 1, 2, 3$ and $\ell = 1$
Interindividual collision avoidance	$\beta_{ij} = 20$ for $i = j = 1, 2, 3$ and $j \neq i$
Convergence	$\alpha_{i1} = \alpha_{i2} = \alpha_{i3} = 0.001$ for $i = 1, 2, 3$

units of time, green sphere at $t = 2110$ units of time, and purple sphere at $t = 8000$ units of time. Table 3 provides all the values of the initial conditions, constraints, and different parameters utilised in the simulation, if different from the previous scenario. The evolution of the Lyapunov function and its time derivative together with its control inputs along the trajectories are depicted in Figure 9, respectively.

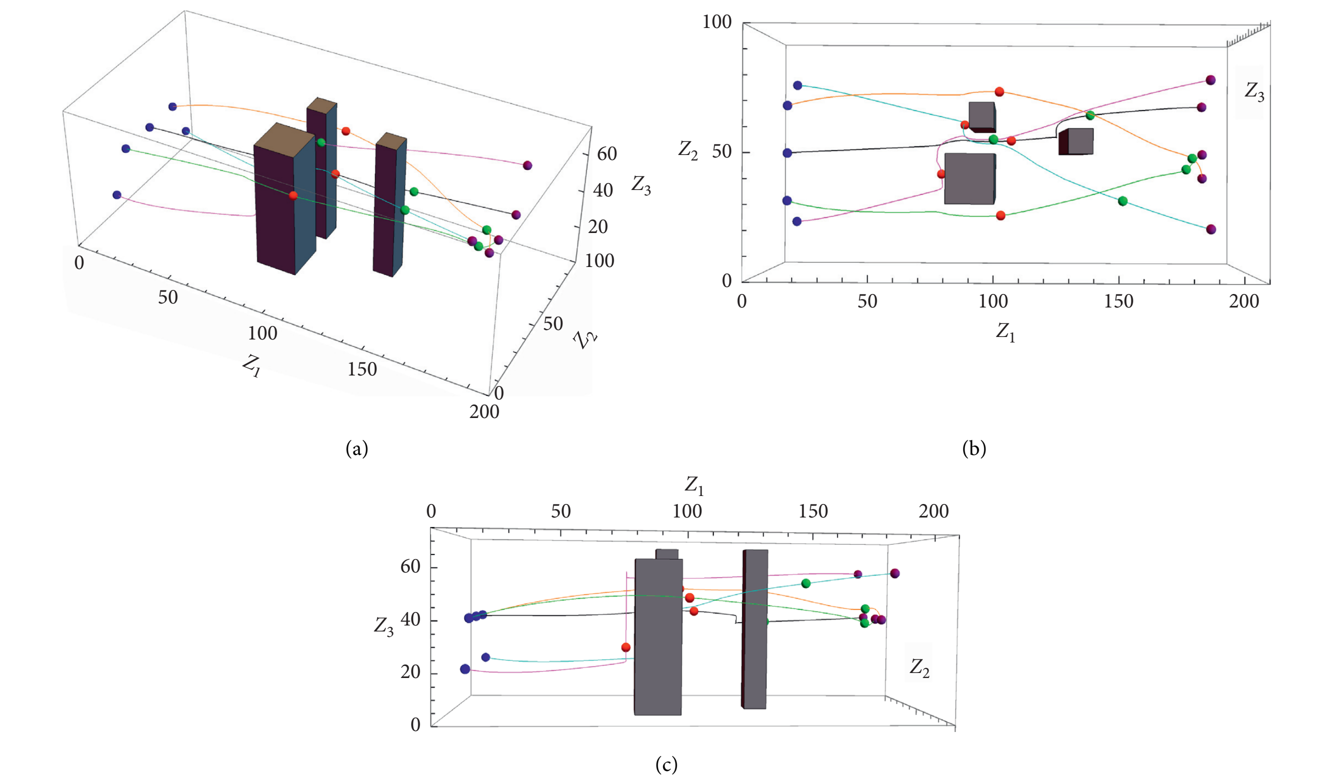

FIGURE 8: Scenario 2. The different viewpoints of $\mathscr{P}_i$ while it is in motion to its target with towers constructed from the rectangular planes. (a) Default 3D motion view. (b) Top 3D motion view. (c) Front 3D motion view.

TABLE 2: Scenario 2. The parameters utilised in the numerical simulation, with $n = 3$ and $\overline{m} = 15$.

Description	Value
Initial state of the point-mass mobile robots	
Initial position, radius	$(x_3, y_3, z_3) = (10, 50, 40)$, $\text{rp}_3 = 2$ $(x_4, y_4, z_4) = (10, 70, 40)$, $\text{rp}_3 = 2$ $((x_5, y_5, z_5) = (10, 30, 40)$, $\text{rp}_3 = 2$
Constraints	
Target centre, radius	$(\tau_{31}, \tau_{32}, \tau_{33}) = (190, 70, 40), r\tau_3 = 1$ $(\tau_{41}, \tau_{42}, \tau_{43}) = (190, 40, 40), r\tau_3 = 1$ $(\tau_{51}, \tau_{52}, \tau_{53}) = (190, 50, 40), r\tau_3 = 1$
Control and convergence parameters	
Avoidance of workspace	$\wp_{i\bar{s}} = 20$ for $i = 1, \ldots, 5 i = 1, \ldots, 5$ and $\bar{s} = 1, \ldots, 6$
Avoidance of rectangular plane	$\varsigma_{i\ell} = 0.5$, for $i = 1, \ldots, 5$ and $\ell = 1, \ldots, 15$
Interindividual collision avoidance	$\beta_{ij} = 5$ for $i = j = 1, \ldots, 5$ and $j \neq i$

TABLE 3: Scenario 3. The parameters utilised in the numerical simulation, with $n = 3$ and $\overline{m} = 8$.

Description	Value
Initial state of the point-mass mobile robots	
Initial position, radius	$(x_1, y_1, z_1) = (10, 70, 65)$, $\text{rp}_1 = 2$ $(x_2, y_2, z_2) = (10, 10, 10)$, $\text{rp}_2 = 2$ $(x_3, y_3, z_3) = (10, 50, 40)$, $\text{rp}_3 = 2$
Constraints	
Target centre, radius	$(\tau_{11}, \tau_{12}, \tau_{13}) = (150, 30, 20), r\tau_1 = 1$ $(\tau_{21}, \tau_{22}, \tau_{23}) = (160, 80, 60), r\tau_2 = 1$ $(\tau_{31}, \tau_{32}, \tau_{33}) = (180, 50, 40), r\tau_3 = 1$
Control and convergence parameters	
Avoidance of workspace	$\wp_{i\bar{s}} = 10$ for $i = 1, 2, 3 i = 1, 2, 3$ and $\bar{s} = 1, \ldots, 6$
Avoidance of rectangular plane	$\varsigma_{i\ell} = 5$ for $i = 1, 2, 3 i = 1, 2, 3$ and $\ell = 1, \ldots, 8$

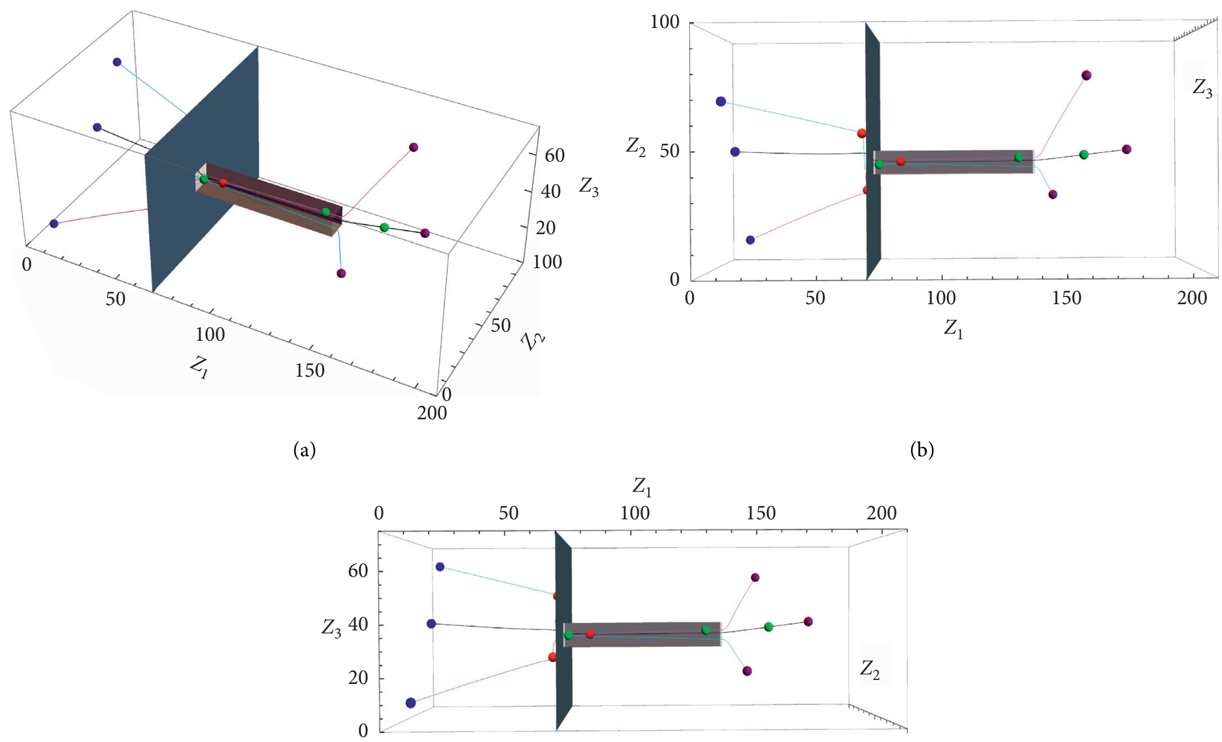

(a) (b) (c)

FIGURE 9: Scenario 3. The evolutionary behavior of the Lyapunov function, its time derivative, and its control inputs along the trajectories of Figure 10. (a) Lyapunov function. (b) Lyapunov function time derivative. (c) Controllers.

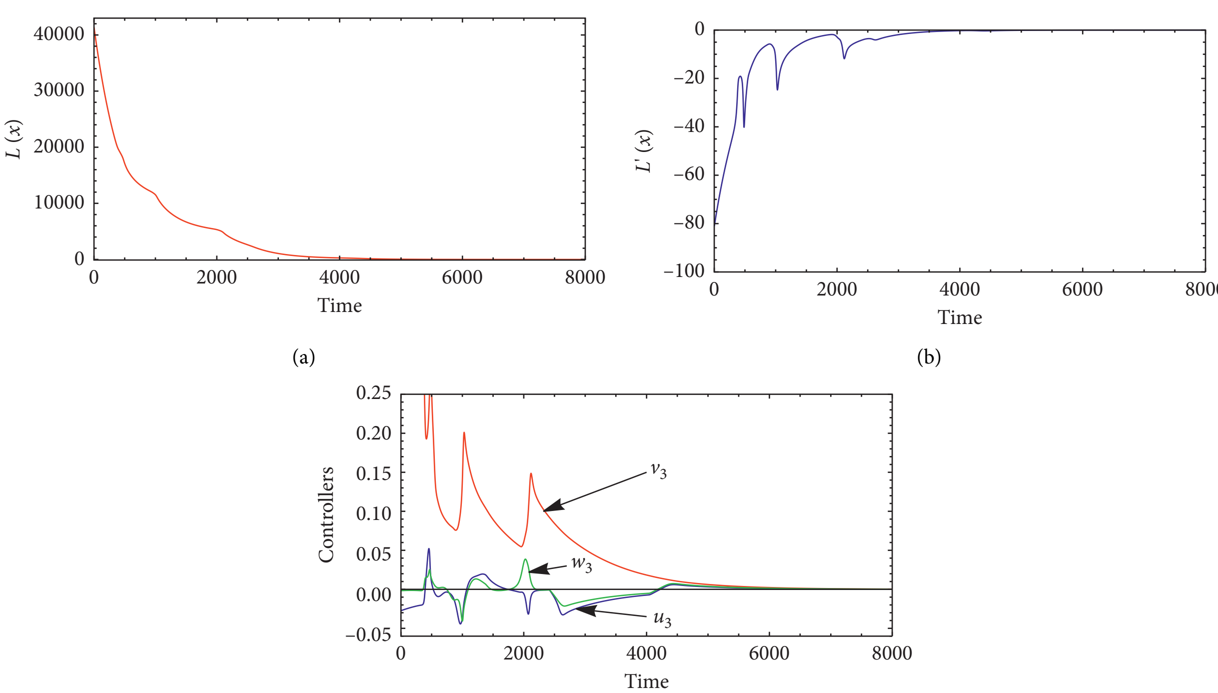

(a) (b) (c)

FIGURE 10: Scenario 3. The different viewpoints of $\mathscr{P}_i$ while it is in motion to its target with tunnel passing maneuvers. (a) Default 3D motion view. (b) Top 3D motion view. (c) Front 3D motion view.

Interestingly, the behavior exhibited in this scenario can be seen in nature, namely, the leader-follower strategy, where the leader guides the followers to food sources, safety, and so on. We note that the leader-follower strategy, cooperative hunting, and avoidance in the military are drone-based applications considered common nowadays.

7. Conclusions and Future Work

Mathematical modelling and the design of motion planners for robotic systems are a complex, computationally expensive yet a fascinating research area. In this paper, the LbCS was applied to derive a set of robust, unique continuous time-invariant velocity-based control inputs that effectively handle the problem of MPC of point-mass mobile robots in a dynamic environment that, for the absolute first time, incorporates rectangular-plane obstacles. The convergence of the mobile robots to a neighborhood of a predefined target is ensured by the Lyapunov direct method. The effectiveness and robustness of the control scheme were illustrated via computer simulation of virtual scenarios that depicts real-life situations.

To the authors' knowledge, this is the first time in literature whereby the MDT was used to derive the mathematical functions for the successful avoidance of rectangular-plane-shaped obstacles. The introduction of the rectangular-plane obstacle into the MPC problem has created new dimensions and potentials for research. The advantages of the MDT are numerous such as making it possible for plane-shaped (and other irregular) obstacles to be treated within the motion planners, help in simplifying collision-avoidance algorithms, and permit maximum free-space for the robots traversing the workspace.

This work paves the way for numerous future directions. Our principal objective is to extend the rectangular-plane obstacles in a workspace for the MPC of a flock of quadrotors performing hovering maneuvers and undergoing split-and-rejoin maneuvers when encountered with towers and tunnels.

Data Availability

The research data for this article are purely simulation-based. These would be available upon request.

Conflicts of Interest

The authors declare that there are no conflicts of interest regarding the publication of this paper.

References

[1] K. Molloy, D. Laurent, M. Vaisset, T. Siméon, and Juan Cortés, "Simultaneous system design and path planning: a sampling-based algorithm," *The International Journal of Robotics Research*, vol. 38, no. 2-3, pp. 375–387, 2019.

[2] A. Gasparetto, P. Boscariol, A. Lanzutti, and R. Vidoni, *Path Planning and Trajectory Planning Algorithms: A General Overview*, Springer International Publishing, Berlin, Germany, 2015.

[3] N. Lashkari, M. Biglarbegian, S. X. Yang, and Yang, "Development of novel motion planning and controls for a series of physically connected robots in dynamic environments," *Journal of Intelligent & Robotic Systems*, vol. 95, no. 2, pp. 291–310, 2019.

[4] B. N. Sharma, J. Raj, and J. Vanualailai, "Navigation of carlike robots in an extended dynamic environment with swarm avoidance," *International Journal of Robust and Nonlinear Control*, vol. 28, no. 2, pp. 678–698, 2018.

[5] M. Liu, H. Ma, J. Li, and S. Koenig, "Task and path planning for multi-agent pickup and delivery," in *Proceedings of the 18th International Conference on Autonomous Agents and MultiAgent Systems, AAMAS '19*, Richland, SC, USA, May 2019.

[6] D. Ali and V. Sezer, "Motion planning and control with randomized payloads using deep reinforcement learning," in *Proceedings of the 2019 Third IEEE International Conference on Robotic Computing (IRC)*, Naples, Italy, February 2019.

[7] J. Raj, K. Raghuwaiya, and J. Vanualailai, "Novel lyapunov-based autonomous controllers for quadrotors," *IEEE Access*, vol. 8, no. 1, pp. 47393–47406, 2020.

[8] F. Ho, A. Salta, R. Geraldes, A. Goncalves, M. Cavazza, and H. Prendinger, "Multi-agent path finding for uav traffic management," in *Proceedings of the 18th International Conference on Autonomous Agents and MultiAgent Systems, AAMAS '19*, Richland, SC, USA, May 2019.

[9] J. T. Ebert, M. Gauci, and R. Nagpal, "Multi-feature collective decision making in robot swarms," in *Proceedings Of the 17th International Conference On Autonomous Agents and MultiAgent Systems, AAMAS '18*, Richland, SC, USA, May 2018.

[10] B. Sharma, J. Vanualailai, and S. Singh, "Motion planning and posture control of multiple n-link doubly nonholonomic manipulators," *Robotica*, vol. 35, no. 1, pp. 1–25, 2017.

[11] D. A. L. Burbano, P. Delellis, and M. dibernardo, "Self-tuning proportional integral control for consensus in heterogeneous multi-agent systems," *European Journal of Applied Mathematics*, vol. 27, no. 6, pp. 923–940, 2016.

[12] J. Raj, R. Krishna, S. Singh, B. Sharma, and J. Vanualailai, N. Che, "Swarming intelligence of 1-trailer systems," *Hamzah Asyrani Sulaiman, Mohd Azlishah Othman, Mohd Fairuz Iskandar Othman, Yahaya Abd Rahim, and*, pp. 251–264, Springer International Publishing, Berlin, Germany, 2016.

[13] R. Krishna, B. Sharma, and J. Vanualailai, "Leader-follower based locally rigid formation control," *Journal of Advanced Transportation*, vol. 2018, Article ID 5278565, 14 pages, 2018.

[14] J. Raj, R. Krishna, J. Vanualailai, and B. Sharma, "Navigation of car-like robots in three-dimensional space," in *Proceedings of the 2018 5th Asia-Pacific World Congress on Computer Science and Engineering (APWC on CSE)*, Nadi, Fiji, December 2018.

[15] T. S. A. Ebtehal, "A complete multi-robot path-planning algorithm: jaamas track," in *Proceedings of the 18th International Conference on Autonomous Agents and MultiAgent Systems, AAMAS '19*, Richland, SC, USA, May 2019.

[16] B. Sharma, J. Vanualailai, and A. Prasad, "A dϕ-strategy: facilitating dual-formation control of a virtually connected team dϕ- strategy: facilitating dual-formation control of a virtually connected team," *Journal of Advanced Transportation*, vol. 2017, Article ID 9213805, 17 pages, 2017.

[17] R. Krishna and S. Singh, "Formation types of multiple steerable 1-trailer mobile robots via split/rejoin maneuvers," *New Zealand Journal of Mathematics*, vol. 43, no. 7–21, 2013.

[18] J. Vanualailai, "Stable emergent formations for a swarm of autonomous car-like vehicles," *International Journal of Advanced Robotic Systems*, vol. 16, no. 5, pp. 1–17, 2019.

[19] D. Albani, T. Manoni, D. Nardi, and V. Trianni, "Dynamic uav swarm deployment for non-uniform coverage," in *Proceedings of the 17th International Conference on Autonomous Agents and MultiAgent Systems, AAMAS '18*, Richland, SC, USA, May 2018.

[20] E. Hartuv, N. Agmon, and S. Kraus, "Scheduling spare drones for persistent task performance under energy constraints," in *Proceedings Of the 17th International Conference On Autonomous Agents and MultiAgent Systems, AAMAS '18*, Richland, SC, USA, May 2018.

[21] B. Sharma, J. Vanualailai, and S. Singh, "Tunnel passing maneuvers of prescribed formations," *International Journal of Robust and Nonlinear Control*, vol. 24, no. 5, pp. 876–901, 2014.

[22] M. d. S. Arantes, C. F. M. Toledo, B. C. Williams, and M. Ono, "Collision-free encoding for chance-constrained nonconvex path planning," *IEEE Transactions on Robotics*, vol. 35, no. 2, pp. 433–448, 2019.

[23] K. Ariu, F. Cheng, M. . da Silva Arantes, C. Toledo, and B. C. Williams, "Chance-constrained path planning with continuous time safety guarantees," in *Proceedings of the Workshops at the Thirty-First AAAI Conference on Artificial Intelligence*, Palo Alto, CA, USA, February 2017.

Hindawi
Journal of Advanced Transportation
Volume 2020, Article ID 8894812, 16 pages
https://doi.org/10.1155/2020/8894812

Research Article

Research on Urban Traffic Signal Control Systems Based on Cyber Physical Systems

Li-li Zhang[1,2] **Qi Zhao,**[2] **Li Wang,**[2] **and Ling-yu Zhang**[2]

[1]*College of Information Engineering, Beijing Institute of Petrochemical Technology, Beijing 102617, China*
[2]*Beijing Key Lab of Urban Intelligent Control Technology, North China University of Technology, Beijing 100144, China*

Correspondence should be addressed to Li-li Zhang; zllphd2012@163.com

Received 26 June 2020; Revised 24 September 2020; Accepted 6 October 2020; Published 23 October 2020

Academic Editor: Sang-Bing Tsai

Copyright © 2020 Li-li Zhang et al. This is an open access article distributed under the Creative Commons Attribution License, which permits unrestricted use, distribution, and reproduction in any medium, provided the original work is properly cited.

In this paper, we present a traffic cyber physical system for urban road traffic signal control, which is referred to as UTSC-CPS. With this proposed system, managers and researchers can realize the construction and simulation of various types of traffic scenarios, the rapid development, and optimization of new control strategies and can apply effective control strategies to actual traffic management. The advantages of this new system include the following. Firstly, the fusion architecture of private cloud computing and edge computing is proposed for the first time, which effectively improves the performance of software and hardware of the urban road traffic signal control system and realizes information security perception and protection in cloud and equipment, respectively, within the fusion framework; secondly, using the concept of parallel system, the depth of real-time traffic control subsystem and real-time simulation subsystem is realized. Thirdly, the idea of virtual scene basic engine and strategy agent engine is put forward in the system design, which separates data from control strategy by designing a general control strategy API and helps researchers focus on control algorithm itself without paying attention to detection data and basic data. Finally, considering China, the system designs a general control strategy API to separate data from control strategy. Most of the popular communication protocols between signal controllers and detectors are private protocols. The standard protocol conversion middleware is skillfully designed, which decouples the field equipment from the system software and achieves the universality and reliability of the control strategy. To further demonstrate the advantages of the new system, we have carried out a one-year practical test in Weifang City, Shandong Province, China. The system has been proved in terms of stability, security, scalability, practicability and rapid practice, and verification of the new control strategy. At the same time, it proves the superiority of the simulation subsystem in the performance and simulation scale by comparing the different-scale road networks of Shunyi District in Beijing and Weifang City in Shandong Province. Further tests were conducted using real intersections, and the results were equally valid.

1. Introduction

Advances in technologies such as optimization algorithm [1–3], vehicle-based collaboration, hybrid driving, autonomous driving, and artificial intelligence enable researchers to develop more innovative signal control strategies and build more traffic scenarios to accommodate changes in transportation demand. At the same time, many innovative signal control strategies s not only break through the traditional signal control theory, but also propose a lot of new control logic architecture, which requires it to be tested in the field, and often involves modifying the field equipment. This project requires the close cooperation of traffic managers, control strategy researchers, information technology professionals, and implementers. It is not only time-consuming and labor-intensive, but also has certain traffic safety risks. Therefore, few traffic control systems have advanced control strategies in the past, and these control strategies have been verified in practice, such as SCOOT [4], SCATS [5], etc., and test new in such mature systems. Control strategies are also very difficult. In order to solve this problem, we propose a new urban traffic signal control and control architecture based on information physics system theory and parallel system theory and carry out thorough tests to bridge the gap between research and practice of traffic signal control strategies (hereinafter referred to as UTSC-CPS). China's traffic signal control field has experienced 20 years of development. Although advances have been made in the function and performance of signal control equipment, there are still major problems in the standardization of communication protocols. Different brands of traffic signal controllers and control systems are not compatible, and the traffic control language in the industry is not uniform. Not to mention the combination of VISSM [6], PARAMICS [7], and other traffic simulation software with the signal controller to achieve the control strategy [8], although there have been some attempts, the results are minimal. In sharp contrast, in North America, traffic signal controllers have adopted the NTCIP [9] protocol in a unified manner, and simulation software providers such as PTV have also embedded the most fully functional traffic signal simulator into their latest version, which not only simulates the function of the hardware traffic signal controller but also provides a comprehensive communication module conforming to the NTCIP standard [10]. Nonetheless, traditional simulation software is still very complex and difficult in parameter calibration and control strategy development. Taking into account the above issues, UTSC-CPS mainly provides a real-time simulation system, which can automatically calibrate parameters based on detection data and GIS data, can simulate macroscopic and microscopic traffic flow characteristics, and provides control strategy APIs and programming templates. The interaction between the real-time control system and the real-time simulation system facilitates the rapid test, iteration, and practice of the control strategy and provides a protocol conversion platform, which can access various types of signal controllers through the solution system and traffic control equipment, and computing and edge computing platforms to improve computing power and information security. Therefore, the UTSC-CPS system is expected to promote the research and deployment of innovative signal control strategies in future urban traffic.

The rest of this paper is organized as follows: first, the literature on the development of traditional traffic signal control system and the application of CPS in traffic management are reviewed. Then, the UTSC-CPS architecture and related technologies are elaborated. Thirdly, an intersection overflow control strategy is proposed to demonstrate the application of UTSC-CPS system. In the end, two case studies are used to verify the intersection overflow control strategy and the real-time simulation system.

2. Literature Review

In this section, we divide the development of urban road traffic signal control in China into four stages, namely, traffic control 1.0 (mechanization), traffic control 2.0 (electrification), traffic control 3.0 (information), and traffic control 4.0 (intellectualization), as shown in Figure 1 (the object, target, method, actuator, and detection of traffic control are listed in four stages and the development of evaluation). Among them, traffic control 1.0 is called the era of mechanization. The first manual traffic light switch in Shanghai is the initial stage of traffic control in China [11]. Traffic control 2.0 and traffic control 3.0 are the longest and most important stages in China. The entry of SCOOT [4] and SCATS [5] systems into China in the 1980s marked the process of information of urban traffic control in China and also promoted the investment of Chinese researchers in the research and development of traffic signal control systems. After 2000, especially in recent years, the demand for urban traffic trips in China has doubled, and the mixed traffic flow characteristics with Chinese regional characteristics have emerged. Diversity of traffic demand, complexity of traffic flow, unbalance of urban development, and uncertainty of controlled objects all put forward new requirements for the theory, control strategy, and control means of urban traffic control. Especially, in today's rapid development of technologies such as big data, cloud computing, edge computing, artificial intelligence, Internet of Things, and vehicle networking, urban traffic control in China is advancing. In the era of intelligent traffic control 4.0, it emphasizes the integration of information, calculation, and control under the background of future urban traffic control. In the era of traffic control 4.0, the most obvious changes should be controlled objects, control objectives, and actuators. Among them, the controlled objects change from traffic flow to human, vehicle, and road coordination, the control objectives change from traffic safety and traffic efficiency to the feelings of traffic participants, and the actuators change from signal controller to signal controller, traffic signs, and intelligent vehicles. All these indicate that the subject of urban traffic control has changed from vehicle to human. This is the "people-oriented" concept that China has always emphasized.

2.1. CPS and Transportation System. The requirements of traffic control 4.0 for information, calculation, and control coincide with the characteristics of Information Physics System (CPS). The concept of CPS first appeared in the United States Natural Fund in 2005 [12], then quickly received the response of the Chinese and American governments and researchers, and has carried out fruitful early work in biological, military, industrial, and other fields [13–17]. The complex characteristics of urban traffic and the difficulties it faces make it the best test site and application area of CPS [18–22]. CPS plays a more and more important role in the supervision and security control function of transportation system, which will contribute to the actual control decision-making in transportation system [23]. T-CPS mainly includes the interaction between control software, communication network, and physical devices in its structure, in which network mainly refers to the integration and integration of traffic information [24–26]. T-CPS is new in expanding application. The improvement of the first-generation transportation system provides the possibility, mainly in terms of reliability, effectiveness, and transparency. Trusted computing, time predictability, and system robustness will be the focus of the design [27–31]. Considering the compatibility of traffic control 4.0 and CPS, we designed UTSC-CPS system based on CPS architecture

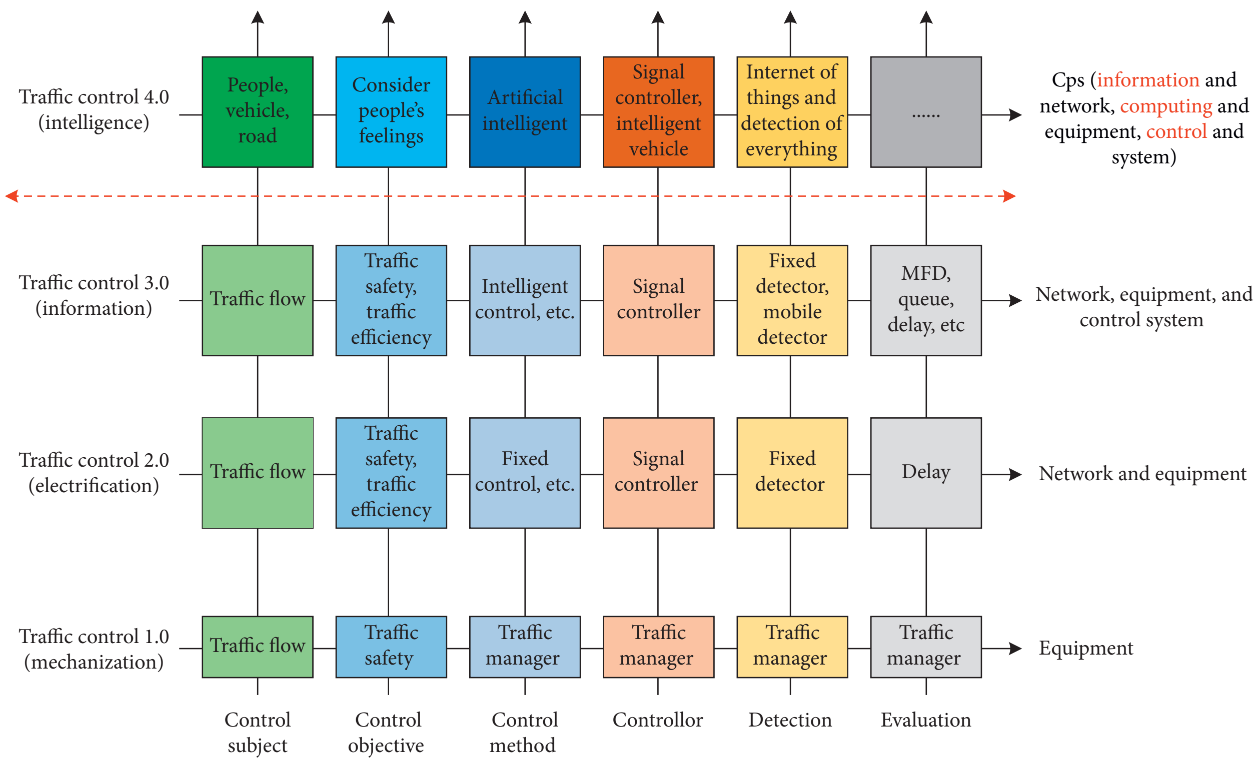

Figure 1: Development form of traffic control.

and fully considered the existing problems in the field of traffic signal control in China and the characteristics of future network-connected traffic. We focused on the design of protocol conversion, information security, artificial intelligence, real-time simulation, and other functions.

2.2. ACP and PTMS. While CPS is applied in the field of urban transportation, Professor Wang proposed CPSS [32, 33], which has a dimension expansion, based on CPS and the research results of complex systems and intelligent science, taking into account the complex characteristics of urban transportation system. Among them, Intelligent Transportation System (ITS) based on ACP [34] has put forward new concepts in traffic control modeling, experimental problems, optimization problems, and so on. It has also pushed the traditional traffic control and simulation technology to a better level and a broader perspective. This kind of research has aroused the interest of scholars all over the world. ACP [35] method can be described in the following three steps: first, considering engineering, social, human, and environmental factors as a whole, synthesizing theoretical model, empirical model, and data model, establishing an equivalent artificial system for the actual system to solve the model problem of complex system (A); through the calculation experiment of artificial system under normal and abnormal conditions, the actual system is studied. The law of interaction and evolution of elements in system (C); thirdly, connect the artificial system with the actual system, and realize parallel execution by comparing and analyzing the behavior of the two systems. System-type, reference, and forecast the future situation, and adjust the control and management methods of the two systems accordingly (P). Based on the ACP method, Professor Wang put forward the concept of parallel transportation management and control system to solve the optimization and evaluation of transportation system. By connecting the actual transportation system with the artificial transportation system, the artificial transportation experiment can be carried out, and the optimization and evaluation can be carried out conveniently. Based on ACP method, a parallel traffic management and control system PTMS [36, 37] is proposed. In this paper, we refer to the concept of ACP and PTMS when we design the interaction between real-time control system and real-time simulation system and visualization software and hardware in the loop system.

3. Significance of the Research

The innovative design of UTSC-CPS is reflected in the development, testing, simulation, and practical application of new control strategies. First, the new control strategy can be quickly implemented through the system's control strategy API, because the variables of the input and output data have been defined, and some of the control logic is also encapsulated into a function, and a programming template is provided, whether it is a researcher or a traffic manager who can quickly implement their own control strategies. Secondly, considering that traditional simulation software such as VISSIM [6] and PARAMICS [7] need a lot of manual work to complete complex parameter calibration, which is time-consuming, laborious, and error-prone, the real-time simulation system in UTSC-CPS provides automatic calibration function of simulation parameters based on detector data and GIS data, which can effectively solve the previous problems. Thirdly, the new control strategy can be implemented through real-time simulation. The system can be quickly optimized and upgraded. When the evaluation index meets the field application conditions, it can be quickly input into the real-time control system, without the need for professional programmers and implementation of manual implementation to the field. Fourthly, it also simulates various types of traffic scenarios, such as road congestion, green wave control, emergency management, and so on, using visual hardware and software in-the-loop system and simulation system, which enables researchers and managers to quickly analyze and design schemes. More importantly, these data are from the field detectors.

UTSC-CPS has also done a lot of work in system expansion, information security, universality, and so on. Firstly, it uses cloud computing platform to provide powerful computing and storage capabilities for control strategy and simulation. At the same time, considering that the method based on artificial intelligence will become the basis of signal control, it also provides GPU cluster computing resources for this purpose. Secondly, it does not pay attention to information security content in the traditional signal control field, when in the future vehicle network and automatic driving. When it is widely used, information security will be the key problem. Therefore, two layers of information security perception and protection are innovatively designed in the architecture of UTSC-CPS, which can effectively block network attacks targeting at signal controllers or as springboards. Thirdly, most of the communication protocols of signal controllers in China are private. Although a lot of work has been done in relevant parts of China, this phenomenon is still very common. This system has considered this problem at the beginning of the architecture and designed a protocol conversion middleware, which innovatively decouples the field equipment from the control system, so that users will not need to pay attention to the field equipment. Specific details are also provided to illustrate that the middleware has integrated NTCIP, which can be quickly applied to China and the United States and other areas of signal control.

4. UTSC-CPS Traffic Signal Control Framework

Considering the requirements of control, information, and computing in CPS architecture, four supporting platforms are constructed when designing and developing UTSC-CPS system. They consist of control and simulation platform, private cloud computing platform, intelligent gateway, and edge computing platform, as shown in Figure 2. (A) In the design of control and simulation platform, the idea of parallel system theory and the needs of some urban traffic managers in China are used for reference. The real-time control system and the real-time simulation system are effectively connected through the visual hardware-in-the-loop system. Therefore, the real-time simulation system provides the rapid realization, verification, and optimization of new control strategies and traffic management concepts. The real-time control system provides the field execution of the verified control strategies. Visual hardware-in-the-loop system as a bridge and display way provides a macro perspective for managers and researchers to understand urban traffic. (B) Private cloud computing platform provides flexible storage, computing, and information security capabilities through virtualization technology. In particular, the UTSC-CPS system also designs GPU resources, which can provide computational support for the application of artificial intelligence technology. (C) We are particularly proud of the design of UTSC-CPS intelligent gateway, which fully takes into account the existing problems in the field of urban road traffic control devices in China. It is also based on the research results of various types of traffic signal controllers in Beijing, China, from 2008 to 2013. Through the intelligent gateway, the system and traffic control equipment are decoupled, and letters of different protocols and control concepts are made. No. 1 controller can be connected to UTSC-CPS. (D) Edge computing platform is designed as a key node to support future urban road traffic. It mainly provides information security and on-site computing capabilities. It needs to be explained that future urban intersections will be the key nodes for data aggregation of various traffic scenarios, such as automatic driving, vehicle networking, public transport, mobile travel, etc. Therefore, information security and computing capabilities on the edge side are provided. It is always important.

4.1. Architecture and Function of UTSC-CPS

4.1.1. Real-Time Traffic Control System. In different regions of China, there are traffic demand mainly for motor vehicles and mixed traffic demand for nonmotor vehicles and motor vehicles, which are different from the regional characteristics of traffic travel in the United States and European countries. For this reason, the real-time control system in UTSC-CPS also takes full account of this special feature and provides a variety of controlled objects and control objectives. According to the traffic demand that may arise from this feature, a variety of control strategies including regional coordinated control, trunk green wave control, single-point adaptive control, antioverflow control, multiperiod timing control, and special light color control are designed. In particular, it should be pointed out that the above control strategies support a variety of detection data types, including geomagnetic detectors, wide-area radar detectors, video detectors, and floating car detectors. Considering the importance of evaluation, an evaluation index set, such as imbalance index and saturation index, is designed to provide more intuitive and reasonable feedback for the evaluation of control strategies. Most importantly, the system provides verification and protection mechanism of VPN online upgrade and backup and signal control timing scheme data. The design inspiration of online upgrade comes from the design of smartphone online upgrade and the problems and experiences of some urban traffic

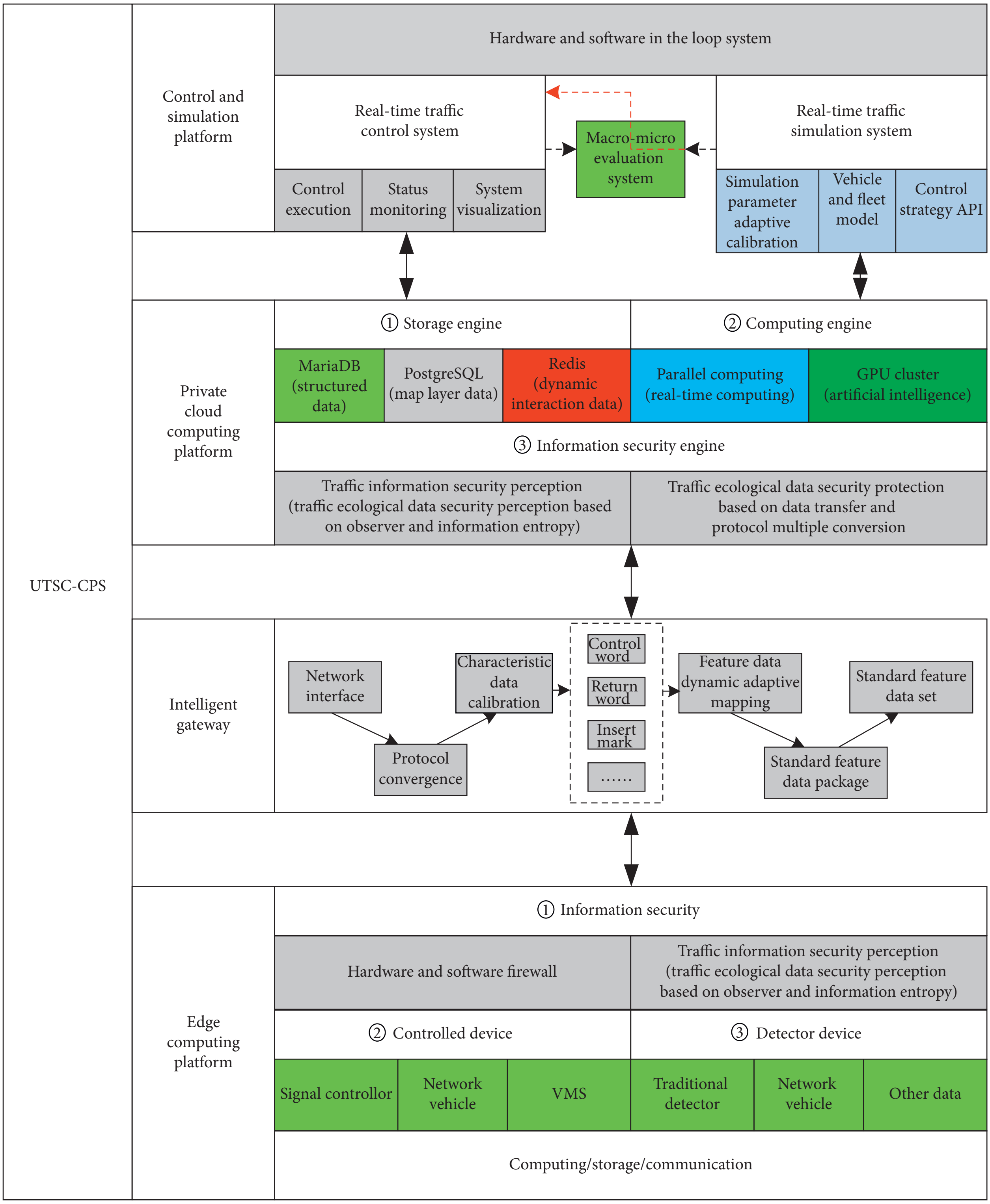

FIGURE 2: System architecture of the "UTSC-CPS" urban road traffic signal control platform.

management departments in China in the past system upgrade and the design of verification and protection mechanism of signal control timing scheme data. It can effectively prevent traffic safety problems caused by staff negligence and unprofessional timing schemes, as shown in Figures 3(a) and 3(b).

4.1.2. Real-Time Traffic Simulation System. Real-time simulation system aims at fast analysis and validation of new signal control strategies, so it is different from microsimulation software VISSIM [6], PARAMICS [7], and macroplanning simulation software TRANSCAD [38]. It mainly simulates traffic flow under the influence of control

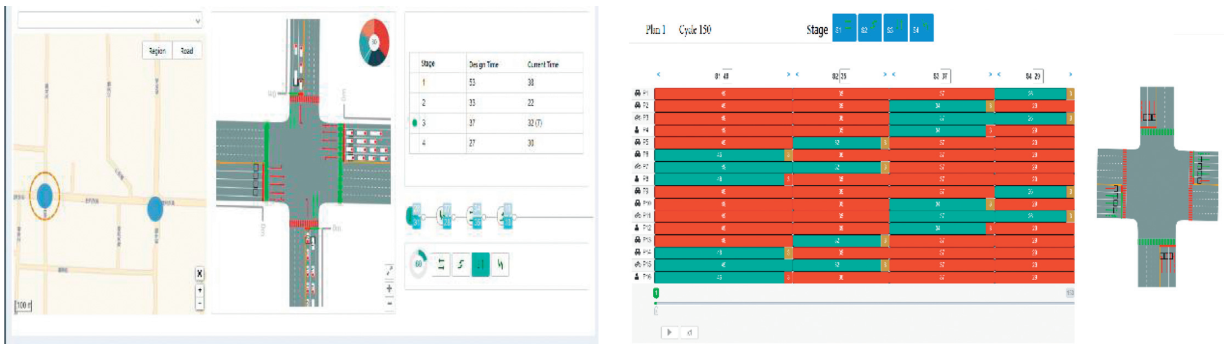

(a) (b)

Figure 3: System architecture of the "UTSC-CPS" urban road traffic signal control platform. (a) Traffic signal control. (b) Traffic signal control plan.

strategies, so as to promote the iterative optimization of control strategies. In order to realize visualization of traffic flow, calibration of dynamic parameters of traffic flow, and calibration of basic parameters of road network in simulation, the design of simulation driver engine refers to SUMO [39] simulation software, as shown in Figures 4(a) and 4(b).

(1) Autocalibration of Simulation Parameters. It should be emphasized that the dynamic characteristics of a single vehicle and the calibration of simulation parameters based on manual work are neglected actively in the design of the simulation system. The system uses detector data and GIS data to automatically calibrate static data (road properties: road length, lane width, intersection shape, etc.) and dynamic data (vehicle type ratio, velocity distribution, steering ratio, headway time, and so on). At the same time, traffic flow characteristics and car-following characteristics are based on the accumulation of historical detection data, and real-time detection data are corrected.

(2) Control Strategy Architecture and API Design. Real-time simulation system provides good support for the development of new control strategies through the architecture shown in Figure 5. This architecture consists of three parts: data preparation, control strategy, and equipment engine. (A) The data preparation part encapsulates the test data as standard input and output variables and stores the signal control, vehicle, and variable sign as control variables in the database. (B) In the control strategy part, traffic demand is first constructed into different virtual scenes. Control strategies are designed for different scenarios. The set of control strategies is called agent, and control strategies are called agent. That is to say, the new control strategy designed by researchers is defined as agent, and the corresponding agent is run through given conditions in the simulation system. (C) The device engine part realizes the interaction between the real-time simulation system and the real-time control system. When the new control strategy is proved to be reliable, it can be pushed directly into the real-time control system through the engine and executed in the real environment at the right time. We call the implementation of this control strategy architecture Scene Driven, Software Definitions (SD), have encapsulated a wealth of functions in the software, and designed a standard programming template, so that managers and researchers without programming technology can quickly implement their own control strategies and be verified, as shown in Figure 6.

4.1.3. Visual Hardware and Software in the Loop System. In ancient and modern wars of China, military experts were good at carrying out war deduction through sand table and carrying out corresponding strategies and tactics. Referring to this form and idea of combat, we design a visual hardware-software in-the-loop system for urban road traffic control as shown in Figure 7, in which the real-time control system and the real-time simulation system are its foundation. The system can simulate traffic control and road state. The data used in the system can be real-time data on the spot, making it a mapping of real traffic. At the same time, it can also use real-time simulation system data to make it a presentation of simulated traffic. Urban traffic managers can discover and screen traffic control effects from a macro perspective and can also construct different traffic scenarios to test new control strategies, as shown in Figure 8(a). It should also be noted that the cellular automata model is also designed in the architecture of the system, which can provide researchers with simulation based on cellular automata, as shown in Figure 8(b).

4.1.4. Cloud Computing and Edge Computing Platform

Computing Power Output. The complexity of urban traffic is reflected in the variability of traffic demand, the dynamic nonlinearity of traffic flow, and the randomness of traffic participants. Considering the large-scale and scalable computing power required by control strategies and other core algorithms, we design a cloud computing platform based on virtualization, which can provide the required storages

At the same time, considering that edge devices and controlled individuals will be integrated into the system in

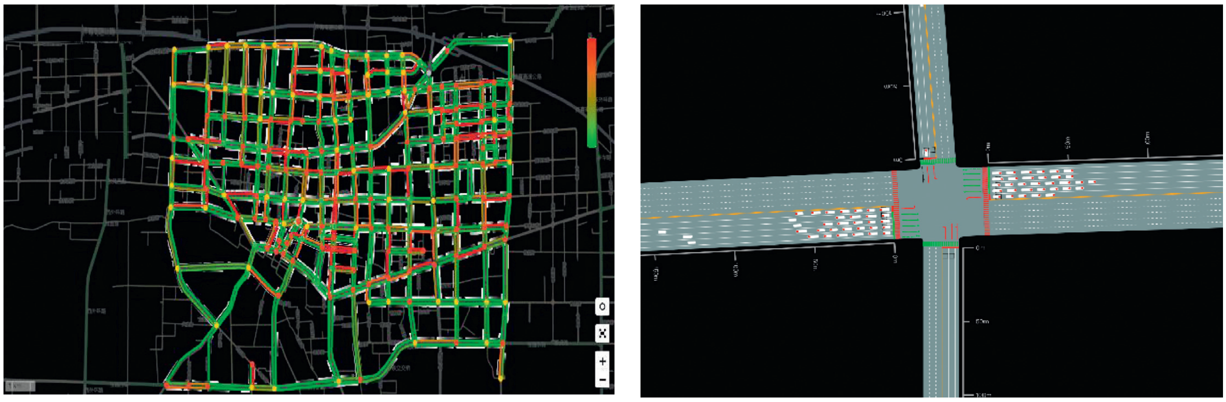

(a) (b)

Figure 4: Real-time simulation functional structure design. (a) Simulation of road network. (b) Simulation of intersection.

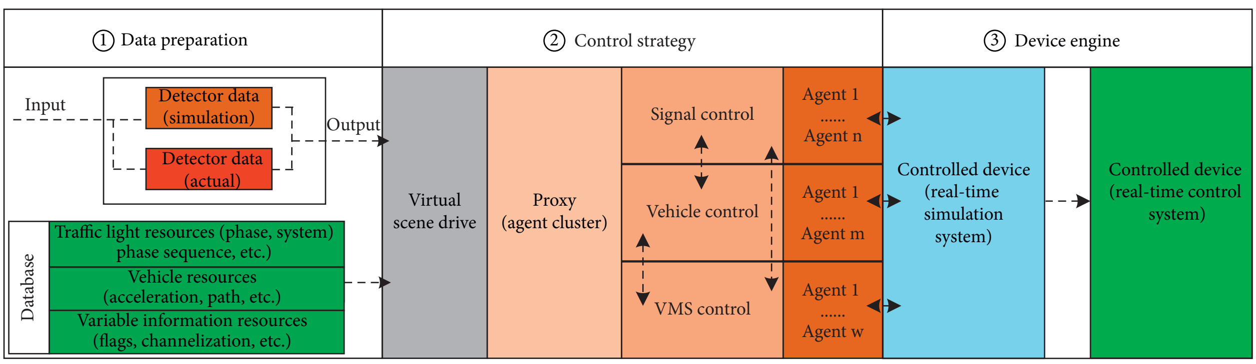

Figure 5: Control strategy API architecture of real-time simulation system.

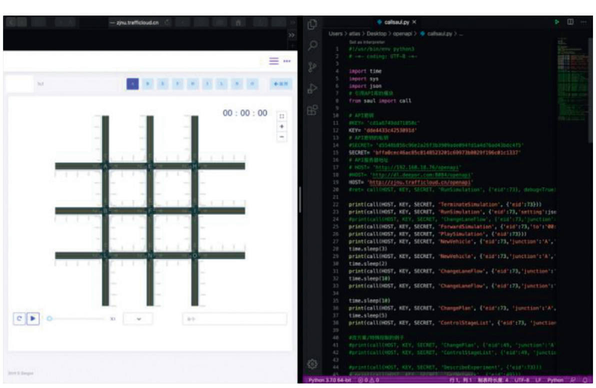

Figure 6: Control strategy software diagram.

the future, and the key technology of centralized large data processing based on cloud computing model cannot satisfy the efficient processing of data generated by edge devices, four key issues are focused on the following: (A) linear growth of centralized cloud computing capability cannot match explosive growth of massive edge data; (B) slave network as network edge devices transmit massive data to the cloud center, resulting in a sharp increase in the load of network transmission bandwidth, resulting in long network delay; (C) network edge data involve personal privacy, making privacy security issues become particularly prominent; and (D) network edge devices with limited power transfer data to the cloud center consume larger power. In order to solve the above four key problems, edge computing platform and cloud computing platform are designed.

It is noteworthy that AI technology has been applied in urban traffic field, such as traffic flow forecasting, image processing, automatic driving, etc. AI technology for urban traffic control and management is also being studied. Therefore, when we design UTSC-CPS architecture, we also fully consider the support of AI and can provide GPU cluster computing power output and edge meter for it. Computing power can be output for system applications.

What is urban traffic control? In 2010, Iran's nuclear facilities were attacked by Stuxnet [34], which proved to be the first virus specifically targeting the real world infrastructure. Since then, this kind of attack has been well known from the background to the front and has also brought new challenges to information security. Vehicles are controlled by hackers in "The Fate of the Furious" [31]. The scene of hitting targets from all directions has also become a highlight of the film, but it also arouses our concern. Intelligent Traffic Signal Control (ITC), as an important node equipment for

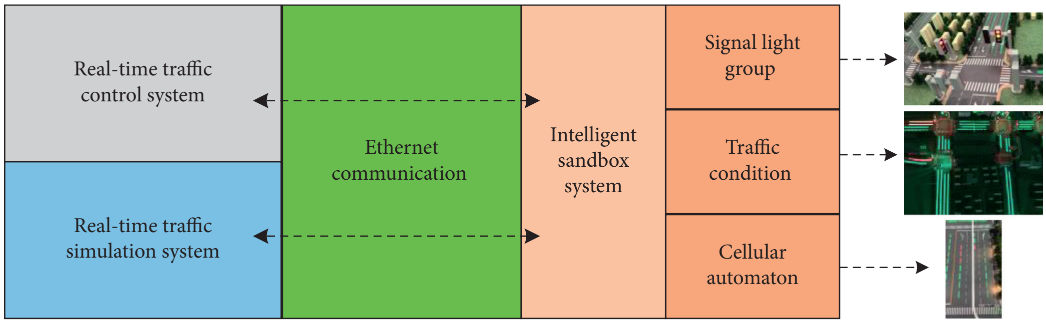

Figure 7: Visualized hardware and software in the loop system architecture.

(a) (b)

Figure 8: Visualized hardware and software in the loop system of Weifang City in Shandong Province, China. (a) Visualized hardware and software in the loop system. (b) Cellular automata.

urban road traffic linking traffic participants, not only undertakes the implementation of control strategies, but also acquires and transmits all kinds of traffic in real time. *T-Type Traffic Information*. Under the background of Internet traffic, the safety of input and output data, which is the key node, must be paid attention to. Taking the signal controller as an example, it can be divided into four categories (as shown in Figure 9): (A) the signal controller as the main body is attacked directly (not through other extended devices); (B) the extended device is the springboard, and the attack signal controller (detector); (C) the external device is the springboard, and the attack signal controller (vehicle networking-signal controller); and (D) the signal controller is the springboard, and the attack signal controller is the springboard. Hit the peripheral equipment (signal controller-vehicle networking). Therefore, in the framework of UTSC-CPS, the importance of information security is considered in both cloud computing platform and edge computing platform, and the ways of information security perception and protection are designed and developed. Among them, the combination of data state perception and information entropy is used in information security perception, and the firewall of hardware and software is used in protection mode. However, with the change and deepening of hacker attack mode and technology, the future urban traffic information security will become a key issue for researchers and managers, because it is not only related to government security, but also related to government security. It is about the safety of traffic participants.

4.1.5. Intelligent Gateway of UTSC-CPS. UTSC-CPS intelligent gateway not only provides powerful network throughput capability for traffic signal controller, but also provides access protocol aggregation and standard conversion functions for various detection and control devices. In order to ensure that the network connection needs to meet the transmission time certainty and data integrity, the unified technical standard time-sensitive networking (TSN) [40, 41] defined by IEEE for key services such as real-time priority and clock is adopted. At present, the interface and protocol of detection and control equipment in China's traffic field are not unified, which brings great difficulties for equipment access and data use. For this reason, the control plane of the network is decoupled from the data forwarding plane by using software-defined networking (SDN) [40, 41] design to realize the programmable control of convergence and conversion of multi-nonstandard protocols, as shown in Figures 10 and 11.

4.2. Technical Characteristics of UTSC-CPS

(1) *Coexistence and Covariance of Virtual and Real.* UTSC-CPS should have the functions of real-time monitoring and real-time online simulation of

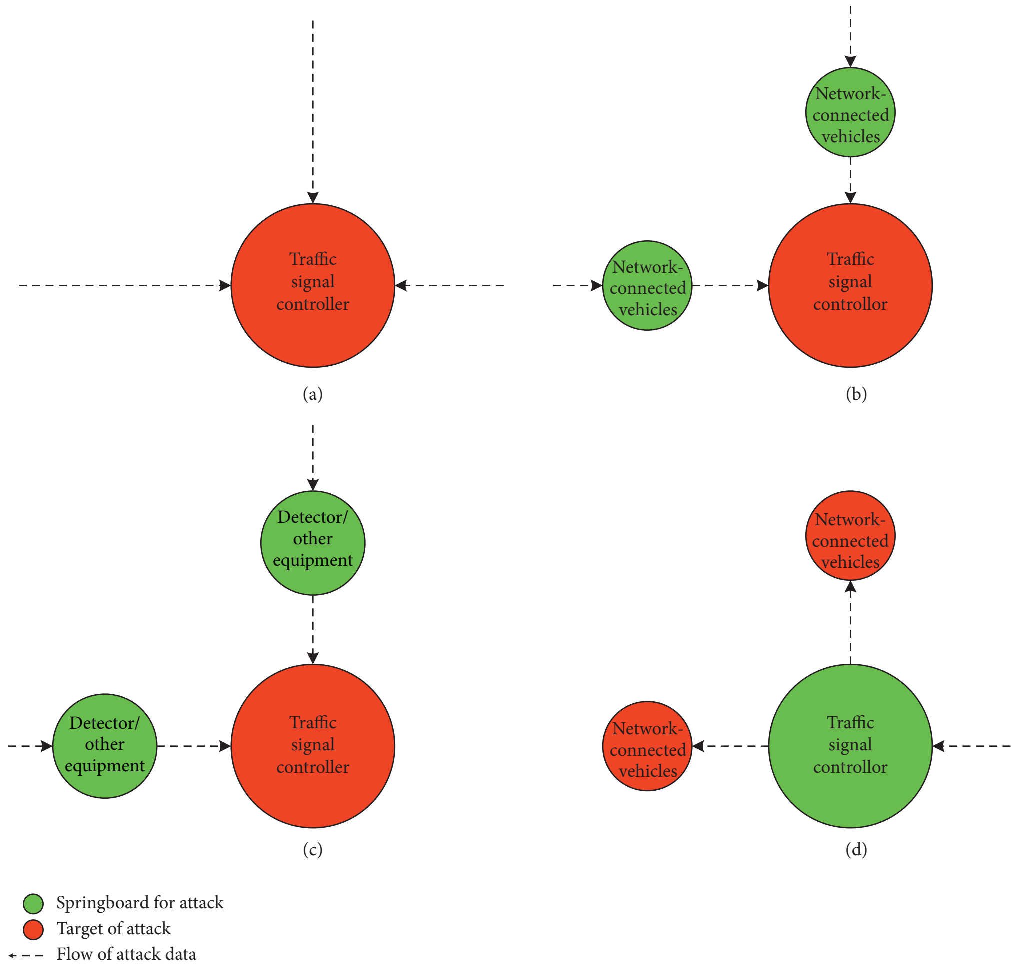

Figure 9: Classification of information security attack scenarios of traffic field equipment.

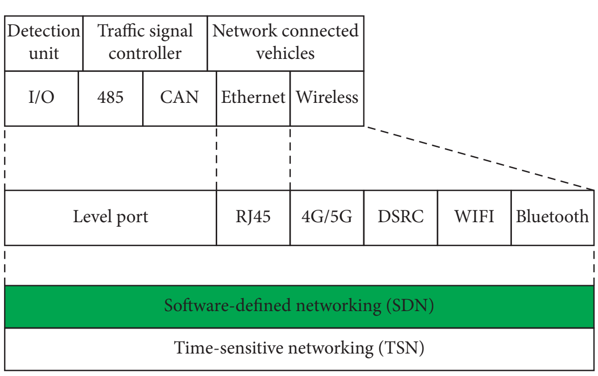

Figure 10: Structure of intelligent gateway.

information system and physical system based on urban road traffic control. Data-driven UTSC-CPS uses real-time information from physical systems to automatically calibrate and modify simulation models and parameters to improve simulation accuracy; simulation results affect the behavior of physical systems through UTSC-CPS control.

(2) *Multi-to-Multi Dynamic Connection*. UTSC-CPS system links traffic elements including people, vehicles, roads, and environment through large-scale heterogeneous networks to form a multilayer information network to realize the interaction and sharing of dynamic information.

(3) *Real-Time Parallel Computing and Information Processing*. UTSC-CPS system framework includes multisource data fusion and processing, large-scale online real-time data-driven simulation, large-scale distributed computing, and other requirements, so it is necessary to use cloud computing to build a macroelastic computing platform and use edge computing to build a microdedicated computing platform to meet the requirements of UTSC-CPS centralized control and decentralized control.

(4) *Self-Organization, Self-Adaptation, Self-Diagnosis, and Self-Healing*. Facing the future, a large number of mobile terminals, including people and vehicles, will quickly access UTSC-CPS system, which requires UTSC-CPS system to have self-organizing and self-adaptive functions. At the same time, the increasingly large and complex system should have

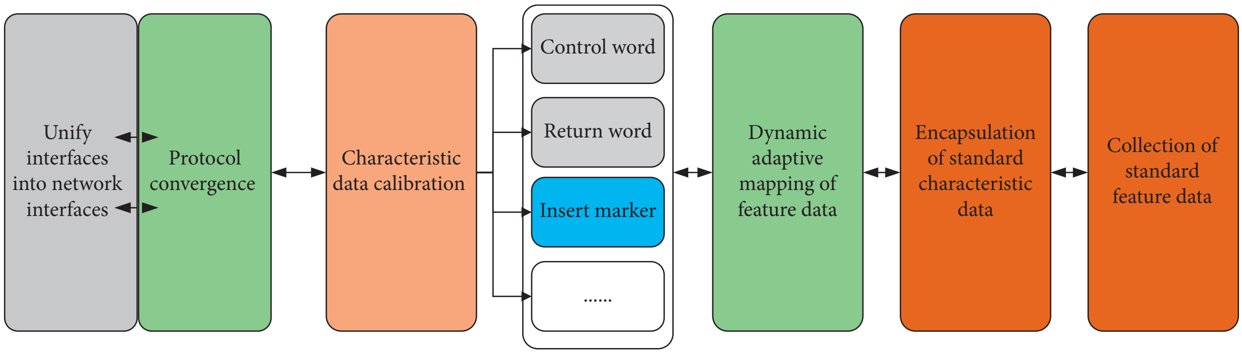

Figure 11: SDN-protocol interface aggregation and conversion.

self-diagnosis and self-healing capabilities in the face of various failures and information security.

4.3. Key Technologies of UTSC-CPS

(1) *Collaborative Technology of Global Optimization and Local Control.* The combination of centralized control and decentralized control to achieve the optimal coordination of global optimization and local control is the first technical problem to be solved by UTSC-CPS.

(2) *Large-Scale Distributed Computing and Layered Information Security.* Cloud computing and edge computing collaboration: cloud computing effectively integrates the computing, storage, and communication resources of the system, realizes the distributed computing requirements of large-scale macrosystems, and uses edge computing to realize fast computing, communication, and control of data measurement. At the same time, information security perception and protection are realized at cloud end and edge side, respectively, effectively blocking attacks based on communication.

(3) *UTSC-CPS Communication Protocol.* In order to realize the deep integration of information system and physical system, a new UTSC-CPS communication protocol is needed to meet the requirements of computing synchronization, data management, and information transmission.

(4) *Dynamic Networks and Delay/Interrupt-Tolerant Networks.* In order to meet the requirements of UTSC-CPS for reliability and speed of online computing and analysis, it is necessary to enhance the ability of communication network to handle delay, packet loss, and interruption and construct dynamic network and delay/interrupt-tolerant network.

(5) *Automatic Mapping Consistency in Virtual and Real Spaces.* It is an important function of UTSC-CPS to realize the comprehensive analysis and simulation of information system and physical system. The consistency of automatic mapping of virtual and real space includes (1) ensuring the synchronization and consistency of real-time information of the system with the actual situation and (2) ensuring the accuracy of simulation model and results.

(6) Cooperation between UTSC-CPS and vehicle cyber physical system (V-CPS): the goal of UTSC-CPS control system with traffic control as its core should be combined with that of V-CPS control system, and the integrated management of urban road traffic in the future can be realized through information sharing and collaborative control.

5. Experiment and Analysis

5.1. Simulation Study on Weifang City in Shandong Province and Shunyi District in Beijing. In order to simulate the scale, real-time performance, stability, and reliability of the real-time simulation system, different-scale urban road network and traffic flow were used to test the system.

(i) Select two different levels of urban road network and traffic flow for simulation test. In order to ensure authenticity and accuracy, the simulation network and fleet data are provided by relevant departments in Shunyi District of Beijing and Weifang City of Shandong Province, as shown in Figures 12(a) and 12(b).

(ii) In order to test the real-time performance and stability of the platform, the refresh rate of the simulation is 1–125 ms (refresh rate is set according to the transmission frequency of the geomagnetic detector data provided by the relevant departments to ensure the authenticity of the simulation), running continuously for 24 hours.

(iii) In Table 1, the hardware and software parameters of cloud computing platform based on VMware virtualization and the scale of simulation road network and traffic flow in Shunyi District of Beijing and Weifang City of Shandong Province are given in Table 2.

Simulated road network diagram: according to the traffic flow data provided by the relevant departments in Shunyi District of Beijing and Weifang City of Shandong Province, the simulation load of the fleet is correlated with the traffic time (morning peak, evening peak, and night), and the

(a)

(b)

Figure 12: Simulation test road network. (a) Shunyi District road network of Beijing. (b) Weifang City road network of Shandong.

Table 1: VMware virtualization of cloud hardware and software parameters.

Name	Configuration requirements
CPU	Two Intel 8-core Xeon E7-4809 V4 processors (2.1 GHz, 20 M cache)
RAM	Two memory 64 GB (4 × 16 GB) 2133 MHz DDR4
Storage	Standardized 8 2.5″ SAS hot swap hard disk slots, 8 ∗ 300 GB
Network card	Four Realtek RTL8111F 10/100/1000 Mbs
Virtualization	VMware ESXI6.5 + Vphere6.5
Operating system	CentOS6.8_64_min_base
Development	Lua5.1 + C + python3 + PHP7.0

Table 2: Simulation of road networks and traffic flow scales.

Position	Intersection scale	Road scale	Traffic flow scale	Refresh rate (ms)
Shunyi District	31	84	252	125
Weifang City	134	446	1624	125

Explanation: the fleet size is modeled as a medium fleet. The number of vehicles represented by the fleet is converted to the maximum detection length of the geomagnetic detector, which is about 10–30 vehicle size.

refresh rate of the simulation platform and the CPU load capacity of the server are tested, respectively. The test results are displayed in Table 3.

As shown in Figures 13(a) and 13(b) above, the refresh ratio (actual refresh time/125 ms) of simulation platforms with different sizes of intersections, sections, and fleets can be found. With the increase of fleet size, the refresh ratio of simulation platforms increases, i.e., the actual refresh time increases, which indicates that the performance of simulation platforms decreases, but it can still be accepted. Figures 13(c) and 13(d) show the CPU resources required by the simulation platform. The private cloud platform can support large-scale simulation requirements by mobilizing computing power and release computing power quickly when the simulation demand decreases to achieve dynamic load balancing adjustment.

5.2. Case Study: Real Intersection Test. In order to test and prove the reliability and advanced nature of the system, a one-year construction and application was carried out with the support of the Weifang City Traffic Detachment in Shandong Province, and the following example tests were conducted based on the single intersection. Modeling and simulation of static data such as lanes, road sections, and canalization at intersections are completed. Calibration of simulation dynamic data uses detection data of wide-area radar, as shown in Figure 14(a). Among them, the selected detection data is workday data and covers morning peak (7:30–8:30), flat peak (10:00–11:00), and evening peak (17:30–18:30); traffic scenarios include four types: undersaturated, oversaturated, undersaturated and transit, and oversaturated and transit. In the programming template provided by the UTSC-CPS system, the detector data and traffic control data (phase, phase sequence, phase, interval time, green light time, lane, period, etc.) have been defined as variables, and the timing control has also been defined., Multiperiod control, induction control, space-time resource allocation control, and traffic scene recognition methods are packaged into functions for direct call, as shown in Figure 14(b). For the test intersection of Shengli East Road and Fushou Street, four control strategies of static-phase sequence multiperiod control, static-phase sequence induction control, dynamic-phase sequence control, and dynamic resource scheduling control were mainly formulated and analyzed.

Table 3: Simulation platform performance test results.

Shunyi District of Beijing							
Time	7:00–9:00	9:01–11:30	11:31–13:00	13:01–16:30	16:31–19:30	19:31–22:30	22:31–6:59
Traffic flow scale	240	152	177	120	250	210	80
Refresh rate (ms)	10.3	8.1	8.5	7.6	12.5	10	3.2
CPU load capacity (%)	25	17	18	10	27	22	6
Weifang City of Shandong Province							
Time	7:00–9:00	9:01–11:30	11:31–13:00	13:01–16:30	16:31–19:30	19:31–22:30	22:31–6:59
Traffic flow scale	1580	1092	1290	1100	1620	1310	820
Refresh rate (ms)	82.3	62.2	70.1	65	88.5	72.4	54.2
CPU load capacity (%)	55	44	48	45	57	50	41

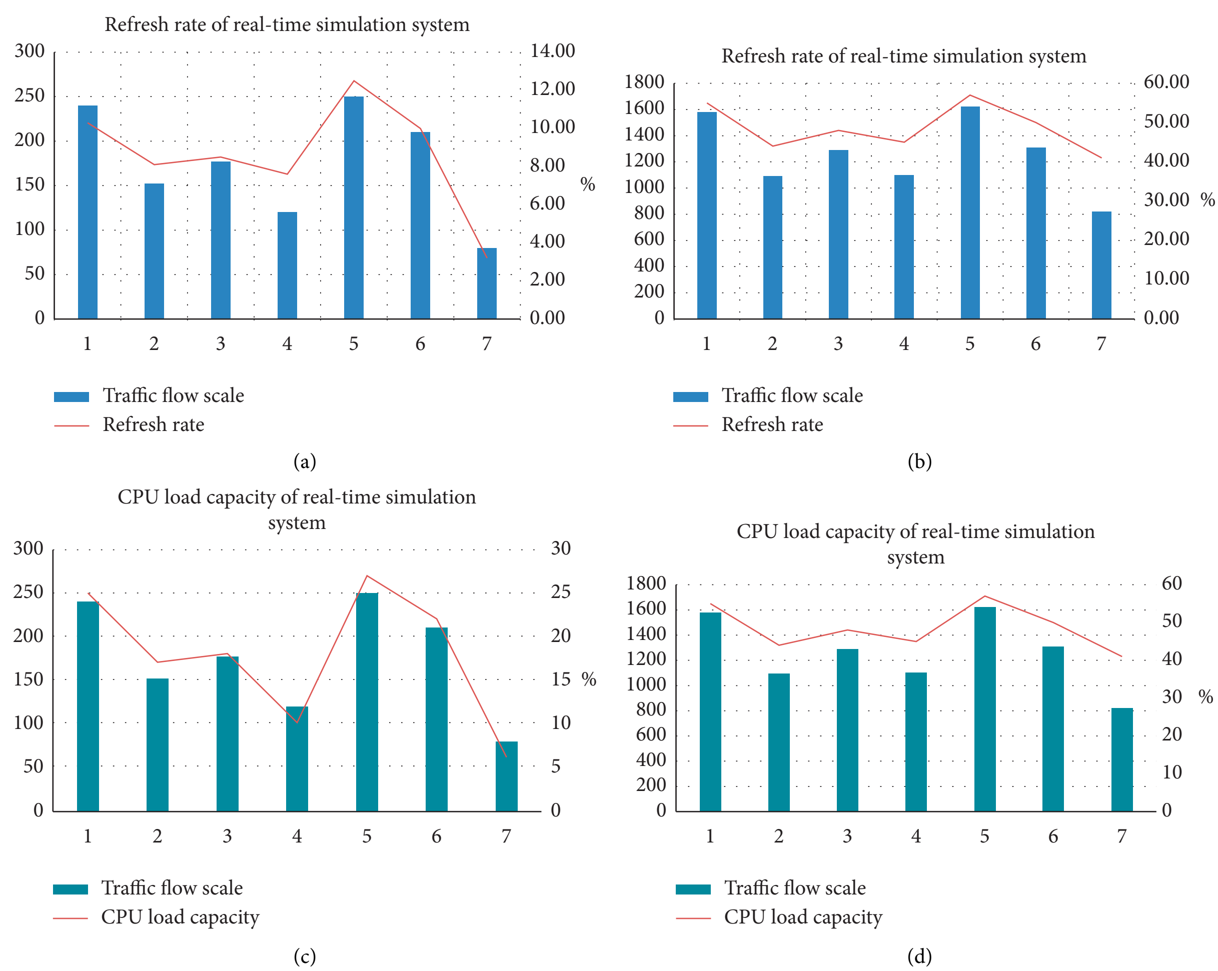

Figure 13: Simulation platform performance test results.

Simulate the four-phase control of static phase sequence multiperiod control (SSMTC), static-phase sequence induction control (SSATC), dynamic-phase sequence control (DSTC), and space-time resource allocation control (DRSTC) at the test intersection and use UTSC-CPS. The three evaluation indexes (through rate, average parking, and queuing length) designed in the system (as shown in Figure 15) analyze and evaluate the simulation control effects under the four control modes. The simulation time for each period is 3600s, and the number of simulations is 10 times. Since the simulation used in this article is directly generated from the raw data of the wide-area radar, there is no need to consider the initial time in traditional simulation software. After the simulation, data sorting and analysis are performed. The evaluation index data is the arithmetic average of ten simulation results. Figure 15 shows the comparison of the three types of evaluation indexes of the four control methods of the test intersection in the morning peak, flat peak, and evening peak hours.

Note: the direct pass rate indicates the proportion of buses passing through intersections without stopping; the average number of stops indicates the average number of stops for all vehicles at the intersection within 5 minutes; the

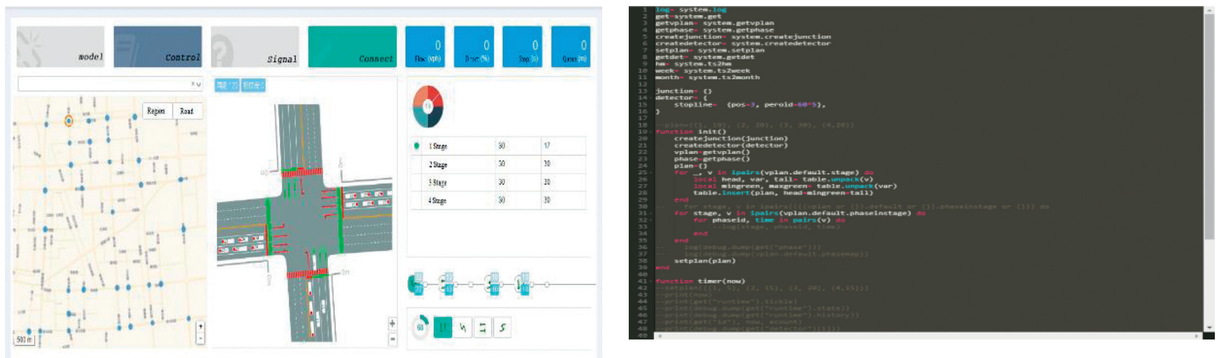

(a) (b)

Figure 14: Intersection test. (a) Model of road network. (b) Algorithm implementation and simulation.

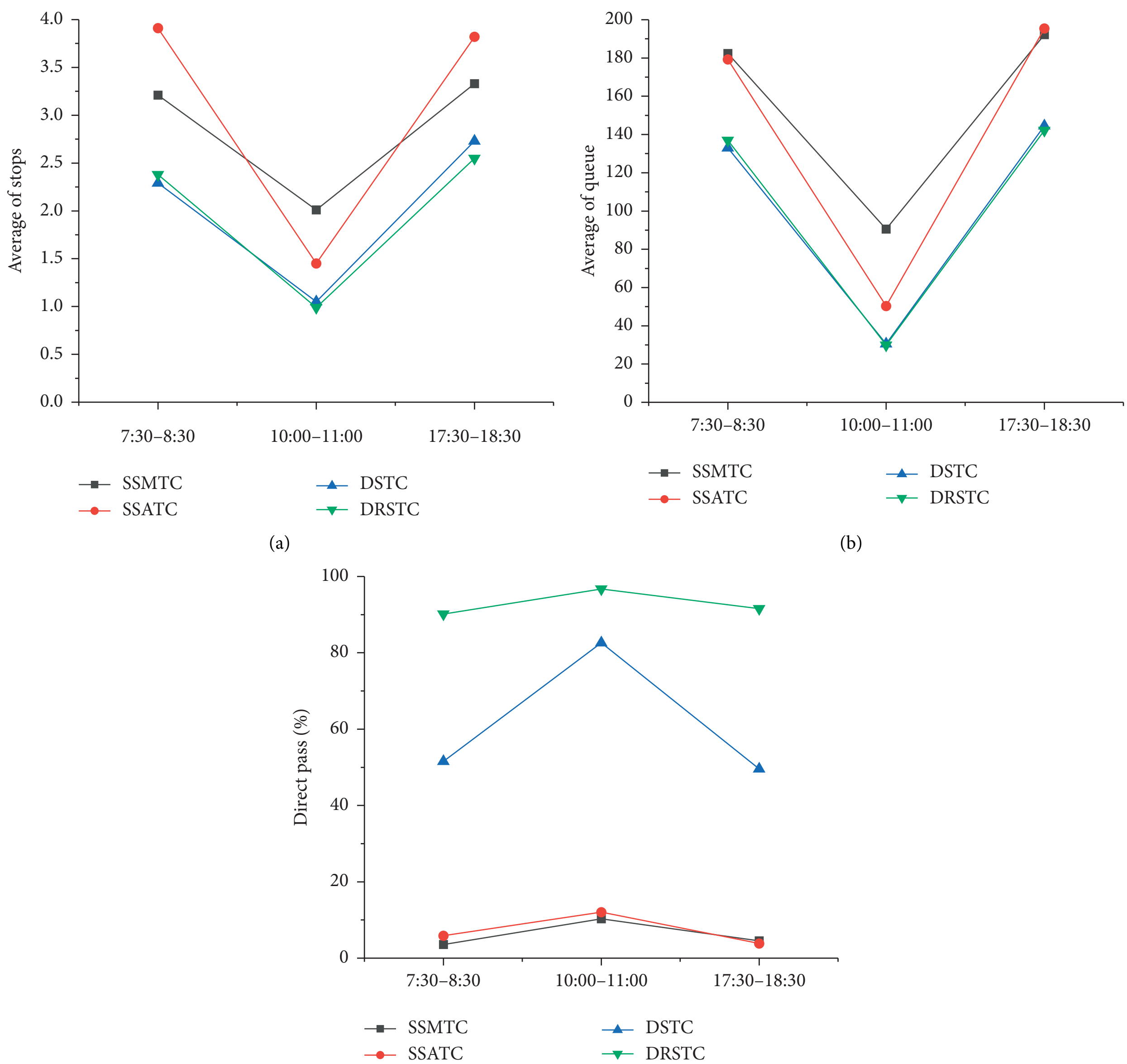

(a) (b) (c)

Figure 15: Comparison of evaluation indicators of four control methods. (a) Comparison of average of stops. (b) Comparison of average of queue. (c) Comparison of direct pass rate.

queue length indicates the average queue length of all lanes within 5 minutes at the intersection.

From Figures 15(a) and 15(b), it can be seen that the average number of stops and the average queue length at the intersection when using the two control strategies of DSTC and DRSTC are significantly lower than those of the two control strategies of SSMTC and SSATC. However, it is worth noting that the SSATC strategy only outperforms the SSMTC strategy during average peak times. This is because the static-phase sequence multiperiod control scheme adopted in this chapter is derived from the actual operation plan of the test intersection, and the plan is optimized. It can be seen from Figure 15(a) that when the DRSTC control strategy is adopted, the bus pass rate is greatly improved compared to the other three control strategies. The reason is that DRSTC can accurately identify “undersaturated and bus” and through the scene recognition method “oversaturation and bus” two scenarios, and when these two scenarios appear, priority control can be provided through lane control. Although the DSTC control strategy can also accurately identify the scene, due to the limitation of the lane control cannot be implemented, the direct rate can only be improved by dynamically adjusting the phase sequence; the two control strategies SSMTC and SSATC cannot recognize the above two scenarios, and intersections that do not adopt public transport priority control, the pass rate is not comparable. Buses may also pass through intersections without stopping.

6. Conclusion Remark and Future Work

In this paper, the urban road traffic signal control information physical system UTSC-CPS is proposed. The system expands the shortcomings of current traffic signal control in control strategy development, testing, simulation, and practical applications and has made innovative work in system extension capabilities, information security, and universality.

UTSC-CPS uses the parallel system concept to establish the interaction mechanism between the real-time control system and the real-time simulation system. It bridges the research and practice of traffic signal control and fully considers the complex characteristics of urban road traffic, through the design of visual hardware and software. In the ring system to simulate a variety of traffic scenarios, the level of traffic management is improved. It also fully considers the requirements of control, information, computing, and simulation under the information physics system architecture and designs cloud computing and edge computing platforms to provide computing power, storage capacity, and information security, especially in the future network communication background. The next is more important.

Compared with other traffic signal control systems, this paper has achieved breakthroughs in three problems. First, through the self-developed real-time simulation system, the data-based parameter adaptive calibration is realized, and the real-time simulation system and real-time control system are constructed. The general underlying data architecture. Second, through the definition of good input and output data variables, packaged control logic functions are provided to researchers through programming templates, enabling them to quickly implement control strategies and use real-time online simulation systems for verification and upgrade Optimization. Third, the protocol middleware is a universal system that can adapt to most signal controllers in China and the United States without changing its physical structure.

In order to test and prove the advantages of UTSC-CPS, it was built and applied for one year with the help of the traffic detachment of Weifang City, Shandong Province, China. The results from the current results are good. At the same time, in order to verify the availability of the simulation system developed by ourselves, the performance and stress tests of the simulation system were carried out using the road network of Weifang City and Beijing Shunyi District, and the results also proved that they can be used. Further tests were conducted using real intersections, and the results were equally valid.

Although we mainly introduce the architecture and features of UTSC-CPS in this article, there are still many problems in the specific application. For this, more traffic scenarios and longer tests are needed, and more practice is needed to explore their potential and explore innovative traffic control measures.

Data Availability

The actual verification and test of the system are supported by Weifang Traffic Police Detachment in Shandong Province and the Beijing Shunyi District Traffic Police Detachment. The data provided were for use in this paper only because it involves commercial and government requirements for the use of data. As a result, the data cannot be made public. However, online access to the system can be provided. Technical details of the system can be made available upon request to the authors. The following is the access address of the system and team e-mail: http://dl.deepor.com:8086/auth/login and http://dl.deepor.com:8088/auth/login and e-mail: zllphd2012@163.com.

Conflicts of Interest

The authors declare that they have no conflicts of interest regarding the publication of this paper.

Authors’ Contributions

Conceptualization was carried out by L.L.Z. and Q.Z.; methodology was conducted by L.L.Z. and Q.Z.; resources were provided by L.W.; writing of the original draft was carried out by L.L.Z.; reviewing and editing were done by Q.Z. and L.Y.Z.; visualization was performed by L.Y.Z.; and supervision was done by L.W.

Acknowledgments

This research was supported by grants from the Beijing Municipal Great Wall Scholar Program (CIT & TCD 20190304), the National Key R&D Program of China under

Grant nos. 2017YFC0821102 and 2017YFC0822504, and the Beijing Municipal Natural Science Foundation under Grant no. 4194078.

Supplementary Materials

The actual verification and test of the system are supported by the Weifang Traffic Police Department in Shandong Province and the Beijing Shunyi District Traffic Police Department. The data provided were for use in this paper only because it involves commercial and government requirements for the use of data. (*Supplementary Materials*)

References

[1] Z. Zhou, S. Lin, W. Du, and H. Liang, "Integration of regional demand management and signals control for urban traffic networks," *IEEE Access*, vol. 7, pp. 20235–20248, 2019.

[2] D. Liu, W. Yu, S. Baldi et al., "A switching-based adaptive dynamic programming method to optimal traffic signaling," *IEEE Transactions on Systems, Man, and Cybernetics: Systems*, 2019.

[3] Z. Zhou, B. De Schutter, S. Lin et al., "Two-level hierarchical model-based predictive control for large-scale urban traffic networks," *IEEE Transactions on Control Systems Technology*, vol. 25, no. 2, pp. 496–508, 2016.

[4] P. B. Hunt, D. I. Robertson, R. D. Bretherton et al., "SCOOT-A traffic method of coordinating signals," Laboratory Report No. LR, The National Academies of Sciences, Engineering, and Medicine, Washington, DC, USA, 1981.

[5] A. G. Sims and K. W. Dobinson, "The Sydney coordinated adaptive traffic (SCAT) system philosophy and benefits," *IEEE Transactions on Vehicular Technology*, vol. 29, no. 2, pp. 130–137, 1980.

[6] PTV VISION: VISSIM 5, *40-User Manual*, PTV Group, Karlsruhe, Germany, 2013.

[7] Quadstone, *Paramics 4.2 User Manual*, Quadstone Ltd, Edinburgh, Scotland, 2003.

[8] S. Baldi, I. Michailidis, V. Ntampasi, E. Kosmatopoulos, I. Papamichail, and M. Papageorgiou, "A simulation-based traffic signal control for congested urban traffic networks," *Transportation Science*, vol. 53, no. 1, pp. 6–20, 2019.

[9] "The national transportation communications for ITS protocol," 2013, http://www.ntcip.org/.

[10] in*Asc/3 Software in the Loop Controller—asc/3 sil*Econolite Group, Inc., Anaheim, CA, USA, 2013, https://www.econolite.com/files/1214/1384/0766/2014-Product-Suite-Controllers.pdf.

[11] "The traffic lights have a history of hundreds of years. Who invented the first signal light in the world? https://baijiahao.baidu.com/s?id=1616556025696965492&wfr=spider&for=pc.

[12] CPS Steering Group, "Cyber-physical systems executive summary," June 2011, http://precise.seas.upenn.edu/events/iccps11/doc/CPS-Executive-Summary.pdf.

[13] J. R. Wang, M. Q. Wu, and J. F. Su, "Cyber-physical system," *Acta Automatica Sinica*, vol. 38, no. 4, pp. 507–517, 2012.

[14] P. Derler, E. A. Lee, and A. S. Vincentelli, "Modeling cyber-physical systems," *Proceedings of the IEEE*, vol. 100, no. 1, pp. 13–28, 2012.

[15] Y. Tan, M. C. Vuran, and S. Goddard, "Spatio-temporal event model for cyber-physical systems," in *Proceedings of the 29th IEEE International Conference on IEEE Distributed Computing Systems Workshops, 2009. ICDCS Workshops'09*, pp. 44–50, Montreal, Canada, June 2009.

[16] R. A. Thacker, K. R. Jones, C. J. Myers et al., "Automatic abstraction for verification of cyber-physical systems," in *Proceedings of the 1st ACM/IEEE International Conference on Cyber-Physical Systems*, ACM, Stockholm Sweden, pp. 12–21, April 2010.

[17] M. C. Bujorianu, M. L. Bujorianu, and H. Barringer, "A unifying specification logic for cyber-physical systems," in *Proceedings of the 17th Mediterranean Conference on Control and Automation, 2009. MED'09*, IEEE, Thessaloniki, Greece, pp. 1166–1171, June 2009.

[18] S. Jianjun, W. Xu, G. Jizhen, and C. Yangzhou, "The analysis of traffic control cyber-physical systems," *Procedia - Social and Behavioral Sciences*, vol. 96, pp. 2487–2496, 2013.

[19] H. Liu, W. D. Sun, and W. Liu, "Lattice hydrodynamic model based traffic control: a transportation cyber-physical system approach," *Physica A: Statistical Mechanics and Its Applications*, vol. 461, pp. 795–801, 2016.

[20] Y. Gong and S.-j. Li, "Fusion framework of urban traffic control and route guidance based on cyber-physical system theory," *Journal of Highway and Transportation Research and Development (English Edition)*, vol. 7, no. 1, pp. 82–89, 2013.

[21] Y. Gong and S. J. Li, "Fusion framework of urban traffic control and route guidance based on CPS theory," *Journal of Highway and Transportation Research and Development*, vol. 29, no. 5, pp. 114–120, 2012.

[22] Z. H. Wang, Y. J. Zhang, and K. Du, "Traffic CPS architecture design," *Journal of Highway and Transportation Research and Development*, vol. 8, no. s1, pp. 142–14, 2012.

[23] E. M. Clarke, B. Krogh, A. Platzer et al., "Analysis and verification challenges for cyber-physical transportation systems," in *Proceedings of the National Workshop for Research on High-Confidence Transportation Cyber-Physical Systems: Automotive, Aviation and Rail*, National Science Foundation, Washington, DC, USA, pp. 20–25, November 2008.

[24] A. Tiwari, "Formal verification of transportation cyber physical systems," in *Proceedings of the National Workshop for Research on High-Confidence Transportation Cyber-Physical Systems: Automotive, Aviation and Rail*, National Science Foundation, Washington DC, USA, pp. 30–35, November 2008.

[25] N. Gaddam, G. S. A. Kumar, and A. K. Somani, "Securing physical processes against cyber attacks in cyber-physical systems," in *Proceedings of the National Workshop for Research on High-Confidence Transportation Cyber-Physical Systems: Automotive, Aviation and Rail*, National Science Foundation, Washington, DC, USA, pp. 26–29, November 2008.

[26] C. Pu, "Intelligent, integrated, and intermodal transportation services," in *Proceedings of the National Workshop for Research on High-Confidence Transportation Cyber-Physical Systems: Automotive, Aviation and Rail*, National Science Foundation, Washington, DC, USA, pp. 51–54, November 2008.

[27] C. Wakter, B. L. Valley, P. Ellis et al., "Dependable automotive cyber-physical system," in *Proceedings of the National Workshop for Research on High-Confidence Transportation Cyber-Physical Systems: Automotive, Aviation and Rail*, National Science Foundation, Washington, DC, USA, pp. 60–64, November 2008.

[28] F. Zhang and W. Wolf, "Cyber-physical control for future transportation systems," in *Proceedings of the National Workshop for Research on High-Confidence Transportation*

Cyber-Physical Systems: Automotive, Aviation and Rail, National Science Foundation, Washington, DC, USA, pp. 115–119, November 2008.

[29] R. Cartwright, A. Cheng, P. Hudak et al., "Cyber-physical challenges in transportation system design," in *Proceedings of the National Workshop for Research on High-Confidence Transportation Cyber-Physical Systems: Automotive, Aviation and Rail*, National Science Foundation, Washington, DC, USA, pp. 220–224, November 2008.

[30] S. Ghiasi, "Design methodologies for synthesis and execution of cyber-physical systems," in *Proceedings of the National Workshop for Research on High-Confidence Transportation Cyber-Physical Systems: Automotive, Aviation and Rail*, National Science Foundation, Washington, DC, USA, pp. 210–215, November 2008.

[31] M. Iqbal and H. B. Lim, "A cyber-physical middleware framework for continuous monitoring of water distribution systems," in *Proceedings of the 7th ACM Conference on Embedded Networked Sensor Systems*, ACM, Berkeley, CA, USA, pp. 401-402, November 2009.

[32] F.-Y. Wang, "The emergence of intelligent enterprises: from CPS to CPSS," *IEEE Intelligent Systems*, vol. 25, no. 4, pp. 85–88, 2010.

[33] W. Guo, Y. Zhang, and L. Li, "The integration of CPS, CPSS, and ITS: a focus on data," *Tsinghua Science and Technology*, vol. 20, no. 4, pp. 327–335, 2015.

[34] F.-Y. Wang, "Toward a paradigm shift in social computing: the ACP approach," *IEEE Intelligent Systems*, vol. 22, no. 5, pp. 65–67, 2007.

[35] F. Zhu, G. Li, Z. Li, C. Chen, and D. Wen, "A case study of evaluating traffic signal control systems using computational experiments," *IEEE Transactions on Intelligent Transportation Systems*, vol. 12, no. 4, pp. 1220–1226, 2011.

[36] F.-Y. Wang, "Parallel control and management for intelligent transportation systems: concepts, architectures, and applications," *IEEE Transactions on Intelligent Transportation Systems*, vol. 11, no. 3, pp. 630–638, 2010.

[37] F. Zhu, Z. Li, S. Chen, and G. Xiong, "Parallel transportation management and control system and its applications in building smart cities," *IEEE Transactions on Intelligent Transportation Systems*, vol. 17, no. 6, pp. 1576–1585, 2016.

[38] Caliper Corporation, *TransCAD User's Guide*, Caliper Corporation, Newton, MA, USA, 2000.

[39] D. Krajzewicz, G. Hertkorn, C. Rössel et al., "SUMO (Simulation of Urban MObility)-an open-source traffic simulation," in *Proceedings of the 4th middle East Symposium on Simulation and Modelling (MESM20002)*, pp. 183–187, Sharjah, UAE, 2002.

[40] Edge Computing Consortium, "White paper of edge computing consortium," 2016, http://www.ecconsortium.org/Lists/index/cid/11.html.

[41] Edge Computing Consortium, "Edge computing reference framework 2.0," 2017, http://www.ecconsortium.org/Lists/index/cid/11.html.

Hindawi
Journal of Advanced Transportation
Volume 2020, Article ID 8849356, 14 pages
https://doi.org/10.1155/2020/8849356

Research Article

Supply Chain Financial Risk Evaluation of Small- and Medium-Sized Enterprises under Smart City

Keyu Wang,[1] Fuhai Yan,[2] Yangjingjing Zhang,[2] Yunlong Xiao,[2] and Lexi Gu[3]

[1]*Department of Mechanical, Aerospace and Civil Engineering, The University of Manchester, Manchester, UK*
[2]*Business School, Sichuan University, Chengdu, China*
[3]*Department of Applied Mathematics, The Hong Kong Polytechnic University, Hung Hom, Hong Kong*

Correspondence should be addressed to Lexi Gu; lexii.gu@connect.polyu.hk

Received 16 June 2020; Revised 13 July 2020; Accepted 5 August 2020; Published 12 September 2020

Academic Editor: Aijun Liu

Copyright © 2020 Keyu Wang et al. This is an open access article distributed under the Creative Commons Attribution License, which permits unrestricted use, distribution, and reproduction in any medium, provided the original work is properly cited.

Prevention and control of risks are an eternal theme of financial institutions. Although, to some extent, the emergence of supply chain finance can enhance the financing capacity of small- and medium-sized enterprises (SMEs) and reduce financial risks of financial institutions, with the development of smart city and smart finance, the financial risks of SMEs are more complex, infectious, dormant, and difficult to accurately identify and measure. Facing this status, financial institutions have been required to understand and evaluate the financial risks of SMEs from a new perspective. Therefore, this paper, based on the study of financial risks assessment of SMEs under the smart city and smart finance, innovatively constructs a new index evaluation system for supply chain finance, based on improved hesitant fuzzy linguistic PROMETHEE method, and the effectiveness and advantages of the model have been verified through an example. To a certain degree, the SMEs financing the evaluation model and improved PROMETHEE method can not only help financial institutions reduce the risks in the specific financial transactions but also reduce the survival threat of financial institutions. Moreover, it is of positive significance to the stable operation of the financial system.

1. Introduction

According to statistics, China's SMEs (including individual industrial and commercial households) accounted for 94.15% of the total number of enterprises. Their final product and service value created was equivalent to 60% of China's total GDP [1]. In terms of promoting China's national economic development, this sector has becoming increasingly important. Unfortunately, the amount of successful loan applications for these small- and medium-sized enterprises (SMEs) has been steadily decreasing over the years. Small scale, weak financial strength, and lack of credit ethics might bring operational risks to financial institutions [2, 3].

With the development of China's economy and society, the market environment is getting better and better. Supply chain finance has emerged as an effective and innovative financial service. It is a kind of credit business relying on the core enterprises in the supply chain and providing effective capital injection to the upstream and downstream enterprises to ensure the normal operation of industrial chain enterprises [4]. This new development model has brought great opportunities to all aspects of the economy and society, especially to the financing of SMEs [5]. Many financial institutions have begun to develop and design new supply chain financing services and products to solve the financing problems faced by SMEs [6]. However, to solve the capital problems of SMEs facing the traditional supply chain is difficult and challenging. The main reason is that traditional supply chain finance still relies on the credit investigation of transaction subjects and stable business relations. Under smart city and smart finance, supply chain finance urgently needs to shift from traditional interpersonal trust to digital trust [7].

Smart city is the general trend of today's economic and social development. It is a new idea and a new model of using the new generation of information technology to promote smart urban planning, construction, management, and service [8]. In the context of smart city, smart technology has swept all traditional industries, including finance. In recent years, relying on Internet technologies and platforms, intelligent financial services using cloud computing, artificial intelligence, big data, blockchain, and other fintech means have developed rapidly; the age of smart finance has arrived [9]. Technological innovation can help expand financial service channels and improve operational efficiency, but it cannot replace the basic functions of finance, nor does it change the hidden, contagious, and sudden nature of financial risks. In other words, prevention and control of risks are an eternal theme of financial institutions, in particular, to guard against financial risks of SMEs.

With the development of the financial industry, rather than financial risk assessment focusing on a single issue, credit status of the entire supply chain is now used [10]. When it comes to loan assessments, financial institutions no longer simply use industry, enterprise scale, and guarantee methods associated with the applied SMEs as the sole bases in their risk assessments. Now they would take a more holistic approach and consider the applicants' entire supply chain as a whole instead [11]. Such changes encourage financial nstitutions to provide loans to SMEs on the basis of fully mastering the logistics, information flow, and capital flow of supply chain and financing SMEs [12]. At the same time, financial institutions could gain a better understanding of the real operating conditions of SMEs and significantly reduce their risks.

Moreover, such model is far from perfect. Under smart city and smart finance, on the one hand, the use of technology and supply chain finance models to boost financing efficiency at the same time broke the limit of time and space of risk conduction, financial risk of companies is more complex, infectious, spread-faster and concealment, and financial risk is more difficult to accurately identify and measure. On the other hand, with the development of fintech, financial services have become more virtual, business boundaries have become more ambiguous, and the challenges faced by risk management and control have become more and more severe. In the end, the large number of participants in supply chain finance with flexible financing mode and complicated contract designs [13], the issues on how to systematically identify and evaluate the specific risks of supply chain finance, and how to effectively control them have increasingly become an urgent subject that needs to be addressed.

Current literature reviews have shown that domestic and foreign scholars have mainly focused on the causes [14], countermeasures [15, 16], and evaluation index system [17] that associated with SMEs supply chain finance risk management. For example, Liang et al. proposed an SME financing evaluation model for supply chain finance based on the theory of the triple bottom line (economy, environment, and society) from a sustainable development perspective [18]. Rosen and Saunders analyzed the risks of supply chain financing which are associated with information sharing. After a discussion on the advantages and disadvantages in supply chain financing, some corresponding solutions are provided [19]. Meanwhile, Demica observes that supply chain finance tends to be carried out by international banks. This is because they have the capacity to bear greater risk than other traditional credit businesses. Providing opportunities for banks to strengthen potential big customer relationships aside, the banks could make a higher margin by charging a higher fee [20]. By analyzing the credit risks of core enterprises in supply chain finance, Mou et al. measured and evaluated the credit risks of core enterprises with a fuzzy analytic hierarchy process. In such way, Mou et al. have established a credit risk evaluation system of supply chain finance [21]. According to the business characteristics of supply chain finance, a credit risk evaluation index system has been put forward by Xia et al., which consists of three subevaluation systems: credit risk evaluation of financing subjects, credit risk evaluation of financing debts, and macroenvironmental risk evaluation. Such index can be used as a reference for financial institutions to carry out their credit risk evaluations [22].

By applying the fuzzy analytic hierarchy process on four aspects, an index weight system for supply chain risk assessment has been established by Zhao and Li [23]. By using the multilevel gray comprehensive evaluation method to evaluate the risks associated with different financial evaluation systems, a risk evaluation index for SMEs has been constructed by Yan [24]. Xiong et al. put forward a credit risk evaluation system for main body rating and debt rating. By combining the principal component analysis method and logistic regression method, a credit risk evaluation model has been established by them. They have also proposed that the construction of the customer basic database should be strengthened. Such move would make the new credit risk evaluation system more accurate and robust [25].

Overall, the above literature reviews have indicated that there is still a lack of a comprehensive and practical method to evaluate supply chain financial risks. The traditional supply chain finance mainly analyzes the operation condition, financing mode, and development prospect of enterprises from the single economic factor [26]. With the advent of globalization and global warming, organizations around the world found that they increasingly have to balance their economic performance and environmental performance [27]. Moreover, whether the enterprise can fulfill the corresponding social responsibility and pass the environmental friendly audit of relevant departments has become an important factor for the survival and operation of the enterprises [28, 29]. However, they have not taken the overall consideration for the development of SMEs (such as industrial risks and new information technology application) into account. As supply chain finance is a financial service for the whole supply chain system, it is also indispensable to assess the overall industry risk of SMEs [30]. In addition, industry risk is also affected by technological evolution [31].

Current evaluation models on supply chain financial risks are based on multilevel gray comprehensive evaluation and principal component analysis method. The former has the problem of relying heavily on expert scoring and being too subjective. Although the latter is more scientific and can improve objectivity in the evaluation process, due to its large sample requirements, its prediction accuracy is not very high [32].

After years of research, the multiattribute decision-making method has achieved outstanding results in political and economic fields [33, 34]. In a multidecision environment, decision-makers can now use a single linguistic term to express their preferences and ideas. They can also express their views based on different influencing factors or uncertain problems.

Among them, the PROMETHEE method put forward by Brans et al. in 1986 is a multiattribute decision-making method [35]. This is a method that is based on the precedence relation of two comparison schemes; the precedence relation between different schemes is determined by preference function and the weight of each attribute given by the decision-maker. Compared with ELECTRE, the PROMETHEE method has very good performance and can be explained directly by using indexes. Such method has drastically improved information accuracy. As its proposed hesitation fuzzy linguistic ranking is based on multiattribute decision-making, it has a good linear preference advantage over other methods.

Under smart city and smart finance, this paper establishes an effective risk evaluation mechanism for SMEs in supply chain finance. The evaluation index expands from traditional single financial evaluation to economic, social, environmental, and industrial risks. By applying the improved hesitant fuzzy PROMETHEE method, it first constructs a multiobjective decisions model to set out the risks that are associated with supply chain financing for SMEs. The uncertainties of uncertain information and decision-makers' perceptions are then transformed into fuzzy concepts; qualitative problems are then quantified.

2. Constructing a Supply Chain Financing Evaluation Index System

With the continuous development of smart finance, it is changing not only the traditional financial channels but also the financial risk control system. The financial evaluation system is a comprehensive evaluation model that includes the following factors into account: corporate economic growth, social responsibility, environmental governance, and industry risk factors. Such comprehensive system would provide financial institutions with more risk assessment options and help them to reduce further financial risk.

In 2012, Ahi and Searcy tried to pick out some key indicators from 445 existing sustainable supply chain management articles. Out of this exercise, they had identified 2555 unique indicators in total, yet most of them were used only once [36]. This shows there is a lack of consensus on how to measure performance in these areas on the subject. Nevertheless, this paper selects some commonly used specific indicators from the economic, social, and environmental risks from the analysis and the summary indicators of Ahi and Searcy as the bases for its financing evaluation indicators.

2.1. "Economic Risk" Evaluation Indicators. The economic performance study identified asset management indicators, development capability indicators, debt indicators, and financial indicators as "economic risks." Based on the value of corporate performance evaluation criteria, this paper constructs an economic risk indicator system from five aspects, asset investment, financial quality, asset quality, capital structure, and operational level, and explains different evaluation indicators.

2.2. "Social Risk" Evaluation Indicators. The "social risk" measures the ability and effectiveness of companies to fulfill their social responsibilities. Corporate social responsibility is composed of two parts: general responsibility and narrow responsibility. Among them, general responsibility refers to corporate responsibility and economy [37]. According to the Global Reporting Initiative, narrow social responsibility includes five aspects of employment compensation, labor security, training, education, occupational safety, and social donations, and further specific indicators such as employment status and labor contract signing rates.

2.3. "Environmental Risk" Evaluation Indicators. Based on the theory of sustainable development, this paper uses the indicators recommended in the Global Sustainability Reporting Guidelines [38] to analyze the actual situation of SMEs supply chain financing. These environmental risks are divided into four specific indicators: waste discharge, energy consumption, resource utilization, and environmental protection.

2.4. "Industry Risk" Evaluation Indicators. This paper will explain the existing credit risk indicators based on the enterprise, such as industry barrier and new information technology application. At last, the industry risk indicator system is constructed and six specific indicators are selected.

Based on the analysis of economic risk, social risk, environmental risk, and industry risk assessment indicators, Table 1 is prepared as follows:

3. Evaluation Using the Hesitation Fuzzy Linguistic PROMETHEE Method

3.1. Preliminary Knowledge. When making multiattribute decisions, because of the uncertainty and complexity of objective things and the fuzziness of human thinking, numerical scale cannot reflect the preference of decision-maker effectively and accurately. Therefore, in order to reasonably express the subjective judgment of decision-makers, scholars put forward the method of expressing with language variables and quantified the qualitative problems by setting a unified language terms set and corresponding language transformation methods. We discuss preliminary knowledge as follows.

Table 1: Summary table of supply chain financing evaluation index system.

Target layer	Subtarget layer	Criterion layer	Indicator layer	References
Supply chain financing evaluation index system	B1 economic criteria	C1 asset investment	D1 actual total investment	[18, 22, 24, 25, 30]
		C2 financial quality	D2 return on equity	[18, 21–25, 30]
			D3 return on total assets	[18, 21–25, 30]
		C3 asset quality	D4 asset turnover rate	[18, 22, 23,25, 30]
			D5 accounts receivable turnover rate	[18, 22, 23, 25, 30]
		C4 capital structure	D6 asset-liability ratio	[18, 21–25, 30]
		C5 operational level	D7 sales growth rate	[18,21,22,24,25,30]
	B2 social criteria	C6 employment contribution	D8 employment opportunities	[18, 26, 30]
			D9 average wage level of workers	[18, 30, 36]
		C7 labor security	D10 labor contract signing rate	[18, 30, 36]
			D11 employee social security purchase rate	[18, 30, 36]
		C8 training education	D12 average annual training time of employees	[18, 26, 30, 36]
		C9 occupational safety	D13 casualty rate	[18, 36]
		C10 social contribution	D14 social contribution	[18, 36]
	B3 environmental criteria	C11 waste discharge	D15 exhaust emissions	[18, 30, 36]
			D16 sewage discharge	[18, 30, 36]
			D17 solid waste discharge	[18, 30, 36]
		C12 energy consumption	D18 total direct energy consumption	[18,30, 36]
		C13 resource utilization	D19 recycling rate	[18, 30, 36]
		C14 environmental protection	D20 environmental protection investment proportion	[18, 30, 36]
	B4 industry criteria	C15 industry cycle	D21 industry life cycle	[21–24]
		C16 industry barrier	D22 technology monopoly	[21, 22, 25]
			D23 government controlled monopoly	[21, 22, 25]
		C17 corporate relationship	D24 upstream and downstream industry concentration	[22–25]
		C18 industry informatization level	D25 new information technology application breadth and depth	[22, 24–26, 32]
		C19 industry technology evolution	D26 rate of industry technology evolution	[22, 24–26, 32]

Definition 1 (see [39, 40]). Set

$$S = \left\{ S_g \,\middle|\, g = 0,\ 1, \ldots, \tau \right\}. \tag{1}$$

For the linguistic terms set, $\alpha_i\, \varepsilon\, A$, $\{i = 1, 2, \ldots, N\}$; the mathematical form of the hesitant fuzzy linguistic set on A is

$$H_S = \left\{ < \alpha_i, h_S(\alpha_i) > \,\middle|\, \alpha_i \in A \right\}, \tag{2}$$

where function $h_s(\alpha_i)$: $A \longrightarrow S$ is the possible membership of the element $\alpha_i \in A$ mapped to the collection $X \subset A$ and $h_S(\alpha_i)$ is a continuous list of possible values in the linguistic terms set S. While $h_s(\alpha_i) = \left\{ s_c(\alpha_i) \mid s_\varphi(\alpha_i) \in S, \quad l = 1, 2, 3, \ldots, L(\alpha_i) \right\}$, $\varphi \in \{0,\ 1,\ 2, \ldots, \tau\}$ is the subscript of the linguistic terms set. For the sake of simplicity, $h_s(\alpha_i)$ is called hesitant fuzzy linguistic number, and H_S is the set of all hesitant fuzzy linguistic numbers on the linguistic terms set S.

Definition 2 (see [39, 40]). Set S as linguistic terms set and set G_H as text-free grammar. Then the elements of the text-free grammar $G_H = (V_N, V_T, I, P)$ can be defined as follows: V_N = {subject, compound, unary, binary, conjunction}; V_T = {"more than," "less than," "at most," "at least," "between," "and," "s_0,, "s_1,, . . ., "s_τ"}; $I \in V_N$; P = {I refers to a subject or compound, while subject is "s_0," "s_1," . . ., "s_τ,". Compound words refer to one-way relationship + subject or binary relationship + conjunction + subject; one-way relationship means "less than" or "more than," binary relationship means "between," and conjunction means "and."

Definition 3 (see [39, 40]). Set E_{GH} as the conversion of a language expression generated by text-free grammar G_H into a function of hesitant fuzzy linguistic set; S is the set of linguistic terms used in grammar. S_{ll} is a collection of all expressions generated for the grammar G_H. The language expression generated by the grammar G_H generation rule can be converted to a hesitant fuzzy linguistic set by the conversion formula $E_{GH} : s_{ll} \longrightarrow H_s$. For example,

$$E_{GH}\left(S_g \middle| S_g \in S\right)$$
$$E_{GH}\left(\text{no more than } S_\alpha\right) = \left\{S_g \middle| S_g \in S, \quad S_g \le S_\alpha\right\},$$
$$E_{GH}\left(\text{less than } S_\alpha\right) = \left\{S_g \middle| S_g \in S, \quad S_g < S_\alpha\right\},$$
$$E_{GH}\left(\text{at least } S_\alpha\right) = \left\{S_g \middle| S_g \in S, \quad S_g \ge S_\alpha\right\},$$
$$E_{GH}\left(\text{more than } S_\alpha\right) = \left\{S_g \middle| S_g \in S, \quad S_g > S_\alpha\right\},$$
$$E_{GH}\left(\text{between } S_\alpha \text{ and } S_\beta\right) = \left\{S_g \middle| S_g \in S, \quad S_\beta \le S_g \le S_\alpha\right\}. \quad (3)$$

In order to understand the characteristics of different hesitant fuzzy linguistic terms more clearly, we should also calculate the two hesitant fuzzy linguistic terms. Liao et al. [39] used the method of linguistic terms for verification and assume that $b = \{b_l \mid l = 1, 2, \ldots, \#b\}$ means hesitant fuzzy linguistic number and $\#b$ denotes the number of hesitant fuzzy linguistic terms in b; then b^+ and b^-, respectively, represent the largest language and the smallest language in b. Meanwhile $\xi\,(0 \le \xi \le 1)$ is optimization parameter; then $b = \xi b^+ \oplus (1-\xi) b^-$ represents at least a few elements in the number. Set $\xi = 0.5$.

Definition 4 (see [41]). The positive ideal solution A^+ and the negative ideal solution A^- of hesitant fuzzy linguistic are $A^+ = \{h_s^{1^+}, h_s^{2^+}, \ldots, h_s^{n^+}\}$ and $A^- = \{h_s^{1-}, h_s^{2-}, \ldots, h_s^{n-}\}$:

$$h_s^{j+} = \begin{cases} \max\limits_{i=1,2,\ldots,m} h_s^{ij+} = \max\limits_{\substack{i=1,2,\ldots,m \\ j=1,2,\ldots,\#h_s^{ij}}} \{S_{\delta^{ij}}\}, & \text{for benefit criterion } C_j, \\ \min\limits_{i=1,2,\ldots,m} h_s^{ij+} = \min\limits_{\substack{i=1,2,\ldots,m \\ j=1,2,\ldots,\#h_s^{ij}}} \{S_{\delta^{ij}}\}, & \text{for cost criterion } C_j, \end{cases} \quad \text{for} \quad j = 1, 2, \ldots, m,$$
$$h_s^{j-} = \begin{cases} \max\limits_{i=1,2,\ldots,m} h_s^{ij+} = \max\limits_{\substack{i=1,2,\ldots,m \\ j=1,2,\ldots,\#h_s^{ij}}} \{S_{\delta^{ij}}\}, & \text{for cost criterion } C_j, \\ \min\limits_{i=1,2,\ldots,m} h_s^{ij-} = \max\limits_{\substack{i=1,2,\ldots,m \\ j=1,2,\ldots,\#h_s^{ij}}} \{S_{\delta^{ij}}\}, & \text{for benefit criterion } C_j, \end{cases} \quad \text{for} \quad j = 1, 2, \ldots, m. \quad (1)$$

Definition 1 shows the relationship between the elements after the quantitative evaluation results, and Definition 2 introduces how to extract the key elements and obtain the quantified indicators. Definition 3 transforms the text-free grammar into a corresponding set of hesitant fuzzy linguistic. Definition 4 determines the positive ideal solution and the negative ideal solution.

3.2. Hesitant Fuzzy Linguistic PROMETHEE Multiattribute Decision-Making Method Based on Improved Preference Function. There are some decision-making problems that cannot be measured quantitatively but can only be evaluated qualitatively in real life. For these decision-making problems, according to the needs of the actual decision-making process, hesitant fuzzy language allows decision-makers to qualitatively describe objective things when information is incomplete or there are uncertainties generated between multiple different language information. This paper combined the hesitant fuzzy linguistic PROMETHEE method based on the improved linear standard preference function and constructed a new supply chain financial risk measurement model.

This measure model consists of two main steps: the construction of hesitant fuzzy linguistic sets and the calculation of PROMETHEE method. In the step of construction of hesitant fuzzy linguistic sets, firstly, every expert will make a qualitative evaluation of each SME based on the evaluation indicators system. Then, by the text-free grammar conversion and the conversion function transition, we can convert the qualitative evaluations of SMEs to the hesitant fuzzy linguistic set used for the calculation of PROMETHEE method. Finally, by the calculation of PROMETHEE method and the comparison of the net flow of each SME, we can choose the reasonable investment decision-making scientifically. The logic of the measure model is shown in Figure 1.

3.2.1. Improved Preference Function. The method adopted in this paper is based on the improvement of the linear standard in the PROMETHEE method. The following mainly introduces the original linear standard, the improved steps, and the application method of the improved hesitant fuzzy linguistic PROMETHEE method.

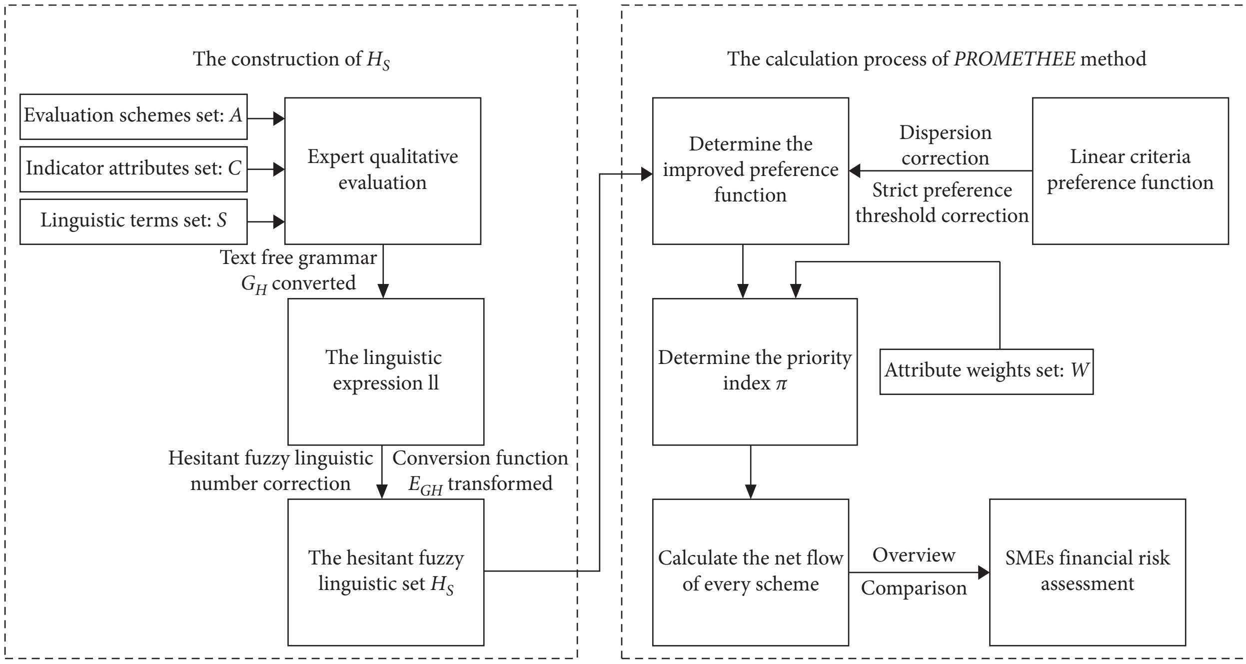

Figure 1: Research framework.

There are six forms of preference functions in the PROMETHEE method [35], where the linear criteria are given as follows:

$$P_j(a_i,a_k)=\begin{cases}0, & d_j(a_i,a_k)\le 0,\\ \dfrac{d_j(a_i,a_k)}{\nu}, & 0<d_j(a_i,a_k)\le\nu,\\ 1, & d_j(a_i,a_k)>\nu.\end{cases}\quad (5)$$

Regardless of which preference function is chosen, it should be calculated.

$d_i(\alpha_i,\alpha_k)=f(\alpha_i)-f(\alpha_k)$, which characterizes the preference difference of any two alternatives. However, in the hesitant fuzzy linguistic environment, the two attributes are described in a hesitant fuzzy linguistic. This cannot be directly operated and thus cannot be directly used in the above preference function of PROMETHEE to calculate the dispersion $d_i(\alpha_i,\alpha_k)$ of the two schemes under the same attribute. Therefore, the preference function of the PROMETHEE method cannot be used effectively, and the above preference function of the PROMETHEE method needs to be further improved as follows:

Step 1: set $h_s^{ij}=\{s_{\delta_i}^{ij}\mid l=1,2,\ldots,\#h_s^{ij}\}(i=1,2,\ldots,m;j=1,2,\ldots,n)$ indicates the degree of satisfaction of the scheme a_i on the attribute c_j. For each hesitant fuzzy linguistic set, define $\sigma_s^{ij}=\sum_{l=1}^{\#h_s^{ij}}\delta_l^{ij}$ as the sum of all hesitant languages in the episode. On the attribute c_j, the dispersion of any pair of schemes a_i and a_k is

$$d_i(\alpha_i,\alpha_k)=\sigma_s^{ij}-\sigma_S^{kj},\quad i,k=\{1,2,\ldots,n\}.\quad (6)$$

Step 2: determine the positive and negative ideal solutions A_j^+ and A_j^- under the criterion c_j, and calculate the dispersion $d_j(A_j^+,A_j^-)$.

Step 3: using the linear preference standard function in the preference function, the strict preference threshold is taken as $\nu=\theta d_j(A_j^+,A_j^-),0<\theta<1$. The decision-maker chooses the value of the parameter θ according to the actual needs of the decision-making process and its subjective preference. When the difference between the sums is 0, it indicates that the schemes a_i and a_k are indistinguishable; when the difference between the sums is greater than $\theta d_j(A_j^+,A_j^-)$, it indicates that the scheme a_i is strictly superior to the scheme a_k. Therefore, the linear criteria preference function can be modified shown as follows:

$$
P_j(a_i, a_k) = \begin{cases} 0, & d_j(a_i, a_k) \le 0, \\[2ex] \dfrac{d_j(a_i, a_k)}{\theta d_j\left(A_j^+, A_j^-\right)}, & 0 < d_j(a_i, a_k) \le \theta d_j\left(A_j^+, A_j^-\right), \\[2ex] 1, & d_j(a_i, a_k) > \theta d_j\left(A_j^+, A_j^-\right), \end{cases}
$$

$$
P_j(a_i, a_k) = \begin{cases} 0, & d_j(a_i, a_k) \le 0, \\[2ex] \dfrac{d_j(a_i, a_k)}{\theta d_j\left(A_j^+, A_j^-\right)}, & 0 < d_j(a_i, a_k) \le \theta d_j\left(A_j^+, A_j^-\right), \quad \text{for benefit criterion,} \\[2ex] 1, & d_j(a_i, a_k) > \theta d_j\left(A_j^+, A_j^-\right), \end{cases} \tag{7}
$$

$$
P_j(a_i, a_k) = \begin{cases} 1, & d_j(a_i, a_k) > \theta d_j\left(A_j^+, A_j^-\right), \\[2ex] \dfrac{d_j(a_i, a_k)}{\theta d_j\left(A_j^+, A_j^-\right)}, & \theta d_j\left(A_j^+, A_j^-\right) < d_j(a_i, a_k) \le 0, \quad \text{for cost criterion.} \\[2ex] 0, & d_j(a_i, a_k) > 0, \end{cases}
$$

$$
0 < \theta < 1.
$$

Considering that the selected indicator may contain the cost attribute, the above preference function only reflects the degree of superiority to the income attribute, so the preference function is adjusted as formula (7).

3.2.2. Hesitant Fuzzy Linguistic PROMETHEE Method. The evaluation steps of the hesitant fuzzy linguistic PROMETHEE method based on the improved linear standard preference function are given as follows:

Step 1: define a multiattribute decision-making problem: determine the set of programs consisting of n schemes $A = \{\alpha_1, \alpha_2, \ldots, \alpha_n\}$ and the set of attributes consisting of m attributes $C = \{c_1, c_2, \ldots, c_m\}$; the set of weights of each attribute is $\omega = (\omega_1, \omega_2, \ldots, \omega_m)^T$, where $0 \le \omega \le 1$ and $\sum_{i=1}^{m} \omega_i = 1$.

Step 2: for the above decision-making problem, the linguistic expression is used to give a qualitative evaluation of the performance of each scheme a_i under each attribute c_j. According to the text-free grammar G_H given by Definition 2, the linguistic expression is generated as ll.

Step 3: according to the conversion function E_{GH} given by Definition 3, the linguistic expression ll is transformed into the hesitant fuzzy linguistic set H_s. For the convenience of operation, a new linguistic term is added, and the hesitant fuzzy linguistic number is the same number of linguistic terms.

Step 4: determine the preference function. Under the benefit type and cost type attribute c_j, the degree to which scheme a_i is better than scheme a_k is represented by the preference function. The modified linear standard preference function is shown in formula (3).

Step 5: determine the priority index $\pi(a_i, a_k)$. The priority index indicates the degree to which scheme a_i is better than scheme a_k. The closer to 1, the better the degree of scheme a_i.

$$
\pi(a_i, a_k) = \sum_{r=1}^{m} \omega_j P_j(a_i, a_k), \quad j = \{1, 2, \ldots, m\}; i, \\ k = \{1, 2, \ldots, n\}. \tag{8}
$$

Step 6: according to the priority index, calculate the inflow $\phi^+(a_i)$ and the outflow $\phi^-(a_i)$ of each scheme:

$$\phi^{+}(\alpha_i) = \sum_{r=1}^{m} \pi(\alpha_i, \alpha_k) = \sum_{j=1}^{n}\sum_{r=1}^{m} \omega_j P_j(\alpha_i, \alpha_k), \tag{9}$$

$$\phi^{-}(\alpha_i) = \sum_{r=1}^{m} \pi(\alpha_k, \alpha_i) = \sum_{j=1}^{n}\sum_{r=1}^{m} \omega_j P_j(\alpha_k, \alpha_i), \tag{10}$$

where $j = \{1, 2, \ldots, m\}; i, k = \{1, 2, \ldots, n\}\phi^{+}(a_i)$ indicates the degree to which a_i is superior to other schemes, and the larger the value is, the better a_i is; $\phi^{-}(a_i)$ indicates the possibility that other schemes are better than scheme a_i, and the smaller the value, the higher the superiority of scheme a_i, relative to other schemes.

Step 7: calculate the net flow of the solution a_i:

$$\phi(a_i) = \phi^{+}(a_i) - \phi^{-}(a_i). \tag{11}$$

The larger $\phi(a_i)$ indicates that the scheme is better. If $\phi(a_i) > \phi(a_k)$, scheme a_i is better than scheme a_k. Similarly, the full ordering of the scheme is available.

4. Case Study

Suppose that a financial institution intends to invest five different small- and medium-sized enterprises. The evaluation of the following five SMEs is then considered under the four economic, social, environmental, and industrial criteria. Next, the financial institution sets the weights of each level and its inclusion indicators according to the characteristics of the market environment and the preferences for each indicator. The corresponding weights of the economic, social, environmental, and industrial levels are as follows:

$$\omega = (0.3, 0.2, 0.2, 0.3)^{T}. \tag{12}$$

The following is a calculation of the performance of five companies in four aspects, respectively.

4.1. Economic Criteria (b_1). In this scenario, there are five criteria: asset investment (c_1), financial quality (c_2), asset quality (c_3), capital structure (c_4), and operational level (c_5). Adjust the weights of these five attributes according to the characteristics of economic criteria:

$$\omega = (0.3, 0.2, 0.2, 0.15, 0.15)^{T}. \tag{13}$$

Step 1: the set of linguistic terms S of the above five attributes can be expressed as $S = \{s_0 = \text{very low}, s_1 = \text{low}, s_2 = \text{low}, s_3 = \text{medium}, s_4 = \text{high}, s_5 = \text{high}, s_6 = \text{very high}\}$.

Step 2: in order to obtain a more reasonable and effective evaluation result, investors set up a decision-making group that includes experts to evaluate the economic indicators of small- and medium-sized enterprises. The decision-making data comes from experts' subjective evaluation of economic indicators of different enterprises. In the evaluation process, each expert independently gives an assessment of the economic indicators of the company. Different experts may have different views on the economic indicators of the same company. For example, an expert may think that the financial quality of a_3 is "very high" and another may be considered "high." If they are unable to convince each other, the evaluation information given by the decision-makers in the decision-making group can be expressed as $\{s_5, s_6\}$. If all decision-makers agree that the asset investment performance of company a_3 is "medium," the evaluation information given can be expressed as $\{s_3\}$. After discussion by the decision-making group, qualitative evaluation information-based linguistic expressions were given to evaluate the performance of the five candidate companies under the five attributes.

Step 3: according to the conversion function E_{G_H}, the expert's linguistic expression $\ell\ell$ is transformed into the hesitant fuzzy linguistic number, and the hesitant fuzzy linguistic evaluation matrix H_s is constructed.

Step 4: among these five attributes, the capital structure (c_4) is the cost attribute, and the other four attributes are the return attribute, which determines the positive ideal solution of the fuzzy hesitant language. $A^{+} = \{s_6, s_6, s_5, s_0, s_6\}$ and $A^{-} = \{s_2, s_1, s_1, s_6, s_0\}$ compute $d_j(A^{+}, A^{-})$. The degree to which enterprise $a_i(i = 1, 2, 3, 4, 5)$ is better than another enterprise $a_k(k = 1, 2, 3, 4, 5)$ is calculated by the improved linear standard preference function, and the calculation result is as follows in Table 2 (set $\theta = 0.6$).

Step 5: according to formula (8), calculate the priority index. The results are shown in Table 3.

Step 6: calculate the inflow $\phi^{+}(a_i)$ and the outflow $\phi^{-}(a_i)$ of each scheme according to formula (9) and formula (10), and finally calculate the net flow $\phi(a_i)$ of the scheme according to formula (11). The results can be seen in Table 4.

4.2. Social Criteria (b_2). According to the characteristics of social norms, the weights of the five attributes employment contribution (c_6), labor security (c_7), training and education (c_8), occupational safety (c_9), and social contribution (c_{10}) are adjusted; the weights are

$$\omega = (0.3\ ,\ 0.2, 0.1, 0.3, 0.1)^{T}. \tag{14}$$

Step 1: same as step 1 in Section 4.1.

Step 2: same as step 2 in Section 4.1.

Step 3: according to the conversion function E_{G_H}, the expert's linguistic expression ll is transformed into the hesitant fuzzy linguistic number, and the hesitant fuzzy linguistic evaluation matrix H_s is constructed.

Table 2: Economic criteria dispersion.

	c_1	c_2	c_3	c_4	c_5
$P_j(a_1,a_2)$	0	2/3	0	0	0
$P_j(a_1,a_3)$	0	0	0	0	0
$P_j(a_1,a_4)$	0	1/6	0	5/36	0
$P_j(a_1,a_5)$	0	0	0	0	0
$P_j(a_2,a_1)$	5/12	0	1	1	1
$P_j(a_2,a_3)$	0	0	1	5/18	1
$P_j(a_2,a_4)$	0	0	0	1	5/9
$P_j(a_2,a_5)$	0	0	0	5/6	5/36
$P_j(a_3,a_1)$	1	5/6	5/12	1	5/18
$P_j(a_3,a_2)$	5/8	1	0	0	0
$P_j(a_3,a_4)$	0	1	0	1	0
$P_j(a_3,a_5)$	5/12	1/6	0	5/6	0
$P_j(a_4,a_1)$	1	0	1	0	5/6
$P_j(a_4,a_2)$	5/6	1/2	0	0	0
$P_j(a_4,a_3)$	5/24	0	1	0	5/9
$P_j(a_4,a_5)$	5/8	0	0	0	0
$P_j(a_5,a_1)$	5/8	2/3	1	5/9	1
$P_j(a_5,a_2)$	5/24	1	5/24	0	0
$P_j(a_5,a_3)$	0	0	1	0	35/36
$P_j(a_5,a_4)$	0	5/6	5/24	25/36	5/12

Table 3: Economic criteria priority index.

$\pi(a_1,a_2)$	2/15	$\pi(a_1,a_3)$	0	$\pi(a_1,a_4)$	13/240	$\pi(a_1,a_5)$	0
$\pi(a_1,a_2)$	5/8	$\pi(a_2,a_3)$	47/120	$\pi(a_2,a_4)$	7/30	$\pi(a_2,a_5)$	7/48
$\pi(a_3,a_1)$	89/120	$\pi(a_3,a_2)$	31/80	$\pi(a_3,a_4)$	7/20	$\pi(a_3,a_5)$	17/60
$\pi(a_4,a_1)$	5/8	$\pi(a_4,a_2)$	7/20	$\pi(a_4,a_3)$	49/120	$\pi(a_4,a_5)$	3/16
$\pi(a_5,a_1)$	181/240	$\pi(a_5,a_2)$	103/240	$\pi(a_5,a_3)$	83/240	$\pi(a_5,a_4)$	3/8

Table 4: The net of economic criteria.

SMEs	$\phi^+(a_i)$	$\phi^-(a_i)$	$\phi^{b_1}(a_i)$
a_1	3/16	659/240	−2.5583
a_2	67/48	13/10	0.0958
a_3	227/120	55/48	0.7458
a_4	377/240	81/80	0.5583
a_5	457/240	37/60	1.2875

$$\begin{bmatrix} (S_3,S_4) & (S_2,S_3,S_4) & (S_5,S_6) & (S_4,S_5) & (S_0,S_1,S_2) \\ (S_1,S_2) & (S_0,S_1) & (S_4,S_5,S_6) & (S_2,S_3) & (S_4,S_5,S_6) \\ (S_4,S_5) & (S_4,S_5) & (S_0) & (S_1,S_2) & (S_5,S_6) \\ (S_2,S_3) & (S_6) & (S_4,S_5) & (S_3,S_4) & (S_2,S_3,S_4) \\ (S_4,S_5,S_6) & (S_1,S_2) & (S_5,S_6) & (S_4) & (S_4,S_5) \end{bmatrix}. \quad (15)$$

Step 4: among these five attributes, the occupational safety (c_9) is the cost attribute, and the other four attributes are the return attribute, which determines the positive and negative ideal solutions of the fuzzy hesitant language. $A^+ = \{s_6, s_6, s_6, s_1, s_6\}$ and $A^- = \{s_1, s_0, s_0, s_5, s_0\}$. We can calculate the improved linear standard preference function. The results are shown in Table 5 (set $\theta = 0.6$).

Step 5: according to formula (8), calculate the priority index. The results are shown in Table 6.

Table 5: Social criteria dispersion.

	c_6	c_7	c_8	c_9	c_{10}
$P_j(a_1,a_2)$	2/3	25/36	5/36	0	0
$P_j(a_1,a_3)$	0	0	1	0	0
$P_j(a_1,a_4)$	1/3	0	5/8	0	0
$P_j(a_1,a_5)$	0	5/12	0	0	0
$P_j(a_2,a_1)$	0	0	0	5/6	1
$P_j(a_2,a_3)$	0	0	1	0	0
$P_j(a_2,a_4)$	0	0	5/36	5/12	5/9
$P_j(a_2,a_5)$	0	0	0	5/8	5/36
$P_j(a_3,a_1)$	1/3	5/12	0	1	1
$P_j(a_3,a_2)$	1	1	0	5/12	5/36
$P_j(a_3,a_4)$	2/3	0	0	5/6	25/36
$P_j(a_3,a_5)$	0	5/6	0	1	5/18
$P_j(a_4,a_1)$	0	5/6	0	5/12	5/9
$P_j(a_4,a_2)$	1/3	1	0	0	0
$P_j(a_4,a_3)$	0	5/12	1	0	0
$P_j(a_4,a_5)$	0	1	0	5/24	0
$P_j(a_5,a_1)$	1/2	0	0	5/24	35/36
$P_j(a_5,a_2)$	1	5/18	5/35	0	0
$P_j(a_5,a_3)$	1/6	0	1	0	0
$P_j(a_5,a_4)$	5/6	0	5/18	0	5/12

Step 6: calculate the inflow $\phi^+(a_i)$ and the outflow $\phi^-(a_i)$ of each scheme according to formula (5) and formula (6), and finally calculate the net flow $\phi(a_i)$ of the scheme according to formula (11). The results are shown in Table 7.

Table 6: Social criteria priority index.

$\pi(a_1,a_2)$	127/360	$\pi(a_1,a_3)$	1/10	$\pi(a_1,a_4)$	13/80	$\pi(a_1,a_5)$	1/12
$\pi(a_2,a_1)$	7/20	$\pi(a_2,a_3)$	1/10	$\pi(a_2,a_4)$	7/36	$\pi(a_2,a_5)$	29/144
$\pi(a_3,a_1)$	7/12	$\pi(a_3,a_2)$	23/36	$\pi(a_3,a_4)$	187/360	$\pi(a_3,a_5)$	89/180
$\pi(a_4,a_1)$	25/72	$\pi(a_4,a_2)$	3/10	$\pi(a_4,a_3)$	11/60	$\pi(a_4,a_5)$	21/80
$\pi(a_5,a_1)$	223/720	$\pi(a_5,a_2)$	233/630	$\pi(a_5,a_3)$	3/20	$\pi(a_5,a_4)$	23/72

Table 7: The net flow of social criteria.

SMEs	$\phi^+(a_i)$	$\phi^-(a_i)$	$\phi^{b_2}(a_i)$
a_1	503/720	229/144	−0.8917
a_2	203/240	4189/2520	−0.8165
a_3	161/72	8/15	1.7028
a_4	787/720	287/240	−0.1028
a_5	5791/5040	25/24	0.1073

4.3. Environmental Criteria (b_3). The weights of the four attributes waste discharge (c_{11}), energy consumption (c_{12}), resource utilization rate (c_{13}), and environmental protection (c_{14}) are adjusted according to the characteristics of environmental criteria; the weight set is

$$\omega = (0.4, 0.2, 0.3, 0.10)^T. \quad (16)$$

Step 1: same as step 1 in Section 4.1.

Step 2: same as step 2 in Section 4.1.

Step 3: the hesitant fuzzy linguistic evaluation matrix H_s is constructed:

$$\begin{bmatrix} (s_1,s_2) & (s_2,s_3) & (s_3,s_4) & (s_1) \\ (s_4) & (s_2) & (s_4,s_5) & (s_5,s_6) \\ (s_5,s_6) & (s_4,s_5) & (s_0,s_1) & (s_3,s_4) \\ (s_3,s_4) & (s_1,s_2) & (s_4) & (s_5,s_6) \\ (s_4,s_5) & (s_4,s_5,s_6) & (s_1,s_2) & (s_2) \end{bmatrix}. \quad (17)$$

Step 4: among these five attributes, waste discharge (c_{11}) and energy consumption (c_{12}) are the cost attributes. The positive and negative ideal solutions of the fuzzy hesitant language are $A^+ = \{s_1, s_1, s_5, s_6\}$ and $A^- = \{s_6, s_6, s_0, s_1\}$. Then the improved linear standard preference function can be calculated. The results are shown in Table 8 (set $\theta = 0.6$).

Step 5: according to formula (8), calculate the priority index. The results are shown in Table 9.

Step 6: calculate the inflow $\phi^+(a_i)$ and the outflow $\phi^-(a_i)$ of each scheme according to formula (5) and formula (6), and finally calculate the net flow $\phi(a_i)$ of the scheme according to formula (11). The results are shown in Table 10.

Table 8: Environmental criteria dispersion.

	c_{11}	c_{12}	c_{13}	c_{14}
$P_j(a_1,a_2)$	5/6	0	0	0
$P_j(a_1,a_3)$	1	2/3	1	0
$P_j(a_1,a_4)$	2/3	0	0	0
$P_j(a_1,a_5)$	1	5/6	2/3	0
$P_j(a_2,a_1)$	0	1/6	1/3	1
$P_j(a_2,a_3)$	1/2	5/6	1	2/3
$P_j(a_2,a_4)$	0	0	1/6	0
$P_j(a_2,a_5)$	1/6	1	1	1
$P_j(a_3,a_1)$	0	0	0	5/6
$P_j(a_3,a_2)$	0	0	0	0
$P_j(a_3,a_4)$	0	0	0	0
$P_j(a_3,a_5)$	0	1/6	0	1/2
$P_j(a_4,a_1)$	0	1/3	1/6	1
$P_j(a_4,a_2)$	1/6	1/6	0	0
$P_j(a_4,a_3)$	2/3	1	1	2/3
$P_j(a_4,a_5)$	1/3	1	5/6	1
$P_j(a_5,a_1)$	0	0	0	1/3
$P_j(a_5,a_2)$	0	0	0	0
$P_j(a_5,a_3)$	1/3	0	1/3	0
$P_j(a_5,a_4)$	0	0	0	0

Table 9: Environmental criteria priority index.

$\pi(a_1,a_2)$	1/3	$\pi(a_1,a_3)$	5/6	$\pi(a_1,a_4)$	4/15	$\pi(a_1,a_5)$	23/30
$\pi(a_2,a_1)$	7/30	$\pi(a_2,a_3)$	11/15	$\pi(a_2,a_4)$	1/20	$\pi(a_2,a_5)$	2/3
$\pi(a_3,a_1)$	1/12	$\pi(a_3,a_2)$	0	$\pi(a_3,a_4)$	0	$\pi(a_3,a_5)$	1/12
$\pi(a_4,a_1)$	13/60	$\pi(a_4,a_2)$	1/10	$\pi(a_4,a_3)$	49/60	$\pi(a_4,a_5)$	41/60
$\pi(a_5,a_1)$	1/30	$\pi(a_5,a_2)$	0	$\pi(a_5,a_3)$	7/30	$\pi(a_5,a_4)$	0

Table 10: The net flow of environmental criteria.

SMEs	$\phi^+(a_i)$	$\phi^-(a_i)$	$\phi^{b_3}(a_i)$
a_1	11/5	17/30	1.6333
a_2	101/60	13/30	1.25
a_3	1/6	157/60	−2.45
a_4	109/60	19/60	1.5
a_5	4/15	11/5	−1.9333

4.4. Industry Criteria (b_4). The weights of the five attributes industry cycle (c_{15}), industry barrier (c_{16}), corporate relationship (c_{17}), industry informatization level (c_{18}), and industry technology evolution (c_{19}) are adjusted according to the characteristics of industry criteria; the weight set is

$$\omega = (0.2, 0.3, 0.2, 0.2, 0.1)^T. \quad (18)$$

Step 1: same as step 1 in Section 4.1.

Table 11: Industry criteria deviation.

	c_{15}	c_{16}	c_{17}	c_{18}	c_{19}
$P_j(a_1,a_2)$	5/8	5/6	1	0	5/8
$P_j(a_1,a_3)$	0	5/18	0	0	5/24
$P_j(a_1,a_4)$	5/24	0	1	5/12	1
$P_j(a_1,a_5)$	0	0	1	0	0
$P_j(a_2,a_1)$	0	0	0	5/12	0
$P_j(a_2,a_3)$	0	0	0	0	0
$P_j(a_2,a_4)$	0	0	0	5/6	5/12
$P_j(a_2,a_5)$	0	0	5/36	0	0
$P_j(a_3,a_1)$	5/6	0	0	5/6	0
$P_j(a_3,a_2)$	1	5/9	1	5/12	5/12
$P_j(a_3,a_4)$	1	0	1	1	5/6
$P_j(a_3,a_5)$	5/8	0	1	5/24	0
$P_j(a_4,a_1)$	0	5/18	0	0	0
$P_j(a_4,a_2)$	5/12	1	0	0	0
$P_j(a_4,a_3)$	0	5/9	0	0	0
$P_j(a_4,a_5)$	0	5/18	5/36	0	0
$P_j(a_5,a_1)$	5/24	0	0	5/8	0
$P_j(a_5,a_2)$	5/6	5/6	0	5/24	5/8
$P_j(a_5,a_3)$	0	5/18	0	0	5/24
$P_j(a_5,a_4)$	5/12	0	0	1	1

Step 2: same as step 2 in Section 4.1.

Step 3: the hesitant fuzzy linguistic evaluation matrix H_s is constructed.

$$\begin{bmatrix} (S_3,S_4) & (S_2,S_3,S_4) & (S_0,S_1) & (S_2,S_3,S_4) & (S_4,S_5,S_6) \\ (S_2) & (S_1,S_2) & (S_4,S_5) & (S_2) & (S_3,S_4) \\ (S_5,S_6) & (S_2,S_3) & (S_0,S_1) & (S_1) & (S_4,S_5) \\ (S_3) & (S_3,S_4) & (S_4,S_5) & (S_3,S_4,S_5) & (S_2,S_3) \\ (S_3,S_4,S_5) & (S_3) & (S_4,S_5,S_6) & (S_1,S_2) & (S_5) \end{bmatrix}. \quad (19)$$

Step 4: among these five attributes, corporate relationship (c_{17}) and industry informatization level (c_{18}) are the cost attributes. The positive and negative ideal solutions of the fuzzy hesitant language are $A^+ = \{s_6, s_4, s_0, s_1, s_6\}$ and $A^- = \{s_2, s_1, s_6, s_5, s_2\}$. The results are shown in Table 11 (set $\theta = 0.6$).

Step 5: according to formula (8), calculate the priority index. The results are shown in Table 12.

Step 6: calculate the inflow $\phi^+(a_i)$ and the outflow $\phi^-(a_i)$ of each scheme according to formula (5) and formula (6), and finally calculate the net flow $\phi(a_i)$ of the scheme according to formula (11). The results are shown in Table 13.

4.5. Results Processing. According to each company's performance in four aspects and the weights preferences, through the formula $\phi^*(a_i) = \sum_{i=1}^{5} \phi^{b_j}(a_i)\omega_b$, $(i = 1, 2, 3, 4, 5)$ calculate the scores and rankings of each company. The results are shown in Table 14.

According to the results of the hesitant fuzzy PROMETHEE method analysis, as shown in the table above, from the perspective of the net outflow of the enterprise, the ranking of the five enterprises is $a_3 > a_4 > a_5 > a_1 > a_2$.

Table 12: Industry criteria priority index.

$\pi(a_1,a_2)$	51/80	$\pi(a_1,a_3)$	5/48	$\pi(a_1,a_4)$	17/40	$\pi(a_1,a_5)$	1/5
$\pi(a_2,a_1)$	1/12	$\pi(a_2,a_3)$	0	$\pi(a_2,a_4)$	5/24	$\pi(a_2,a_5)$	1/36
$\pi(a_3,a_1)$	1/3	$\pi(a_3,a_2)$	83/120	$\pi(a_3,a_4)$	41/60	$\pi(a_3,a_5)$	11/30
$\pi(a_4,a_1)$	1/12	$\pi(a_4,a_2)$	23/60	$\pi(a_4,a_3)$	1/6	$\pi(a_4,a_5)$	1/9
$\pi(a_5,a_1)$	1/6	$\pi(a_5,a_2)$	25/48	$\pi(a_5,a_3)$	5/48	$\pi(a_5,a_4)$	23/60

Table 13: The net flow of industry criteria.

SMEs	$\phi^+(a_i)$	$\phi^-(a_i)$	$\phi^{b_4}(a_i)$
a_1	41/30	2/3	0.7
a_2	23/72	67/30	1.9139
a_3	83/40	3/8	1.7
a_4	67/90	17/10	−0.9556
a_5	47/40	127/180	0.4694

Table 14: Evaluation results.

SMEs	$\phi^*(a_i)$	Rank
a_1	−0.4092	4
a_2	−0.4587	5
a_3	0.5843	1
a_4	0.1630	2
a_5	0.1619	3

Therefore, enterprise 3 has the best risk control performance and is the most suitable target.

At present, there are few related researches on this kind of scientific problems. In terms of engineering practice, it still mainly relies on the subjective experience judgment of the decision-maker, which may affect the objectivity of the research results. Such inconsistent evaluation criteria lead to decision-making errors. In addition, as some indicators data are not easy to obtain in the process of scientific research, this makes researches difficult to carry out.

4.6. Sensitivity Analysis. The purpose of the sensitivity analysis is to detect whether there is a difference in the evaluation results when selecting different decision-makers or different evaluation criteria for SMEs that need financing. In order to judge the degree of influence of the evaluation factors on the decision-making results, eight different evaluation criteria with specific details are selected (see Table 15).

Figure 2 is a graphical representation of the evaluation results under different evaluation criteria. Among them, conditions 1, 2, 3, and 4 only consider single economic, social, environmental, and industrial factors. From analyzing the ranking changes of SMEs, we can deduce that using traditional single economic indicators to assess SMEs financing decisions may bring about considerable risks.

Table 15: Sensitivity analysis conditions comparison table.

Condition	Decision criteria	Ranks
1	c1, c2, c3, c4, c5	5 > 3 > 4 > 2 > 1
2	c6, c7, c8, c9, c10	3 > 5 > 4 > 2 > 1
3	c11, c12, c13, c14	1 > 4 > 2 > 5 > 3
4	c15, c16, c17, c18, c19	3 > 1 > 5 > 4 > 2
5	c1, c2, c3, c4, c5, c6, c7, c8, c9, c10	3 > 5 > 4 > 2 > 1
6	c6, c7, c8, c9, c10, c11, c12, c13, c14	4 > 1 > 2 > 3 > 5
7	c11, c12, c13, c14, c15, c16, c17, c18, c19	1 > 4 > 3 > 5 > 2
8	c1, c2, c3, c4, c5, c6, c7, c8, c9, c10, c11, c12, c13, c14, c15, c16, c17, c18, c19	3 > 4 > 5 > 1 > 2

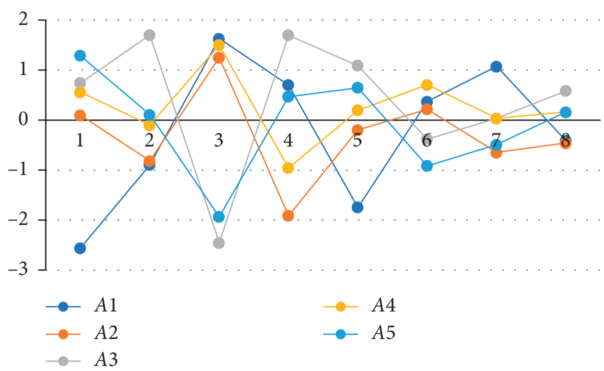

Figure 2: Sensitivity analysis results.

Conditions 5, 6, and 7 are assessments that have taken economic and social indicators, social and environmental indicators, and environmental and industry indicators into their accounts; their various choices depend on the focus of the evaluation indicators. Meanwhile condition 8 considers economic, social, environmental, and industry indicators. It can be seen that as the number of selected indicators increases, the score gap between different enterprises decreases, and the ranking of enterprises also changes.

According to the sensitivity analysis, the selection of the standard type and the standard quantity in the evaluation process is sensitive to evaluation results. This means that when applying risk evaluation system to corresponding enterprises, financial institutions should select the evaluation criteria and quantity carefully in their evaluation process. Comprehensive and scientific evaluation of supply chain financing can further reduce the risk of making supply chain financing decisions.

5. Conclusion

With the progress of financial industry and the rapid development of information technology, the concepts of smart city and smart finance have attracted a lot more attention from financial institutions than ever before. This change has led to differentiating in the financial evaluation system of financial institutions. Single-focus assessments were disappearing and they are replaced by more holistic approaches. At present, most of the evaluations of supply chain financial risks only consider the impact of economic unilateral factors on supply chain financial risks. While other factors such as the wealth of the industry and its operating environment as a whole were ignored, such negligence had exposed financial institutions with considerable unnecessary risks.

In order to ameliorate the situation, this paper constructs a more complete supply chain financial evaluation system for SMEs from the perspectives of economy, society, environment, and industry. By taking these factors into account, the new model would provide a more scientific and less subjective footing to enable financial institutions to reach better investment decisions. This is beneficial to SMEs in the long run also. With a clearer and quantifiable assessment system, they could take actual practical steps to adjust their enterprises and meet the new environmental criteria that had been set forth by the financial institutions. In such way, these enterprises could get the loans they badly needed to avoid credit crunches. At the same time, social and economic growth can be achieved on a sustainable basis. From a macro perspective, such comprehensive assessment method would also help government agencies to regulate and allocate appropriate credits to SMEs more efficiently in the future.

Through the above case analysis, the following can be seen:

(1) In the context of smart finance, taking into account the economic conditions, social benefits, industry characteristics, and other indicators related to the measurement of supply chain financial risk, this paper establishes a relatively comprehensive index system for the evaluation of supply chain financial risk, which provides a reliable reference for the objective completion of multiobjective measurement.

(2) The improved PROMETHEE method proposed in this paper not only solves the calculation problem of hesitant fuzzy linguistic dispersion but also proposes a more scientific approach to determine strict preference threshold value. As the values are based on the hesitant linguistic fuzzy number characteristics of each scheme under different attributes, this avoids the influence of subjective experience. In addition, the improved PROMETHEE method is not affected by missing index data. This new model can deal with multiattribute decision-making problem in uncertain and fuzzy environment successfully.

Even though by expanding the evaluation content of financial institutions' credit financial risks for SMEs this paper has enriched the theory of supply chain financial risk assessment, there are still many limitations:

(1) When applying the evaluation method, the weight selection of each evaluation index would still contain a certain degree of subjectivity. Further research on how to eliminate the problem with subjectivity (particularly on consensus bias) is needed.

(2) In the background of smart finance, financial risks are very complex. Different regional financial institutions may have different financial preferences on their evaluation subjects. This means that deviations in the performance of the indicators from one financial institution to the next are unavoidable. Further research on how to expand the system into dealing with regional specificities is also required.

Data Availability

The data used to support the findings of this study were supplied by a decision-making group that includes experts to evaluate the risk indicators of small- and medium-sized enterprises. These risk indicators of different enterprises are from experts' subjective evaluations. Data are available from Yunlong Xiao (xiaoyunlongg@163.com) for researchers who meet the criteria for access to confidential data.

Conflicts of Interest

The authors declare no conflicts of interest.

Authors' Contributions

The study was designed by Keyu Wang. The data were collected by Yunlong Xiao. The results were analyzed by Yangjingjing Zhang. The policies related to the research were reviewed by Yangjingjing Zhang and Yunlong Xiao. This paper was edited by Fuhai Yan and Lexi Gu.

Acknowledgments

This research was funded by the Foundation of Sichuan University (skyb201709).

References

[1] J. Lv, "On financing constraints of small and medium enterprises," *Journal of Financial Research*, vol. 11, pp. 115–123, 2015, in Chinese.

[2] A. G. Berger and G. F. Udell, "The economics of small business finance: the roles of private equity and debt markets in the financial growth cycle," *Journal of Banking & Finance*, vol. 22, no. 6–8, pp. 613–673, 1998.

[3] M. Schiffer and B. Weder, *Firm Size and the Business Environment: Worldwide Survey Results*, World Bank Publications, Washington DC, USA, Discussion Paper No. 43, 2001.

[4] F. Fan, G. Su, and X. Wang, "Study on assessment and management of SMEs' credit risk under the model of supply chain finance," *Journal of Central University of Finance & Economics*, vol. 12, pp. 34–43, 2017.

[5] W. Wang, "Research on the impact of supply chain finance mode on SME financing," *Logistics Engineering and Management*, vol. 6, pp. 90–92, 2020.

[6] X. Feng, I. Moon, and K. Ryu, "Supply chain coordination under budget constraints," *Computers & Industrial Engineering*, vol. 88, pp. 487–500, 2015.

[7] H. Song, "Pattern innovation of the supply chain finance enabled by the digital platform," *China Business and Market*, vol. 34, no. 7, pp. 17–24, 2020.

[8] Y. Zhang, Z. Shan, and C. Ma, "Practical studies of Public-Private Partnership in the smart city," *Urban Development Studies*, vol. 25, no. 1, pp. 18–22, 2018.

[9] X. L. Chen, H. C. Zhang, L. Y. Guo, and B. Cong, "Wisdom bank system," *Advanced Materials Research*, vol. 791–793, pp. 2155–2158, 2013.

[10] F. Caniato, L. M. Gelsomino, A. Perego, and S. Ronchi, "Does finance solve the supply chain financing problem?" *Supply Chain Management: An International Journal*, vol. 21, no. 5, pp. 534–549, 2016.

[11] T. Dunn, "21st century supply chain finance," *Global Finance*, vol. 8, no. S6, 2010.

[12] W. A. Abbasi, Z. Wang, and A. Alsakarneh, "Overcoming SMEs financing and supply chain obstacles by introducing supply chain finance," *International Journal of Business and Management*, vol. 13, no. 6, pp. 165–173, 2018.

[13] Q. Guo, "Research on supply chain finance model and its risk management," *Financial Teaching and Research*, vol. 2, pp. 2–5+9, 2010.

[14] H. Wan, "Analysis and countermeasures on the discouraging factors of increasing incomes for farmers," *Economic Problem*, vol. 11, pp. 109–112, 2008.

[15] Y. Yang, "The risk prevention in financial supply chain of commercial banks," *Finance Forum*, vol. 10, pp. 42–45, 2007.

[16] Y. Yang, X. Chen, J. Gu, and H. Fujita, "Alleviating financing constraints of SMEs through supply chain," *Sustainability*, vol. 11, no. 3, p. 673, 2019.

[17] Y. Shi, X. Xie, and Z. Guan, "Risk evaluation model building of logistics financial business for the bank and empirical research," *Journal of System Management*, vol. 4, pp. 53–61, 2014.

[18] X. Liang, X. Zhao, M. Wang, and Z. Li, "Small and medium-sized enterprises sustainable supply chain financing decision based on triple bottom line theory," *Sustainability*, vol. 10, no. 11, p. 4242, 2018.

[19] D. Rosen and D. Saunders, "Risk factor contributions in portfolio credit risk models," *Journal of Banking & Finance*, vol. 34, no. 2, pp. 336–349, 2010.

[20] Demica, "The growing role of supply chain finance in a changing world," *Demica Report Series*, pp. 1–8, Demica, London, UK, 2007.

[21] W. Mou, W.-K. Wong, and M. McAleer, "Financial credit risk evaluation based on core enterprise supply chains," *Sustainability*, vol. 10, no. 10, p. 3699, 2018.

[22] L. Xia, H. Zong, and L. Meng, "The construction of assessment index system of SME credit risks—based on the perspective of supply chain finance," *Finance Forum*, vol. 10, pp. 73–79, 2011.

[23] Z. Zhao and B. Li, "Credit risk evaluation of the supply chain finance based on FAHP method," *Henan Science*, vol. 1, pp. 112–116, 2011.

[24] J. Yan, "The financing models and credit risk management of supply chain finance," Master thesis, Northwestern Polytechnical University, Xian, China, 2007.

[25] X. Xiong, J. Ma, W. Zhao, X. Wang, and J. Zhang, "Credit risk analysis of supply chain finance," *Nankai Business Review*, vol. 4, pp. 92–98+106, 2009.

[26] D. More and P. Basu, "Challenges of supply chain finance," *Business Process Management Journal*, vol. 19, no. 4, pp. 624–647, 2013.

[27] B. M. Beamon, "Designing the green supply chain," *Logistics Information Management*, vol. 12, no. 4, pp. 332–342, 1999.

[28] Y. Chen, R. Simon, C. Reich-Weiser, and J. Woo, "Green supply chain," in *Green Manufacturing*, pp. 83–105, Springer, Boston, MA, USA, 2013.

[29] B. A. Gema Perez, "Sustainable supply chain financing How financial institutions could enhance supply chain sustainability," Master thesis, Georgetown University, Washington, DC, USA, 2012.

[30] S. Young and M. Marais, "A multi-level perspective of CSR reporting: the implications of national institutions and industry risk characteristics," *Corporate Governance: An International Review*, vol. 20, no. 5, pp. 432–450, 2012.

[31] K. Y. Chen, *Investment Economics*, Shanghai University of Finance and Economics Press, Shanghai, China, 2013.

[32] H. Hu, L. Zhang, and D. Zhang, "Research on SMEs credit risk assessment from the perspective of supply chain finance—a comparative study on the SVM model and BP model," *Business Review*, vol. 11, pp. 70–80, 2012.

[33] I. Beg and T. Rashid, "TOPSIS for hesitant fuzzy linguistic term sets," *International Journal of Intelligent Systems*, vol. 28, no. 12, pp. 1162–1171, 2013.

[34] H. Liao, Z. Xu, and X.-J. Zeng, "Hesitant fuzzy linguistic VIKOR method and its application in qualitative multiple criteria decision making," *IEEE Transactions on Fuzzy Systems*, vol. 23, no. 5, pp. 1343–1355, 2015.

[35] J. P. Brans, P. Vincke, and B. Mareschal, "How to select and how to rank projects: the Promethee method," *European Journal of Operational Research*, vol. 24, no. 2, pp. 228–238, 1986.

[36] P. Ahi and C. Searcy, "A comparative literature analysis of definitions for green and sustainable supply chain management," *Journal of Cleaner Production*, vol. 52, pp. 329–341, 2013.

[37] Y. Chen, S. Wang, J. Yao, Y. Li, and S. Yang, "Socially responsible supplier selection and sustainable supply chain development: a combined approach of total interpretive structural modeling and fuzzy analytic network process," *Business Strategy and the Environment*, vol. 27, no. 8, pp. 1708–1719, 2018.

[38] S. O. Idowu, N. Capaldi, L. Zu, and A. D. Gupta, *Encyclopedia of Corporate Social Responsibility*, Springer, Berlin, Germany, 2013.

[39] H. Liao, Z. Xu, X.-J. Zeng, and J. M. Merigó, "Qualitative decision making with correlation coefficients of hesitant fuzzy linguistic term sets," *Knowledge-Based Systems*, vol. 76, pp. 127–138, 2015.

[40] H. C. Liao, "Multiple criteria decision making methods and applications with complicated fuzzy information," Master thesis, Science Press, Beijing, China, 2016.

[41] H. Liao and Z. Xu, "Multi-criteria decision making with intuitionistic fuzzy PROMETHEE," *Journal of Intelligent & Fuzzy Systems*, vol. 27, no. 4, pp. 1703–1717, 2014.

Hindawi
Journal of Advanced Transportation
Volume 2020, Article ID 8854082, 14 pages
https://doi.org/10.1155/2020/8854082

Research Article

Research on a Shared Bicycle Deposit Management System Based on Blockchain Technology

Daozhi Zhao,[1] Di Wang ,[1] and Baosen Wang[2]

[1]*College of Management and Economics, Tianjin University, Tianjin 300072, China*
[2]*School of Economics, Beijing Wuzi University, Beijing 101149, China*

Correspondence should be addressed to Di Wang; wangdi666@tju.edu.cn

Received 17 June 2020; Revised 23 July 2020; Accepted 21 August 2020; Published 3 September 2020

Academic Editor: Aijun Liu

Copyright © 2020 Daozhi Zhao et al. This is an open access article distributed under the Creative Commons Attribution License, which permits unrestricted use, distribution, and reproduction in any medium, provided the original work is properly cited.

As a green travel mode, bike sharing is developing rapidly across China. At present, charging deposits from users is the common operation mode adopted by shared bicycle enterprises. The large number of shared bicycle enterprises generates fierce market competition, and the eliminated enterprises always refuse to return user deposits. Even regular running enterprises still have trouble with the immediate return of deposits. This situation severely affects the reputation of shared bicycle enterprises, and concerns have been shared widely across the society. Meanwhile, there is a general expectation among users that their deposits could be refunded timely and a broad appeal for technical management to resolve this problem. This article uses blockchain technology to reform the current management mode for shared bicycle deposits and constructs a decentralized, user information and deposit visualized, and multidimensional supervised management system. The proposed management system makes the real-time flow direction supervision of user deposits to be realized. Furthermore, a smart contract of shared bicycle deposits with punishment mechanism is also designed. Finally, the differences between the proposed deposit management mode and the current deposit management mode are analyzed, and a simulation experiment is conducted. In the simulation experiment, the deposit theft rate of our deposit management system is 0%, which is far better than the two existing bike deposit management systems. The results show that the outstanding advantages of the proposed deposit management mode, which include improving deposit supervision and guaranteeing user deposit security, are also conducted. This article has made effective technical management exploration to reduce deposit management risks and improve deposit management institutions for shared bicycles. It has important practical reference value for accelerating the sustainable development of shared bicycle enterprises.

1. Introduction

After its introduction to the China market at 2016, bike sharing, with vigorous support from the government, has become an indispensable part of urban green public transport system [1]. According to the statistics, shared bikes are distributed in over 200 cities in China; the highest daily usage of shared bikes has surpassed 700 million person-times [2]. Shared bicycles positively affect low-carbon transportation and environmental protection. Nevertheless, the common drawbacks such as not open, not transparent, not visible, and delay refund of the current deposit management mode of shared bicycles have aroused the anxiety of users. In this situation, the reputation damages and widespread criticisms toward shared bicycle enterprises are inescapable.

After fierce competitions for the occupation of market shares among numerous shared bike enterprises, the failed enterprises exit markets and refuse to return user deposits. According to the statistics, up to 25 million-yuan deposits belong to about 125,000 users which could not be returned after the bankruptcy of "Xiao Ming" shared bikes in June 2018. The well-known company OFO has also been exposed as having difficulty for the deposit refund. According to the incomplete statistics, the number of active users of shared bikes in China had grown to 221 million [3], and the deposit scale of shared bikes can reach 40 billion yuan. Meanwhile, several shared bike enterprises have embezzled user deposits to invest and manufacture more bicycles [4]. This situation has raised concerns among the majority of users.

Currently, the lack of a scientific deposit management mode is a common problem among shared bicycle companies. The drawbacks of deposit management have caused social contradictions between enterprises and users, severely impaired the reputation of shared bike enterprises, and restricted the sustainable, healthy development of the bike-sharing industry. Meanwhile, there is a widespread appeal for protecting the legitimate rights and interests of bicycle users. Thus, establishing a wholesome, scientific management system for shared bike deposits has aroused great concern from the government and the academic community.

On May 16, 2019, "user deposit administrative measures for the new industry forms of communication and transportation (trial)" was jointly issued by the Ministry of Transport, People's Bank of China, National Development and Reform Commission, Ministry of Public Security, State Administration for Market Regulation, and China Banking Regulatory Commission (http://www.mot.gov.cn/zxft2019/xinyetgl/). This measure enacted detailed regulations toward the management of user deposit and advance fund for internet bicycle rental and made requests such as "store and manage by special account, earmark funds for specified purpose only" and "immediate deposit for rental, immediate refund for return." Meanwhile, this measure pointed out that detailed management measures for user deposits should be carried out as soon as possible, and the rights and obligations of all parties should be clarified to strengthen the management of user deposits, prevent user deposit risks, guarantee legitimate rights and interests of users, and promote the healthy development of new industry forms of communication and transportation.

Under these circumstances, it is widely expected that the deposit management mode of shared bicycle enterprises will be reshaped with advanced technology. As the underlying technology of bitcoin [5, 6], blockchain has the characteristic of decentralized data storage and tamper-resistant data [7, 8]. Due to its outstanding advantages for supervising digital asset trading, the blockchain technology has been used to build transparent information management platforms for financial and medical institutions [9, 10]. At the Politburo Meeting, Jinping Xi pointed out that "we should take blockchain as an important breakthrough in independent innovations of core technologies and accelerate the promotion of technological reform and industrial innovation"(http://paper.people.com.cn/rmrb/html/2019/10/26/nw.D110000renmrb201910262-01.htm). Evidently, how to develop and apply blockchain technology has been appreciated at the national level of China.

If the system can be equal and without privilege, it can reduce the opportunism behavior of relevant enterprises. Trading information in blockchains cannot be tampered, and it is traceable. Users could check their balance at any time by using a private key. Meanwhile, supervision organizations have access via a public key to monitor the trading data and capital pools. These merits solve the asymmetrical problems of trade information and effectively ensure the safety of user deposits. Furthermore, this paper designs a smart contract to regulate the behavior of enterprises and users in real time. Finally, with a simulation experiment, this paper shows the deposit theft rate of the system which is 0%, which verifies its security and effectiveness.

This article is organized as follows: in Section 1, we introduce the research background and main research content. In Section 2, we introduce related research reviews of shared bicycle deposit, blockchain technology, and smart contract. In Section 3, we construct a management system of shared bicycle deposits based on blockchain technology and introduce the process of data upload and encryption, transaction data storage, verification methods of payment information, and smart contract. In Section 4, the safety performance index of the management system for shared bicycle deposits is illustrated, and experimental simulation and numerical analysis are conducted. Section 5 gives the research conclusion. Section 6 gives future research and applications.

2. Literature Review

2.1. Shared Bicycle Deposits. Since shared bicycle services entered the China market, collecting user deposits has become a common operation procedure for shared bicycle enterprises [11, 12]. For example, Mo-bike charges 299 yuan as deposit from each user [13], and the deposits charged by OFO and Bluegogo are 199 yuan and 99 yuan, respectively [14, 15]. Different viewpoints for the property of shared bicycle deposit are held by the academic community. Deemed by Chen et al. [16], users and shared bicycle enterprises formed a rental relationship, and the deposit was the guarantee fund for users to rent bikes. The property of deposit was discriminated from a legal perspective by Marselli [17], and charging deposit was deemed to be a disguised form of financing. Hence, fund custody regulations should be carried out to provide supervision for the shared bicycle deposits. Deemed by Nakamura and Abe [18], the manufacturing and operating costs of shared bicycles were very high, and normal running of related enterprises could not be maintained merely by charging low use fee. And deemed by Vallurupalli and Bose [19], using the deposits to reinvest is the main source of profit for the enterprises.

According to this paper, the purpose of enterprises for charging deposits is to insure proper and reasonable use of shared bicycles by the users and guarantee priority compensation to enterprises when bicycles are deliberately damaged by the users. However, the supervision system for shared bicycle deposits is outdated, which has created a series of problems.

First of all, different with the common rental mode, shared bicycle users not always apply for deposit refund immediately after they return shared bicycles. This situation will result in a shared bicycle is bounded with multiple user deposits. It brings enormous sum of funds to the deposit pools of enterprises. Secondly, the flow directions of huge deposits are opaque, and there is a risk of corporate misappropriation. Furthermore, the current shared bicycle deposit system fails to achieve the purpose of restraining misconducts of users, and the phenomena of damaging and hiding shared bicycles occur occasionally.

Deemed by us, the reasonability of charging user deposits remains controversial and should be determined by the current industry conditions and legal institutions. However, users have the rights to check the flow direction of deposits, and enterprises should refund deposits timely under the requests of users. Therefore, the realization of the transparency and publicity of deposit flow direction is a problem demanding prompt solution. This article uses blockchain technology to resolve the shortcomings of the current shared bicycle deposit management system. It sets up a specified account for deposit, prevents enterprises from concealing and transferring user deposits, and fulfills the user demands of checking the flow direction of deposit in real time.

2.2. Blockchain. Blockchain is the underlying technology of bitcoin developed by Nakamoto [20]. Its essence is that everyone participated and is trustworthy, secure, and a shareable encrypted distributed account book [21]. Each new transaction is packaged into a block and linked to the previous block after being confirmed by the majority or all nodes in the system. It forms a valid, tamper-proof part of the data layer [22]. Also, there is no central institution with special rights in the application of blockchain technology, and there are no privileges between participants [23]. Blockchain technology could provide strong technical support for the establishment of safe and transparent application systems in this age of gradual virtualization of money and gradual digitization of assets [24–26]. The blockchain technology has the following advantages.

(i) Decentralization [27]: blockchain-based applications could eliminate the intermediate links of transaction processes, and they do not need the arbitration and management of a third party. Meanwhile, any node could participate in the process of information validation; however, no node could control blockchain individually. (ii) Tamper resistance: blockchain technology uses hash algorithm to store data information, that means the data is hard to tamper with [28]. Any node that tampers or adds invalid data will be detected by the system as a potential threat. (iii) Transparency: information on blockchain is open and transparent due to system-validated nodes could view data in the data layer at any time [29].

The blockchain technology is changing the application of digital currency. In 2017, the donation query system was established based on blockchain technology by Alipay charity donation platform to guarantee the reasonable use of donation (http://www.sohu.com/a/122224160_254472). In 2018, based on the real transaction data and running resources in a supply chain scenario, by the use of blockchain technology, Tencent company released "Tencent blockchain + supply chain finance solutions," which enabled to improve the financing difficulties of small, medium, and microcompanies and support the transformation and upgrade of local industries (https://tech.qq.com/a/20180413/012603.htm). Li et al. [30] proposed P2P cloud storage network, which could realize transfer and sharing of data by users without having to rely on third-party data providers. Zyskind and Nathan [31] proposed cloud storage solutions based on blockchain to improve the data storage security.

2.3. Smart Contract. Smart contract is a contract performed automatically on blockchain and programmed in the form of code [32]. The essence of the smart contract is a digital formally defined commitment containing trigger conditions and execution results [33]. The data storage and reading processes of blockchain are transparent and tamper-resisted. These merits of blockchain could provide underlying technical support for running of the smart contract [34, 35], and the development of the smart contract makes it possible to monitor digital currencies in real time.

The smart contract based on blockchain technology could replace original arbitration and enforcement processes, not only reduce the arbitration enforcement costs but also avert the interference of human factors, and minimize fraud losses. The nodes in blockchain conform to the vested provisions of the smart contract and are punished by the smart contract based on the performance of violations.

This article establishes a deposit management system for shared bicycles by the use of blockchain and smart contract technologies, with aims to monitor the conducts of enterprises in real time, eradicate the misconducts of enterprises, eliminate the possibility of disguised financing in the bike-sharing industry, and guarantee scientific running of the shared bicycle service system.

3. Shared Bicycle Deposit Management System

The core which sets shared bicycle use right as exchange exists in the shared bicycle system [36]. This section constructs a blockchain deposit management system for shared bicycles based on different authorities and responsibilities for the three nodes of enterprises, users, and supervisory organizations around this core. As shown in Figure 1, this system contains a data layer, network layer, and consensus layer.

As can be seen from the figure, in the data layer, the blocks constitute a blockchain according to the occurrence of the time sequences of transactions and guarantee the safety of data stored in the blockchain by the utilization of SHA256 algorithm [37] and Merkle hash value [38]. In the network layer, the nodes are connected with a flat topological structure, and there is no centralized node. Meanwhile, related nodes could view data of any node in the network layer by using a public or private key. As shown in the consensus layer, all the nodes of the network layer should comply with the enacted rules and conform to the identical smart contract. This section individually introduces the four important composing structures: uploading and encryption

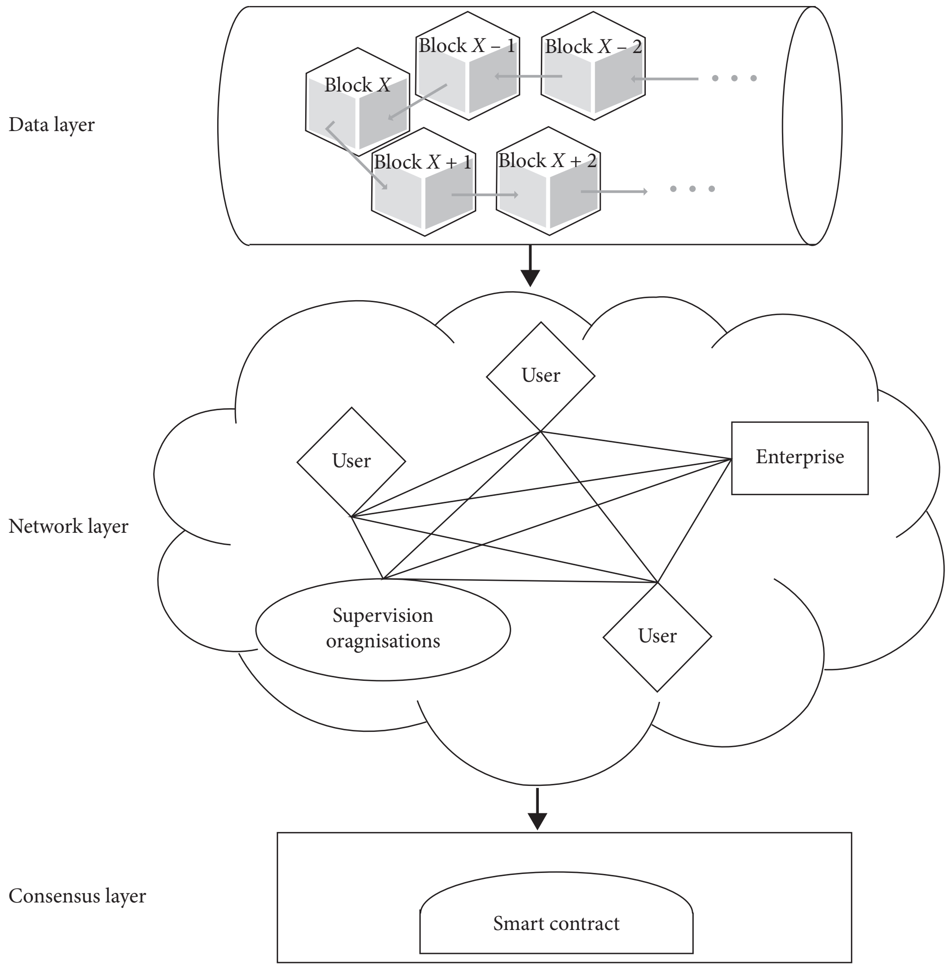

Figure 1: Blockchain shared bicycle deposit management system.

of the data of shared bicycle users, transaction data of users use shared bicycle store, verification of payment information for deposit refund, and smart contract for deposit transfer according to the usage flow of shared bicycles.

3.1. Uploading and Encryption of the Data for Shared Bicycle Users. After shared bicycle users log in and access the nodes of the client, the basic information containing user identities, locations, and so on, is compressed as 32 MB file package and stored in the node block of users. The submitted deposits of registration, the resulting cost record, and transaction data for bicycle using are also preserved in the user block. As shown in Figure 2, each block is composed of a block head and a block body [39]. The block head contains block number, hash value of the previous block, Meckel root, and time stamp [40], and the block body contains all the target transaction lists [41]. The hash value of the previous block ensures the trading order of blockchain, and the Meckel root hash value ensures the authenticity of the transaction record in the blocks. The blocks link together orderly according to the order of trading time, and each block cites the previous block via the “hash value of previous block” of its block head, in turn creating an integral chain of blocks.

The encryption and decryption processes of blocks rely on the RSA and elliptic curve cryptosystem [42]. In our deposit management system for digital signatures and the locking and unlocking of script, the generation of private and public keys is realized with the secp256k1 curve asymmetric encryption algorithm that was proposed by Pote et al. [43]. Encryption code for the private key and public key is given in Algorithm 1.

The private key is secretive, and the public key is available systemwide. The nodes after identity authentication could view data information by the utilization of the public key for the verification of integrity degree and reliability. Especially, this proposed system implants privacy into the permission design of nodes. In this situation, the basic information of users could only be consulted by themselves, and other nodes could only check trading information by the use of the public key. Hence, the privacy of personal information, asset status, and credit status of users could be guaranteed. Decryption code for the private key and public key is given in Algorithm 2.

3.2. Store Transaction Data for Shared Bicycle Using of Users. Merkle tree is used to store transactions taking place in the user node blocks in the proposed deposit management

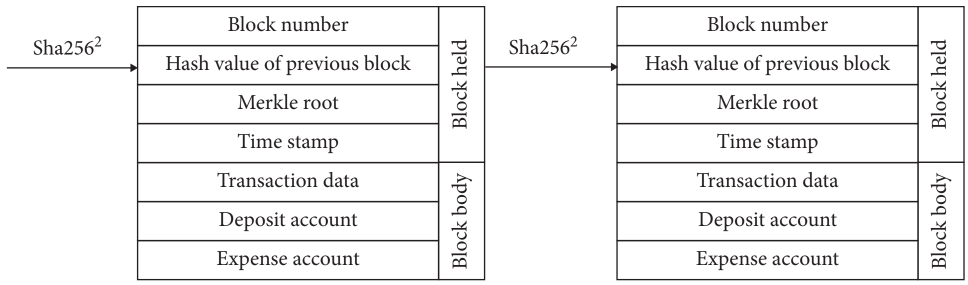

Figure 2: Block structure.

```
Package encryp
import {
   "crypto/rand"
   "crypto/rsa"
   "crypto/x509"
   "encoding/pem"
   "errors"
}
   var privateKey = []byte(`
   —begin RSA private key—
   var publicKey = []byte(`
   —begin public key—
   —end public key—
```

Algorithm 1: Encryption code for private key and public key.

```
//Decry the public key in pem format
   block, _ : = pem.Decode (publicKey)
   if block == nil {
      return nil, errors.New ("public key error")
   }
   // Parsing the public key
   pubInterface, err : = x509.ParsePKIXPublicKey(block.Bytes)
   if err ! = nil {
      return nil, err
   }
   // Type discriminant
   pub : = pubInterface.( * rsa.PublicKey)
   //Encryption
   return rsa.EncryptPKCS1v15 (rand.Reader, pub, origData)
}
// Decryption
func RsaDecrypt (ciphertext []byte) ([]byte, error) {
   // Decryption
   block, _ : = pem.Decode (privateKey)
   if block == nil {
      return nil, errors.New ("private key error!")
   }
   //Resolves the private key in PKCS1 format
   priv, err : = x509.ParsePKCS1PrivateKey (block.Bytes)
   if err ! = nil {
      return nil, err
   }
   // Decryption
   return rsa.DecryptPKCS1v15 (rand.Reader, priv, ciphertext)
}
```

Algorithm 2: Decryption code for private key and public key.

system. Merkle tree is a kind of hash binary tree, which could conclude and check the integrity of large-scale data rapidly [44]. As shown in Figure 3, six transactions are hypothesized to exist in a user node block, with hash values of H_1~H_6. Each hash value is stored in a "leaf" node [45], and all nodes of the same level are divided into groups with two nodes. The hash values of nodes in the same group are tandem calculated by the hash algorithm until the top root node is only left over. The hash value stored in the root node is the Meckel root hash value. The above procedure is described by formulas as follows:

$$H_{12} = \text{sha256d}\ (H_1 + H_2)$$
$$H_{34} = \text{sha256d}\ (H_3 + H_4)$$
$$H_{56} = \text{sha256d}\ (H_5 + H_6)$$
$$H_{1234} = \text{sha256d}\ (H_{12} + H_{34})$$
$$H_{123456} = \text{sha256d}\ (H_{1234} + H_{56})$$

The system performs Algorithm 3 for the hash calculation of each transaction to generate leaf hashes. Merkle tree like Figure 3 is established, and Merkle root is also calculated according to the leaf hashes.

As shown in Figure 4, differing from the current bike-sharing system, the trading information of the proposed deposit management system is not stored in shared bicycle enterprises or specific nodes but in the node blocks where transactions are taking place. The number of blocks is a series of hash values without regularity [46]. The hash values of the previous blocks are stored in the current blocks and are used to connect all blocks to form a chain structure.

When a new block is generated in the system, all nodes will add it to their own blockchains to guarantee data integrity. The heights of blocks are associated with their sequential order of joining blockchain. Block joined earlier has less height, and blocks joined later have more height. The data storage of the chain structure is orderly as the traditional account book and could give early warning towards the modification of block data. By checking the previous block hash value stored in the latter block, users could estimate whether the block data have been tampered.

The hash values of block heads are obtained by calculating the trading information of block bodies, and the hash values of block heads change accordingly when trading information is deleted or tampered. Thus, nodes could check the account security by observing hash values, which can reduce the probability of data tampering. As can be seen in the program, when certain information is deleted, the Merkle root of a block body changes, and the hash value of a block head varies accordingly (Algorithm 4).

The blockchain technology makes the transaction conducts between users and enterprises to be a distributed account book and solve the opacity problem of information between users and enterprises. Consequently, introducing blockchain technology to the deposit system of shared bicycles could realize the tamper-proof property of trading information.

In the proposed system, all transactions related to shared bicycles could be caught, and supervision organizations could comprehend the using condition of any user at any time and location, as well as the flow direction of any fund. Hence, this system could provide technical support to supervision organizations for authenticity checking of deposit refund for enterprises.

3.3. Verification of Payment Information for Deposit Refund. In the current bike-sharing system, purchasing and selling of shared bicycle use rights have nothing to do with supervision organizations. Comparing with the nodes of enterprises and users, the nodes of supervision organizations are incomplete with the function of payment information checking. The proposed system endows the nodes of supervision organizations with Simplified Payment Verification (SPV) permission [47] so that supervision organizations could check the existence of any payment in the network, as shown in Figure 1.

As indicated in Section 3.2, the transactions between users and enterprises will be saved in the transaction data package of block bodies and in the block heads as the hash values of the Merkle root by virtue of the hash algorithm. If the deposit is really refunded to user A by a related enterprise, the resulting transaction record will be saved in the block body, and the hash value of this block and the "hash value of the previous block" stored in the latter block head will change simultaneously. As shown in Figure 5, supervision organizations need to verify the hash value authenticity of H_{1234}, H_{12}, and H_3 to check the authenticity of Transaction 4. If the calculated hash value, according to the Meckel number path of the latter block by related supervision organization, is identical with the hash value of the user A block, Transaction 4 is verified.

The supervision organizations perform Algorithm 5 to compare the Merkle root of user A calculated by them with the Merkle root submitted by the shared bicycle enterprise. If the two Merkle roots are equal, confirming no transaction was false, returning of deposit to user A could be verified. On the contrary, if the two roots are not equal, a selective packet dropping attack would take place in the enterprise reports, confirming the enterprise has not returned the deposit to user A. Original hash sent by the shared bicycle enterprise is denoted with the symbol (').

Overall, the verification of enterprises' deposit refunds conducted by supervision organizations is simplified as verifying whether the two Merkle roots are equal. Therefore, this system provides a scientific, convenient checking mode to supervisory organizations. Simplified Payment Verification (SPV) could enhance the supervisory force of the government and remove the advantage of information asymmetry from enterprises.

The shared bicycle deposit management system based on blockchain technology could ensure visuality of trading data, tamper-proof property of generating the transaction, and checking of the authenticity of payment information. It could also realize automatic supervision of the conduct of enterprises and users via the vsmart contract to guarantee their legitimate rights and interests.

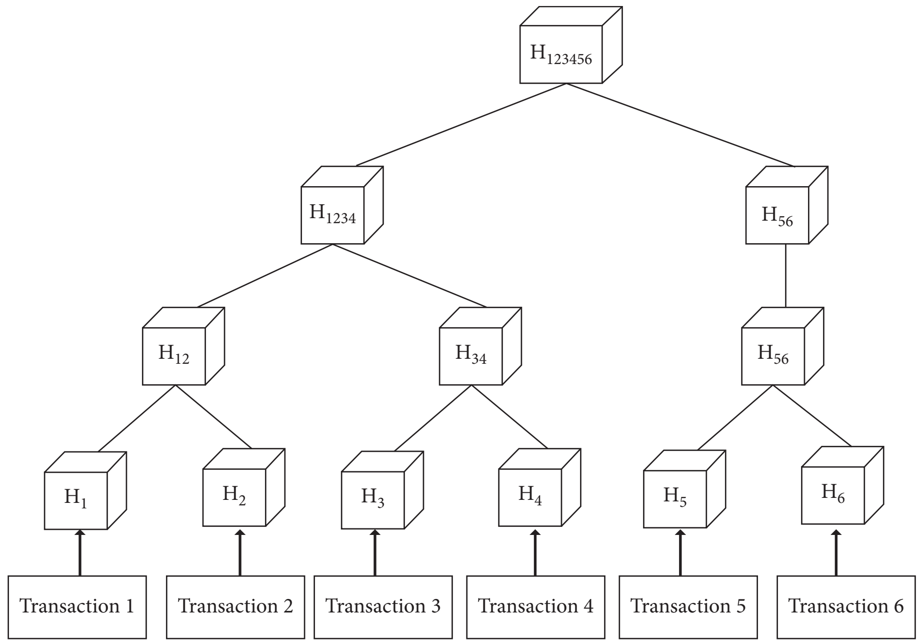

Figure 3: Merkle tree.

```
READ: Transactions
For all transactions
hash[i]=create Hash(transaction[i])
For all hashes in each level
if number of hashes = even then
    Hash[i]=create Hash(hash[i]+hash[i])
else
    if! Last Hash then
        hash[i]=create Hash(hash[i]+hash[i+1])
    else
        hash[i]=create Hash(hash[i]+hash[i])
    end if
    if level=last then
        rootvalue=hash[i]
    end if
end if
```

Algorithm 3: Hash each transaction, build Merkle tree, and compute the Merkle root.

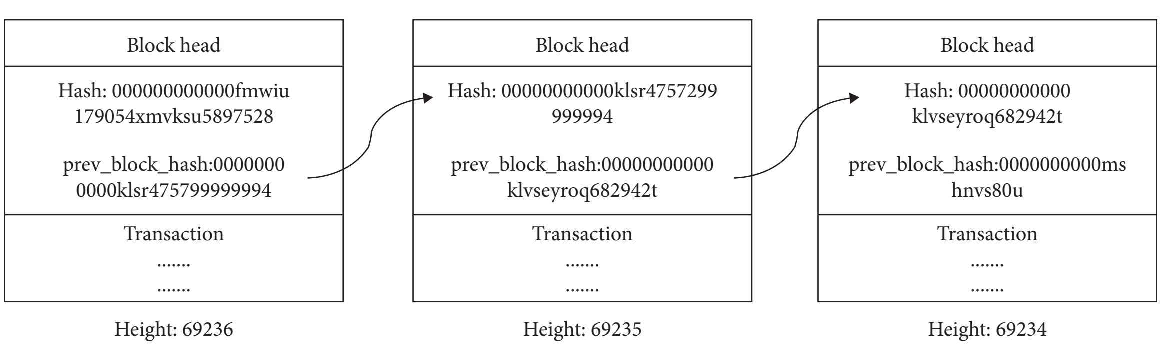

Figure 4: Blockchain structure.

```
#Delete the last transaction in the block transaction
>>>block.txs.pop()
>>>block
#The hash value of the block has changes
Block(hash:4r4i4nv5ny6m6iiih6i390u68b690b5m388569j40)
#The hash value of Meckel root has changes
>>>block.merkle_root_hash
'4n4u4nt843t3nv5394mtvj5m9vj54854v9i8v9vm034,f0j538'
```

Algorithm 4: Check the account security.

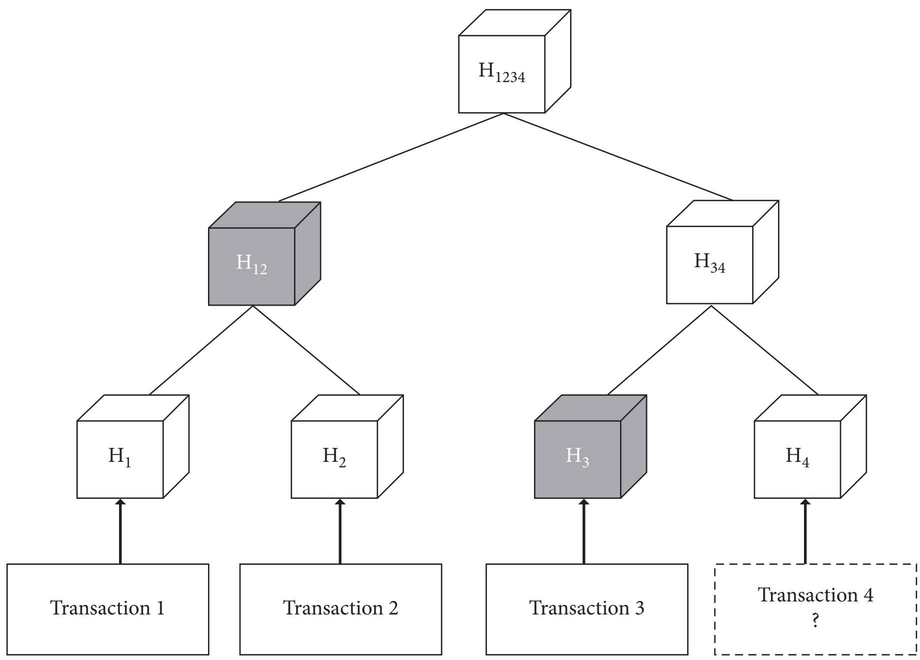

Figure 5: Supervision organizations verify transaction payments.

```
(1) READ: merkleRoot'
(2) if merkleRoot= merkleRoot' then
(3)     Transactions are all legitimate
(4) else
(5)     A selective transaction dropping attack has happened
(6) end if
```

Algorithm 5: Identify malicious paths.

3.4. Smart Contract for Deposit Transfer. Smart contract is the executed agreement among nodes in the blockchain technology [48]. Smart contract typically consists of properties, which contain statements and values and contract terms, trigger conditions, and corresponding response actions of which are linked by "if-then" conditionals [49, 50]. Ethereum uses gas to prevent unlimited contract execution as well as DoS attacks [51]. An account must enclose adequate amounts of gas to successfully call a contract function. Although the proposed system should be carried out based on a platform similar to Ethereum, the blockchain-based shared bicycle deposit management system designed by us theoretically supports all smart contract frameworks. For this reason, detailed gas consumption is not our primary consideration. However, we still optimized the system implementation to minimize operating costs.

In this system, the contract terms related to the enterprise and the users are designed in detail. Every transaction between users and enterprises will be broadcasted in the blockchain network layer, which will be verified by each node and stored in the block. The operating mechanism diagram of the system smart contract is shown in Figure 6.

The smart contract could automatically supervise the flow direction of deposits. Specifically, enterprises can only use the deposits of users for predetermined purposes. As shown in trigger condition 1, if a deposit goes into a nondesignated account, the smart contract would automatically execute a punishment mechanism, locking deposit accounts of enterprises and recording negative information. Meanwhile, the smart contract could also be used to supervise trading information. When an enterprise updates a transaction record, the smart contract could verify it and the deposit value automatically and release this information to the network. Moreover, each transaction record is added to the node blocks when the conformity of the transaction and deposit value are verified by users. A smart contract could also automatically trigger a punishment mechanism, freeze circulating funds, and record negative information, as shown in the corresponding action 2. As shown in Contract Terms 1 and 2, this article demonstrates how a smart contract can be used to supervise capital flow directions and control the deposit usage permissions of enterprises. Smart contract could be used to supervise transaction information and standardize the operating behavior of enterprises. Thus, the possibility of disguising financing for shared bicycle enterprises can be ruled out, and the risk of out-of-control deposit management can be significantly reduced.

In addition, the supervision mechanism for the user conduct is also set in the smart contract. Users purchase the right to shared bicycle usage, not shared bicycle ownership. Thus, users are obliged to avoid damaging the shared bicycles, and maliciously damaging shared bicycles is strictly forbidden in the use rules of enterprises. Nevertheless, the damage conduct to shared bicycles of users occurs occasionally. In this situation, the proposed system binds the behavior of users with their deposits and sets conditions for permitting enterprises to transfer user deposits. After use, the shared bicycle will be checked. If a returned bicycle is not damaged, enterprises could transfer the use fee of users according to the corresponding action 3. Conversely, as shown in the corresponding action 4, if a shared bicycle is returned damaged, the smart contract can deduct a partial deposit from the user to compensate the account of the enterprise according to the damage level of the shared bicycle. Contract Term 5 shows the smart contract would transfer the entire user deposit of anyone who does not return a bicycle or seriously damages it in order to compensate the enterprise. The core code for smart contracts is shown in Appendix A.

4. Experiment and Analysis

This article sets the theft rate of deposit as the evaluation index of safety. The safety and effectiveness of the proposed system are analyzed by comparing its deposit theft rate with the current deposit management system of shared bicycles. In the following section, the experiment settings are first introduced. Then, the parameters of the deposit theft rate are introduced. Finally, simulation experiment is carried out, and related results are compared.

4.1. Experimental Setup

4.1. Experimental Setup. The experiment is conducted with Java1.8 on a desktop computer (Inter(R) Pentium(R) G34603.5 GHz, RAM4 GB, DISK1 TB, bandwidth100 MB/s) equipped with Windows 7 operating system.

4.2. Deposit Theft Rate of the Shared Bicycle Deposit Management System

4.2.1. The Current Deposit Management System for Shared Bicycles. The current deposit management systems for shared bicycles are mainly managed by enterprises or comanaged by enterprises and signing banks. These deposit management systems ensure the security of deposits by establishing an allopatric disaster preparedness system [52]. However, these systems have only one or two centralized nodes with high risk of being stolen since the breakdown of a single node will lead to the crash of the whole system [53]. The basic symbols of the deposit management system for shared bicycles are shown in Table 1.

In enterprise-led deposit management systems, deposits are stored in a central node. Once the node crashes, all deposits will be stolen, and the enterprise and users will suffer huge losses. The number of hacker attacks is shown as follows:

$$NAT_1 = f \cdot U \cdot p, \quad (0 \le NAT_1 \le CN). \tag{1}$$

The central node crashes when $NAT_1 = CN$; the deposit theft rate of the enterprise-led deposit management system is shown as follows:

$$T_1 = NAT_1 \cdot A. \tag{2}$$

In the deposit management system jointly managed by the enterprise and its signatory bank, the deposits are randomly stored in two central nodes and subject to a Poisson distribution with parameter $\lambda_1 = A/CN \cdot p$. In this system, the number of hacker attacks is shown as follows:

$$NAT_2 = \sum_{k=1}^{f\cdot U} \frac{\lambda_1^k \cdot e^{-\lambda_1}}{k!}, \quad (0 \le NAT_2 \le CN). \tag{3}$$

The deposit theft rate of system T_2 can be obtained by calculating the number of central nodes CN, the total amount of deposit accounts A, the probability of nodes attacked successfully p, and system security parameter η:

$$T_2 = NAT_2 \cdot \frac{A}{CN} \cdot p\eta. \tag{4}$$

According to (2) and (4), as the amount of deposit accounts increases, the rate of deposit theft increases. Thus, the two current types of the deposit management model are extremely insecure.

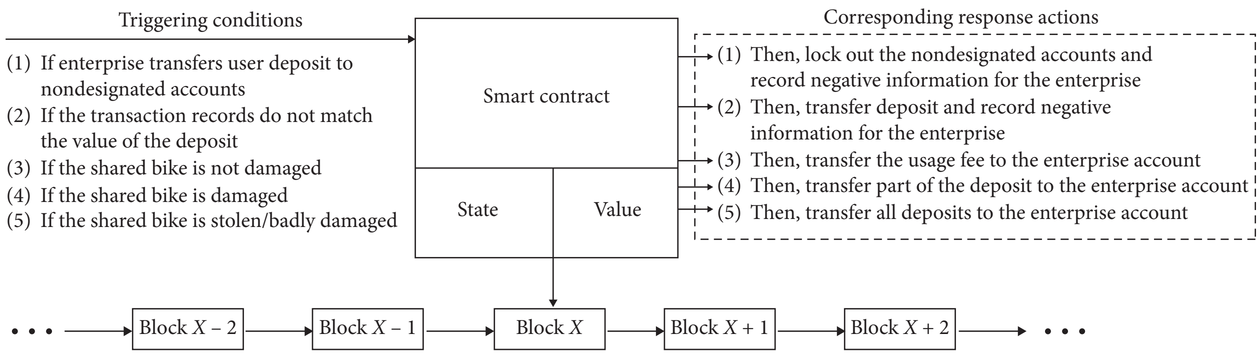

Figure 6: Operational mechanism of the smart contract.

Table 1: Basic symbols of the deposit management system for shared bicycles.

Symbol	Meaning
T	Deposit theft rate
NAT	Number of attacks
CN	Number of node centers
f	Percentage of malicious nodes
U	Number of users
p	Probability of a successful attack on a node
A	Amount of deposit accounts
m	Number of blocks
r	Number of copies of deposit accounts
n	Number of nodes
q	Number of fake blocks forged by an attacker
$m-q$	Actual number of blocks
Q	Probability of successful attacks on all blocks

4.2.2. The Deposit Management System for Shared Bicycles Based on Blockchain Technology. In the deposit management system for shared bicycles based on blockchain technology, there is no central node for storing user deposits. User deposits are stored in the deposit account of each block, and the copy of each user deposit account is randomly stored in the nearby block. In this system, the crash of a block does not affect the whole system; only more than half of the system blocks crashing at the same time would affect the whole system. In this system, the number of deposit accounts that hackers need to attack simultaneously is at least $m/2$, and the probability of correctly attacking the copy of each deposit account is $(r/m)^m$. If the number of blocks in the system is large enough, the probability of tampering the password to steal the deposit by a hacker is infinite close to 0.

To compare the proposed system with the two existing systems, this paper assumes that a hacker has successfully tampered the block with a serial number of z. The probability of tampering all blocks and stealing all deposit accounts by the hacker is as follows:

$$Q=\begin{cases}1, & \text{if} m-q\leq q,\\ \left(\dfrac{q}{m-q}\right)^{z}, & \text{if} m-q\leq q.\end{cases} \quad (5)$$

According to the above formula, when the number of real blocks in the system is greater than the number of fake blocks, the probability of all deposit accounts being stolen by attackers decreases exponentially with the increase of blocks. When the number of real blocks is less than the number of fake blocks, suppose the process of forging fake blocks by the hacker obeys a Poisson process with parameter $\lambda_2 = z\cdot q/m-q$, the number of attack times needed by the hacker to tamper with the whole system NAT_3 is as follows:

$$NAT_3 = 1-\sum_{k=0}^{z}\frac{\lambda_2^k\cdot e^{-\lambda_2}}{k!}\cdot\left[1-\left(\frac{q}{m-q}\right)^{z-k}\right]. \quad (6)$$

The deposit theft rate of the blockchain shared bicycle deposit management system is

$$T_3 = NAT_3\cdot\left(\frac{r}{n}\right)^m. \quad (7)$$

4.3. Simulation and Analysis. In the simulation experiment, the number of central nodes in the enterprise-led deposit management system CN is equal to 1. The probability of hacking the center node successfully by an attacker is set to 0.1. The number of central nodes in the deposit management system led by enterprises and signing banks CN is equal to 2, the security parameter of the deposit η is set to 0.9, and the probability of hacking the center node successfully by an attacker is set to 0.1. The number of copies of deposit accounts in the deposit management system of shared bicycles using blockchain technology is set to 3. As an extreme case, we set the number of blocks forged by the attacker as $q = n/3$. With the increase in the number of deposit accounts, the deposit theft rates for the three systems are shown in Figure 7.

As shown in Figure 7, when the amount of deposit accounts increases from 50 to 500, the deposit theft rates of three deposit management systems for shared bicycles T_1, T_2, and T_3 vary greatly. The security of the deposit management system led by enterprises is very low. Once the only deposit storage node is breached, the deposit theft rate T_1 is almost 100%, the system will crash, and all deposits will be stolen. For the deposit management system led by enterprises and signing banks, the deposit theft rate T_2 gradually increases with the increase in the amount of

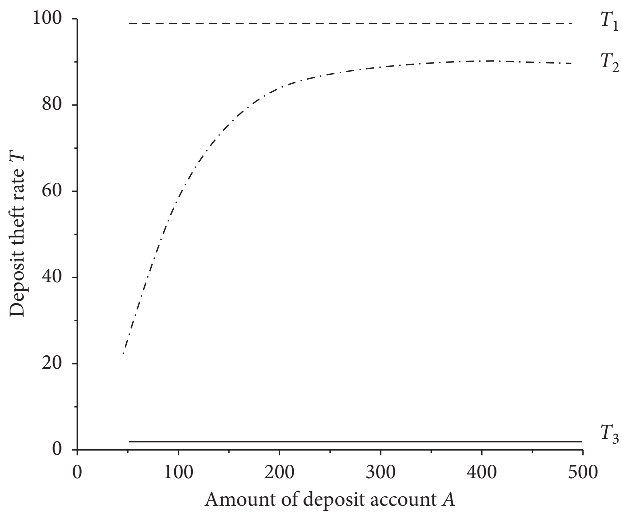

Figure 7: Operational deposit theft rate of the shared bicycle deposit management system.

deposit accounts. When the amount of deposit accounts is more than 200, the deposit theft rate tends to be 90%. For the blockchain-based shared bicycle deposit management system, the deposit theft rate T_3 is almost 0%, showing an outstanding performance in security.

5. Conclusion

As a green transportation mode, shared bicycles are experiencing rapid development all over China. However, the current management mode of shared bicycle deposits has several defects, such as the nonpublic storage of deposit, the opaque flow directions of deposit, and the delay in deposit refunds. These issues have aroused the dissatisfaction of shared bicycle users and wide attention from the society. To correct these defects in the deposit management mode of shared bicycles and promote the sustainable development of the service, this paper combines the concept of blockchain with the shared bicycle system. It is the first time this type of research has been undertaken, to our knowledge. This paper creatively constructs a deposit management system for shared bicycles based on the blockchain technology. In the deposit management system for shared bicycles built in this paper, the user deposit accounts, personal information, and transaction data are stored in blocks of the same specification. Asymmetric encryption algorithm and SHA256 algorithm are used to guarantee the security of blocks, and Merkle algorithm is used to ensure that transaction data, deposit value, and other information could not be tampered. Moreover, this system endows the supervision organizations with SPV permission to verify the authenticity of deposit refunds. Meanwhile, the smart contract of the consensus layer can monitor the transaction behaviors and deposit flows of enterprises and users in real time. It can punish enterprises transferring user deposits illegally and punish users who damage shared bicycles. Finally, in the simulation experiment, the deposit theft rate of our deposit management system is 0%, which is far better than the two current deposit management systems. Thus, the security and effectiveness of our shared bicycle deposit management system are verified. Our system eliminates the problem of information asymmetry among enterprises, users, and supervision organizations, eradicates the possibility of enterprises transferring user deposits unilaterally, and realizes the visualization of deposit accounts, the transparency of deposit whereabouts, and the management requirement of immediate deposit refunds.

The research results of this article improve the theoretical system of deposit management for the shared bicycle industry and design a set of operational programs for the scientific management of shared bicycle deposit. Meanwhile, these results are also endowed with important theoretical significance and practical value for the guarantee of user deposit security, improving the industry supervision system, reinforcement of antecedent and real-time scientific and effective supervision conducted by the government, and accelerating the innovative development of shared bicycle enterprises.

Firstly, the system proposed in our paper eliminates the centralization advantage of shared bicycle enterprises and eradicates the possibility of transferring users' deposits by enterprises at will. In this system, the transfer of deposit needs to meet the trigger conditions stipulated in the smart contract. Also, each deposit is transferred automatically by the smart contract, which means the enterprises have no right to transfer the deposits. If the deposit transfer records meet the trigger conditions, the smart contract will automatically review the rationality of related deposit transfer and publish the transaction record, and block the status and deposit value on the network layer in the form of broadcast. Therefore, users and the supervision organizations can verify the rationality of any deposit transfer in real time. Thus, our system puts an end to the transfer of user deposits caused by false transaction and finally guarantees the legitimate rights and interests of users.

Secondly, our deposit management system realizes the management requirements of deposit account visualization and the immediate deposit refunds. The deposit of the user is kept in the deposit account of the user block body. Technically, enterprises have no right to interfere with the deposit accounts of users, and the users can withdraw the deposits without waiting for the review of the enterprise or regulatory agency. At the same time, the smart contract designed by our system can monitor the user behavior in real time. If a user intentionally damages shared bicycles, the smart contract will withdraw part of the deposit to compensate related enterprise, thereby protecting the legitimate rights and interests of the enterprise.

Moreover, the proposed system increases the capability of supervision organizations to check deposit returns and realizes a multidimensional deposit supervision management mode. In this system, the deposit return record is saved in the block head by generating a hash value with the hash algorithm. Adding or deleting a deposit return record will affect the hash value. By checking the hash values between users and enterprises, the supervision organizations could verify the authenticity for deposit refunds by enterprises, in turn guaranteeing the legitimate rights and interests of related enterprises and users.

Finally, the blockchain deposit management system for shared bicycles constructed in this paper eliminates the management shortcomings of the current shared bicycle industry and reconstructs its management system. This system could record the behavior of enterprises and users comprehensively and provide real and reliable data support for the supervision of the shared bicycle market. In general, this paper provides blockchain technical support and a creative management mode for building a shared bicycle system that features honest operations of enterprises, standardized user conducts, and multidimensional regulation of supervision organizations.

6. Prospective Directions

The decentralization, visualization, and information tamper-proof characteristics of the blockchain technology could realize the openness and transparency of the industrial transaction mode and social management structure. Thus, implementation of blockchain technology can help meet the technical requirements for the revolution of the industrial structure and form in the context of supply-side reforms. In this paper, the deposit management system for shared bicycles constructed with the blockchain technology complies with the development of the society, solves the problem of unreliable enterprise deposit management credit, ensures the reasonable use of user deposits, and provides scientific technical support for the sustainable development of shared bicycles. Beyond the management of shared bicycle deposits, the proposed system still has many other aspects that deserve attention and are worth expanding. In future research, we will seek to predict user demand and plan bike delivery quantity by utilizing user transaction records stored in this system in combination with cloud computing and other technologies.

Appendix

A

```
pragma solidity ˆ0.4.2;
contract Token { //Account query
//issue Function can recharge the contract account
//transfer Function can send tokens to other accounts
//getBalance Function gets the token balance for an account
  address issuer;
  mapping (address => uint) balances;
  event Issue(address account, uint amount);
  event Transfer(address from, address to, uint amount);
  function Token() {
    issuer = msg.sender;
  }
  function issue(address account, uint amount) {
    if (msg.sender != issuer) throw;
    balances[account] += amount;
  }
  function transfer(address to, uint amount){
    if (balances[msg.sender]<amount)throw;
    balances[msg.sender] −= amount;
    balances[to] += amount;
    Transfer(msg.sender, to, amount);
  }
  function getBalance(address account)constant returns (uint) {
    return balances[account];
  }
}
contract LockAccount {//
  mapping(address => uint) private userBalances;
  function transfer(address to, uint amount){
    if (userBalances[msg.sender] ≥amount){
      userBalances[to]+=amount;
      userBalances[msg.sender] −= amount;
    }
  }
  function withdrawBalance()public{
    uint amountToWithdrew = userBalances [msg.sender];
    if (!(msg.sender.call.value(amountToWithdrew))) { throw; }
    userBalances[msg.sender] = 0;
  }
  _mapping (address => uint)private userBalances;
  mapping(address => bool)private claimedBonus;
  mapping (address => uint) private rewardsForA;
  function untrustedWithdrew(address recipient) public{
    uint amountToWithdrew = userBalances [recipient];
    rewardsForA[recipient] = 0;
    if (!(recipient.call.value(amountToWithdrew) ())) { throw; }
  }
  function untrustedGetFirstWithdrewalBonus(address recipient)public{
    if (claimedBonus[recipient]) { throw; }
    claimedBonus[recipient] = true’
    rewardsForA[recipient] += 100;
    untrustedWithdrew(recipient);
  }
```

```
    function deposit() payable public returns(bool){
      if (!lockBalances) {
        lockBalances = true;
        balances[msg.sender] += msg.value;
        lockBalances = false;
        return true;
        {throw;}
    }
    function withdraw(uint amount) payable public
returns(bool){
      if (!lockBalances && amount>0 && balances
[msg.sender] ≥ amount) {
        lockBalances = true;
        if (msg.sender.call(amount)()) {// Normally
insecure, but the mutex saves it
          balances[msg.sender] −= amount;
      }
      lockBalances = false;
      return true;
      {throw; }
    }
}
contract StopContract{//
      bool private stopped = false;
      2address private owner;
      modifier isAdmin(){
        if (msg.sender != owner){throw;}
        }
      }
      function toggleContractActive() isAdmin public{
        stopped =! stopped;
      }
      modifier stopInEmergency{if (!stopped)_;}
      modifier onlyInEmergency{if (!stopped)_;}
      function deposit()stopInEmergency public{
      }
}
```

Data Availability

No data were used to support this study.

Conflicts of Interest

The authors declare no conflicts of interest.

Authors' Contributions

All the authors contributed to the idea of this paper. D. Z. supervised the overall work. D. W. wrote the whole manuscript and polished the language of this paper. B. W. provided constructive advice to improve the manuscript.

Acknowledgments

This research was funded by the National Natural Science Foundation of China (Grant no. 71472134) and School-level major project of Beijing Wuzi University in 2020—design and function of hedging strategy calculator (Grant no. 035200120918).

References

[1] D. Zhao and D. Wang, "The research of tripartite collaborative governance on disorderly parking of shared bicycles based on the theory of planned behavior and motivation theories-a case of Beijing, China," *Sustainability*, vol. 11, no. 19, p. 54, 2019.

[2] Y. Cao and D. Shen, "Contribution of shared bikes to carbon dioxide emission reduction and the economy in Beijing," *Sustainable Cities and Society*, vol. 51, p. 10, 2019.

[3] L. Gao, Y. Ji, X. Yan et al., "Incentive measures to avoid the illegal parking of dockless shared bikes: the relationships among incentive forms, intensity and policy compliance," *Transportation*, vol. 51, pp. 1–28, 2020.

[4] B. Bachand-Marleau, *Better Understanding of Factors Influencing Likelihood of Using Shared Bicycle Systems and Frequency of Use*, Transportation Research Record, New York, NY, USA, 2018.

[5] S. Ølnes, *Beyond Bitcoin Enabling Smart Government Using Blockchain Technology*, Springer, Berlin, Germany, 2016.

[6] R. Beck, "Beyond bitcoin: the rise of blockchain world," *Computer*, vol. 51, no. 2, pp. 54–58, 2018.

[7] D. Zhao, L. Feng, and G. Liang, "Blockchain: a secure, decentralized, trusted cyber infrastructure solution for future energy systems," *Journal of Modern Power Systems and Clean Energy*, vol. 6, no. 5, pp. 958–967, 2018.

[8] T. Nugent, D. Upton, and M. Cimpoesu, "Improving data transparency in clinical trials using blockchain smart contracts," *F1000Research*, vol. 5, p. 2541, 2016.

[9] D. Knezevic, "Impact of blockchain technology platform in changing the financial sector and other industries," *Montenegrin Journal of Economics*, vol. 14, no. 1, pp. 109–120, 2018.

[10] Z. Shae and J. J. P. Tsai, *On the Design of a Blockchain Platform for Clinical Trial and Precision medicine*, IEEE, New York, NY, USA, 2017.

[11] J. Zhao, W. Deng, and Y. Song, "Ridership and effectiveness of bikesharing: the effects of urban features and system characteristics on daily use and turnover rate of public bikes in China," *Transport Policy*, vol. 35, pp. 253–264, 2014.

[12] B. Shen, Y. Shan, Y. Jia, D. Xie, and S. Zhu, "Modeling the cashflow management of bike sharing industry," Springer, Berlin, Germany, 2019.

[13] X. Liu, T. Gao, and X. B. Wang, *From High-Tech to Business Model Innovation. Regional Innovation Index of China*, Springer, Singapore, 2018.

[14] H. Xu and X. Liu, *Research on Social Governance Innovation of Shared Bikes*, Atlantis Press, Berlin, Germany, 2018.

[15] D. Yu and L. Shang, "Opportunities and challenges faced by share economy: taking sharing bicycle as an example," *DEStech Transactions on Environment, Energy and Earth Sciences*, vol. 47, 2017.

[16] M. Chen, D. Wang, Y. Sun, E. O. D. Waygood, and W. Yang, "A comparison of users' characteristics between station-based

bikesharing system and free-floating bikesharing system: case study in Hangzhou, China," *Transportation*, vol. 47, no. 2, p. 689, 2018.

[17] R. Marselli, "Treasury financing and bank lending-reserves causality: the case of Italy, 1975–1990," *Journal of Post Keynesian Economics*, vol. 15, no. 4, pp. 571–588, 1993.

[18] H. Nakamura and N. Abe, "Evaluation of the hybrid model of public bicycle-sharing operation and private bicycle parking management," *Transport Policy*, vol. 35, pp. 31–41, 2014.

[19] V. Vallurupalli and I. Bose, "Rabbit or tortoise? Rethinking customer acquisition at dravya bank," *Communications of the Association for Information Systems*, vol. 43, no. 1, pp. 378–403, 2018.

[20] S. B. Nakamoto, "A peer-to-peer electronic cash system," *Consulted*, vol. 43, 2008.

[21] S. Bogart and K. Rice, *The Blockchain Report: Welcome to the Internet of Value*, Needham Insights, New York, NY, USA, 2015.

[22] S. A. Abeyratne and R. P. Monfared, "Blockchain ready manufacturing supply chain using distributed ledger," *International Journal of Research in Engineering and Technology*, vol. 05, pp. 1–10, 2016.

[23] M. Attaran and A. Gunasekaran, "Blockchain-enabled technology: the emerging technology set to reshape and decentralise many industries," *International Journal of Applied Decision Sciences*, vol. 12, no. 4, pp. 424–444, 2019.

[24] M. L. D. Silvestre, P. Gallo, J. M. Guerrero et al., "Blockchain for power systems: current trends and future applications," *Renewable and Sustainable Energy Reviews*, vol. 10, 2019.

[25] V. K. Chattu, A. Nanda, S. K. Chattu, S. M. Kadri, and A. W. Knight, "The emerging role of blockchain technology applications in routine disease surveillance systems to strengthen global health security," *Big Data and Cognitive Computing*, vol. 3, no. 2, p. 25, 2019.

[26] S. Fernandez-Vazquez, R. Rosillo, and D. De La Fuente, "Blockchain in FinTech: a mapping study," *Sustainability*, vol. 11, no. 22, p. 6366, 2019.

[27] Q. Priore and K. Li, "Decentration transaction method based on blockchain technology. 2018 international conference on intelligent transportation, big data & smart city (ICITBS)," *IEEE*, vol. 11, pp. 416–419, 2018.

[28] A. Hari and T. V. Lakshman, "The internet blockchain: a distributed, tamper-resistant transaction framework for the internet," *ACM*, vol. 11, pp. 204–210, 2016.

[29] J. Hwang, M.-i. Choi, T. Lee et al., "Energy prosumer business model using blockchain system to ensure transparency and safety," *Energy Procedia*, vol. 141, pp. 194–198, 2017.

[30] J. Li, J. Wu, and L. Chen, "Block-secure: blockchain based scheme for secure P2P cloud storage," *Information Sciences*, vol. 465, pp. 219–231, 2018.

[31] G. Zyskind and O. Nathan, "Decentralizing privacy: using blockchain to protect personal data," *IEEE*, vol. 465, pp. 180–184, 2015.

[32] R. Wang, W. T. Tsai, J. He, C. Liu, Q. Li, and E. Deng, "Logistics management system based on permissioned blockchains and RFID technology," *White Paper*, vol. 465, 2019.

[33] V. Buterin, "A next-generation smart contract and decentralized application platform," *White Paper*, vol. 3, p. 37, 2014.

[34] R. Lai and D. L. K. Chuen, "Blockchain–from public to private," *White Paper*, vol. 2, pp. 145–177, 2018.

[35] T. Bocek and B. Stiller, *Smart Contracts–Blockchains in the Wings*, Springer, Berlin, Germany, 2018.

[36] P. DeMaio, "Bike-sharing: history, impacts, models of provision, and future," *Journal of Public Transportation*, vol. 12, no. 4, p. 41, 2009.

[37] W. Feng, Y.-G. He, H.-M. Li, and C.-L. Li, "Image encryption algorithm based on discrete logarithm and memristive chaotic system," *The European Physical Journal Special Topics*, vol. 228, no. 10, pp. 1951–1967, 2019.

[38] M. Szydlo, *Merkle Tree Traversal in Log Space and Time*, Springer, Berlin, Germany, 2004.

[39] Z. Tian, M. Li, M. Qiu, Y. Sun, and S. Su, "Block-DEF: a secure digital evidence framework using blockchain," *Information Sciences*, vol. 491, pp. 151–165, 2019.

[40] Z. Zheng, S. Xie, H. N. Dai, and X. Chen, "Blockchain challenges and opportunities: a survey," *International Journal of Web and Grid Services*, vol. 14, no. 4, pp. 352–375, 2018.

[41] B. Wang, J. Park, and J. H. Park, "A lightweight hash-based blockchain architecture for industrial IoT," *Applied Sciences*, vol. 9, no. 18, p. 3740, 2019.

[42] D. Johnson, A. Menezes, and S. Vanstone, "The elliptic curve digital signature algorithm (ECDSA)," *International Journal of Information Security*, vol. 1, no. 1, pp. 36–63, 2001.

[43] S. Pote, V. Sule, and B. K. Lande, "Arithmetic of koblitz curve SECP256K1 used in bitcoin cryptocurrency based on one variable polynomial division," 2019.

[44] P. Wei, D. Wang, Y. Zhao, S. K. S. Tyagi, and N. Kumar, "Blockchain data-based cloud data integrity protection mechanism," *Future Generation Computer Systems*, vol. 102, pp. 902–911, 2020.

[45] S. Philippe, A. Glaser, and E. W. Felten, "A cryptographic escrow for treaty declarations and step-by-step verification," *Science & Global Security*, vol. 27, no. 1, pp. 3–14, 2019.

[46] A. Aggarwal, P. Chaphekar, and R. Mandrekar, "Cryptanalysis of bcrypt and SHA-512 using distributed processing over the cloud," *International Journal of Computer Applications*, vol. 128, no. 16, pp. 13–16, 2015.

[47] W. Dai, J. Deng, Q. Wang, C. Cui, D. Zou, and H. Jin, "SBLWT: a secure blockchain lightweight wallet based on trustzone," *IEEE Access*, vol. 6, pp. 40638–40648, 2018.

[48] G. Governatori, F. Idelberger, Z. Milosevic, R. Riveret, G. Sartor, and X. Xu, "On legal contracts, imperative and declarative smart contracts, and blockchain systems," *Artificial Intelligence and Law*, vol. 26, no. 4, pp. 377–409, 2018.

[49] S. Wang, L. Ouyang, Y. Yuan, X. Ni, X. Han, and F.-Y. Wang, "Blockchain-Enabled smart contracts: architecture, applications, and future trends," *IEEE Transactions on Systems, Man, and Cybernetics: Systems*, vol. 49, no. 11, pp. 2266–2277, 2019.

[50] N. Liu, M. Xu, B. Gao, and G.-Q. Liu, "A novel intelligent classification model for breast cancer diagnosis," *Information Processing & Management*, vol. 56, no. 3, pp. 609–623, 2019.

[51] W. Qi, Z. Wang, X. Wang, K. Qiu, C. Jia, and C. Jiang, "LSC: online auto-update smart contracts for fortifying blockchain-based log systems," *Information Sciences*, vol. 512, pp. 506–517, 2020.

[52] D. Wang, D. Zhao, B. Wang et al., "Industrial engineering and engineering management," 2019.

[53] F. Tian, "A supply chain traceability system for food safety based on HACCP, blockchain & internet of things," 2017.

Hindawi
Journal of Advanced Transportation
Volume 2020, Article ID 8868533, 10 pages
https://doi.org/10.1155/2020/8868533

Research Article

The Robustness and Sustainability of Port Logistics Systems for Emergency Supplies from Overseas

Yanyu Chen,[1] **Wenzhe Zheng**,[1] **Wenbo Li**,[1] **and Yimiao Huang**[2]

[1]*College of Economics and Management, Zhejiang Normal University, Jinhua 321004, Zhejiang, China*
[2]*School of Public Administration, Changchun University of Technology, Changchun 130012, Jilin, China*

Correspondence should be addressed to Yanyu Chen; tyler4585@zjnu.edu.cn

Received 30 May 2020; Revised 14 July 2020; Accepted 8 August 2020; Published 1 September 2020

Academic Editor: Sang-Bing Tsai

Copyright © 2020 Yanyu Chen et al. This is an open access article distributed under the Creative Commons Attribution License, which permits unrestricted use, distribution, and reproduction in any medium, provided the original work is properly cited.

When the epidemic comes, in addition to eliminating people's panic, quickly enacting corresponding laws and implementing corresponding policies, and isolating infected people, providing emergency supplies are of course essential. The purpose of this article is to study the robustness and sustainability of the port logistics system for outbreak emergency supplies from overseas. This paper analyzes the sustainable development capability of the port logistics system for outbreak emergency supplies from overseas and formulates response strategies and robust collaborative optimization methods. The optimized and robust system is obtained through formula derivation and analysis, which realizes the coordinated optimization of emergency logistics infrastructure positioning and emergency rescue vehicle path positioning and minimizes the economic loss caused by the outbreak. Research data show that the shortest path can be planned between each material supply location. The research results show that the proportion of demand fluctuations during the outbreak is 6.5%, the time window needs to be controlled between 0 and 600, and the robustness and sustainability of the port logistics system have saved the time of the entire process by about 45%, greatly optimizing the delivery route and delivery time. The robustness of the logistics system can be widely used in emergency events.

1. Introduction

The logistics industry is known as the "third profit source," and the logistics industry has now become an indispensable strategic industry for development at home and abroad [1]. As consumption in modern society begins to diversify, material production begins to soften, and economic circulation begins to become more efficient; everyone's requirements for the level and quality of logistics services begin to increase. Therefore, the quality of logistics services is extremely important in the future development of the logistics industry, that is, to provide customers with high-quality products at a specified time and a specified location in an appropriate quantity and at a price generally acceptable to the public [2].

With the deepening of China's internationalization, domestic and foreign exchanges are becoming more frequent, and the port logistics system has developed by leaps and bounds. However, in recent years, major foreign epidemics have occurred frequently. Port logistics is the place most affected by overseas epidemics. Being able to carry out the exchange of port logistics without affecting the production and life of our people requires serious consideration. This also requires us to study the robustness and sustainability of the port logistics system for outbreak emergency materials from overseas. At present, China's emergency logistics planning system in the organization link is not yet perfect. Although each department of the government has its own emergency plan, the plans between the departments cannot be well communicated and communicated [3]. This has led to the inability to effectively establish effective communication in the face of overseas epidemics, to prevent the overseas epidemic from being introduced into China in port logistics in time and ultimately to avoid the paralysis of port logistics, which requires us to deal with the epidemic from overseas. The robustness and sustainability of the port logistics system of emergency supplies are carefully studied to ensure the production and life of our people [4].

In the era of rapid development of science and technology in our country, once the epidemic situation comes, our country must respond within the first time and timely plan the human and material resources for rescue. After purchasing emergency supplies in large quantities abroad, they should be promptly transported back to the epidemic location for support. At this time, the powerful port logistics system directly determines the progress of effective epidemic control [5, 6]. In our country, if the logistics system presents obstacles in any logistics node such as outbound, transportation, and transshipment, a small one will reduce the distribution efficiency and a large one may lead to the paralysis of the entire logistics system. This paper analyzes the sustainable development capabilities of the port logistics system for outbreak emergency materials from overseas and formulates coping strategies and robust collaborative optimization methods. The optimized and robust system is obtained through formula derivation and analysis, which realizes the coordinated optimization of emergency logistics infrastructure positioning and emergency rescue vehicle path positioning and minimizes the economic loss caused by the outbreak. Research data show that the robustness and sustainability of the port logistics system can help plan the shortest path between material supply locations. No problem in the logistics system is allowed to fail during this time period, so the robustness of a logistics system is very important. In the logistics transportation process, optimizing the shortest route and increasing the number of warehouse centers and the amount of stored materials will also decide the sustainable development of China's port logistics system [7].

2. Proposed Method

2.1. Architecture and Process of Emergency Logistics System. The emergency logistics system is composed of emergency command department, emergency logistics node, and emergency logistics information system [8]. The main work of the emergency command department is to consider the needs of emergency supplies, customize emergency logistics plans, make a backup support plan coordinated by various departments, adjust emergency logistics, and organize the information on the supply and demand of materials [9]. Emergency logistics nodes mainly include warehouses for emergency supplies, emergency distribution centers, rescue and transportation centers, and economic assistance stations [10]. The main task of the logistics node is to be responsible for the management of procurement, warehousing, transportation, distribution, recycling, and other aspects. The emergency logistics information system runs through all links in logistics. The main functions of the system are to save emergency-related resources, monitor real-time logistics dynamics, handle emergency events, and manage data [11]. The emergency logistics system process mainly includes procurement, warehousing, transportation, distribution, recycling, and other links. Each link is important to ensure that emergency supplies can be transported to the designated location in a timely and accurate manner, improve emergency equipment protection, and save costs [12, 13].

2.1.1. Emergency Logistics Procurement. When an epidemic occurs in an area, the reserves of emergency supplies are small and cannot meet the needs in front of the front [14]. Many daily supplies of daily supplies are not enough. In general, most supplies of living supplies and medical supplies do not promote storage. Therefore, emergency storage can be combined with actual item reserves and negotiated agreement reserves [15]. The signing of the agreement means that the civil affairs department signs the purchase agreement after consulting with the overseas company providing emergency supplies in advance; in case the epidemic situation suddenly comes, the contracted company quickly dispatches overseas resources to provide sufficient high-quality materials [16]. This can not only reduce the series of expenses consumed for storing materials but also meet the material needs of the front line in time and avoid inflation caused by the shortage of materials.

2.1.2. Emergency Logistics Warehousing. Tianjin, Guangzhou, and other coastal cities need to be built into overseas epidemic emergency supplies storage bases, gradually increasing the number of emergency storage material warehouses and gradually forming a complete emergency logistics infrastructure [17]. In addition to tents, the types of storage materials should also increase the storage capacity of warehouses that use more materials during the period when epidemics spread such as medical materials and daily necessities. There are also optimization of storage capacity and professional equipment in warehouses, proper arrangement of storage plans, and optimization of warehouse space [18].

2.1.3. Emergency Logistics and Transportation. Various logistics companies need to set up emergency logistics transportation fleets to ensure sufficient capacity and reasonable coordination when the epidemic situation comes. After its establishment, it is necessary to conduct emergency drills from time to time to fully explore the stamina of transportation and, at the same time, pay attention to the connection between port material supply and transportation using GIS and GPS technology to control the emergency logistics transportation in real time and receive the latest developments at any time during the transportation of materials [19, 20]. Relevant departments and people must cooperate to provide a "green channel" for emergency logistics and transportation and implement the principle of priority. The transportation department and the public security department are responsible for arranging the safety protection of emergency logistics transportation, timely handling of various problems that may occur in the transportation process, and providing safe transportation guarantee [21].

2.1.4. Emergency Logistics and Distribution. The emergency distribution center needs to be located in a convenient location around the epidemic area, and the space needs to be sufficient to ensure that the emergency supplies are smoothly loaded and unloaded. The distribution center is responsible for the recycling of emergency supplies for reuse [22]. After the epidemic has passed, return the position to the local emergency supplies storage warehouse. In addition, the distribution center must collect the types and quantities of the missing materials in detail and respond quickly and accurately to the emergency command department according to the epidemic situation and the lack of emergency supplies [23].

2.1.5. Emergency Supplies Distribution Link. Reusable emergency supplies such as tents need to be cleaned, repaired, and recycled on time. Relevant departments need to formulate recycling requirements to tell everyone to cherish the materials. The recovered materials are stored in emergency reserve warehouses at all levels of the government. Improving the recovery and repair quality of emergency supplies are the two most important requirements for handling materials. The entire process is shown in Figure 1.

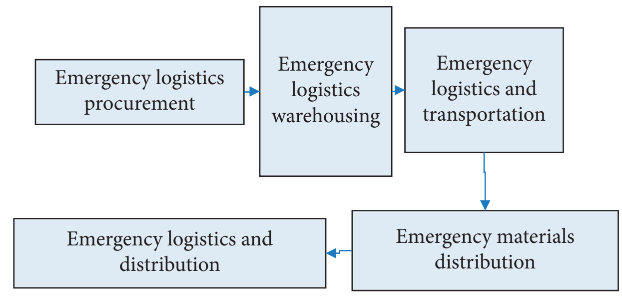

Figure 1: Emergency logistics system structure.

2.2. Countermeasures for the Development of China's Port Logistics

2.2.1. Scientific Planning. Optimize China's port system. Only after detailed planning can the port resources be used rationally [3]. When using resources, extravagance or taste is avoided.

2.2.2. Taking Advantage of Development. Give play to the role of bonded areas. Full freedom is given to the company's asset size, capital investment, and business scope in the bonded zone, and the establishment of a bonded zone rule suitable for its own port is in line with overseas economic development.

2.2.3. Reasonable Layout. Speed up the construction of the port transportation network and adopt the waterway transportation method. Strengthen the construction of port hub railways. Improve the technical level of highway passages, properly allocate some materials to waterways and railways to prevent congestion of transportation passages, and ensure the sustainability of ports [24, 25].

2.2.4. Changing Roles. Constantly update the logistics service concept. Continuously create new products for discovery services, with a focus on accelerating the construction of logistics areas and taking service diversification as the focus of service innovation. To meet the needs of the public as the ultimate goal, China's port logistics system will be built into a new type of logistics center that mainly relies on modern transportation, integrating storage, packaging, distribution, processing, information services, and other service functions. The transportation node is transformed into a higher level logistics location [26].

2.2.5. Scientific and Technological Innovation. Improve logistics technology and information level. Increase investment in the construction of information infrastructure, and at the same time, introduce cutting-edge technology from overseas [27]. Make full use of advanced information technology, establish a port logistics information network and a logistics public information communication platform, and formulate a unified port logistics system information standard as soon as possible so that the transport port has the function of logistics information, in order to provide better quality, efficient, and comprehensive port services in science and technology [28].

2.2.6. People-Oriented. Emphasis is provided on personnel training in the logistics service industry. It is necessary to increase investment in logistics professional colleges, especially in the fields of future work and port logistics enterprises. In addition to formal logistics courses offered by formal colleges and universities, enterprises train and educate employees within a certain period of time so that their professional knowledge can keep up with the development trend of the modern social logistics industry. In addition, the training of corporate leaders is also very important. Only if the corporate leaders accept the cutting-edge logistics concepts earlier than the employees can they lead the employees of his company to participate more actively in the reform and development of the enterprise and the logistics industry [29].

2.3. LRP Robust Two-Layer Optimization Model for Emergency Logistics

2.3.1. Structure of Problems in Emergency Logistics. The emergency logistics facility positioning-configuration problem (LAP) and emergency supplies transportation route selection problem (VRP) are two important places in the optimization design process of emergency logistics transportation system. LAP means that there are many demand points and alternative material equipment in a designated area. From each point, the location of the alternative material equipment points, the number of materials in each alternative material equipment point, and the corresponding demand can be determined. The distribution plan and VRP are mainly designed when the location of the candidate equipment location has been determined, and the vehicle transports the material route between the locations where each material is lacking so that it reaches the shortest total route or the lowest distribution cost [30]. Rescue emergency logistics equipment positioning-vehicle routing problem is simply considered to be the integration of LRP and VRP, which effectively integrates the attributes of LAP and VRP. By constructing a robust two-layer optimization model with uncertain coefficients in order to collaboratively optimize the port logistics system of emergency supplies, in this paper, the robust optimization method is used to establish the LRP of the port logistics system of emergency supplies with hierarchical correlation. The model was deterministically transformed, and a hybrid algorithm was designed to solve the transformed deterministic planning model below [31, 32].

The construction of the model relies on the following four assumptions:

(1) There are many places that need material support and material storage warehouses, and many rescue vehicles can be purchased.
(2) The rescue vehicles depart from their respective material storage warehouses and return to the original warehouses after successfully completing the delivery task.
(3) Any two material reserve warehouses are not on the same path.
(4) There is only one rescue vehicle for each place where supplies are needed.

2.3.2. Model Construction. In the context of uncertain requirements, a model with uncertain data is constructed as follows. The upper planning from the perspective of the logistics system as a whole, considering how to meet the warehouse storage capacity constraint conditions determine the total cost of LRP (logistics equipment positioning and purchase cost of different rescue vehicles, implement emergency warehouse construction costs, buy store supplies cost, purchase cost of rescue vehicles, and rescue vehicle fixed cost and shipping costs) to achieve a smaller one. Given the location of logistics equipment and the number of vehicles purchased. The lower planning only starts from the perspective of vehicle route planning and considers the minimization of operation cost and transportation cost within a specified time. In the upper and lower planning, $d_r\,(r \in G)$ is an undetermined parameter. Upper planning: consider the minimum cost of LRP from the perspective of port logistics system of emergency supplies. The decision variable:

$$F = \min \sum_{i\in H} f_i x_i + \sum_{K\in V} \beta Q_i + \sum_{K\in V} g_K y_K + \sum_{K\in V}\sum_{i\in V} c_K z_{Ki} + \sum_{g\in S}\sum_{h\in S}\sum_{K\in V} r_K l_{gh} w_{kgh}. \tag{1}$$

(1) Objective Function. The lower-level planning minimizes the cost in the pursuit of vehicle path selection from a local perspective, mainly including the fixed operating cost and transportation cost of rescue vehicles:

$$f = \min \sum_{K\in V}\sum_{i\in V} c_K z_{Ki} + \sum_{g\in S}\sum_{h\in S}\sum_{K\in V} r_K l_{gh} w_{kgh}. \tag{2}$$

(2) Constraints. The volume of materials transported to the demand point on the same route shall not be greater than that of the rescue vehicle:

$$a \sum_{g\in S}\sum_{h\in S}\sum_{i\in H} w_{kgh} K_r \le y_K q_K, \quad \forall K \in V. \tag{3}$$

The driving distance limit of rescue vehicles is

$$\sum_{g\in S}\sum_{h\in S} I_{gh} w_{kgh} \le \mathrm{dis}_K, \quad \forall K \in V. \tag{4}$$

Formula (5) guarantees that the selected warehouse has vehicles to send out, formula (6) guarantees that the unselected warehouse cannot send out, and formula (7) guarantees that the rescue vehicles can only be allocated to the selected warehouse:

$$\sum_{r\in G}\sum_{K\in V} w_{kir} - x_i \ge 0, \quad \forall k \in V, \tag{5}$$

$$\sum_{r\in G} w_{kir} - x_i \le 0, \quad \forall k \in V, \tag{6}$$

$$z_{ki} \le x_i, \quad \forall i \in H, \forall k \in V. \tag{7}$$

The following formula indicates that the path of each vehicle is only issued from the warehouse:

$$\sum_{r\in G} w_{kir} = z_{ki}, \quad \forall i \in H, \forall k \in v. \tag{8}$$

The following formula represents two selected warehouses that are not on the same path:

$$\sum_{k\in V} w_{kgh} = 1, \quad \forall g, h \in H. \tag{9}$$

The exit point of each vehicle must be the vehicle's entry point, as shown in formula (10). Considering that the arrival time of materials cannot be determined, the parameters t_{kgh} can be assumed to be indeterminate data in this model:

$$\sum_{k\in V} w_{khg} - \sum_{k\in V} w_{kgh}, \quad \forall k \in V, \forall k \in S. \tag{10}$$

3. Experiments

3.1. Experimental Background. Since the model established above takes into account the unresolvable data of the demand for emergency supplies, it is assumed that the demand for materials in locations where the materials are lacking fluctuates within the box set. However, when an epidemic occurs, the road network is often damaged, affecting the time when the rescue vehicles actually deliver the emergency relief materials. Therefore, this experiment is based on the optimization model and then improved according to the actual measurement situation.

3.2. Source of Experimental Data. The experimental data select the basic experiment carried out by a port in Tianjin. Firstly, the relationship between the decision variables of logistics location and the decision variables of the path selection of rescue vehicles is established to establish a statistical model, and then, LAP and VRP are used for simulation. Randomly select 3 places as alternative emergency supplies distribution centers in the 100 data of the country, get three random numbers in the range of 1–99, and use these 3 numbered positions as alternative emergency supplies distribution in this calculation example The position of the center, simulating the situation of the vehicle, and the travel time of the vehicle between the points all follow the normal distribution, and the average speed of the vehicle on the way is 60 km/h. In LAP, the alternative material transportation and tour routes from the location of the material equipment to the place where the material is needed are all radial. Each alternative material equipment location transportation vehicle needs to be responsible for the alternative material transportation in multiple material shortage locations. After the transportation is completed from the alternative material facility point and returned to the nearby material facility point, this fully considers the material vehicle tour route planning using simulation models and field operations to verify the port logistics system and sustainability of the outbreak emergency from overseas.

3.3. Experimental Setup. This experiment aims at the two interconnected problems of emergency logistics equipment positioning and rescue vehicle route in the emergency logistics system. Considering that it is difficult to accurately grasp the exact epidemic occurrence area and the corresponding area's demand for materials in emergencies, the model optimizes LAP and VRP together. Although there is a relationship between the decision variables of logistics site location and the decision variables of rescue vehicle routing, there is also a sequence of decisions for the two. In the established bilevel planning model, the leading role of facility positioning decision is emphasized. To put it simply, the location decision of emergency equipment greatly affects the vehicle road planning for the rescue epidemic, and the vehicle path planning also affects the location of emergency facilities. But the positioning decision of emergency equipment has always been a priority.

The steps are as follows:

(1) The planning of the upper layer starts from the perspective of the overall emergency logistics system, and the pursuit of LRP costs should be reduced to the greatest extent.

(2) The lower-level planning is only from the perspective of vehicle route planning [33], plus the consideration of minimizing transportation costs, so as to achieve the overall optimization of port logistics equipment positioning and rescue vehicle route planning for epidemic emergency supplies from overseas as a whole and to minimize the losses caused by the epidemic.

(3) Next, the data measured by the actual situation are used to verify the practicality and transportation effect of the optimized transportation efficiency of the robust system.

4. Discussion

4.1. Logistics Analysis. From the data in Table 1 and Figure 2, it can be seen that the optimized formula of the port point under different serial numbers theoretically solves the two interrelated problems of emergency logistics equipment positioning and rescue vehicle route in the emergency logistics system, but it has not been used in real situations. Therefore, this article will use the data in the simulation of real-life training to test whether the optimized port logistics system and sustainability research have ensured the outbreak emergency response from overseas.

Randomly select 3 places from the 100 data of RC208 as candidate emergency supplies distribution centers, obtain 3 random numbers in the range of 1–99, and use these 3 numbered positions as the example alternative emergency supplies distribution center location. The data in Table 2 are mainly based on the RC208 in the RC type question bank, and based on the robustness and sustainability of the port logistics system of epidemic emergency supplies from overseas studied in this article, it supplements the fluctuation ratio of demand. Randomly choose 3 places from the 100 data of RC208 as alternative emergency supplies distribution centers, get three random numbers in the range of 1 to 99, and use these 3 numbered positions as alternative emergency in the calculation example of the location of the material distribution center. In a similar way, we can obtain data on 15 locations where emergency supplies are missing. As shown in Table 2, the time windows in nos. 1–20 are controlled between [0, 600], and the demand of each demand location fluctuates within the box set, where the data of $d*$ are shown in Table 2 and Figure 3, by calculating the demand fluctuation ratio of 6.5%.

4.2. Material Analysis. Assume that there are 5 vehicles of 2 types each as shown in Table 3, all of which are 9 yuan/km. When dealing with random delivery time, this paper will follow the normal distribution of the travel time of vehicles between each point. The average traveling speed of vehicles on the way is 60 km/h. In LAP, the alternative material transportation and tour routes from the location of the material equipment to the place where the material is needed are all radial. Each alternative material equipment location transportation vehicle needs to be responsible for the alternative material transportation in multiple material shortage locations. After the transportation is completed from the alternative material facility point and returned to the nearby material facility point, this fully considers the material vehicle tour route planning solves the problem of

Table 1: Port logistics system data.

Serial number	X coordinate (km)	Y coordinate (km)	Capacity (piece)	The construction of running
A	50	10	1510	25
B	53	70	1900	30
C	21	65	1900	25

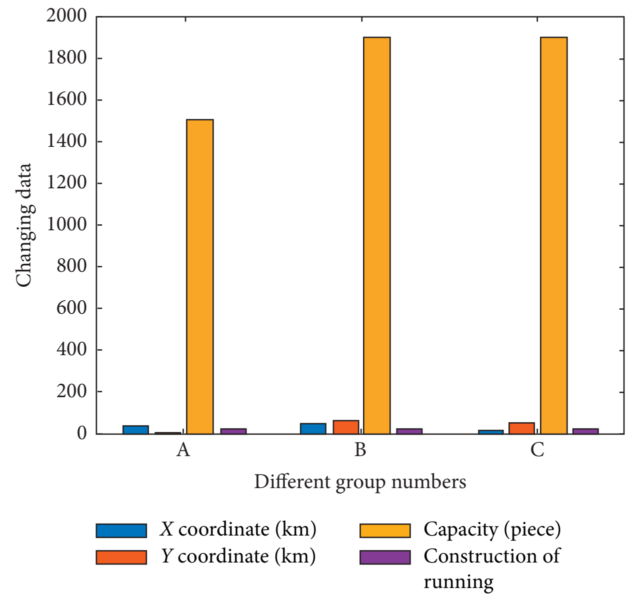

Figure 2: Port logistics system data.

Table 2: Data of emergency supplies demand points.

Serial number	X coordinate (km)	Y coordinate (km)	Demand 1 (piece)	Demand 2 (piece)	Demand 3 (piece)	Time window (m)
1	20	80	130	130	150	[0.520]
2	6	45	369	375	388	[0.560]
3	44	20	65	80	84	[0.515]
4	40	25	140	153	165	[0.534]
5	90	30	128	138	153	[0.535]
6	83	25	69	78	82	[0.555]
7	62	80	180	198	212	[0.591]
8	80	60	129	135	150	[0.569]
9	56	82	65	75	82	[0.520]
10	30	80	270	275	282	[0.550]
11	20	30	60	70	74	[0.575]
12	15	10	130	136	142	[0.568]
13	46	46	62	70	78	[0.600]
14	65	30	245	252	257	[0.520]
15	30	50	165	178	186	[0.527]
16	2	60	40	45	50	[0.538]
17	5	6	100	111	120	[0.561]
18	57	35	120	135	135	[0.506]
19	6	16	160	168	169	[0.506]
20	25	35	296	305	305	[0.256]

time and total distance of transportation. The robustness and sustainability of the port logistics system saves the time of the entire process by about 45% so that transportation costs and economic pressure will be greatly reduced. In VRP, the coordination characteristics of the transportation vehicles to the transportation of various material vehicles and the transportation of the materials and the locations of the tour routes have been fully considered; that is, the efficiency of emergency supplies transportation is improved, and it is in line with the actual situation. During this process, the

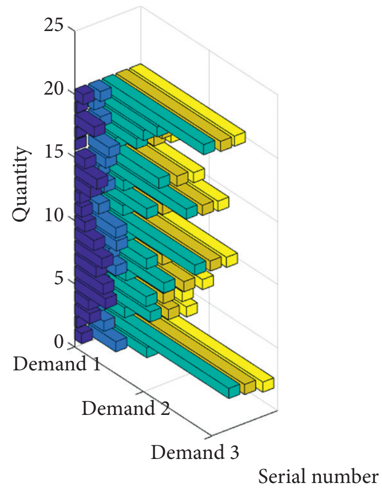

FIGURE 3: Data of emergency supplies demand points.

TABLE 3: Data from emergency supplies vehicles.

Vehicle number	Capacity (piece)	Purchase cost (yuan)	Fixed cost (yuan)	Maximum range (km)
1–5	100	200000	500	350
6–10	155	350000	600	360

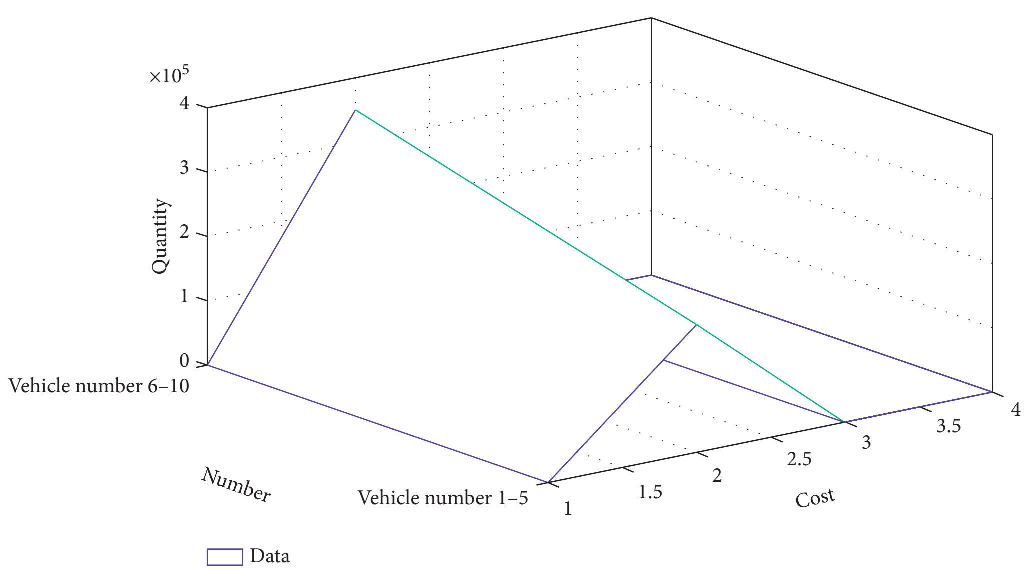

FIGURE 4: Data from emergency supplies vehicles.

transportation vehicle has accurately positioned the material facilities so that the entire logistics cost reaches the minimum. Specific data are shown in Table 3 and Figure 4.

This experiment stipulates a series of material shortage locations and alternative material equipment locations that are consistent with the actual rescue problem within the specified range. It can be seen from Table 4 and Figure 5 that the number and time of the planned road map, from which to choose the largest number, the best location, the largest material capacity of the material setting location, and to determine the best material, is missing the location of the material distribution and simple and specific transportation schemes and, at the same time, rationally arrange the corresponding best material transportation plans and

Table 4: Location, distribution vehicles, and route selection.

Alternative distribution center number	Vehicle number	Corresponding distribution route
A	4	A-6-5-14-A
	9	A-12-19-17-A
	10	A-4-3-18-A
B	6	B-9-1-10-16-2-B
	7	B-8-7-B
	8	B-15-20-11-13

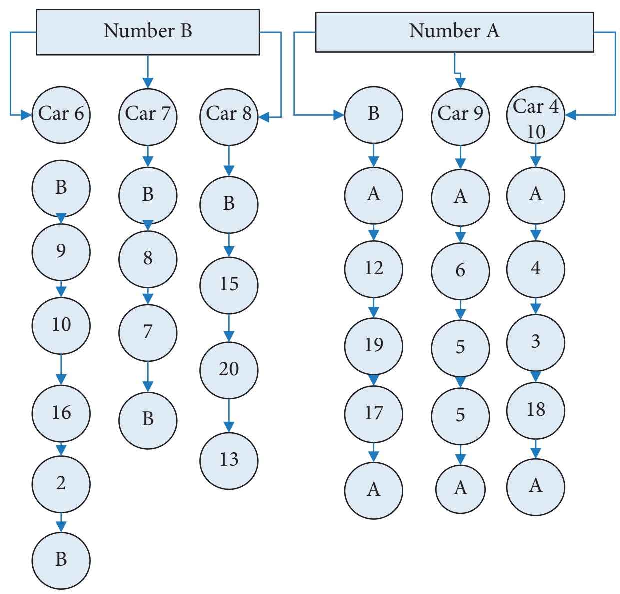

Figure 5: Location, distribution vehicles, and route selection.

alternative roads with shorter distances according to needs. In a real situation, you can make full use of the relationship between the two to better solve the problem and quickly formulate all corresponding response measures. The entire specific data are shown in Table 4 and Figure 5.

5. Conclusions

(1) Based on the study of port logistics system problems, this paper considers the optimization problems of LAP and VRP in the logistics system, as well as the uncertainty of the demand that exists in the port emergency logistics system, and emphasizes the premise of equipment positioning planning as a guide. Next, the optimized model is constructed based on the model. Among them, the upper level planning pursues the reduction of the maximum scope of LRP cost from the perspective of the port logistics system of emergency supplies. Under the conditions of the given logistics equipment location and the number of different rescue vehicles purchased, the lower-level planning only pursues the operation cost and transportation cost to the minimum when meeting the prescribed time from the perspective of vehicle driving route selection. The algorithm in the paper is used to answer the converted bilevel programming model with determinable parameters, so as to finally obtain a robust solution to the LRP problem of the emergency logistics system under uncertain conditions and realize the location of emergency logistics equipment and rescue vehicles. The roads are optimized to minimize the losses caused by sudden outbreaks and to maintain the robustness and sustainability of the port logistics system from overseas outbreak emergency logistics.

(2) Because the epidemic situation and the location of the epidemic situation are unpredictable, the location of the epidemic situation is uncertain about the location and demand for rescue emergency supplies and facilities. After the outbreak, the transportation efficiency of emergency supplies plays an important role in the rescue process. In this paper, during the process of emergency logistics mobilization and material delivery, the problem of slow dispatching time or insufficient inventory supply in the warehouse, which leads to insufficient rescue capabilities, is solved to the greatest extent. In addition, the risks in the emergency logistics process are random and may exist in a certain link. If one link destroys the entire emergency logistics system, it may be destroyed and causes greater losses. In the process of risk spreading, the improvement of the resilience of nodes in the region has a greater impact on risk spreading than the increase in the level of risk infection. Therefore, it is necessary to strengthen the reliability of its own material retention, attach importance to external communication, and ensure the smooth access of rescue channels. The increase in rescue speed has a good inhibitory effect on the spread of risks. The effectiveness of rescue speed should be considered. Excessive rescue will weaken the effect of controlling the spread and spread of risks.

(3) This paper analyzes the sustainable development capability of the port logistics system from overseas epidemic emergency supplies and formulates coping strategies and robust collaborative optimization methods. The optimized and robust system is obtained through formula derivation and analysis, which realizes the coordinated optimization of emergency logistics infrastructure positioning and emergency rescue vehicle path positioning and minimizes the economic loss caused by the outbreak. Research data show that the robustness and sustainability of the port logistics system can help plan the shortest path between material supply locations. The research results show that the proportion of demand fluctuations during the outbreak is 6.5%, the time window needs to be controlled between 0 and 600, and the robustness and sustainability of the port logistics system has saved the time of the entire process by about 45%, greatly optimizing the delivery route and delivery time, and the robustness of the

logistics system can be widely used in emergency events.

Data Availability

The data in the article are actually available.

Conflicts of Interest

The authors declare that there are no conflicts of interest in our paper.

Acknowledgments

This work was supported by the Jinhua City Federation of Social Sciences (No. YB2020060) and Jinhua City Bureau of Commerce 2020 Jinhua City E-commerce Work Research Project "Turning Crisis into Opportunity: Countermeasures and Suggestions for SMEs in Jinhua City to Resume Work and Production by Digital Trade under the Globalization of the Epidemic" (No. 22), Zhejiang Province in China.

References

[1] Q. Qu, K. Y. Chen, Y. M. Wei, Y. Liu, S. B. Tsai, and W. Dong, "Using hybrid model to evaluate performance of innovation and technology professionals in marine logistics industry," *Mathematical Problems in Engineering*, vol. 2015, Article ID 361275, 8 pages, 2015.

[2] Y. C. Wu and S. J. Y. Zhao, "Supply chain management theory and its application in animal livestock logistics," *Revista Cientifica-Facultad De Ciencias Veterinarias*, vol. 29, no. 1, pp. 43–51, 2019.

[3] J. D. Vanvactor, "Healthcare logistics in disaster planning and emergency management: a perspective," *Journal of Business Continuity & Emergency Planning*, vol. 10, no. 2, pp. 1–20, 2017.

[4] J. Guo, J. Pan, J. Guo, F. Gu, and J. Kuusisto, "Measurement framework for assessing disruptive innovations," *Technological Forecasting & Social Change*, vol. 139, pp. 250–265, 2018.

[5] S. Mustari, "Strategic port management – between tradition and reform," *Jurnalul De Studii Juridice*, vol. 1-2, no. 1-2, pp. 123–132, 2018.

[6] V. Mirzabeiki, P. V. Sjöholm, and Per Sjöholm, "Collaborative tracking and tracing applied on dry ports," *International Journal of Logistics Systems and Management*, vol. 25, no. 3, p. 425, 2016.

[7] L. R. d. O. Andr eacute a and d. O. M. C. Lucas, "Evaluating the logistics performance of Brazils corn exports: a proposal of indicators," *African Journal of Agricultural Research*, vol. 11, no. 8, pp. 693–700, 2016.

[8] C. Nguyen and T. Notteboom, "Dry ports as extensions of maritime deep-sea ports: a case study of vietnam," *Journal of International Logistics and Trade*, vol. 14, no. 1, pp. 65–88, 2016.

[9] A. K. Y. Ng, Z. Yang, S. Cahoon, and P. T.-W. Lee, "Introduction: port, maritime logistics, and regional development," *Growth and Change*, vol. 47, no. 3, pp. 346–348, 2016.

[10] T. G. Péra and J. V. Caixeta-Filho, "Impact of vertically integrated road transport on Brazilian sugar export logistics: a mathematical programming application," *International Business Research*, vol. 9, no. 12, p. 85, 2016.

[11] A. Suárez-Alemán, T. Serebrisky, and O. Ponce de León, "Port reforms in Latin America and the Caribbean: where we stand, how we got here, and what is left," *Maritime Economics & Logistics*, vol. 20, no. 4, pp. 495–513, 2018.

[12] R. Mangiaracina, A. Perego, and G. Salvadori, "A comprehensive view of intelligent transport systems for urban smart mobility[J]," *International Journal of Logistics*, vol. 20, no. 1, pp. 1–14, 2016.

[13] R. D. Soliani and P. P. d. S. Guedes, "Logistics aspects of transport modalities on the exports of raw sugar," *European Scientific Journal, ESJ*, vol. 12, no. 16, pp. 345–362, 2016.

[14] G. Zhang and B. Zhang, "Optimization model of emergency medical supplies dispatching," *Investigacion Clinica*, vol. 60, no. 3, pp. 603–608, 2019.

[15] Y. Gu and S. Gao, "Analysis on the logistics cost control of self-logistics system in the electric business enterprise," *American Journal of Industrial and Business Management*, vol. 6, no. 12, pp. 1113–1121, 2016.

[16] X. Huang and L. Song, "An emergency logistics distribution routing model for unexpected events," *Annals of Operations Research*, vol. 269, no. 6, pp. 1–17, 2018.

[17] H. Zhao, C. Niu, T. Zhang, and S. Cai, "Review and prospect of emergency logistics under uncertainty conditions," *Journal of Risk Analysis and Crisis Response*, vol. 8, no. 2, p. 101, 2018.

[18] M. Benabdouallah, C. Bojji, and O. E. Yaakoubi, "Sector prioritisation in Rabat region for emergency management," *International Journal of Emergency Management*, vol. 14, no. 1, p. 1, 2018.

[19] J. Clarke, J. A. V. Gascon, and J. A. Ferland, "A capacitated vehicle routing problem with synchronized pick-ups and drop-offs: the case of medication delivery and supervision in the DR Congo," *IEEE Transactions on Engineering Management*, vol. 64, no. 3, pp. 327–336, 2017.

[20] A. M. Eassa, M. Elhoseny, M. Hazem, El-Bakry, and A. S. Salama, "NoSQL injection attack detection in web applications using RESTful service," *Programming and Computer Software*, vol. 44, no. 6, pp. 435–444, 2018.

[21] V. K. Senthil Ragavan, M. Elhoseny, and K. Shankar, "An enhanced whale optimization algorithm for vehicular communication networks," *International Journal of Communication Systems*, Article ID e3953, 2019.

[22] J. Meng, "Teaching research and practice of logistics management," *Journal of Jilin Education Institute*, vol. 32, no. 11, pp. 98–100, 2016.

[23] D. Hrušecká, M. Pivnička, and R. B. Lopes, "Logistics management as a system constraint," *Polish Journal of Management Studies*, vol. 15, no. 1, pp. 76–87, 2017.

[24] M. V. Kajresheva, "The system of effective management of transport and logistics company," *Proceedings of the Voronezh State University of Engineering Technologies*, vol. 79, no. 1, pp. 432–437, 2017.

[25] T. Gaber, S. Abdelwahab, M. Elhoseny, and A. E. Hassanien, "Trust-based secure clustering in WSN-based intelligent transportation systems," *Computer Networks*, vol. 146, pp. 151–158, 2018.

[26] G. Jie and Z. Mingliang, "Internet of things management mode and multi-dimensionally collaborative evaluation method for agricultural product logistics service," *International Journal of Smart Home*, vol. 10, no. 10, pp. 1–8, 2016.

[27] Z. Lv, B. Hu, and H. Lv, "Infrastructure monitoring and operation for smart cities based on IoT system," *IEEE Transactions on Industrial Informatics*, vol. 16, no. 3, pp. 1957–1962, 2020.

[28] U. Sallnäs, “Coordination to manage dependencies between logistics service providers and shippers,” *International Journal of Physical Distribution & Logistics Management*, vol. 46, no. 3, pp. 316–340, 2016.

[29] H. Fu, “Integration of logistics simulation technology and logistics learning factory in a two-stage teaching method for logistics management courses,” *International Journal of Emerging Technologies in Learning (iJET)*, vol. 12, no. 9, p. 62, 2017.

[30] M. Giuffrida, R. Mangiaracina, and A. Perego, “Cross border B2C e-commerce to Greater China and the role of logistics: a literature review,” *International Journal of Physical Distribution & Logistics Management*, vol. 47, no. 6, 2017.

[31] V. Santén, “Towards more efficient logistics: increasing load factor in a shipper’s road transport,” *The International Journal of Logistics Management*, vol. 28, no. 2, pp. 228–250, 2017.

[32] W. J. Rose, D. A. Mollenkopf, C. W. Autry, and J. E. Bell, “Exploring urban institutional pressures on logistics service providers,” *International Journal of Physical Distribution & Logistics Management*, vol. 46, no. 2, pp. 153–176, 2016.

[33] S. Wan, X. Li, Y. Xue et al., “Efficient computation offloading for Internet of vehicles in edge computing-assisted 5G networks,” *The Journal of Supercomputing*, vol. 76, no. 4, 2019.

Hindawi
Journal of Advanced Transportation
Volume 2020, Article ID 8856360, 11 pages
https://doi.org/10.1155/2020/8856360

Research Article

Safety Monitoring of Expressway Construction Based on Multisource Data Fusion

Dianliang Xiao,[1] Tiantao Zhang,[2] Xudong Zhou,[3] Guangshun Zheng,[2] and Haoran Song [1]

[1]*Transportation Safety Research Center, China Academy of Transportation Sciences, Beijing 100029, China*
[2]*Qilu Transportation Development Group, Jinan 250014, Shandong, China*
[3]*Guangdong Highway Construction Co., Ltd., Guangzhou 510699, Guangdong, China*

Correspondence should be addressed to Haoran Song; songhr@motcats.ac.cn

Received 16 June 2020; Revised 14 July 2020; Accepted 31 July 2020; Published 1 September 2020

Academic Editor: Sang-Bing Tsai

Copyright © 2020 Dianliang Xiao et al. This is an open access article distributed under the Creative Commons Attribution License, which permits unrestricted use, distribution, and reproduction in any medium, provided the original work is properly cited.

China's terrain is complex, both plain, microhill (heavy-hill) and mountainous terrain; the hidden dangers of highway construction are prominent. Construction site management, production safety management, and construction personnel management are difficult, and it is necessary to borrow advanced technology to establish information, and it is necessary to borrow advanced technology to establish information system to realize the visualization of safety monitoring. In the construction of highways, mountainous terrain is often complicated due to complex terrain, high mountains, and deep valleys. Excavation of the mountain mass is required to form high and steep slopes. For successful projects, safety monitoring is particularly important. Multisource data fusion is one of the computer application technologies. It is an information processing technology that is automatically analyzed and synthesized under certain criteria to complete the required decision-making and evaluation tasks. This paper analyzes high-speed data in the context of multisource data fusion. *Study on highway slope construction safety monitoring.* BP neural network fusion technology of multisource data fusion technology is used. A high-speed breccia-bearing silty clay slope is taken as the research object. The feedback information about the deployed monitoring system is fully used in the slope design and construction. The construction design parameters are reversed to predict the stability of the slope and ensure the safety of construction and operation of similar slopes of the entire expressway. The research in this paper finds that the maximum deviation between the slope displacement value and the measured value obtained by the slope monitoring based on multisource data fusion in this paper is 7.53%, which is less than 10%, which verifies the feasibility of the method in this paper. The research methods and ideas of this paper can also provide a reference for similar engineering research.

1. Introduction

At present, general highway construction project companies and higher-level units cannot implement real-time, comprehensive, and image-based safety monitoring of construction sites due to traffic and environmental reasons: construction management efficiency is not high and managers are struggling with high-load and high-intensity inspections on construction sites or unannounced inspections; many safety management actions are ex post facto. Generally, it is not until a hidden safety hazard appears or a safety accident occurs after some time that it is discovered. It may even take some time for the safety problem to be effectively corrected. The existing methods are difficult to implement real-time command on the construction site, which requires the personnel of all parties to be concentrating on the site. It lacks intuitive on-site video data, and it is difficult to supervise the work of the supervision station, which will inevitably affect the analysis of the cause of the accident and the division of responsibilities. Safety production management is difficult and has also gradually increased. Under some occasions, certain environments, and other major dangerous sources, there is a dire need to use advanced science and technology to establish real-time traceable dynamic engineering archives and information-oriented construction site safety monitoring systems, to provide powerful technical means to improve the work efficiency of on-site management personnel, reduce the probability of accidents in highway construction, and create a “safe construction site” through visualization and information technology, which can provide a strong guarantee for the safe production and emergency rescue of engineering projects.

The highway construction project has the characteristics of many construction points, long lines, remote geographical locations, inconvenient transportation, and many units participating in the construction. The hidden safety hazards are particularly prominent [1]. Nowadays, the proportion of bridges and tunnels on expressways is generally high, and there are many key projects such as long tunnels, high pier bridges, and high slopes, such as a large number of waterworks, cross-road bridges, cross-rail bridges, and overpasses; the terrain and geological conditions are complex and result in extensive Karst development, rich groundwater, faults, and other bad geology, complex construction site management, difficult construction conditions, and difficult access roads [2]. Slopes are used to protect the stability of the roadbed. Slopes with a certain slope are made on both sides of the roadbed. However, under certain conditions, landslides and collapses may occur. Buried houses increase huge operation and maintenance costs, so the monitoring of slopes in highway construction safety monitoring is of great significance to ensure the safe operation of highways [3, 4].

HUANG Yong used the support mechanism of the high slope of the roadway in the highway reconstruction project and optimized the support scheme. Taking the left side of the K1415 + 200 high slope on the Liunan (Liuzhou to Nanning) highway as an example, the FLAC3D numerical method was first used. The influence of slope excavation on the stability of the slope and then an orthogonal test was designed to analyze the influence of anchor angle, anchor length, and anchor spacing on the safety factor of the slope during anchor support. In another study, Huang Yong changed slope safety factor under the conditions of antislide piles and excavation before the original slope construction. Monitoring points were set by the slope height. The author analyzed the horizontal and vertical displacement, and the stress of slope soil was studied with a strain increment cloud map. The results indicate that although the author’s method is difficult to construct, it is economical and safe and its coefficient is high. Finally, the support effects of the two support schemes were compared in his study [5, 6]. The representative design elements of road geometry are longitudinal slope, flat curve radius, superelevation, and gentle curve. The design criteria of these elements are combined in various ways according to the function of the road. WU Hai-bao divided highways into homogeneous sections based on longitudinal slopes and flat curve radii. The author matched the data required for analysis of various links and used the established data to establish a safety performance function. Finally, a collision correction factor that could explain the exposure rate of traffic accidents was calculated. When the threshold of the horizontal curve radius $R = 1000$ m is set to 1.0, the collision correction coefficient of $R = 300$ m is calculated as 1.33, and the accident exposure rate is increased by 33%. When the critical 0% threshold is set to 1.0, the collision correction coefficient indicates that the accident exposure rate decreases on the uphill and rises on the downhill. The research results can be used as the basic data for the geometric design of expressways during the improvement period [7, 8]. Yang et al. targeted the current situation of single safety monitoring information for construction projects, slow information feedback analysis, and the inability of participants to work together. The proposed system was also suitable for modern information technology and monitoring indicators and control points of the existing construction projects, to obtain comprehensive information on monitoring targets, including building entity information, construction site environmental information, and security ontology knowledge information. From the perspective of information collaboration, Yang et al. proposed a security monitoring information collaboration system for construction projects based on the integrated information of the data warehouse integrated monitoring target, including an information acquisition module, information processing module, and information collaboration module. All the participants can work together based on the security information control center and finally realize real-time visualization, automation, and informationization of security monitoring [9, 10]. Okumura et al. introduced the research status of ACSDINS based on analyzing the background and current research status of building safety monitoring. The system used acoustic vector sensors as the main equipment to realize signal acquisition and selected steel mold as the monitoring object. Okumura et al.’s experiments and analysis results proved the feasibility of ACSDINS. This research result was broadly applied and had important practical significance in the field of safety monitoring [11, 12].

The present study uses the BP neural network data fusion method in multisource data fusion technology to monitor and study slope safety in highway construction safety. In this paper, the data of field monitoring points are substituted into the inversion system for parameter inversion. The slope model at the monitoring points is established based on the inversion results. The analysis and calculation are compared with the measured data of the monitoring points. It is 7.53% and less than 10%. It indicates that the mechanical parameters of breccia-bearing silty clay obtained through inversion are reasonable and can be used as predictive analysis parameters of the slope stability.

2. The Proposed Method

2.1. Multisource Data Fusion Technology

2.1.1. Multisource Data Fusion. Multisource data fusion is also called multisensor information fusion [13]. Multisource data fusion technology studies how to integrate multisource data information or related auxiliary data to obtain more accurate and reliable results than using a single data [14]. It is an information processing technology that is automatically analyzed and integrated under certain criteria to complete the required decision-making and evaluation tasks. The cognitive process of objective things by humans and other animals in nature is a process of fusion of multisource information.

Multisource data fusion is divided into data-level fusion, feature-level fusion, and decision-level fusion according to the level of fusion [15]. Data-level fusion is the lowest level of fusion. It directly performs fusion processing on the sensor's observation data and then performs feature extraction and judgment decisions based on the fusion result. For example, in imaging sensors, the sensor performs image processing on a blurred image containing a certain pixel. The process is to confirm target attributes. This level of fusion is mostly used for image analysis and direct synthesis of similar radar waveforms [16].

Feature-level fusion refers to the extraction of a set of feature information from the original information provided by each sensor to form a feature vector, and the fusion of each group of information before classifying or other processing of the target, sometimes called intermediate-level fusion, a commonly used method. There are cluster analysis methods, artificial neural networks, and K-order nearest neighbor methods.

(1) Data Layer Fusion. Data layer fusion is a level of fusion that uses the direct data collected by the sensors to perform preliminary analysis and integration based on expert experience and description [17]. The main advantage of this fusion is that it processes first-level data, including proofreading and identification, analysis, and synthesis, and the resulting results can be imported into the database, can be used by system users, and can provide accuracy that cannot be provided by other fusion levels. However, its shortcomings are also obvious. Because the raw data of all sensors is collected, the system needs more storage space, the central processor that needs to process the raw data is more demanding, and the system software needs more powerful error correction capabilities. Both require high costs. This fusion level is mainly used for the synthesis, analysis, and organization of the initial image data collected by various inspection methods. Data layer fusion is shown in Figure 1.

From Figure 1, the data layer fusion first collects data information from multiple sensors, filters out the associated data information and passes it to the data layer for fusion, performs feature extraction and attribute judgment, and finally performs joint attribute judgment to output relevant data.

(2) Feature Layer Fusion. Feature-level fusion uses the feature information collected by sensors at various levels to improve target recognition capabilities. Using feature-level fusion algorithms, efforts are made to combine different types of fault features to make a comprehensive judgment [18]. The characteristic factors used in this system are as follows: connection layer, normalization, number of components, spatial information, and multiscale. Compared with a single feature recognition system, this fusion system has higher accuracy and stability and will be more widely used in applications. Feature layer fusion mostly adopts a distributed or centralized fusion structure. The specific model is shown in Figure 2.

Figure 2 demonstrates that feature layer fusion refers to extracting locally representative data information from different sensors, then combining these local data to obtain vectors with significant features.

(3) Decision-Level Integration. Decision-level fusion requires a database and expert decision-making system to analyze and reason about raw data or intermediate-level data to obtain expert-level decision-making results. This method requires a large amount of calculation, and the use of expert decision-making systems will bring high costs [19]. Decision-level fusion is a high-level fusion. The specific model is shown in Figure 3.

Figure 3 illustrates that the preliminary conclusions on the object are formed after the basic processing operations, such as preprocessing, feature extraction, and judgment and recognition, are performed on the information of different types of sensors locally. The fusion center then performs further fusion processing on the local decision results. Because the decision-making layer is the overall decision result obtained by fusion processing based on the decision results of each sensor.

2.1.2. Information Fusion Method. With the development of sensor technology, information fusion technology is also developing rapidly. Many scholars proposed a variety of effective information fusion methods, which are summarized as weighted average method, D-S evidence reasoning algorithm, Bayesian reasoning algorithm, Mann filter method, fuzzy logic reasoning algorithm, artificial neural network algorithm [20]. Each method has different advantages and disadvantages and its application scope. In practical applications, corresponding algorithms should be selected for different situations.

2.1.3. Process of Information Fusion. The process of information fusion mainly includes the following five categories:

(1) Data Input/Data Output (DAI-DAO). This is the most basic and lowest-level form of fusion, which belongs to data-level fusion. This process is mainly the fusion processing of the raw data input from multiple information sources, such as traffic flow data preprocessing.

(2) Data Input/Feature Output (DAI-FEO). This process belongs to data-level fusion, and its main function is to extract the traffic flow state characteristic information of the target road section through the fusion of multisource data according to the needs of solving practical problems.

(3) Feature Input/Feature Output (FEI-FEO). This process belongs to feature-level fusion, and its main function is to analyze and merge the spatial and temporal characteristics of the extracted traffic flow state characteristics of the target road section.

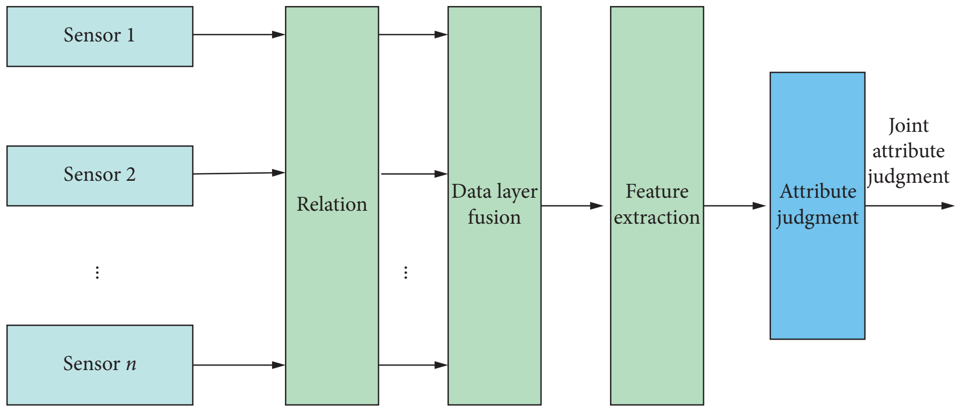

Figure 1: Data layer fusion structure.

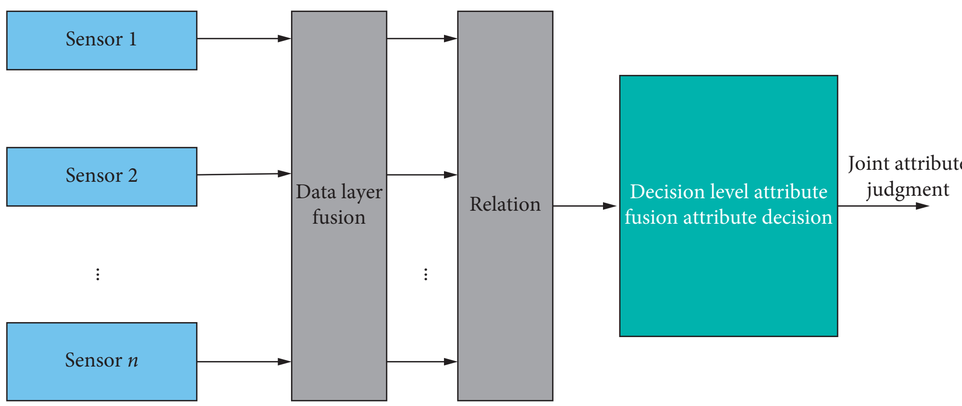

Figure 2: Feature layer fusion structure.

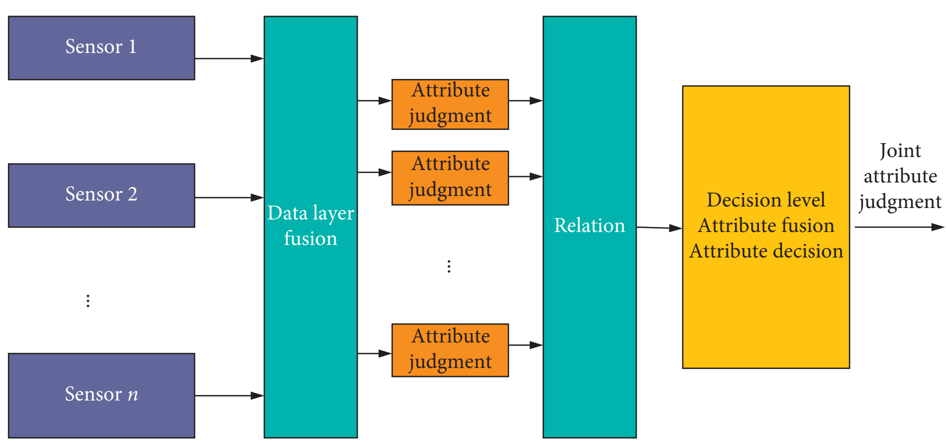

Figure 3: Decision-level fusion structure.

(4) Feature Input/Decision Output (FEI-DE). This process is a decision-level fusion. Based on the characteristics of the traffic flow state of the existing target road segment, the classification result is obtained by classifying and identifying the characteristics from different information sources.

(5) Decision Input/Decision Output (DEI-DEO). This process belongs to decision-level fusion. Its main function is to further fuse local decision-making results, making the final fusion result more accurate and reliable.

2.2. Multisource Data Fusion Model

2.2.1. First-Level Data Fusion Method. At present, the most commonly used method for preprocessing the raw data is the weighted average method [21]. The weighted average fusion algorithm uses a mathematical average formula, which is difficult to overcome the influence of some sensor failures on the measured values and the measurement speed memory. Based on the weighted average algorithm, the optimal weighting fully considers the influence of each sensor system on the measurement data and has a good strain handling ability for some sensor failures in the system; and the optimal weighted fusion algorithm is used to fuse the measurement data only. There is a need to know the variance of the sensor's measurement noise.

2.2.2. The Estimation Model of Optimal Weighted Fusion. For the measurement equation of the sensor, the mean square error is often used as the evaluation criterion for the fusion result. The optimal weighted fusion is to find the minimum mean square error. Multiply the measurement data of each sensor by a certain weight coefficient and add them. The results of data fusion are in [22]. When n sensors detect the same index parameter at different positions, the measurement equation of the i sensor is

$$Y_i = X + M_i, \quad i = 1, 2, \ldots, n. \tag{1}$$

Among them, X is the true value of the estimated parameter, Y_i is the measurement value, and M_i is the measurement noise. The measurement noise of each sensor is independent of each other. Let each sensor's weighting factor be $W_i\,(i = 1, 2, \ldots, n)$ and then get

$$\widehat{X} = \sum_{i=1}^{n} w_i \cdot Y_i, \qquad \sum_{i=1}^{n} w_i = 1. \tag{2}$$

The mean square error of the weighted estimate is

$$\sigma^2 = E[(X - \widehat{X})] = \frac{1}{\sum_{i=1}^{n} \sigma_i^2}. \tag{3}$$

It can be known from the above formula that the smaller the measurement noise variance is, the larger the sensor weight is, and the proportion of the corresponding measurement data in the weighted estimation value is higher; on the contrary, the larger the sensor noise value is, the smaller the weight is, and the measurement data is in the weighted estimation. The proportion in the value is low. The mean square error of the optimal weighted estimate is less than the variance of the measurement noise of any sensor in the system.

2.2.3. BP Neural Network Two-Level Fusion Model. An artificial neural network, which is also referred to as a neural network, is a research area used to simulate the structure and intelligence of the human brain. An important feature of it is that the output of the network is consistent with expectations through network learning ability [23, 24]. BP neural network is a feedforward network and is one of the most important models in ANN. It can be used to approximate any nonlinear continuous function with arbitrary accuracy and has good self-adaptation and fault tolerance in nonlinear systems.

(1) BP Neural Network Structure. Mostly, BP neural network has one input layer and one output layer, one or several hidden layers. Each layer is connected, and neurons in the same layer are not connected. The multilevel network architecture can ensure that the BP network can obtain more comprehensive information from the input layer and then can handle more complicated information. The structure of the BP neural network is shown in Figure 4.

X_1, X_2, ..., X_n are input values of the network, Y_1, ..., Y_n are output values of the network, and W_{ij} and W_{jk} are weights of the neural network. When the number of input nodes is n and the number of output nodes is m, a function mapping relationship from n independent variables to m dependent variables is formed.

(2) BP neural network training is required to give the network storage memory and prediction ability before BP network prediction. BP network training process:.

Step 1. The first step defines network initialization. According to the network input and output sequence (X, Y), select the number of input layer nodes n; the number of hidden layer nodes is 1, and the number of output layer nodes is m. Initially, the connection weight between the input layer and the hidden layer is W_{ij}, and the connection weight between the hidden layer and the output layer is W_{jk}, the hidden layer threshold is initialized to a, and the initial output layer threshold is set to b. At the same time, the learning rate and neuron excitation function is assigned.

Step 2. Hidden layer output calculation: according to the input variable X, the connection weight is W_{ij} between the input layer and the hidden layer, and for the hidden layer threshold a, the output H of the hidden layer is calculated:

$$H_j = f\left(\sum_{i=1}^{n} w_{ij} x_i - a_j\right), \quad j = 1, 2, \ldots, I. \tag{4}$$

In the formula, I is the number of nodes in the hidden layer and f is the excitation function of the hidden layer.

$$f(x) = \frac{1}{1 + e^{-x}}. \tag{5}$$

Step 3. Output layer output calculation: according to the output H of the hidden layer, the connection weight is Wij between the hidden layer and the output layer, and for the output layer threshold b, the predicted output O of the BP neural network is calculated:

$$O_k = \sum_{j=1}^{I} H_j w_{jk} - b_k, \quad k = 1, 2, \ldots, m. \tag{6}$$

Step 4. Error calculation: according to the predicted output O and expected output Y of the network, the prediction error e of the neural network is calculated:

$$e_k = Y_k - O_k, \quad k = 1, 2, \ldots, m. \tag{7}$$

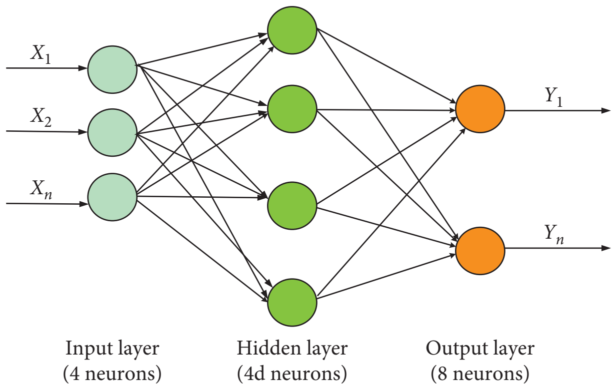

Figure 4: Structure of BP neural network.

Step 5. Weight update: update the network connection weights *wij*, *wjk* according to the prediction error *e* of the neural network:

$$w_{jk} = w_{jk} + \eta H_j e_k, \quad j = 1, 2, \ldots, I; k = 1, 2, \ldots, m, \quad (8)$$

where η is the learning rate.

Step 6. Threshold update: update the network node thresholds *a* and *b* according to the prediction error *e* of the neural network:

$$a_j = a_j + \eta H_j \left(1 - H_j\right) \sum_{k=1}^{m} w_{jk} e_k, \quad j = 1, 2, \ldots, I. \quad (9)$$

Step 7. According to the requirements of the condition, determine whether the algorithm iteration ends or not. If not, return to the second step.

(3) Multilayer Network Design Based on BP Algorithm. Multilayer network design based on the BP algorithm has different layers of the hidden layers, which can be divided into single hidden layers and multiple hidden layers [107-108]. Compared with a single hidden layer, a multihidden layer has stronger generalization ability and higher prediction accuracy, but the disadvantage is that it takes longer training time. Therefore, the choice of the number of hidden layers should be considered from the accuracy and time. For complex mapping relationships, multiple hidden layers can be selected to improve the prediction accuracy. For the recognition of general patterns, the accuracy can meet the requirements, the choice of a single hidden layer. A three-layer network can be well solved, speed up, and save time. The information capacity of the neural network (the weight of the neural network and the total number of thresholds) has a significant impact on the actual application of the network and is closely related to the number of training samples and training errors, as shown in the following formula:

$$P \approx \frac{n_w}{\varepsilon}. \quad (10)$$

In the formula, *P* is the number of training samples and is the training error and *wn* is the total number of weights and thresholds of the neural network. Therefore, under the condition of guaranteed training error, when the training samples are not enough, the information capacity of the neural network should be appropriately reduced by reducing the sample dimension.

2.3. In Situ Monitoring of Site Displacement during Highway Slope Construction

2.3.1. Slope Displacement Monitoring and Burying Design of Inclined Pipe. Expressway slopes are permanent slopes that are in service during operation. To ensure the safety of the slope, prevent slope instability and damage, and ensure the smooth passage of high-speed sections, the slope of the highway must be monitored for a long period. Obtain the stability of the slope for timely construction control and remediation [25].

(1) Monitoring purpose: the slope monitoring can be mainly used for the following two points: First, data monitoring during the construction period will guide the data results to the construction and feedback of the construction design. Secondly, based on the monitoring data of the longer observation period of the construction period, relevant geotechnical parameters, protection measures design plan, and other data, the slope stability is analyzed and calculated, and relevant reasonable suggestions are provided for maintenance and repair work during the operation period.

(2) The monitoring points are based on the actual geological conditions of the slopes of the Chang'an Expressway and the characteristics of the existing structures and carry out horizontal displacement monitoring of the slope surface, deep displacement monitoring of the slope body, vertical displacement (subsidence) monitoring of the slope surface, groundwater level monitoring, and so forth four items. This monitoring plan is designed to arrange a total of 12 observation points for horizontal displacement of the slope, 6 monitoring points for vertical displacement (settling) on the slope surface, and 6 monitoring points for the groundwater level.

2.3.2. Principle of Inclined Pipe and Slope Excavation Displacement and Water Level Monitoring. Inclinometer can measure the internal lateral displacement of rock and soil with high accuracy and is widely used for in situ monitoring of slope engineering [26]. The inclinometer consists of a probe, a cable, and a reader. Before monitoring, the inclinometer pipe must be buried in the rock and soil layer in advance, and the guide roller card of the instrument can be moved up and down in a symmetrically distributed groove in the pipe. When measuring, the sensing direction of the instrument needs to be aligned with the sliding direction of the slope, so that the sensor slowly slides into the bottom of the tube, and then remains stable for 5 to 10 minutes, so that the temperature of the sensor is close to the external underground temperature, then lifting the cable from the bottom of the measuring tube. The distance to the measuring nozzle is measured at a distance of 0.5 m and is recorded after the reading of the reading instrument is stable until the nozzle position, and then the reverse measurement is performed in the same way, and the corresponding data value is read and recorded. The inclinometer works. The principle is to use the internal pendulum of the sensor probe affected by gravity to measure the internal angle between the sensor and the plumb line and then calculate the gap between the hole axis and the plumb line by geometric theory. The horizontal displacement is calculated, and then, it is accumulated to obtain the total displacement and the deep displacement change in the entire hole along the axis of the tube.

When measured with an inclinometer, the error caused by the instrument itself and external influences should be reduced as much as possible. The forward displacement and reverse measurement should be used to measure the deep soil displacement of the slope once, and the measured value should be taken twice, mean of algebraic differences.

The MCU remote monitoring system can realize the automatic monitoring of surface displacement. Both the surface displacement monitoring data and the slope water level monitoring data can be transmitted to the computer through the instrument, and then the data can be summarized and processed for slope stability analysis and research.

2.3.3. Processing Method of Slope Monitoring Data. Obtain soil deformation monitoring data through a borehole inclinometer and then arrange the deformation process curve. Demonstrate the changes and current status of deformation traits. The monitoring results are comprehensively analyzed from space, time, and environmental factors to find the cause of curve deformation, accurately explain the deformation curve, identify the stability of the soil, provide a basis for design, construction, and engineering treatment, and provide reference data for forecasting.

2.3.4. Causes of Error in Monitoring Data and Avoiding Measures. In slope monitoring, the occurrence of errors will inevitably affect the reliability of the inclinometer monitoring results, analyze the errors of each link, and establish a scientific and reasonable error elimination method, which will directly affect the scientificity and feasibility of the monitoring results [27]. Any part of the application of the inclinometer instrument may produce errors. The inclinometer itself may have errors: offset error, zero-point drift error, and rotation error; the inclinometer tube may cause distortion errors of the tube during manufacture and installation; during the observation process, it may occur due to different ambient temperature and humidity, environmental errors; human errors are like errors in reading values, misreading values, and misremembering values; calculation errors may also occur during data processing. The above possible errors will affect the accuracy of the subsequent displacement inversion analysis and soil parameter inversion analysis results. Therefore, during the monitoring process, the error caused by the monitored monitoring data must be accurately and reasonably monitored to minimize the monitoring error.

Table 1: Important functions and functions of some BP Networks.

Function name	Corresponding function
tansig	S-type transfer function
purelin	Linear transfer function
logsig	Logarithmic S-type transfer function
deltatan	Delta function of tansig neurons
deltalog	Delta function of logsig neurons
learnbp	BP learning rules

3. Experiments

3.1. Training Sample Preprocessing. Before the BP neural network performs prediction, the input and output data need to be normalized. The data is transformed to [0,1] or [-1,1]. The purpose is to eliminate the order of magnitude difference between the data in each dimension, so that each component of the neural network has the same important status, which can effectively prevent the network prediction error from being too large due to the large order difference. The formula for transforming [0, 1] interval of data is as follows:

$$\overline{X}_i = \frac{X_i - X_{\min}}{X_{\max} - X_{\min}}. \tag{11}$$

In the formula, X_i represents the input or output data, $X_{\min}$ represents the minimum value in the data sequence, and $X_{\max}$ represents the maximum value in the data sequence. The formula for transforming the data [−1, 1] interval is as follows:

$$\overline{X}_i = \frac{2X_i\left(X_{\max} + X_{\min}\right)}{X_{\max} - X_{\min}}. \tag{12}$$

BP network training once runs the training sample forward for one round and reverses the network weight. During the training process, each round of data is best selected in different orders and used repeatedly, usually training up to 10,000 times. The sample set of the network can generally be divided into two parts: one part is used as the training set, which is used for network training; the other part is used as the test set, which is used to test the neural network. To determine whether the neural network has a good generalization ability, it is tested by using a test set. If the generalization ability of the neural network is poor, it expresses that the error is small for the training set but large for the test set. When the number of nodes in the hidden layer of the neural network is constant, there exists an optimal number of times to train, at which time the network generalization ability is optimal. When the number of training times does not reach t_0, it means that network training is insufficient. After t_0, network training is excessive. Some important functions and functions of the BP network are shown in Table 1.

Table 2: Parameters of silty clay with breccia.

Rock and soil layer	Bulk density (KN/m^3)	Modulus of elasticity (MPa)	Cohesive force (KPa)	Internal friction angle (°)	Poisson's ratio
Silty clay with breccia	19	15–27	21.5–30	20–22	0.3

Table 3: Inversion value of soil parameters.

Inversion parameters	Internal friction angle (°)	Cohesion (KPa)	Modulus of elasticity (MPa)
Silty clay with breccia	21.88	29.55	26.90
Strongly weathered marl	34.96	49.70	117.15

3.2. Selection of Input Layer and Output Layer for Building a Network Model. The measured deep displacement of the slope is monitored at intervals of 0.5 m. Model analysis is performed to calculate the displacement value of the number. 3 oblique tube as a network input sample set. During the trial calculation, it was found that the amount of input caused the network structure. It is too large, the network analysis time is long, and the convergence effect of the network is not obvious. This article improves the network design process and simplifies the network design. Considering that the inputs of each soil layer do not affect each other, the input layer is divided into 9 units, which is denoted as Ii ($i = 1, 2, 3, 4, 5$ (6, 7, 8, 9) correspond to the displacement values at the monitoring points in the model at 16.5 m, 14.5 m, 12.5 m, 10.5 m, 8.5 m, 6.5 m, 4.5 m, 2.5 m, and 0.5 m, the output layer is soil parameters, and the internal friction angle, cohesion, and elastic modulus are separately trained using three networks; the method and principle are the same. Each network has 9 input nodes and 2 output nodes, which greatly simplifies the complexity of the network structure and facilitates network convergence and analysis.

3.3. Experimental Design. The multisource data fusion BP neural network model is used to monitor the safety of the highway slope construction, and the monitoring data is analyzed and arranged. The test object is the construction section of a certain highway slope. The date of monitoring data is selected from mid-October to December.

In the early days, the data of 10 monitoring points were selected for analysis. Table 2 shows the parameters of the breccia silty clay soil on the highway slope construction section.

4. Discussion

4.1. Analysis and Comparison of Slope Displacement of Highway Slope Construction Safety Monitoring Based on Multisource Data Fusion. The measured displacement values corresponding to the different depths of the third monitoring point in the field are substituted into the trained BP neural network for inversion to obtain the soil parameters. The parameter inversion values are shown in Table 3. Comparison and analysis of slope displacement calculation analysis and actual measurement of highway safety monitoring based on multisource data fusion are shown in Figure 5 and Table 4.

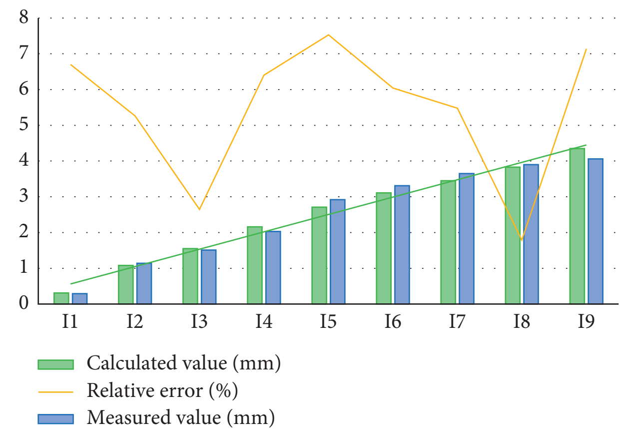

Figure 5: Analysis of the comparison between the calculated value and the measured value of the displacement at different depths at the monitoring point.

To make the comparison result more intuitive, the slope construction in which the soil parameters were simulated was inverted, and the comparison between the calculated displacement values at different depths and the measured displacement values at the fourth monitoring point is shown in Figure 6.

Combining Table 4 with Figures 5 and 6, it can be found that the maximum error between the displacement value and the measured value at different depths is 7.53%, which is less than 10%. It is reasonable, and the numerical results can be used for subsequent analysis and research. In addition, by analyzing three different parameters separately, this research method has fewer errors and can be popularized.

4.2. Analysis of Surface Horizontal Displacement Data. The surface displacement value changes continuously with the slope excavation. The surface displacement value is measured before the slope excavation as the initial displacement value. As the excavation progresses, the measured value of the slope displacement is compared with the initial displacement value to obtain the change in displacement. Then, select a part of the monitoring data of 10 monitoring points in the surface displacement monitoring data of a highway from mid-October to early December and make a displacement change trend chart. The results are shown in Figures 7 and 8.

Table 4: Comparison between calculated and measured displacement values at different depths of monitoring points.

Measuring point	I_1	I_2	I_3	I_4	I_5	I_6	I_7	I_8	I_9
Calculated value (mm)	0.31	1.08	1.55	2.16	2.71	3.11	3.45	3.83	4.35
Measured value (mm)	0.29	1.14	1.51	2.03	2.92	3.31	3.65	3.90	4.06
Relative error (%)	6.70	5.26	2.65	6.40	7.53	6.04	5.48	1.79	7.14

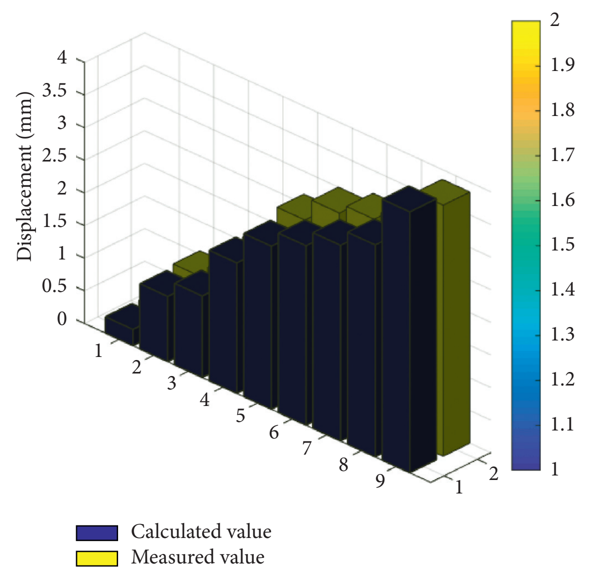

Figure 6: Analysis chart of comparison result between the calculated value and the measured value.

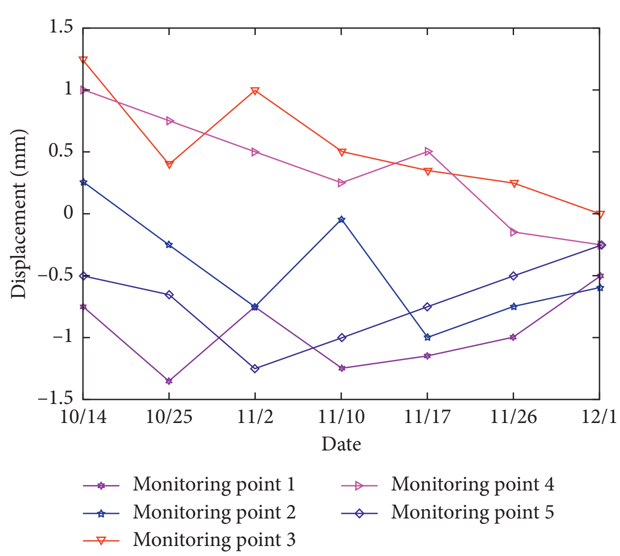

Figure 7: Surface displacement trend of monitoring points 1–5.

The value of the analysis of the surface displacement data of the monitored slope is the maximum value of the current displacement on the day and the analysis of the horizontal surface displacement data. The rainy weather and the infiltration of rainwater cause a significant change in the horizontal displacement. When the weather is fine, the soil surface water evaporates and the internal contraction will cause changes in horizontal displacement shrinkage. Months of August and September were in the rainy season, but due to better drainage facilities and timely drainage, the slope surface displacement did not change significantly. From November to December, weather was mainly sunny. It can be seen from Figures 7 and 8 that with the support of the lower slope of the slope formed, from mid-October to mid-November, the surface displacement of the slope changed a little, without significant fluctuations. By December, the slope displacement stabilized. It is consistent with the actual slope situation.

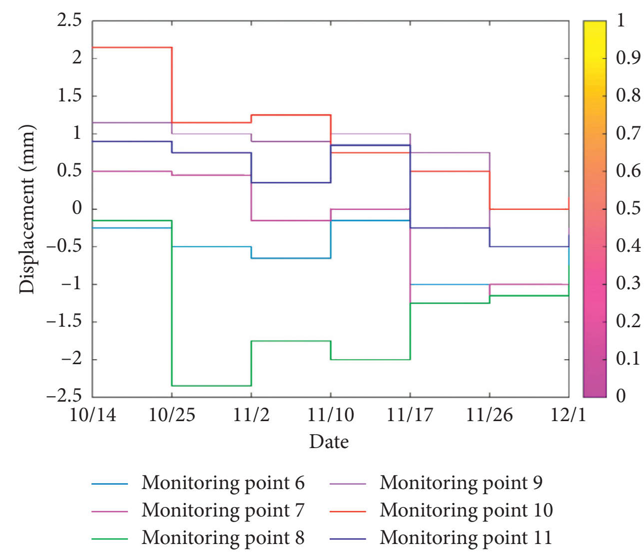

Figure 8: Surface displacement trend of monitoring points 6–11.

5. Conclusions

With the development of large-scale highway engineering construction, under the requirements of safety production and quality supervision, the construction of a construction monitoring system can provide technical support for the project site and safety management informatization construction. It provides a strong guarantee for the safety production and emergency rescue of the engineering construction, strengthens and improves the safety awareness of construction personnel at all levels, and establishes real-time and traceable dynamic engineering archives to bring daily management work to a new level. The information-oriented construction site safety monitoring system provides a powerful technical means for improving the work efficiency of site management personnel and can bring unlimited benefits with limited investment. The present research uses the BP neural network data fusion method based on the multisource data fusion method to build a model to monitor the slope construction of the expressway.

In this paper, the method of multisource data fusion is used to determine the slope parameters based on the slope characteristics of an expressway. In situ monitoring of slope displacement and soil parameter inversion is used to determine the soil parameter values, and then the slope is calculated based on the inverse soil parameter values to research on the influence of slope design parameters and treatment measures on slope stability during construction in unexcavated sections.

This study uses a multisource data fusion method to invert the soil parameters to establish a monitoring point-slope model analyze and calculate the displacement values at different depths at the monitoring points and compare with the measured displacement values. The maximum error is 7.53%, less than 10%. The results of soil parameters are reasonable and can be used for the subsequent analysis of the stability of unexcavated slopes. In addition, this paper also analyzes the horizontal surface displacement data and concludes that the slope stability is in line with the actual situation, and the feasibility of this method is verified again. The research results in this paper play an important paradigm role in the construction safety monitoring of future expressways.

Data Availability

No data were used to support this study.

Conflicts of Interest

There are no potential conflicts of interest in the paper. All the authors have read the manuscript and approved to submit it to the journal.

Acknowledgments

This work was supported by National Key R&D Program of China (no. 2017YFC0805303).

References

[1] Y. Wang, L. Wang, and C. Wang, "How eye movement and driving performance vary before, during, and after entering a long expressway tunnel: considering the differences of novice and experienced drivers under daytime and nighttime conditions[J]," *SpringerPlus*, vol. 5, no. 1, p. 538, 2016.

[2] C.-G. Qi, J.-H. Zheng, and D.-J. Zuo, "Method to reduce bump at bridge approach of open expressway using horizontal drilling replacement," *Geotechnical & Geological Engineering*, vol. 35, no. 3, pp. 1–8, 2016.

[3] D. Cheng and X. Fu, "Change characteristics and forecast research of road surface temperature on huyu expressway(hubei section)," *Meteorological and Environmental Research*, vol. 8, no. 5, pp. 92–99, 2017.

[4] H.-F. Jia, Y.-X. Li, and L.-L. Yang, "Expressway traffic joint control based on traffic state estimation," *Journal of Jilin University*, vol. 47, no. 1, pp. 76–81, 2017.

[5] Y. Huang, Y.-B. Li, and Y. Hong, "The land use change and landscape pattern response driven by YU-YI expressway(chongqing section)," *Journal of Natural Resources*, vol. 30, no. 9, pp. 1449–1460, 2015.

[6] D.-W. Wang and P. Shen, "Support mechanism and effect of cutting high slope in expressway reconstruction and expansion projects," *Changan Daxue Xuebao*, vol. 37, no. 3, pp. 39–46, 2017.

[7] H.-B. Wu, "Program feasibility numerical analysis of rail transport beneath expressway and the study of site construction control," *Value Engineering*, vol. 39, no. 2, pp. 344–352, 2015.

[8] J. Hsi, C. Gunasekara, and V. Nguyen, "Chapter 24 Characteristics of soft peats, organic soils and clays," *Elsevier Geo-Engineering Book Series*, Colombo-Katunayake Expressway, vol. 3, no. 5, pp. 681–722, Sri Lanka, 2015.

[9] G.-L. Yang, Q. Shen, and J.-N. Xu, "Site test and numerical analysis on reinforced earth retaining wall with green gabion on expressway," *Zhongguo Gonglu Xuebao/china Journal of Highway & Transport*, vol. 28, no. 6, pp. 18–23, 2015.

[10] M. A. Yue-mei and X.-G. Zhou, "Gradation ratio design and application of micro-surfacing mixtures in tanbai expressway pavement," *Western China Communications Science & Technology*, vol. 59, no. 1, pp. 123–142, 2015.

[11] U. Okumura, T. Han, and H. Zhu, "Application of the digital image technology in the visual monitoring and prediction of shuttering construction safety," *IOP Conference Series Earth and Environmental Science*, vol. 128, no. 1, Article ID 012059, 2018.

[12] Z. G. Zhu, "Research on construction technology of first pile in an urban expressway under complicated conditions," *IOP Conference*, vol. 100, no. 1, Article ID 012182, 2017.

[13] Y. Wang, X. Jiang, and D. Li, "The robust fusion of multisource gravity data based on the spherical cap harmonic model," *Acta Geodaetica Et Cartographica Sinica*, vol. 44, no. 9, pp. 952–957, 2015.

[14] L. Rui, Y. Zhang, and P. Zhang, "Location-dependent sensing data collection and processing mechanism in vehicular network," *Transactions on Emerging Telecommunications Technologies*, vol. 30, no. 11, Article ID e3283, 2018.

[15] M. Zhang and W. Li, "Collaborative classification of hyperspectral and visible images with convolutional neural network," *Journal of Applied Remote Sensing*, vol. 11, no. 4, p. 1, 2017.

[16] Y. Huang, T. Li, and C. Luo, "Dynamic fusion of multisource interval-valued data by fuzzy granulation," *IEEE Transactions on Fuzzy Systems*, vol. 26, no. 6, 2018.

[17] G. Xiong, F. Zhu, and X. Dong, "A kind of novel ITS based on space-air-ground big-data," *IEEE Intelligent Transportation Systems Magazine*, vol. 8, no. 1, pp. 10–22, 2016.

[18] T. Guo, B. Guo, and Yi Ouyang, "CrowdTravel: scenic spot profiling by using heterogeneous crowdsourced data," *Journal of Zhejiang University*, vol. 9, no. 5, pp. 1–10, 2017.

[19] S. Dong, Z. Yuan, and C. Gu, "Research on intelligent agricultural machinery control platform based on multi-discipline technology integration," *Transactions of the Chinese Society of Agricultural Engineering*, vol. 33, no. 8, pp. 1–11, 2017.

[20] K. Liu, W. Sheng, and D. Zhang, "Big data application requirements and scenario analysis in smart distribution network," *Proceedings of the CSEE*, vol. 35, no. 2, pp. 287–293, 2015.

[21] Y. Xu, Bo Du, and L. Zhang, "Advanced multi-sensor optical remote sensing for urban land use and land cover classification: outcome of the 2018 IEEE GRSS data fusion contest," *IEEE Journal of Selected Topics in Applied Earth Observations and Remote Sensing*, vol. 12, no. 6, pp. 1–16, 2019.

[22] C. Zhang, X. Yang, and H. A. O. Lina, "Lithological classification by synergizing hyperspectral Hyperion and high resolution WorldView-2 satellite images," *Journal of Chengdu University of Technology*, vol. 44, no. 5, pp. 613–622, 2017.

[23] J. Shao, "Design of textile manufacturing execution system based on big data," *Journal of Mechanical Engineering*, vol. 51, no. 5, p. 160, 2015.
[24] K. Alexiev, G. Shishkov, and N. Popova, "Human activity registration using multisensor data fusion," *Cybernetics and Information Technologies*, vol. 15, no. 7, pp. 99–108, 2015.
[25] Y.-C. Shi, G.-J. Yang, and X.-C. Li, "Intercomparison of the different fusion methods for generating high spatial-temporal resolution data," *Journal of Infrared & Millimeter Waves*, vol. 34, no. 1, pp. 92–99, 2015.
[26] W. Liao, F. Van Coillie, and L. Gao, "Deep learning for fusion of APEX hyperspectral and full-waveform LiDAR remote sensing data for tree species mapping," *IEEE Access*, vol. 6, no. 6, pp. 68716–68729, 2018.
[27] X.-F. Gong, Q.-H. Lin, F.-Y. Cong, and L. De Lathauwer, "Double coupled canonical polyadic decomposition for joint blind source separation," *IEEE Transactions on Signal Processing*, vol. 66, no. 13, pp. 3475–3490, 2018.

Hindawi
Journal of Advanced Transportation
Volume 2020, Article ID 8890233, 16 pages
https://doi.org/10.1155/2020/8890233

Research Article

Optimal Pricing Strategy of Electric Vehicle Charging Station for Promoting Green Behavior Based on Time and Space Dimensions

Xiaomin Xu ,[1,2] Dongxiao Niu,[1,2] Yan Li,[1,2] and Lijie Sun[1,2]

[1]*School of Economics and Management, North China Electric Power University, Beijing 102206, China*
[2]*Beijing Key Laboratory of New Energy and Low-Carbon Development (North China Electric Power University), Beijing 102206, China*

Correspondence should be addressed to Xiaomin Xu; xuxiaomin0701@126.com

Received 5 June 2020; Revised 3 July 2020; Accepted 16 July 2020; Published 11 August 2020

Academic Editor: Sang-Bing Tsai

Copyright © 2020 Xiaomin Xu et al. This is an open access article distributed under the Creative Commons Attribution License, which permits unrestricted use, distribution, and reproduction in any medium, provided the original work is properly cited.

Considering that the charging behaviors of users of electric vehicles (EVs) (including charging time and charging location) are random and uncertain and that the disorderly charging of EVs brings new challenges to the power grid, this paper proposes an optimal electricity pricing strategy for EVs based on region division and time division. Firstly, by comparing the number of EVs and charging stations in different districts of a city, the demand ratio of charging stations per unit is calculated. Secondly, according to the demand price function and the principle of profit maximization, the charging price between different districts of a city is optimized to guide users to charge in districts with more abundant charging stations. Then, based on the results of the zonal pricing strategy, the time-of-use (TOU) pricing strategy in different districts is discussed. In the TOU pricing model, consumer satisfaction, the profit of power grid enterprises, and the load variance of the power grid are considered comprehensively. Taking the optimization of the comprehensive index as the objective function, the TOU pricing optimization model of EVs is constructed. Finally, the nondominated sorting genetic algorithm (NSGA-II) is introduced to solve the above optimization problems. The specific data of EVs in a municipality directly under the Central Government are taken as examples for this analysis. The empirical results demonstrate that the peak-to-valley ratio of a certain day in the city is reduced from 56.8% to 43% by using the optimal pricing strategy, which further smooth the load curve and alleviates the impact of load fluctuation. To a certain extent, the problem caused by the uneven distribution of electric vehicles and charging stations has been optimized. An orderly and reasonable electricity pricing strategy can guide users to adjust charging habits, to ensure grid security, and to ensure the economic benefits of all parties.

1. Introduction

Since the 1990s, environmental pollution and fossil-energy shortages have become increasingly serious [1]. Thus, energy-saving and environmentally friendly electric vehicles (EVs) have attracted worldwide attention [2]. The United States, Japan, and many countries in Europe have formulated relative policies to encourage the development of the EV industry [3]. Through a series of policy incentives, the Chinese government has also strongly supported the development of its domestic EV industry to promote the production and sales of EVs, as well as the construction of charging infrastructure [4]. According to statistics from the Ministry of Industry and Information Technology of China, the average fuel consumption of fuel passenger vehicles was 6.7 L/100 km in 2017. Calculated by kilometers traveled, the emission factor of greenhouse gases was 152 g/km. In comparison, the average fuel consumption of pure electric passenger vehicles was 16.2 kWh/100 km, and the emission factor of greenhouse gases was 0 g/km [5]. According to the data released by the Ministry of Ecology and Environment of China, the emission factor of air pollutants for pure electric passenger vehicles during operation phase is 0 g/km. Thus, EVs can reduce not only greenhouse gas emissions [6] but also the emissions of pollutants such as hydrocarbons [7]; both reductions are conducive to achieve green, low-carbon travel, to mitigate the global warming and climate change crisis, and to alleviate environmental pollution [8]. Further, EVs can help promote the consumption of renewable energy and reduce the dependence on fossil energy [9], thereby promoting the development of a low-carbon economy and the sustainable development of society. EVs are therefore an important means in solving energy, environmental, and transportation problems [10]. EVs encourage people to adopt green and low-carbon travel, and EVs have promising development prospects as well [11].

With continuous breakthroughs in key EV technologies and the increasing improvements in charging infrastructure [12], countries around the world have accelerated EV technological innovation and have actively participated in market competition [13, 14]. According to the "Global EV Outlook 2018" released by the International Energy Agency (IEA), the global electric vehicle market has grown to more than 3 million vehicles in 2017, with an increase of 54% year-over-year. According to this estimation, global electric vehicle ownership will reach 13 million by 2030. By the end of June 2018, there were 19.9 million new energy vehicles in China, of which 1.62 million were pure EVs, leading world production. As the Chinese government attaches great importance to the development of the electric vehicle industry, a series of policies has been issued in macroplanning, industry management, financial subsidies, technological innovation, and infrastructure construction [15]. According to data released by the China Association of Automobile Manufacturers, production and sales of EVs have been steadily increasing from 2013 to 2018.

As seen in Figure 1, sales of pure EVs increased the most in 2014 and 2015, indicating that the industry development plan formulated by the government in the earlier period and the current subsidy policy have achieved remarkable results. In 2018, sales of pure EVs increased by more than 50%, showing a strong momentum in the development of the electric vehicle market. With the rapid growth of electric vehicle ownership, China also has the fastest growth in charging infrastructure (according to the data released by China Electric Vehicle Charging Infrastructure Promotion Alliance, there were approximately 7154 new public charging stations installed every month in 2018, which is 18.2% higher than that in 2017). At present, China has become the country with the most charging stations in the world [16]. The distribution of charging stations in various provinces and cities in China (excluding Hong Kong, Macao, and Taiwan) at the end of 2018 is shown in Figure 2. It can be seen that most provinces in China are equipped with charging facilities. Among them, Beijing, Shanghai, Guangdong, and Jiangsu are the leaders with more than 30000 charging stations.

With the promulgation and implementation of a series of policies and incentives by the Chinese government, the use of EVs has been widely promoted [17]. As such, problems related to EV charging have gradually emerged, mainly in the following three aspects.

Firstly, large-scale, unguided, and spontaneous EV charging can affect the safe operation of the electric power grid, which is reflected in load balance, power quality, and power grid construction planning [18]. The rapid increase in the number of EVs and charging stations suggests that EVs are an important load on the power grid. When large numbers of EVs charge during peak hours, it further aggravates the peak-to-valley difference and increases the burden on the power grid. Even worse, when EVs charge in a disordered manner, it enlarges the difficulty of peak shaving, brings incremental cost of generator, increases pressure on electricity transmission and on distribution networks, and reduces the security and reliability of the power grid [19]. In addition, charging EVs will create negative effects on power quality and increase the harmonic content of the power grid. For power generation, the large-scale connection of EVs to the power grid places higher requirements on the capacity of the generator assembly [20]. For transmission and distribution networks, if there is large-scale EV charging at peak hours, the charging may lead to overload, making the construction planning of future power systems much more uncertain [21].

Secondly, unreasonable charging pricing mechanisms and methods have led to a failure of EVs being able to respond effectively to demand [22]. When large numbers of EVs charge in an orderly way, the peak-to-valley difference can be reduced, and the grid load characteristics can be improved. Moreover, as distributed energy storage facilities, EVs can adjust their real-time charging plans to meet the needs of the electric power system [23]. Price is an important means to guide EVs in playing their role in demand response. However, except in Beijing, the EV charging service as a market has not started up in other places. Electric vehicles have uniform prices set by the government, with the pricing mechanism having little effect on guidance and adjustment by EV users. Under this circumstance, it is difficult for EVs to play their role in peak shaving and valley filling [24] and in reducing the operating cost of the system [25].

Thirdly, there also exist some problems in charging stations, such as unbalanced utilization, high maintenance costs, and poor revenue in the charging business. Generally, the utilization rate of charging stations, such as stations for public transportation and logistics, which are constructed and operated according to the specific needs of their users, is relatively high [26]; thus, the result is congestion in the charging queue during peak hours. Meanwhile, other charging stations, especially those located in remote areas, experience low utilization rates. Even a part of the proportion of charging stations is 0%. The utilization rate of charging stations in each area is extremely uneven, causing idleness and wasting of resources to certain extents (from the perspective of revenue, even the charging stations with high utilization rates have very poor economic benefits because of the large preinvestments, high operating costs, and single source of income [27]).

Using the above context, and fully considering the charging demand of users and the impact of safe operation of charging stations, this paper explores how to formulate a reasonable and orderly charging strategy and how to formulate an effective price response mechanism for electric vehicles. Through the reasonable and orderly guidance of user behavior, we can reduce not only the peak-valley difference in grid load but also the charging costs for users. To

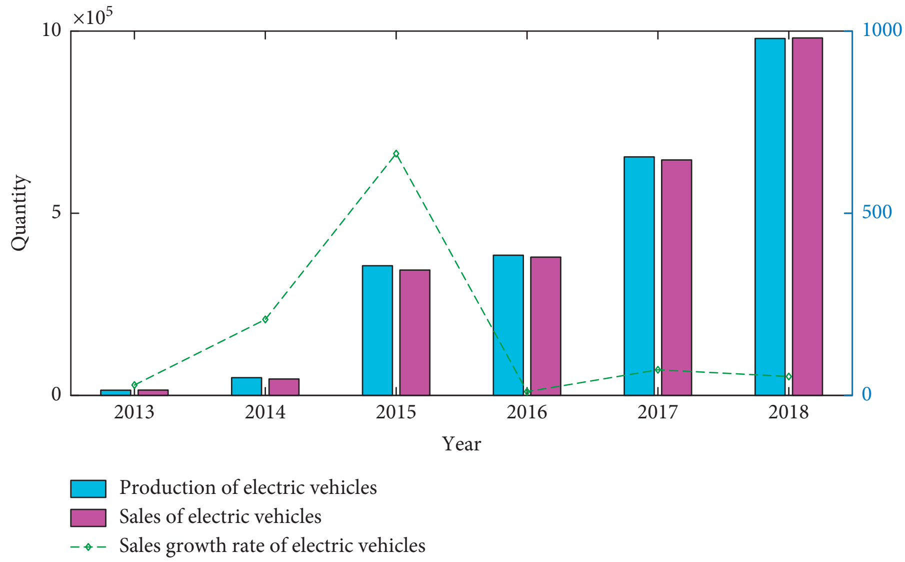

FIGURE 1: Production and sales of pure electric vehicles from 2013 to 2018.

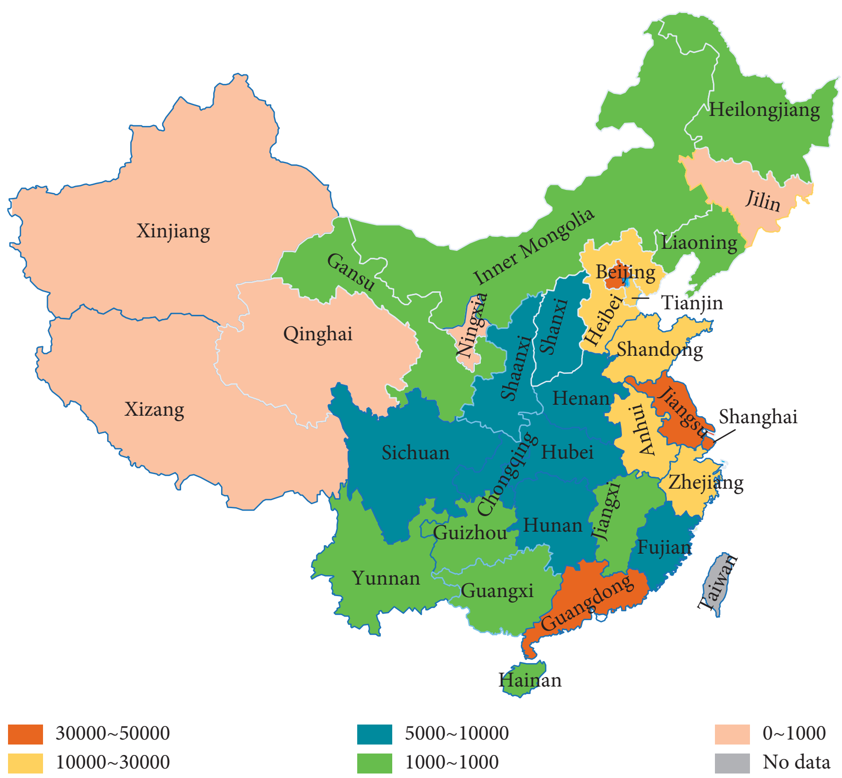

FIGURE 2: Distribution of electric vehicle charging stations in major provinces and cities in China (excluding Hong Kong, Macao, and Taiwan).

guide the orderly charging of electric vehicles, users can assist the grid frequency modulation to ensure the safe and stable operation of the power system. Therefore, it is of great significance to optimize the pricing strategy of electric vehicle charging stations. Thus, the organization of the rest of this paper is as follows. Section 2 summarizes the existing research literature. Section 3 introduces the model description and construction process. Section 4 describes the empirical analysis based on the modeling process and discusses the results. Section 5 summarizes the conclusions.

2. Literature Review

With the depletion of fossil fuels and the aggravation of environmental problems, electric vehicles, as new energy vehicles, have great potential in reducing environmental pollution and greenhouse gas emissions. However, with an increasing number of electric vehicles being connected to the grid for charging, the unreasonable charging plan of electric vehicles may have a great impact on the safe operation and economic benefits of the grid system. Therefore, a reasonable arrangement of the orderly charging of electric vehicles has become a major research trend. In view of the above problems, scholars in China and abroad have put forward many research methods for orderly charging. These methods can be summed up in two principle ways: one method is a direct load control method, and the other method is based on pricing strategy.

The direct load control method describes controlling the charging power of the charging station by the distribution network dispatching center or charging station and charging on the basis of meeting the system safety and vehicle charging requirements [28]. Qi et al. [29] proposed a charging control method combining online control and offline control, which can charge by controlling charging power. The current academic studies on EV charging stations mainly focus on a pricing mechanism. The research can be divided into the following categories. On the one hand, some studies mainly consider the technical factor of EV charging on the power grid to design the pricing mechanism. In other words, the cost of the charging technology is the most important factor. Salah and Flath [30] applied a deadline differentiated pricing scheme to incentivize flexible loads and claimed that varying PV capacity and the costs of conventional generation were the main factors. He et al. [31] formulated a multiclass combined distribution and assignment model, estimated electrical loads on the power distribution network, and optimized electricity prices at public charging stations and road tolls. Due to the high technical cost, this kind of pricing strategy often led to the charging price exceeding affordability for local residents, which is not conducive to the development of EVs.

On the other hand, some studies mainly consider the social and economic factors such as the developmental status of EVs, residents purchasing power, and the public attributes of electric products to the design the pricing mechanism. This kind of pricing strategy can be further divided into three categories: electricity consumption-based pricing, time-of-use pricing, and zonal pricing. The electricity consumption-based pricing strategy aims at reducing the electric load in peak hours and managing the charging behavior by EVs through controlling the amount of power supplied in corresponding time periods. The time-of-use pricing strategy is more mature [32]. The main idea is to encourage EV users to consume less electricity during the peak time period and more electricity during the valley time period, in order to guide the orderly charging of EVs. This method realizes the role of load adjustment for the power grid and reduces load fluctuation and the associated adverse effects when large numbers of EVs access the power grid. According to existing studies, peak–valley pricing [2, 33] and time-of-use pricing [34, 35] can mitigate the negative effects caused by the aggregate charging behavior of EVs to a certain extent and can play a better role in leveraging pricing. However, there exist corresponding deficiencies in flexibility and adaptability. Real-time pricing mechanisms [27, 36, 37] have been less studied due to related technological restrictions. The zonal pricing strategy mainly works by analyzing the utilization ratio of charging stations in different regions to guide users' charging behavior. Dong et al. [38] developed a double-layer optimization model to redistribute the charging load of EVs to optimize the charging pricing scheme and minimize the total voltage magnitude deviation of distribution networks [39]. Li et al. [4] took the users' charging time and space constraints into consideration to minimize the cost of each EV user. From the perspective of the participants, there are three research perspectives. The first is a pricing strategy that prioritizes the interests of the power grid and charging stations. For instance, Li et al. [40] put forward a charging pricing strategy that would improve the economic benefits of electric power enterprises. The second is a pricing strategy with priority given to EV users' interests, such as Pu et al. [41] who established a customer satisfaction model and proposed a coordinated pricing strategy for charging stations based on multiagents. The last pricing strategy considers multiple participants' interests, for example, the multiobjective charging optimization model based on time-of-use price with the security of power grid operation proposed by Cui et al. [42]. In this model, the individual needs of users and the interests of all parties are both addressed. Recent studies have changed from simply ensuring the maximization of one participant's interests to considering the common interests of multiple participants.

In summary, most of the current works only consider a single factor in the design of a pricing strategy. However, a single time-of-use (TOU) pricing strategy cannot solve the contradiction between charging congestion and charging station abandonment by EVs nor can a single zonal pricing strategy alleviate the impact of large-scale EV charging on the power grid during peak usage periods. Only by examining the two dimensions of zonal and TOU pricing simultaneously can we formulate effective strategies to solve the above problems. There are currently few studies focused on comprehensive analysis of multifactor pricing strategies, which is an area that requires further exploration and more detailed work. Accordingly, studies on multifactor, multidimension, and multiobjective pricing strategy are of great significance in motivating and guiding EV users to choose the appropriate time and location for charging. Moreover, it is conducive to improve the utilization efficiency of charging stations, alleviate the negative effects on the power grid, enhance the demand response ability, and improve the economic benefits of EV charging services.

In the previous research, the optimal pricing model and strategy of EV charging stations for the promotion of green and low-carbon behavior are proposed from two dimensions: space and time [43]. A multiobjective optimization model for centralized charging of EVs based on zonal and TOU pricing is put forward to formulate an optimal pricing strategy for EV charging. Firstly, through the demand of EVs for unit charging stations in different regions, the zonal pricing model is constructed based on the demand price function with the goal of maximizing profits. Through price differences, the model can guide users to transfer from regions where the charging stations are in short supply to regions where the charging stations are in oversupply. Secondly, taking the comprehensive consideration of user utility maximum, grid revenue maximization, and grid fluctuation minimum, this paper constructs a TOU pricing objective function and constraints. Thirdly, nondominated sorting genetic algorithm II (NSGA-II), which is a mature multiobjective optimization algorithm, is utilized to optimize the pricing strategy [44]. The empirical data from a municipality directly under the Central Government is used to verify the validity of this model. By exploring the pricing strategies for different periods in different regions and further refining the charging price classification of EVs, the utilization rate of charging stations in different regions can be improved, reducing the impact on the power grid, but it can also decrease users' charging costs and improve the revenue of charging stations through dynamic pricing strategies. Thus, a win-win situation can be achieved.

3. Model Description and Construction

3.1. Zonal Optimal Pricing Model. Based on the demand and price, the demand price function of electric vehicles is constructed, and then the profit function is established. Profit can be obtained from charging revenue and then subtracting costs, which include electricity costs, construction costs, operation and maintenance costs, and bank interest, to obtain the optimal pricing strategy of each region through calculation.

Establish the demand price function of electric vehicle charging in each region:

$$Q_d^i = d\left(P_i\right) = b_i - a\overline{P}_i. \tag{1}$$

Among them, Q_d^i indicates the demand for electric vehicle charging in the area i, b_i is a constant, which presents EV ownership of area i, $\overline{P}_i$ is the price for different regions, and a is a coefficient. The formula reflects the relationship between the quantity of charging demand and the charging price. It is a monotonic decreasing function; that is, the demand decreases with the increase in charging price. We believe that for the regions with high demand for charging, we can set a higher charging price through the demand price function to increase the charging cost of electric vehicles to guide some electric vehicles to the neighboring regions that have lower demand for charging.

On this basis, the benefits of charging station operators cannot be ignored, we can establish a profit function:

$$L\left(\overline{P}\right) = \sum_{i=1}^{n}\left[D_i \times \left(\overline{P}_i - p\right)(1+r)^n\right] - C, \tag{2}$$

$$D_i = Q_d^i \times t, \tag{3}$$

where $L(\overline{P})$ represents a profit function and p expresses the electricity purchase price (units: yuan/kWh). r represents the annual growth rate of electric vehicles. t represents the charging capacity per car. C represents the fixed cost of the charge station. Thus, the profit function is a quadratic function of price P with respect to L, and the optimal solution of the function appears at the point where the first derivative is 0; namely,

$$\text{Max}L = \frac{dL}{d\overline{P}} = 0. \tag{4}$$

Combining the ownership and demand of EVs in different regions, the optimal charging pricing of EVs in different regions can be obtained.

3.2. Multiobjective Optimal Model for Time-of-Use Pricing (TOU Pricing)

3.2.1. Objective Function. Taking the economic benefits of users and power grids, as well as the power quality, into account, this paper establishes a multiobjective pricing optimization model, which has the objective of maximizing the benefits for both users and the power grid and minimizing the fluctuation in the loads.

(1) Maximizing User Benefits. The purpose of setting a TOU price is to guide users to charge when the price of electricity is low to earn the price difference and reduce the peak-valley difference in grid load [45]. However, users are not willing to charge in all areas where price differences exist. Only when the differential value of electricity prices exceeds a certain range will users change their charging behavior and transfer the charging to a different region. In other words, we believe that there is a certain threshold for the transfer of electricity. Within the threshold range, users are willing to change their charging mode (transfer charging capacity). While beyond the threshold range, no matter how much the price changes, users are not willing to change their behavior. Figure 3 shows the relationship.

x is the differential value of electricity price and x_1 represents the start threshold for users to change charging behavior. In the region which is less than x_1, the incentive effect of changing electricity price on users is ineffective. Similarly, electricity price spreads will not endlessly change users' charging behavior. x_2 represents the saturation threshold for users to change charging behavior. After this threshold, no matter how the price increases, the users' charging behavior will not change. y represents the probability that the user will change his/her charging behavior or the probability of a power transfer.

This paper does not take the purchase cost of EVs into consideration, but only considers the user's satisfaction in both the electricity consumption mode and the cost expenditure after the implementation of the TOU price.

Through reading and summarizing the literature, the degree of satisfaction of electricity consumption mode can be calculated by the following formula [42]:

$$\beta_i = 1 - \frac{\sum_{t=1}^{T}\left|\hat{g}_i^t - g_e\right| \times \Delta t}{\sum_{t=1}^{T} g_i^t \Delta t}. \tag{5}$$

The satisfaction degree of the cost expenditure can be expressed as

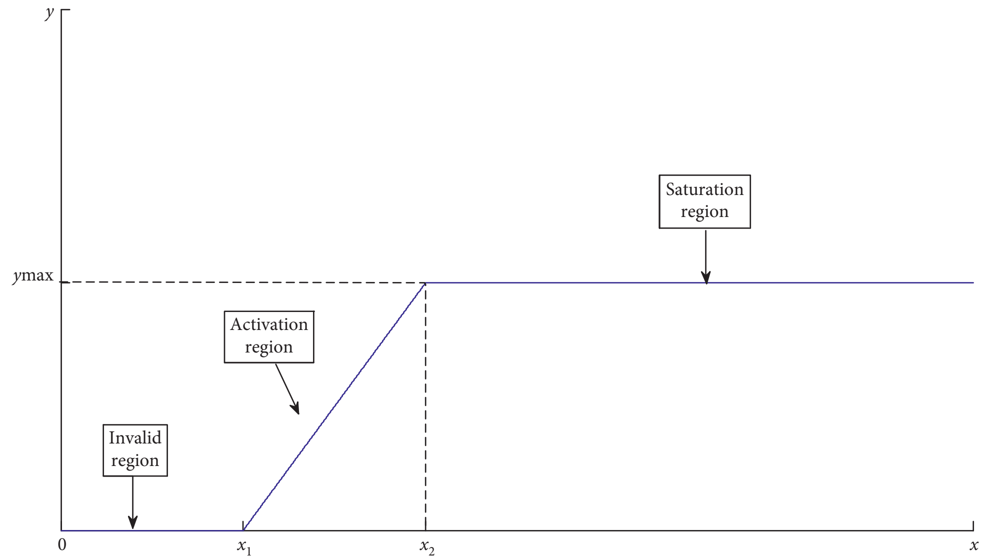

FIGURE 3: Charging behavior change (power transfer probability) diagram.

$$\gamma_i = \frac{\sum_{t=t'}^{t'+m-1}\left(\widetilde{P}_i^t - \widetilde{P_g}\right) \times g_i^t \times \Delta t}{\sum_{t=t'}^{t'+m-1}\left(\widetilde{P_f} - \widetilde{P_g}\right) \times g_i^t \times \Delta t.} \tag{6}$$

Among them, $\widetilde{P}_i^t$ is the price for a period of time i; P_f, P_g represent the peak hour price and trough price, respectively; g_i is the charging power for EV; $\widehat{g}_i^t$ is the charging power of the electric vehicle i in the period t when the single user has the greatest travel satisfaction; Δt is the charging time; and m is a time window for rolling optimization. The greater the difference between the optimized TOU price $\overline{P}_i$ and the original price is, the higher the satisfaction of users with charging charges is, and the greater the utility is.

To maximize user satisfaction, the objective function is set as follows:

$$F_1 = \max \sum_{i=1}^{N} \left(\alpha_1 \beta_i + \alpha_2 \gamma_i\right), \tag{7}$$

where α_1, α_2 are the weight coefficient.

(2) Maximizing the Revenue of Power Grid. For power grid companies, dynamic electricity prices can make users of EVs choose a charging start time that is independent of their own needs for reducing charging costs. However, in the economic market, the goal of all industries is to maximize economic benefits. Power grid companies can also achieve this goal by setting a reasonable TOU price.

$$F2 = \max \sum_{i=1}^{24} \sum_{j=1}^{T} \left[n \times \mu_j \times \left(\widetilde{P}_i - c\right) \times \Delta t\right],$$
$$\mu_j = \frac{1}{N} \sum_{i=1}^{N} g_{i,j}. \tag{8}$$

In this formula, μ_j represents the expected value of charging power for the time periods j of an electric vehicle.

(3) Minimizing Load Fluctuation in Power Grid. A large number of decentralized and disorderly charging stations of EVs will create challenges for the safe and stable operation of the power system. As builders and operators of charging stations, power grid companies need to consider not only their own benefits, but also power quality and grid security as objectives. Through reasonable TOU pricing, users can be guided to charge at staggered peaks to suppress load fluctuations and facilitate the stable operation of the power grid.

The load fluctuation of the power system is incorporated into the objective function. The deviation between the total load and the average load level after considering the charging load of EVs is investigated. The objective functions are shown as follows:

$$F_3 = \min\left[\frac{1}{T}\sum_{t=1}^{T}\left(L_t + \sum_{i=1}^{n} g_i^t - \overline{g}\right)^2\right],$$
$$\overline{g} = \frac{1}{T}\sum_{t=1}^{T}\left(L_t + \sum_{i=1}^{n} g_i^t\right). \tag{9}$$

Among them, L_t is the basic load of the power grid at time t and $\overline{g}$ represents the average load of the grid at time t.

3.2.2. Constraint Conditions

(1) Limit Constraints for TOU Price. The formulation of TOU prices should be within the price range that users can afford. To avoid excessive TOU pricing, it is necessary to restrict the fluctuation limits of TOU prices.

$$\widetilde{P}_{\min} \le \widetilde{P}_i \le \widetilde{P}_{\max},$$
$$\widetilde{P}_{\text{avr}} = \frac{1}{24}\sum_{i=1}^{24} \widetilde{P}_i, \tag{10}$$
$$\left|\widetilde{P}_i - \frac{\widetilde{P}_f + \widetilde{P}_g}{2}\right| \le \varepsilon,$$

where $\widetilde{P}_{\min}$ is the lower limit of the charging price for the ith hour; $\widetilde{P}_{\max}$ is the upper limit of the charging price for the ith hour; and $\widetilde{P}_{\text{avr}}$ is the floating benchmark value for the TOU price.

(2) Benefit Constraints of Power Grid. After implementing the TOU price, power grid companies should be guaranteed no reduction in revenue; that is,

$$R_1 \geq R_0. \tag{11}$$

Specifically,

$$\begin{aligned}
&\left(Q_f - \Delta Q_{\text{fp}} - \Delta Q_{\text{fg}}\right) \times \overline{P}_f + \left(Q_p - \Delta Q_{\text{pg}} + \Delta Q_{\text{fp}}\right) \times \overline{P}_p \\
&\quad + \left(Q_g + \Delta Q_{\text{fg}} + \Delta Q_{\text{pg}}\right) \times \overline{P}_g \geq \left(Q_f + Q_p + Q_g\right) \times P_0, \\
&\Delta Q_{\text{fp}} = \eta_1 \Delta P_{\text{fp}}, \\
&\Delta Q_{\text{fg}} = \eta_2 \Delta P_{\text{fg}}, \\
&\Delta Q_{\text{pg}} = \eta_3 \Delta P_{\text{pg}}.
\end{aligned} \tag{12}$$

According to the analysis of changes in users' charging behavior, it can be seen that the transfer of electricity is related to the price difference. In the formula, Q_f, Q_p, and Q_g express the power demand in peak hours, flat hours, and valley hours, respectively; ΔQ_{fp}, ΔQ_{fg}, and ΔQ_{pg} are peak–flat demand transfer, peak–valley demand transfer, and flat–valley demand transfer, respectively. $\overline{P}_f$, $\overline{P}_p$, and $\overline{P}_g$ are the prices at the peak, flat, and valley time periods, respectively; P_0 is the price before optimization; η_1, η_2, and η_3 are the demand transfer rates of the peak-to-flat, peak-to-valley, and flat-to-valley periods, respectively.

(3) Probability Constraints of Charging Volume Transfer for Users. The power transfer probability of the TOF price is related to the price difference, and there remains a trigger threshold, which should meet the following constraints:

$$c_l \leq \overline{P}_f - \overline{P}_g. \tag{13}$$

(4) Voltage Offset Constraint. According to GB/T 12325–2008, the deviation limits of 20 kV and the following three phases supply voltage are nominal voltage. Therefore, the normal range of node voltage $U_{i,j}$ is

$$(1 - 7\%)U_N \leq U_{i,j} \leq (1 + 7\%)U_N. \tag{14}$$

(5) Expectation Constraints of Voltage Qualification Rate. Voltage qualification rate (VQR) indicators F_{VQR} are the percentage of cumulative runtime t_{VQR} and the total runtime T that the actual operating voltage deviation is within the limits.

$$F_{\text{VQR}} = \frac{t_{\text{VQR}}}{T} \times 100\%. \tag{15}$$

The expected value $M_{\text{VQR},n}$ of voltage qualification rate of charging TOF price node v can be expressed as

$$M_{\text{VQR},n} = \frac{\sum_{j=1}^{96}\left(1 - q_{n,j}\right)}{96} \times 100\%. \tag{16}$$

Among them, $q_{n,j}$ is the probability of voltage overrun of node n in the time period j.

According to the regulation that the qualified rate of voltage in EN50160 is not less than 99%, there are the following constraints:

$$M_{\text{VQR},n} \geq 99\%. \tag{17}$$

3.3. Optimization Algorithm. In engineering practice, the mathematical model of many issues can be generalized as the multiobjective optimization problem, which is not similar to the single-objective optimization problem and its only one optimal solution. The solution is a set called the Pareto solution set. NSGA-II is robust and the noninferior solution has a uniform distribution in the target space and good convergence. With these characteristics, NSGA-II has become one of the popular multiobjective optimization algorithms and widely applied in engineering practice and various disciplines. The NSGA-II, an improved version of the NSGA, was proposed by Deb et al. [46]. The algorithm improved NSGA mainly by enhancing nondominated sorting efficiency, using crowding distance instead of sharing parameters, and introducing elitist-preserving approach, thus effectively overcoming the three major deficiencies of NSGA [47]. Meanwhile, by introducing a fast, nondominant sorting procedure, the computational complexity is greatly reduced, and the optimal preservation mechanism is provided. In this case, it can not only ensure the diversity of the population by using a parameterless niching operator [48] but also improve the ability of the optimization result to approach the Pareto optimal frontier [41]. NSGA-II mainly includes operators such as selection, crossover, and mutation. The selection mechanism is based on nondominated sorting and crowding distance. Simulated binary crossover (SBX) and polynomial mutation are utilized in NSGA-II, as stated by Murugan et al. [49].

The specific procedures of NSGA-II are described as follows and are shown in Figure 4.

Step 1. Set the algorithm parameters and the domain of values of each decision variable.

Step 2. Randomly generate the initial population P_0 in the domain of decision variables, that is, coding the feasible schemes and initializing a majority of pricing strategy schemes that satisfy the constraint conditions.

Step 3. Calculate the fitness value of each individual in the parent population P_0, which means calculating the values of multiple objective functions corresponding to each scheme according to the established multiobjective optimization mathematical model.

Step 4. Perform nondominated sorting on the current population according to their nondomination level based on the objective function values, enable individuals to enter their own front set, and calculate the crowding distance of individuals in each front separately.

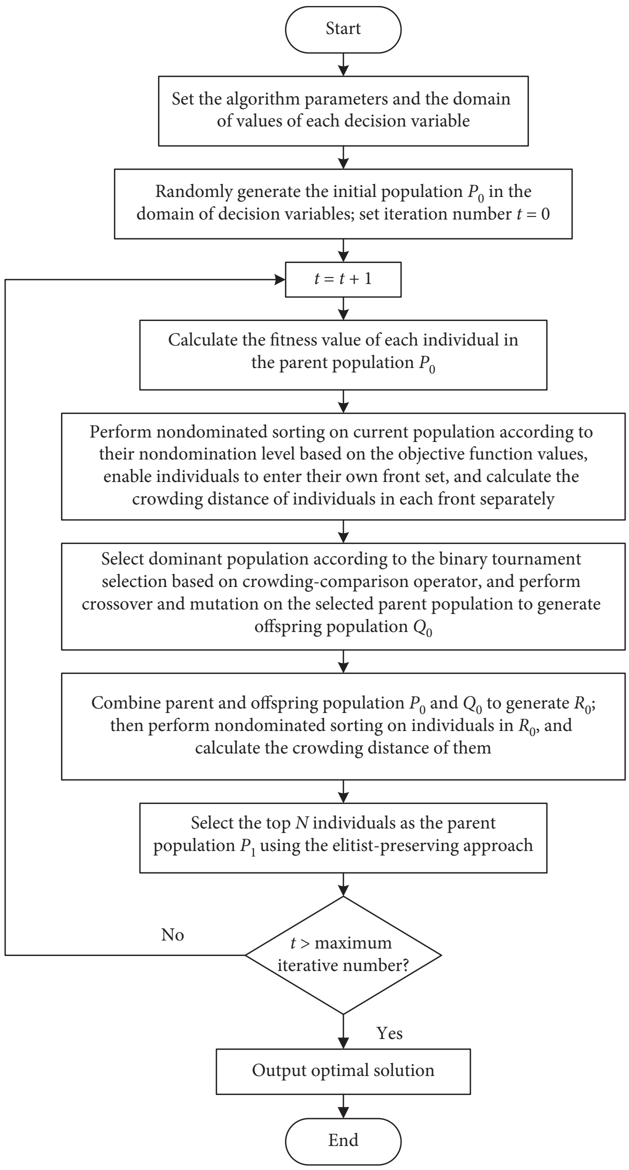

Figure 4: Flowchart of NSGA-II algorithm calculation.

Step 5. Select dominant population according to the binary tournament selection based on crowding-comparison operator, and perform crossover and mutation on the selected parent population to generate offspring population Q_0.

Step 6. Combine parent and offspring populations P_0 and Q_0 to generate R_0; then perform nondominated sorting on individuals in R_0, and calculate the crowding distance of them.

Step 7. Select the top N individuals as the parent population P_1 using the elitist-preserving approach.

Step 8. Determine whether the algorithm has reached the set maximum iteration number. If so, stop optimization and output the optimal solution. Otherwise, return to Step 3 and repeat the above operation until the set maximum number of iterations is reached.

4. Empirical Analysis

4.1. Data Setting and Instructions

4.1.1. Case Background. To verify the feasibility and effectiveness of the strategy proposed in this paper, the data of new energy electric vehicles used in summer in a municipality directly under the Central Government are taken as research objects. We selected six municipal districts in the city for research. For convenience, they are expressed by the letters A–E. The municipal district is a core component and regional development center of the city and is characterized by a concentrated population, close regional connections, and strong mobility. The characteristics of these municipal districts lay the foundations for carrying out the zonal and TOU pricing strategy for this paper.

After collecting the operational data from the charging stations and other relevant information, this paper analyzes the uncertain factors according to the power supply demand of each region and the actual operation of the charging stations; the aim is to improve the operating revenues of the charging station and to guide EV users to charge reasonably according to pricing strategy. Zonal pricing is to price the electricity selling price at charging stations in different regions. Using the data of the number of electric vehicles, charging stations, and the efficiency of charging stations in different regions, the optimal pricing strategies in different regions are analyzed. On this basis, TOU pricing is to price the electricity selling price of different regions in different time periods. According to the peak and valley situation of the traffic flow and the working efficiency of the charging station in different periods, and considering the objectives of user benefit, operator benefit, and grid fluctuation and multiple constraints, the optimal charging price of different regions in different time periods is determined by comprehensive analysis [50]. Thus, we can achieve differentiated pricing strategies in different regions for different time periods.

4.1.2. Data Setting. To facilitate the analysis, we set the following parameters. Due to the characteristic that EVs stay in residential or working areas for a long time, this paper assumes that EVs are charged at a constant power and slow speed. The sample number of EVs was 20000 with 70 kWh battery capacity and 7.3 kW charging power. The minimum control period of charging power of EV charging station is 1 hour, the charging price before optimization is 1.5 yuan/kWh, and the maximum charging power transfer is 95%. On this basis, the initial data of EV ownership and charging stations are shown in Figure 5.

Notes. Number of electric vehicles per charging=The number of electric vehicle/The number of charging stations.

From Figure 5, we can see that in the areas selected in this paper, regions C and D have a sufficient number of EVs, but a relatively inadequate supply of charging stations, while region E, with a relatively small number of EVs, has a

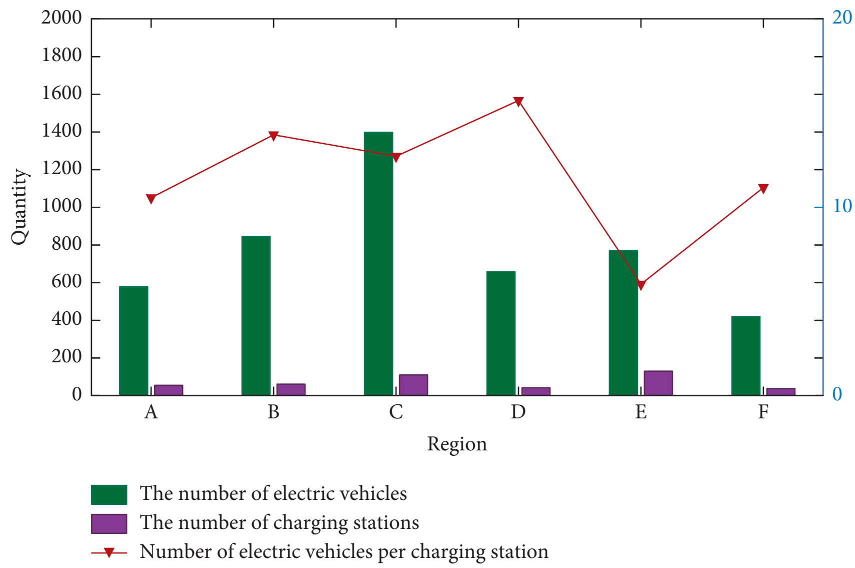

Figure 5: Contrast chart of electric vehicle ownership and charging station.

relatively large number and sufficient supply of charging stations. In the selected case, the demand for charging stations varies in different regions. For instance, in region D, which has a higher number of EVs per charging station, the charging stations may be inadequate, with EV users needing to wait in line during the peak periods of charging, while in region E, which has a lower number of EVs per charging station, the utilization rate is low owing to the desolation of some charging stations for weeks and months. Expanding charging stations in places where EVs are in great demand can solve this problem, but the execution is more difficult and will be restricted by technology, venue, and other aspects. The formulation of electricity pricing policies in different regions that guide users to decentralize charging (charging in adjacent areas with sufficient charging stations) can not only reduce the charging cost of users but also increase the utilization rate of charging stations and reduce the waiting time of charging queues, providing a basis for zonal pricing.

4.1.3. Analysis of the Influence of Unguided EV Charging on Power Grid. To analyze the influence of unguided charging behaviors of electric vehicles on the grid, we have drawn the daily demand data of charging vehicles and the original data of the conventional load of the power grid in the corresponding analysis period. Figure 6 shows the comparison of daily charging demand of EVs and daily load curves of the power grid on a given day.

As seen from Figure 6(a), the daily demand curve of EV charging is a normal distribution. The early peak period of charging commences from 8:00 am to 3:00 pm, and the peak of night charging starts from 18:00 to 20:00, which is consistent with people's life routine. Compared with the changes of daily load curve from Figure 6(b), it can be seen that the trend of charging peak is consistent with that of power consumption peak. That is, this unguided and spontaneous charging behavior increases the fluctuation on the grid. Charging in the peak period of electricity consumption will undoubtedly increase the load pressure on the grid and further widen the gap between the peak load (maximum load) and low load (minimum load). As we all know, electricity cannot be stored. Power generation, transmission, and use should be completed instantaneously, and the ideal load curve should be a horizontal straight line. In this event, the generator unit can operate stably for a long time with the lowest operation cost. However, there will be incapability to emerge frequent starts and stops of electric generating units and frequent dispatching of the power grid. The peak–valley difference refers to the difference between the maximum load and the minimum load in a certain period of time. An increase in the peak–valley difference means that we need to shut down more units in the low valley and start more units in the peak valley. However, frequent starts and stops of a unit will not only shorten its service life but also increase its use cost. Additionally, it will further increase the fluctuation of the power grid, bringing security risks to the power grid and increasing the difficulty of power grid dispatching. Charging during the peak period of the grid load will further increase the peak load and widen the peak-to-valley difference in the load, which will adversely affect the safety and economy of the grid. Under the circumstances, the formulation and implementation of TOU pricing can make users respond to the price and guide users to charge during the lowest periods of power consumption, thus achieving the win-win goals of reducing user charging costs, suppressing load fluctuation of the power grid, and ensuring the safety of the power grid operation.

4.2. Optimization Strategy for Zonal Pricing. According to formulae (1)–(3) and the principle of profit maximization, this paper optimizes the charging price of 6 regions in a city. Combined with the data of electric vehicle ownership and charging demand in different regions, we can get the optimal pricing results for each region, as shown in Table 1 and Figure 7.

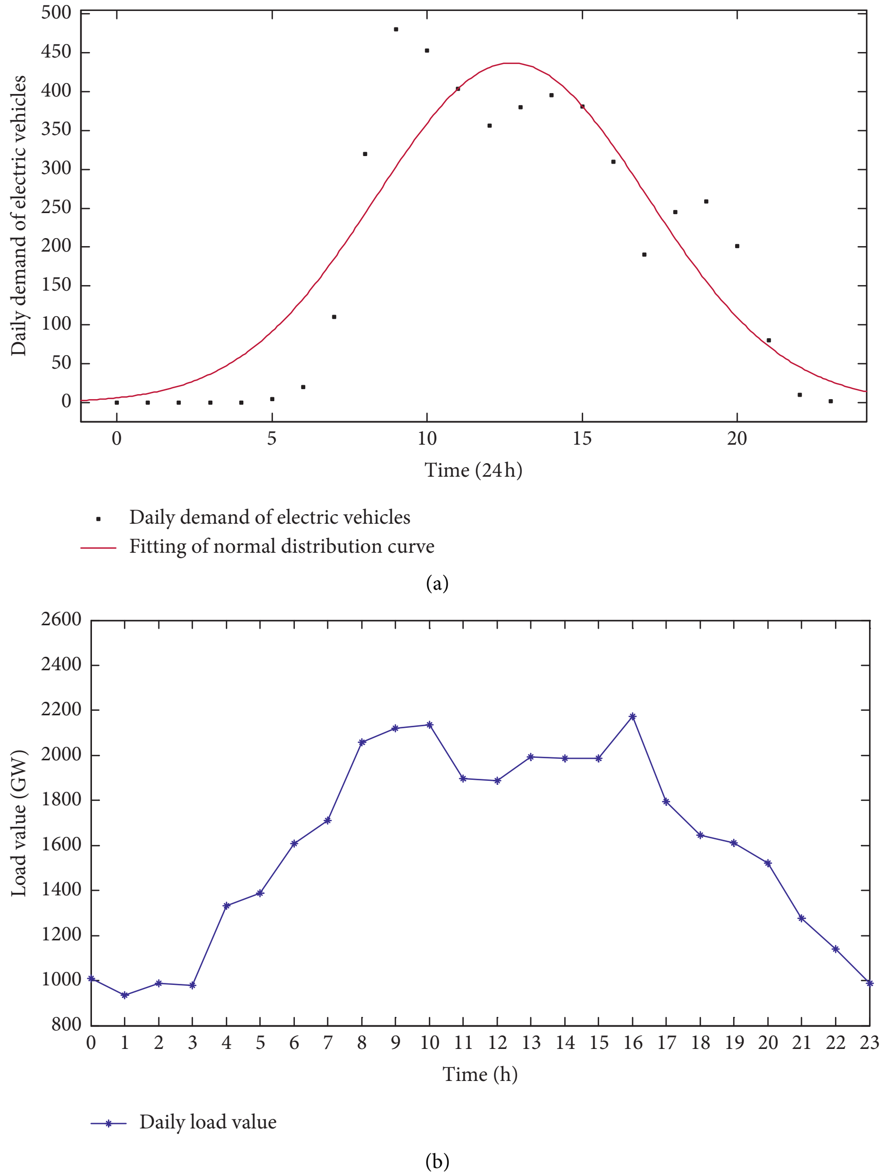

FIGURE 6: Comparison of daily charging demand of electric vehicles and daily load curves of power grid. (a) Daily demand curve of charged vehicles. (b) Graph of basic daily load curve of power grid.

TABLE 1: Optimal pricing of electric vehicle charging in various regions of a city.

Regions	Number of EVs	Supply–demand ratio for charging station	Daily demand (kW) (before and after optimization)		Optimal price (yuan/kWh)
A	578	10.51	245	282	1.77
B	845	13.85	478	351	1.90
C	1398	15.67	835	768	1.87
D	758	12.71	393	275	2.04
E	670	5.92	269	343	1.25
F	420	11.05	260	230	1.81

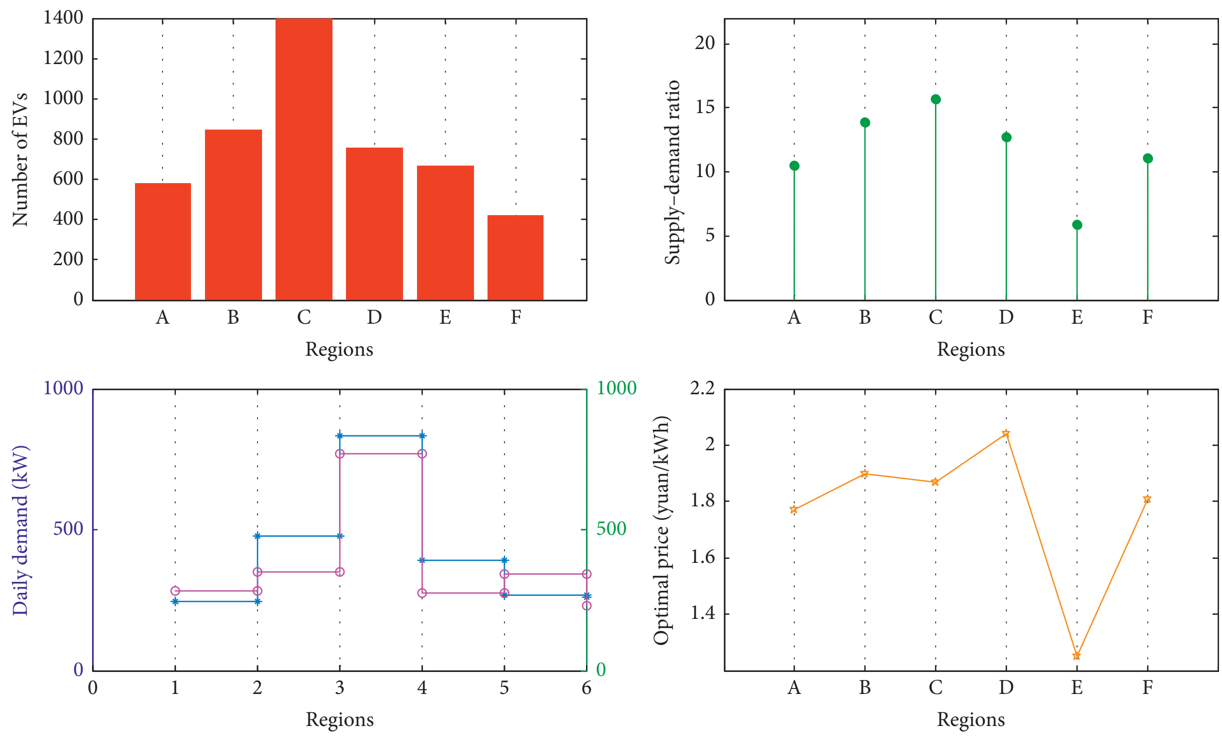

Figure 7: Variations before and after optimization in different regions.

Compared to the previous unified electricity price, different regions have different pricing after optimization. In Region A, for example, the charging price before optimization is 1.5 yuan/kWh (including 0.8 yuan/kWh for electricity price and 0.7 yuan/kWh for service fee), and the optimized charging price is 1.77 yuan/kWh, with an increase of 18%. Compared with the supply–demand ratio for EV charging stations, there is a positive correlation between them. That is, the greater the ratio of supply–demand for EV charging stations is, the higher the charging price for the region is. When the ratio is large, there are more EVs and fewer charging stations in this region. At the same moment, it is likely that there are not enough charging stations and charging needs lead to queuing and other phenomena. According to the theory of supply and demand, when demand exceeds supply, the prices rise. Some users can be guided into changing their charging behavior and charging in adjacent regions with a lower charging price, which can reduce the charging pressure. After optimization, the daily demand for EV charging in each region has also shifted. In Region E, which has a lower charging price, the daily demand has increased from 269 kW to 343 kW, with a 27.5% rise, while in Region D, with the highest charging price, there is a downward trend in daily charging demand. That is, to a certain extent, the charging behavior is transferred from the high-price region to the low-price region. The zonal pricing strategy can effectively guide users to decentralized charging, improve the utilization efficiency of charging stations, and reduce queuing time due to charging congestion. However, relying solely on the zonal pricing strategy cannot solve the impact of large-scale electric vehicle charging load on grid security. Additionally, we believe further study into the guiding role of pricing strategies for users in different periods based on zonal pricing is required.

4.3. Optimization Strategy for TOU Pricing. According to the load change of 24 hours in a day shown in Figure 6, to reduce the peak-to-valley difference in the daily load curve and to make the charging load of electric vehicles reach the effect of peak-cutting and valley-filling, this paper first divides the time period into the peak, flat, and valley of the daily load, as shown in Table 2.

The TOU pricing strategy in this paper is analyzed on the foundation of this division. The optimization model is solved by programming with MATLAB. The parameters of NSGA-II settings are as follows. The population number is 50, the maximum number of iterations is 200, the crossover rate is 0.8, and the variation rate is 0.3. The optimized time window for scrolling is 9.

In this paper, the charging of electric vehicles is arranged in disorderly mode and orderly mode. Disorderly charging refers to the random charging behavior of electric vehicles without a guidance mechanism. Orderly charging refers to the arrangement of charging according to the optimal pricing strategy proposed by the charging station. Before optimization, the impact of disordered charging behavior on grid load is quantitatively analyzed, as shown in Figure 8. The black solid line represents the original load of the power grid, and the purple dotted line indicates the load condition after the superimposing of disordered charging for EVs. It can be seen clearly from the figure that the disordered charging behavior further

Table 2: Time division for TOU price.

Time period	Specific classification
Peak	8:00–12:00; 14:00–16:00; 18:00–20:00
Flat	12:00–14:00; 16:00–18:00; 20:00–24:00
Valley	0:00–7:00

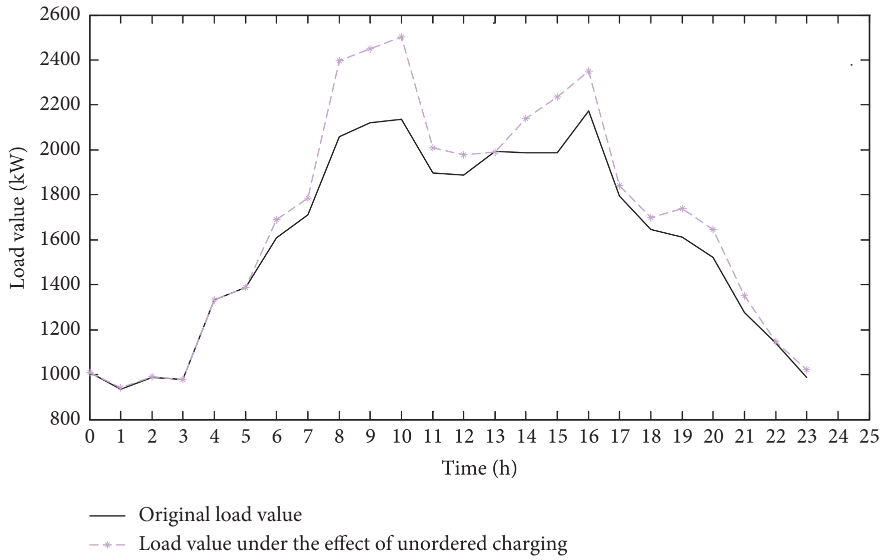

Figure 8: Influence of disordered charging behavior on grid load.

increases the load peak from the original 2173.5 GW to 2503 GW, and the peak-to-valley difference ratio rises from 56.98% to 62.45%, which enlarges the operating pressure on the grid. Thus, there is an urgent need to guide and control the charging behavior of EVs through a price mechanism.

Based on the zonal pricing, this paper studies the impact of TOU pricing in different regions on the charging behavior of EVs, mainly considering the peak, flat, and valley periods. The optimization results are shown in Table 3 by NSGA-II optimization. The corresponding user satisfaction and the grid load curve under the orderly charging are obtained as shown in Figures 9 and 10.

As seen from Figure 9, the user satisfaction with the optimized TOU price has significantly improved [51]. Among them, it mainly reflects in the satisfaction with the amount of electricity expenditure. Under the premise of guaranteeing the trip plan, the user's expenditure on the charging cost has been reduced, which will reach an overall optimal state. Figure 10 shows the guiding effect of optimized TOU price on electric vehicle users. The optimized grid load distribution is more uniform with a lower variance of the load. The load fluctuation is more gradual with a nearly 14% reduction in the peak-to-valley difference, which is conducive to the safety of the grid operation. Moreover, the average rate of electricity transfer of EV users is 65%. That is, comprehensive strategies of zonal pricing and TOU pricing can motivate users to change their original electricity usage habits and transfer the charging period from the peak load period to the low valley period of the grid and transfer the charging region from a dense area with fewer charging stations to areas with sufficient charging stations. This not only improves the utilization efficiency of charging stations in various regions but also plays a role in cutting peaks and filling valleys, which is conducive to the safer and more orderly operation of power grids and charging stations.

For a more intuitive understanding, the impact of the optimized pricing strategy on the charging power arrangement of EVs, this paper randomly selected 150 EVs and plotted the charging power distribution, as shown in Figure 11 below.

By comparing the data of the above graphs, it can be seen that after adopting the optimized pricing strategy, the charging probability of EVs in peak period is significantly reduced, and the charging load time range of EVs is extended, which can distribute the charging load of EVs in a longer period. In this way, the fluctuation of load in the power grid can be smoothed more effectively, and the impact on the power grid can be reduced.

Table 3: TOU tariffs of peak-flat-valley period in different regions.

Region	Peak period	Flat period	Valley period	Price before optimization
A	1.89	1.45	1.53	1.77
B	2.21	1.80	1.65	1.90
C	2.09	1.77	1.60	1.87
D	2.35	1.86	1.74	2.04
E	1.50	0.98	1.12	1.25
F	1.94	1.72	1.58	1.81

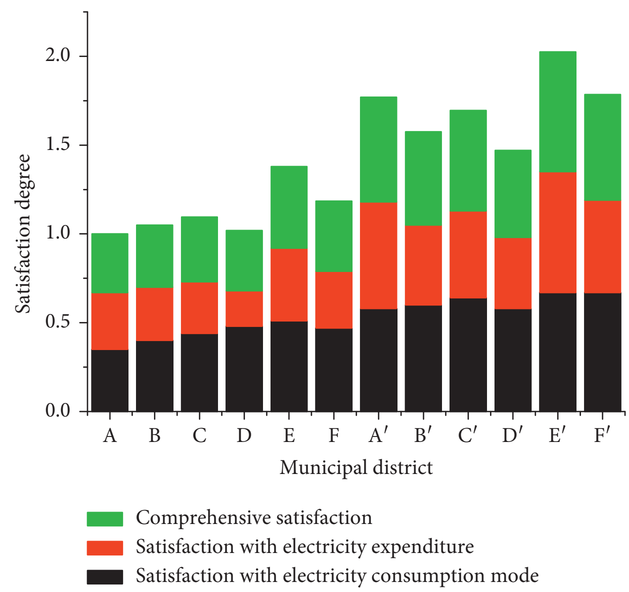

Figure 9: User satisfactions before and after optimization. A to E represent satisfaction before optimization and A′ to E′ represent satisfaction after optimization.

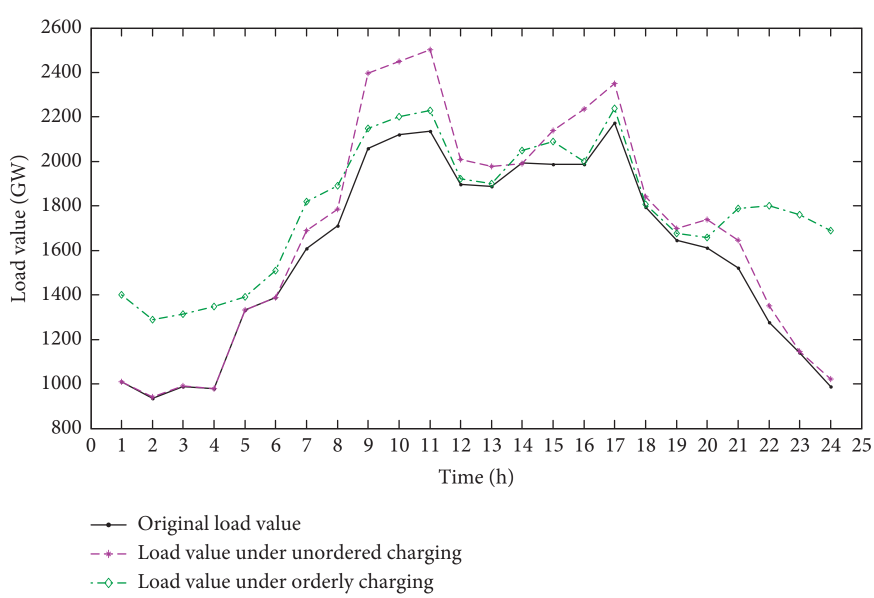

Figure 10: Load curve of power grid under ordered charging behavior.

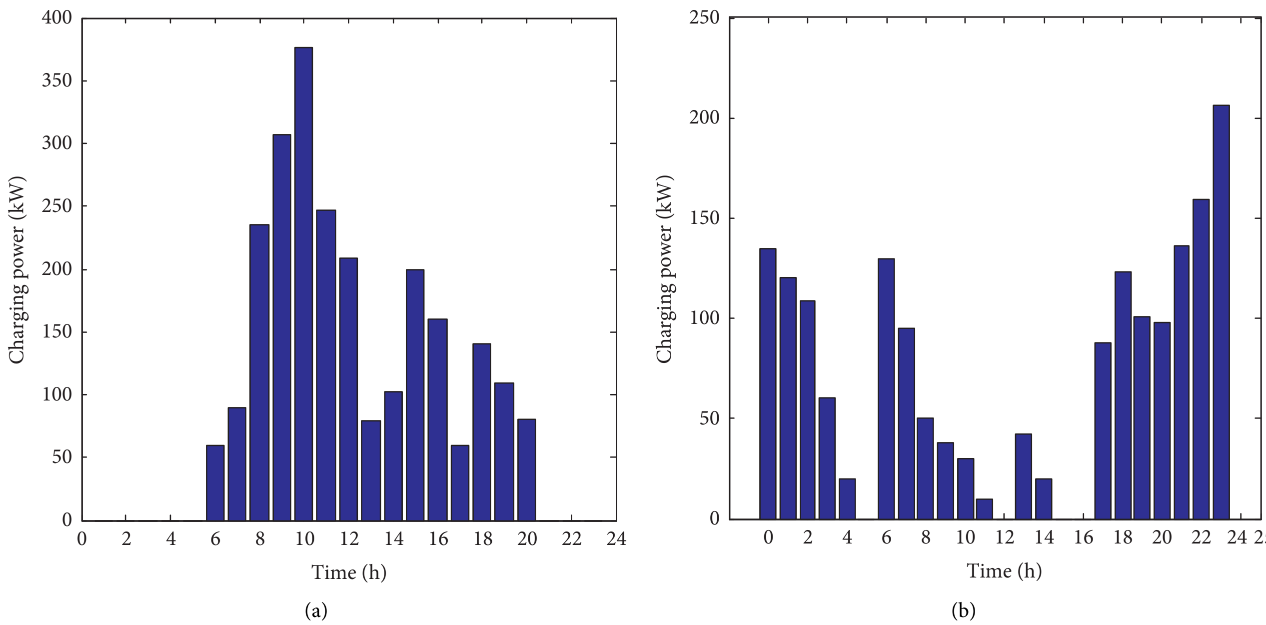

Figure 11: Charging power distribution before and after optimization of 150 EVs.

5. Conclusion

Electric vehicles, with clean electricity as fuel, can lessen dependency on fossil fuels and reduce greenhouse gas emissions. Promoting green and low-carbon behavior is vital. Based on the analysis of the charging characteristics of EVs, and considering the problems of large fluctuation on the grid and the imbalance in distribution and utilization of charging stations, a comprehensive optimization model based on zonal and TOU pricing for EVs is proposed in this paper. The empirical analysis is carried out with 6 municipal regions in a municipality directly under the Central Government as the research object. Compared with the disorderly charging behavior of EVs, the following conclusions are obtained:

(1) Formulating the charging price in different regions is beneficial to guide users to perform decentralized charging. The research shows that reasonable zonal pricing can effectively guide users to charge in adjacent areas and can effectively alleviate the charging pressure in crowded areas. The price signal is conducive in guiding the user to select a suitable charging station in advance, which can not only reduce the charging cost of the user but also improve the utilization efficiency of the charging station and increase the operating income of the power grid.

(2) Establishing a reasonable time-of-use price of peak-valley-flat is conducive to guiding users into choosing a reasonable charging time and optimizing the charging load of electric vehicles. The results show that, under the guidance of TOU pricing, the charging period of EVs is lengthened and the charging load is evenly distributed for a longer period. It can more effectively smooth the fluctuation of the grid load and alleviate the impact on the grid.

(3) Single zonal pricing strategy cannot optimize the daily load curve. Meanwhile, a single TOU pricing strategy cannot change the charging path of users and improve the utilization efficiency of charging stations. The rationality of zonal and TOU pricing strategy determines the user satisfaction, which in turn affects the user's electricity consumption behavior, finally achieving the effect of "shifting the peaks and filling the valley," calming the load fluctuation of the power grid to ensure a benefit for all parties and the safe operation of the power grid.

Data Availability

The data that support the findings of this study are available from the authors upon request.

Conflicts of Interest

The authors declare that there are no potential competing interests regarding the publication of this paper. All authors have seen the manuscript and approved to submit it.

Authors' Contributions

X. X. M., N. D. X., L. Y., and S. L. J. designed the experiments; N. D. X. provided guidance on manuscript preparation and supervised the whole work; X. X. M., L. Y., and S. L. J. conducted the experiments, analyzed the data, and wrote the manuscript.

Acknowledgments

The authors would like to acknowledge the financial support from the National Natural Science Foundation of China

(Grant no.71804045) and the 2018 Key Projects of Philosophy and Social Sciences Research, Ministry of Education, China (Grant no. 18JZD032). This paper is also supported by the 111 Project (B18021) and the Fundamental Research Funds for the Central Universities (2018ZD14 and 2020MS045).

References

[1] J. Guo, X. Zhang, F. Gu, H. Zhang, and Y. Fan, "Does air pollution stimulate electric vehicle sales? Empirical evidence from twenty major cities in China," *Journal of Cleaner Production*, vol. 249, Article ID 119372, 2019.

[2] Z. Hu, K. Zhan, H. Zhang, and Y. Song, "Pricing mechanisms design for guiding electric vehicle charging to fill load valley," *Applied Energy*, vol. 178, pp. 155–163, 2016.

[3] Y. Ma, T. Shi, W. Zhang, Y. Hao, J. Huang, and Y. Lin, "Comprehensive policy evaluation of NEV development in China, Japan, the United States, and Germany based on the AHP-EW model," *Journal of Cleaner Production*, vol. 214, pp. 389–402, 2019.

[4] Y. Li, P. Zhang, and Y. Wu, "Public recharging infrastructure location strategy for promoting electric vehicles: a bi-level programming approach," *Journal of Cleaner Production*, vol. 172, pp. 2720–2734, 2018.

[5] B. Hu, Y. Feng, J. Sun, Y. Gao, and J. Tan, "Driving preference analysis and electricity pricing strategy comparison for electric vehicles in smart city," *Information Sciences*, vol. 504, pp. 202–220, 2019.

[6] A. F. Roberto, "A more realistic approach to electric vehicle contribution to greenhouse gas emissions in the city," *Journal of Cleaner Production*, vol. 172, pp. 949–959, 2018.

[7] R. Ju, "Electric vehicle charging station constraint conditions and comprehensive benefit analysis," *East China Electric Power*, vol. 39, pp. 547–550, 2011, in Chinese.

[8] C. C. Lluc, M. L. Egoitz, A. G. Beatriz, and N. Nerea, "Sustainability analysis of the electric vehicle use in Europe for CO_2 emissions reduction," *Journal of Cleaner Production*, vol. 127, pp. 425–437, 2016.

[9] R. Marco, H. Allan, and M. Denise, "Can electric vehicles significantly reduce our dependence on non-renewable energy? Scenarios of compact vehicles in the UK as a case in point," *Journal of Cleaner Production*, vol. 201, pp. 1043–1051, 2018.

[10] S.-B. Tsai, Y. Xue, J. Zhang et al., "Models for forecasting growth trends in renewable energy," *Renewable and Sustainable Energy Reviews*, vol. 77, pp. 1169–1178, 2017.

[11] X. Zhao, Q. Yu, J. Ma, Y. Wu, M. Yu, and Y. Ye, "Development of a representative EV urban driving cycle based on a k-means and SVM hybrid clustering algorithm," *Journal of Advanced Transportation*, vol. 2018, Article ID 1890753, 18 pages, 2018.

[12] Z. Lv, B. Hu, and H. Lv, "Infrastructure monitoring and operation for smart cities based on IoT system," *IEEE Transactions on Industrial Informatics*, vol. 16, no. 3, pp. 1957–1962, 2020.

[13] T. Yi, C. Zhang, T. Lin, and J. Liu, "Research on the spatial-temporal distribution of electric vehicle charging load demand: a case study in China," *Journal of Cleaner Production*, vol. 242, Article ID 118457, 2020.

[14] P. Hu, Z. Tan, G. Qiu et al., "Overview of the development of electric vehicles," *Electrotechnical Application*, vol. 37, pp. 79–85, 2018, in Chinese.

[15] J. Ma, X. Liu, Y. Chen et al., "Current status and countermeasures for China's new energy automobile industry and technology development," *China Journal of Highway and Transport*, vol. 31, pp. 1–19, 2018, in Chinese.

[16] F. Gu, J. Guo, X. Yao, P. A. Summers, S. D. Widijatmoko, and P. Hall, "investigation of the current status of recycling spent lithium-ion batteries from consumer electronics in China," *Journal of Cleaner Production*, vol. 161, pp. 765–780, 2017.

[17] L. Widijatmoko and Z. Hanwen, "An ontology constructing technology oriented on massive social security policy documents," *Cognitive Systems Research*, vol. 60, pp. 97–105, 2020.

[18] K. M. Tan, V. K. Ramachandaramurthy, and J. Y. Yong, "Integration of electric vehicles in smart grid: A review on vehicle to grid technologies and optimization techniques," *Renewable and Sustainable Energy Reviews*, vol. 53, pp. 720–732, 2016.

[19] K. Guo, "Research on location selection model of distribution network with constrained line constraints based on genetic algorithm," *Neural Computing and Applications*, vol. 32, no. 6, pp. 1679–1689, 2019.

[20] D. Yu, H. Zhu, W. Han, and D. Holburn, "Dynamic multi agent-based management and load frequency control of PV/ Fuel cell/ wind turbine/ CHP in autonomous microgrid system," *Energy*, vol. 173, no. 15, pp. 554–568, 2019.

[21] C. A. Klöckner, A. Nayum, and M. Mehmetoglu, "Positive and negative spillover effects from electric car purchase to car use," *Transportation Research Part D: Transport and Environment*, vol. 21, pp. 32–38, 2013.

[22] B. Zhou, F. Yao, T. Littler, and H. Zhang, "An electric vehicle dispatch module for demand-side energy participation," *Applied Energy*, vol. 177, pp. 464–474, 2016.

[23] P. Finn, C. Fitzpatrick, and D. Connolly, "Demand side management of electric car charging: benefits for consumer and grid," *Energy*, vol. 42, no. 1, pp. 358–363, 2012.

[24] W. Kempton and T. Kubo, "Electric-drive vehicles for peak power in Japan," *Energy Policy*, vol. 28, no. 1, pp. 9–18, 2000.

[25] C. D. White and K. M. Zhang, "Using vehicle-to-grid technology for frequency regulation and peak-load reduction," *Journal of Power Sources*, vol. 196, no. 8, pp. 3972–3980, 2011.

[26] C.-H. Chen, "An arrival time prediction method for bus system," *IEEE Internet of Things Journal*, vol. 5, no. 5, pp. 4231-4232, 2018.

[27] Y. Zhang, Q. He, Y. Xiang et al., "Low-cost and confidentiality-preserving data acquisition for internet of multimedia things," *IEEE Internet of Things Journal*, vol. 5, no. 5, pp. 3442–3451, 2017.

[28] V. K. Senthil Ragavan, M. Elhoseny, and K. Shankar, "An enhanced whale optimization algorithm for vehicular communication networks," *International Journal of Communication Systems*, 2019, In press.

[29] X. J. Qi, D. W. Li, and S. Y. Ji, "Orderly charging strategy of electric vehicles in residential areas with power limitation," *Power Grid Technology*, vol. 40, no. 12, pp. 3715–3721, 2016, in Chinese.

[30] F. Salah and C. M. Flath, "Deadline differentiated pricing in practice: marketing EV charging in car parks," *Computer Science—Research and Development*, vol. 31, no. 1-2, pp. 33–40, 2014.

[31] F. He, Y. Yin, J. Wang, and Y. Yang, "Sustainability SI: optimal prices of electricity at public charging stations for plug-in electric vehicles," *Networks and Spatial Economics*, vol. 16, no. 1, pp. 131–154, 2013.

[32] T. Ikegami, H. Yano, K. Kudo, and K. Ogimoto, "Effects of smart charging of multiple electric vehicles in reducing power generation fuel cost," *Electrical Engineering in Japan*, vol. 193, no. 2, pp. 42–57, 2015.

[33] Y. Cao, S. Tang, C. Li et al., "An optimized EV charging model considering TOU price and SOC curve," *IEEE Transactions on Smart Grid*, vol. 3, no. 1, pp. 388–393, 2012.
[34] K. Lu, S. Liu, X. Niu, W. Xue, Y. zhu, and Z. Zhu, "Pricing method of electric vehicle charging by using cost-benefit analysis," *Proceedings of the CSU-EPSA*, vol. 26, pp. 76–80, 2014, in Chinese.
[35] N. O'Connell, Q. Wu, J. Ostergaard, A. H. Nielsen, S. T. Cha, and Y. Ding, "Electric vehicle (ev) charging management with dynamic distribution system tariff," in *Proceedings of the 2nd IEEE PES International Conference and Exhibition on Innovative Smart Grid Technologies University Manchester*, Manchester, UK, 2011.
[36] A. Ghosh and V. Aggarwal, "Control of charging of electric vehicles through menu-based pricing," *IEEE Transactions on Smart Grid*, vol. 9, no. 6, pp. 5918–5929, 2018.
[37] S. Martinenas, A. B. Pedersen, M. Marinelli, and P. B. Andersen, "Electric vehicle smart charging using dynamic price signal," in *2014 IEEE International Electric Vehicle Conference (IEVC)*, December 2014.
[38] X. Dong, Y. Mu, X. Xu et al., "A charging pricing strategy of electric vehicle fast charging stations for the voltage control of electricity distribution networks," *Applied Energy*, vol. 225, pp. 857–868, 2018.
[39] Y. Cao, Q. Wang, W. Cheng, S. Nojavan, and K. Jermsittiparsert, "Risk-constrained optimal operation of fuel cell/photovoltaic/battery/grid hybrid energy system using downside risk constraints method," *International Journal of Hydrogen Energy*, vol. 45, no. 27, pp. 14108–14118, 2020.
[40] X. Li, H. Li, J. Zhang, Y. Liu, Y. Niu, and N. Song, "Dynamic breakeven analysis on the charging price of electric vehicle charging station," in *2012 China International Conference on Electricity Distribution (CICED)*, Shanghai, China, September 2012.
[41] L. Pu, Q. Ai, W. Yu, and J. Chen, "Multi-agent elecetronic pricing strategy for electric vehicle charging cosidering customer satisfaction degree," *Automation of Electric Power Systems*, vol. 22, pp. 69–75, 2015, in Chinese.
[42] J. Cui, W. Luo, and N. Zhou, "Research on pricing model and strategy of electric vehicle charging and discharging based on multi view," *Proceedings of the CSEE*, vol. 15, 2018 in Chinese.
[43] B. Zhu, M. Zhang, L. Huang, P. Wang, B. Su, and Y. Wei, "Exploring the effect of carbon trading mechanism on China's green development efficiency: a novel integrated approach," *Energy Economics*, vol. 85, p. 104601, 2020.
[44] M. Elhoseny, X. Yuan, H. K. El-Minir, and A. M. Riad, "Extending self-organizing network availability using genetic algorithm," in *Proceedings of the 5th International Conference on Computing Communication and Networking Technologies, ICCCNT*, Hefei, China, July 2014.
[45] Y. Cao, Y. Li, G. Zhang, K. Jermsittiparsert, and M. Nasseric, "An efficient terminal voltage control for pemfc based on an improved version of whale optimization algorithm," *Energy Reports*, vol. 6, pp. 530–542, 2020.
[46] K. Deb, A. Pratap, S. Agarwal, and T. Meyarivan, "A fast and elitist multi-objective genetic algorithm: NSGA-II," *IEEE Transactions on Evolutionary Computation*, vol. 6, pp. 182–197, 2002.
[47] G. B. Elias and W. N. John, "Multi-objective automatic calibration of SWAT using NSGA-II," *Journal of Hydrology*, vol. 341, no. 3-4, pp. 165–176, 2007.
[48] S. Debasis and M. M. Jayant, "Pareto-optimal solutions for multi-objective optimization of fed-batch bioreactors using nondominated sorting genetic algorithm," *Chemical Engineering Science*, vol. 60, no. 2, pp. 481–492, 2005.
[49] P. Murugan, S. Kannan, and S. Baskar, "NSGA-II algorithm for multi-objective generation expansion planning problem," *Electric Power Systems Research*, vol. 79, no. 4, pp. 622–628, 2009.
[50] T. Gaber, S. Abdelwahab, M. Elhoseny, and A. E. Hassanien, "Trust-based secure clustering in WSN-based intelligent transportation systems," *Computer Networks*, vol. 146, pp. 151–158, 2018.
[51] S.-B. Tsai, C.-Y. Huang, C. Yu, Q. Chen et al., "Using a mixed model to evaluate job satisfaction in high-tech industries," *PLoS One*, vol. 11, no. 5, Article ID e0154071, 2016.

Hindawi
Journal of Advanced Transportation
Volume 2020, Article ID 5036792, 14 pages
https://doi.org/10.1155/2020/5036792

Research Article

Blockchain-Based Intelligent Transportation: A Sustainable GCU Application System

Xiaomin Du,[1] Yang Gao,[2] Chia-Huei Wu,[3] Rong Wang,[2] and Datian Bi[4]

[1]*Department of Economic Management, Yingkou Institute of Technology, Yingkou, China*
[2]*School of Economics and Management, Dalian University of Technology, Dalian 116024, China*
[3]*Institute of Service Industries and Management, Minghsin University of Science and Technology, Hsinchu 304, Taiwan*
[4]*School of Management, Jilin University, Changchun 130022, China*

Correspondence should be addressed to Datian Bi; bdt@jlu.edu.cn

Received 20 February 2020; Revised 30 April 2020; Accepted 27 May 2020; Published 25 June 2020

Academic Editor: Wenqing Wu

Copyright © 2020 Xiaomin Du et al. This is an open access article distributed under the Creative Commons Attribution License, which permits unrestricted use, distribution, and reproduction in any medium, provided the original work is properly cited.

The purpose of this study is to explore how to apply blockchain technology to intelligent transportation, create a hierarchical theoretical framework of intelligent transportation, and explore a sustainable application system of intelligent transportation under the blockchain. However, not only this hierarchical theoretical framework must consider unnecessary attributes and the interrelationships between the aspects and the criteria, but also the sustainable application system must be in consideration in multiple stakeholders. Hence, fuzzy set theory is used for screening out the unnecessary attributes, a decision-making trial and evaluation laboratory (DEMATEL) is proposed to manage the complex interrelationships among the aspects and attributes, and interpretive structural modeling (ISM) is used to divide the hierarchy and construct a hierarchical theoretical framework. Finally, the research develops a sustainable GCU application system for intelligent transportation under the blockchain. The results show that (1) solving social problems is the primary link, (2) economic tasks are mainly focused on smart contracts and affected by the social problems, (3) the continuous improvement of environmental issues requires a solution to social problems, and (4) the application system of blockchain in intelligent transportation needs to be built from three levels including the government layer, the company layer, and the user layer. This theoretical hierarchical framework aims to guide intelligent transportation toward the application of blockchain. This study also proposes the engagement of stakeholders for establishing a sustainable application system.

1. Introduction

Urban intelligent traffic aims to give full play to the carrying capacity of the road network, solve all varieties of traffic problems, and improve traffic safety and environmental protection. In the field, this means using physics, computer science, Internet of Things technology, and integrated traffic information to establish a dynamic information service system to realize a rapid response to traffic problems, improve traffic conditions, and increase transport efficiency [1, 2]. Intelligent transportation will greatly improve the management of urban transportation systems to optimize the urban layout and promote the process of smart city development [3]. Blockchain, as a disruptive technological innovation following the emergence of the Internet, is being applied for its tamper-proof, traceable, high-trust, and decentralized distributed accounting system [4, 5], leading to a new round of global technological and industrial changes. Combining blockchain and intelligent traffic to establish a transportation consortium blockchain participated in by government, company, and user, allowing implementation of data upload, storage, and conditional queries, will promote the further upgrade and development of intelligent transportation.

Currently, blockchain has attracted wide attention from all walks of life. Existing research results include the basic underlying technologies of blockchain [6, 7], blockchain credit evaluation systems [8], and blockchain transaction cost analysis [9, 10]. However, studies on blockchain in the intelligent transportation industry are still in the exploratory stage, and most focus on the impact of the characteristics of blockchain on transportation, such as the establishment of blockchain-based traffic safety data sharing systems [11], the creation of electric vehicle safe energy trading schemes [12, 13], or the issue of freely tradable mobile licenses based on the blockchain [14]. The development system for intelligent transportation under blockchain is very vague. In addition, the application of blockchain in the intelligent transportation industry is difficult to explain from a single level because it interacts with all the subjects in intelligent transportation simultaneously in the application process, requiring multiple subjects to cooperate and interact with each other. From the perspective of stakeholders, it is still rare to explore a development system coordinated by multiple subjects. Moreover, few existing studies have studied the combination of blockchain and intelligent transportation from a sustainability perspective, which requires comprehensive consideration of upgrading needs and challenges for intelligent transportation brought by blockchain considering three aspects: the economy, society, and environment. Finally, at present, the application of blockchain to the physical industry lacks exploration at the level of consortium blockchains, as research is more focused on private blockchains [15]. Due to the existence of information controlled by the leading enterprise, the credibility of information is questioned in private blockchains, and their application is limited [16]. Although public blockchains have greater information credibility than private blockchains, they remain difficult to apply and popularize in the real economy. This is because the public blockchain needs to include a large number of participants, making it difficult to guarantee the security of participant's privacy [17], and blockchain's feature of "complete decentralization" brings great obstacles to the system design. By featuring only "partial decentralization," the consortium blockchain just needs to include a limited number of subjects to increase security, reduce cost, increase reliability, and increase the level of trust in the application process to better control and promote the implementation of blockchain in intelligent transportation.

Urban transportation includes a wide range. Considering that underground transportation has its unique operating system such as the subway. Our research focuses on urban ground transportation, including buses, private cars, taxis, and Internet-based traffic. Based on the above, to develop a sustainable application system of blockchain in intelligent transportation based on a consortium blockchain, the following research is carried out in this paper. First, to systematically consider the impact of blockchain on the sustainable development of intelligent transportation, a set of valid criteria are proposed from the three aspects of the economy, society, and environment. Second, considering the mutual restriction and in order to make multiattribute decisions among multiple attributes, the theory of fuzzy sets, decision-making trial and evaluation laboratory (DEMATEL), and interpretation structure model (ISM) are synthetically integrated. Third, combined with the above analysis and the theory of stakeholders, a sustainable application system of blockchain intelligent transportation based on a consortium blockchain is constructed from the three levels.

Through this study, we can draw the following scientific conclusions. First, the impact of blockchain technology on the sustainable development of intelligent transportation is mainly reflected in three aspects, namely, the social level, economic level, and environmental level. Second, the study finds that these three layers have different importance. First, solving social problems is the primary link for the sustainable development of blockchain in intelligent transportation. At the social level, we need to solve two problems: institutional completeness and the impact of blockchain technology characteristics on society. Second, in the whole development process of blockchain in intelligent transportation, the development of the economic level mainly occurs around smart contracts and is affected by the social level. The continuous improvement of environmental issues requires a solution to social problems. In addition, one innovation of this paper is its study of the related issues in the field of blockchain-based intelligent transportation from the perspective of finance and taxation. Finally, the application system of intelligent transportation under the blockchain needs to be built around three levels: the government layer, the company layer, and the user layer. The results of this paper provide an important theoretical reference for the sustainable development of intelligent transportation under the blockchain.

2. Literature Review

As the underlying technology of bitcoin, the blockchain is essentially a decentralized database that comprehensively utilizes distributed data storage, consensus mechanisms, point-to-point transmission, encryption algorithms, intelligent contracts, and other computer technologies. Data with timestamps and digital signatures are packaged into blocks in the blockchain, which are linked by hash pointers to form a chained ledger structure. The distributed storage of the blockchain facilitates data sharing, and the digital signature in the data records can self-verify the correctness of the data. By linking blocks together, hash pointers prevent hackers from falsifying the data and allows the data to be traced back to its source. The technological novelty of blockchain lies in the fact that it is possible to build a consensus on the true state of the ledger without trusting any centralized entity or an intermediary [18]. Therefore, the blockchain has the excellent characteristics of supporting data sharing and being tamper-proof, trustworthy, and traceable, making it suitable for building an information system to deal with multiparty collaborative business.

By applying blockchain technology to intelligent transportation, our research has built a transportation consortium blockchain led by the government and involving multiple parties, giving full play to the carrying capacity of the road network, solving various traffic problems, and improving traffic safety and environmental protection. In this study, we analyzed the economic, social, and environmental aspects of the system based on the triple bottom line principle. The economic focus is on cost analysis, the social aspect focuses on the management of social issues, and the environmental aspect mainly refers to the environmental benefits of blockchain-based intelligent transportation. Combined with new technologies such as the Internet of Things and the characteristics of blockchain, the application system of blockchain in intelligent transportation is built, including 3 aspects and 15 criteria.

2.1. Intelligent Transportation under Blockchain: Economic Aspect. In terms of the economy, we begin with a cost analysis to study the impact of blockchain-based intelligent transportation on the economic cost of government and enterprises. The four criteria include transaction cost, management cost, infrastructure construction cost, and financial cost.

Blockchain, which keeps a permanent record of past transactions and has a tamper-proof system, can reduce well-designed opportunistic behavior. Reliable ledgers can create an economic environment with low transaction cost, which is a prerequisite for achieving economic efficiency and prosperity [19]. Intelligent contracts and information sharing technology can establish a better trust mechanism that can reduce the behavioral uncertainty in the transaction relationship. The distributed accounting system and decentralized nature of blockchain reduce the costs associated with intermediaries. All these factors reduce the transaction cost of government and enterprises [9, 10]. In terms of management cost, automatic data uploading and traceability systems can reduce the cost of monitoring, controlling, and approving the fund flow to prevent fraud and increase the supervision of the fund flow. Immutable and distributed bookkeeping reduces the human cost of information research, monitoring, and management for governments and enterprises [20]. The use of smart contracts can reduce the use of paper and other consumables, realize rapid discussion, and save time, and sharing databases can reduce management work [21]. In terms of infrastructure construction cost, traffic information in the blockchain can be analyzed and processed to support the overall planning of the urban traffic network layout, including logistics and transportation, road planning, road construction, bus station construction, and optimization of the supporting infrastructure construction scheme. In terms of financial cost, the automatic data uploading and traceability system facilitates the electronic bill management of companies. Blockchain technology gives the government and auditing institutions the right to examine company accounts through blockchain, strengthens the supervision of company profits and taxes, and reduces tax fraud. Coyne and McMickle [22] believe that blockchain-based digital currency only exists in the blockchain, while economic transactions exist outside the blockchain records, which will prevent the use of the blockchain model for acceptable transaction verification. However, combining blockchain with the Internet of Things technology can effectively solve this problem and make blockchain accounting possible in the field of transportation.

2.2. Intelligent Transportation under Blockchain: Social Aspect

2.2.1. Blockchain Features Have an Impact on Society. Blockchain is a distributed shared ledger and database involving mathematics, cryptography, the Internet, computer programming, and other fields. It has the characteristics of being decentralized, tamper-proof, and traceable and supporting whole-process marking, collective maintenance, openness, and transparency [23]. These features ensure the reliability of the blockchain. The combination of blockchain and the Internet of Things technology can realize automatic data upload and timely information update, which can improve the timeliness of transactions by instantly forming smart contracts [24]. Therefore, we classify the characteristics of blockchain as reliability and timeliness.

2.2.2. Problem Management. In this section, we discuss how the blockchain can optimize solutions to the existing problems in traffic, relieve traffic pressure, and promote urban development, including Internet-based traffic management, congestion management, urban space optimization, convenient travel, and parking management as 5 criteria.

In terms of Internet-based traffic management, blockchain technology allows the use of the aggregate signature scheme to connect the channels under the chain to build a secure large-scale real-time payment system and improve the capacity of the blockchain system [25]. The blockchain is used to record Internet-based traffic information and make public the basic personal information and credit ratings of Internet-based traffic drivers to ensure that those responsible for traffic accidents can be held accountable. At the same time, transaction information for Internet-based traffic can be tracked and conditions investigated, which will make it easier for the government to collect taxes and facilitate tax administration.

In terms of congestion management, solutions to alleviate traffic congestion are as follows: the traffic management department issues a limited number of mobile licenses, distributes them equally among all users, and conducts free trade in the market through blockchain technology and "smart contracts" [14]; priority is given to emergency vehicles by allocating high prices on all routes; in the "Internet of vehicles" environment, the data exchange between vehicles and between vehicles and infrastructure is regarded as transaction information stored in the blockchain to enrich the traffic information; heavy truck rows are encouraged [26]; payment is made in blockchain digital currency to reduce transaction time [27]; machine vision technology is used to collect the images of relevant sections, solve the problem of image recognition in intelligent vehicles, optimize the judgment of obstacles, and plan the follow-up routes of intelligent vehicles [28].

In terms of urban space optimization, regional industrial agglomeration promotes the optimization of urban structure and space and promotes the sustainable transformation of cities, which in turn will promote the optimization of transportation networks [3]. In terms of convenient travel, users are encouraged to participate in the blockchain platform to share traffic information and improve navigation information. At the same time, the reduction of traffic congestion and the convenience of public transportation will facilitate public travel. In terms of parking management, free parking can be traded through the blockchain, which can generate income for the owner, on the one hand, and alleviate the problem of difficult parking, on the other hand.

2.2.3. Top-Level System Design. The top-level system design, including the reward and punishment system and the credit evaluation system, is the foundation of the whole blockchain-based intelligent traffic index framework and plays an important supporting role in the system. The reward and punishment system refers to virtual currency rewards for users who actively participate in blockchain and publish real information [29]. A credit evaluation system refers to the use of blockchain technology to ensure data integrity and nonrepudiation, evaluate user trust by evaluating service trust, behavior trust, and task trust, and establish a safe and reliable database to support analytical queries with different query timestamps [8, 11]. Yang et al. [30] proposed a blockchain-based decentralized trust management system for vehicle networks.

2.3. Intelligent Transportation under Blockchain: Environmental Aspect. The most serious part of urban traffic pollution is the excessive emission of automobile exhaust. Methods to reduce urban traffic pollution through blockchain include optimizing traffic routes through blockchain, reasonably controlling speed; reducing instantaneous acceleration and idling to reduce carbon dioxide emissions [31, 32]; and encouraging or requiring heavy truck lines to reduce air resistance and fuel consumption [33]. The popularity of energy transactions between electric vehicles and charging stations in the vehicle-to-grid (V2G) environment has increased the use of electric vehicles [12, 13]. A more comprehensive public transport system has increased the rates of public travel. In addition, a reasonable urban greening layout based on multiple pieces of information in the transportation consortium blockchain [34] is also beneficial to urban environmental governance. A detailed explanation of each criterion is shown in Table 1.

3. Method

This paper uses the DEMATEL method to fully consider the number and correlation of influencing factors and gives the importance of the influencing factors. We explore from 15 influencing factors and explain the inner structure of the influencing factor system in a deeper level, including transaction cost (C1), management cost (C2), infrastructure construction cost (C3), financial cost (C4), reliability (C5), timeliness (C6), Internet-based traffic management (C7), congestion management (C8), urban space optimization (C9), convenient travel (C10), parking management (C11), reward and punishment system (C12), credit evaluation system (C13), urban traffic pollution (C14), and urban greening layout (C15). Considering the complexity and ambiguity of the relationship between various influencing factors, this paper introduces the concept of fuzzy sets and uses a semantic conversion table to perform a series of transformations on the original expert data to remove subjective factors. The hybrid DEMATEL method is used to standardize the hybrid matrix given by the experts and obtain a hybrid comprehensive influence factor matrix by matrix calculation. Then, calculate its centrality and causality to reveal the most critical factors affecting the blockchain-based intelligent transportation [35]. The DEMATEL method can calculate the importance of a specific factor in the influencing factor system, but it cannot determine the intrinsic relationship of the factors and the division of the hierarchical structure. It is difficult to effectively manage and control the factors. Therefore, the ISM method is also required to classify the system structure. And the combination of the two methods can reduce the difficulty in matrix calculation [36]. The ISM method can transform nebulous thoughts and ideas into an intuitive model of structural relationships to understand the relationship between the variables [37].

3.1. Fuzzy DEMATEL. Fuzzy mathematics based on fuzzy set theory is applied to the analysis of the fuzzy degree of feature relevance. Triangular fuzzy number (TFN) provides an effective means of quantifying human linguistic preferences into computable form [38]. DEMATEL technique provides a way to elucidate the complex interrelationships among attributes in a given problem [39]. Fuzzy DEMATEL is a method to simulate the human brain processing fuzzy information [40]. This method retains practical and effective advantages of the traditional DEMATEL method for factor identification. In addition, the triangular fuzzy number is used to replace the original accurate value, and this approach can improve the credibility of the analysis results and provide a more valuable reference for managers to make decisions. The steps are as follows [41]:

Step 1: for the problem under study, build a system of influencing factors set to $F1, F2, \ldots, Fn$.

Step 2: determine the influence relationship between two factors by an expert scoring method and express the relationship in matrix form. Invite experts to use the language operators "no impact (N)," "very low influence (VL)," "low influence (L)," "high influence (H)," and "very high influence (VH)." The relationship between the two factors is assessed. Convert the original expert evaluations into triangular fuzzy numbers via a semantic table $w_{ij}^{k} = (a_{1ij}^{k}, a_{2ij}^{k}, a_{3ij}^{k})$ to represent the extent to which k experts consider the influence of the i-th factor on the j-th factor, as shown in Table 2.

Step 3: using the Converting the Fuzzy data into Crisp Scores (CFCS) method to defuzzify the initial values of

Table 1: Proposed attributes.

Aspects	Criteria	Explanation
Economic	C1: transaction cost	Smart contracts; decentralized, tamper-proof, permanent records
	C2: management cost	Automated data upload and traceability systems reduce monitoring costs and labor costs
	C3: infrastructure construction cost	Analyze and process traffic information and plan traffic network
	C4: financial cost	Electronic bill management, blockchain-based audit, blockchain-based tax supervision
Society	C5: reliability	Secure databases, irreversibly distributed accounting systems, traceability, smart contracts
	C6: timeliness	Instantly form a smart contract
	C7: Internet-based traffic management	Blockchain accounting; record transaction information to ensure accountability for drivers
	C8: congestion management	Issue of transportation permits. Give different prices to different roads. Heavy trucks line up. Blockchain transactions
	C9: urban space optimization	Regional industrial agglomeration promotes the optimization of urban space
	C10: convenient travel	Traffic congestion is reduced, public transportation is more convenient, and traffic information is more abundant
	C11: parking management	Trade parking spaces that are not used for a period of time via the blockchain
	C12: reward and punishment system	Virtual currency rewards are offered to users who actively participate in blockchain and publish real messages
	C13: credit evaluation system	Conduct credit assessments for blockchain participants
Environment	C14: urban traffic pollution	Reasonable control of speed, reduce carbon dioxide emissions, and reduce fuel consumption; charging electric cars is easier; improve public transport
	C15: urban greening layout	Make a reasonable greening plan according to the city layout

Table 2: Semantic transformation table.

Linguistic variables	TFN
N (no influence)	(0, 0, 0.2)
VL (very low influence)	(0, 0.2, 0.4)
L (low influence)	(0.2, 0.4, 0.6)
H (high influence)	(0.4, 0.6, 0.8)
VH (very high influence)	(0.8, 1, 1)

the expert scores, the nth order directly affects the matrix Z, and the direct influence matrix reflects the direct effect between the factors, including the following four steps:

(1) Normalize triangular fuzzy numbers:

$$xa_{1ij}^{k} = \frac{\left(a_{1ij}^{k} - \min a_{1ij}^{k}\right)}{\Delta_{\min}^{\max}},\quad xa_{2ij}^{k} = \frac{\left(a_{2ij}^{k} - \min a_{1ij}^{k}\right)}{\Delta_{\min}^{\max}},\quad xa_{3ij}^{k} = \frac{\left(a_{3ij}^{k} - \min a_{1ij}^{k}\right)}{\Delta_{\min}^{\max}}. \tag{1}$$

$$xls_{ij}^{k} = \frac{xa_{2ij}^{k}}{1 + xa_{2ij}^{k} - xa_{1ij}^{k}},\quad xrs_{ij}^{k} = \frac{xa_{3ij}^{k}}{1 + xa_{3ij}^{k} - xa_{2ij}^{k}}. \tag{2}$$

$$x_{ij}^{k} = \frac{\left[xls_{ij}^{k}\left(1 - x\,ls_{ij}^{k}\right) + xrs_{ij}^{k} x\,rs_{ij}^{k}\right]}{\left[1 - xls_{ij}^{k} + xrs_{ij}^{k}\right]},\quad z_{ij}^{k} = \min a_{1ij}^{k} + x_{ij}^{k} \times \Delta_{\min}^{\max}. \tag{3}$$

$$z_{ij}^{k} = \frac{z_{ij}^{1} + z_{ij}^{2} + \cdots + z_{ij}^{k}}{n}. \tag{4}$$

Step 4: normalize the direct influence matrix Z to obtain the standardized direct influence matrix G:

$$\lambda = \frac{1}{\max\limits_{1\le i\le n} \sum_{j=1}^{n} z_{ij}}, G = \lambda Z. \tag{5}$$

Step 5: according to $T = G + G^2 + \cdots + G^n$ or $T = G(E - G)^{-1}$, E is the identity matrix, and the comprehensive influence matrix T is obtained.

Step 6: analyze the comprehensive matrix to reveal the internal structure of the sustainable application system. The elements in matrix T are added by row as the influence degree D_i, which represents the comprehensive influence value of the row factor on all other factors. The elements in matrix T are added as the affected degree R_i by column, indicating the comprehensive influence value of all other factors in that column. The formulas are as follows:

$$D_i = \sum_{j=1}^{n} t_{ij}, \quad i = 1, 2, \ldots, n, \tag{6}$$

$$R_i = \sum_{i=1}^{n} t_{ij}, \quad i = 1, 2, \ldots, n. \tag{7}$$

(2) Normalize the left value (ls) and right value (rs):

(3) Calculate the clear value after defuzzification:

(4) Calculate the average clear value:

The sum of the influence degree and affected degree is called centrality, which indicates the position of the factor in the system and the size of its role. The difference between the influence degree and the affected degree is called causality, which reflects the causal relationship between the influencing factors. If the causality is greater than 0, the factor has a great effect on other factors and is called the factor of cause. If the causality is less than 0, the factor is greatly affected by other factors and is called the factor of result. The formulas are as follows:

$$m_i = D_i + R_i, \quad i = 1, 2, \ldots, n, \tag{8}$$

$$\begin{aligned} n_i &= D_i - R_i, \quad i = 1, 2, \ldots, n, \\ H &= T_i - R_i, \quad i = 1, 2, \ldots, n. \end{aligned} \tag{9}$$

3.2. ISM. The ISM method is also needed to classify the system structure to transform the ambiguous ideas and views into an intuitive model with structural relationships. The direct influence matrix is calculated, and the comprehensive influence matrix is obtained. The comprehensive influence matrix t reflects only the mutual influence relationship and degree between different factors and does not consider the influence of factors on itself. Therefore, it is necessary to calculate the overall influence relationship reflecting system factors, i.e., the overall influence matrix. The calculation formula is as follows:

$$\begin{aligned} H &= T + E = h_{ij}, \\ \lambda &= \alpha + \beta, \end{aligned} \tag{10}$$

where α and β are the mean and standard deviation of all elements in the comprehensive influence matrix T, respectively.

A threshold is used to remove the redundant factors, and the reachable matrix is obtained:

$$\begin{aligned} M &= \left[m_{ij}\right]_{n*n}, \quad i = 1, 2, \ldots, n; j = 1, 2, \ldots, n, \\ m_{ij} &= \begin{cases} 1, & h \geq \lambda, \\ 0, & h \leq \lambda, \end{cases} \quad i = 1, 2, \ldots, n; j = 1, 2, \ldots, n. \end{aligned} \tag{11}$$

1 means there is a direct effect between the two factors, and 0 means there is no direct effect between the two factors.

The reachable set $L(f_i)$, antecedent set $P(f_i)$, and common set

$$C(f_i) = L(f_i) \cap P(f_i), \tag{12}$$

are obtained by hierarchical processing.

Finally, the ISM is determined by the reachable set and common set.

4. Results

In order to standardize the practice of intelligent transportation and ensure the embedding of blockchain technology, it is necessary to evaluate the rationality and standardization of the research through the expert committee. The expert committee is composed of 7 experts who have more than 8 years of experience in intelligent transportation enterprise or working in relevant departments. Prior to the process of evaluation, the committee need to prove that the attributes proposed in the study (including aspects and criteria) can reflect the real situation of the intelligent transportation industry. Once an expert disagrees with the proposed measures, the committee needs to discuss the arguments until all experts agree. Therefore, several rounds of discussion will be repeated to ensure the reliability of the research. Data collection adopts individual face-to-face interviews to improve consistency and prevent the judgment of other experts from being affected. Then, according to the CFCS method, the original data are processed, and finally, the direct impact matrix for the influencing factors of blockchain technology on intelligent transportation is determined, as shown in Table 3.

The direct impact matrix of blockchain technology in intelligent transportation is standardized to obtain the standardized direct impact matrix. Then, according to the formula $T = G\ (E - G) - 1$, MATLAB software is used to calculate the matrix, and the comprehensive impact matrix is obtained, as shown in Table 4.

According to formulas (6)–(9), the influence degree, affected degree, centrality, and causality are calculated as shown in Table 5, and a causal relationship diagram is shown in Figure 1.

According to the positive and negative causality, 15 risk factors are divided into a cause set and a result set. Table 5 shows that there are 7 causal factors, which should be taken into consideration when developing measures, including Internet-based traffic management (C7), transaction cost (C1), credit evaluation system (C13), congestion management (C8), reward and punishment system (C12), timeliness (C6), and reliability (C5). As shown in Tables 4 and 5 and Figure 1, the corresponding influence degrees of C5, C6, and C12 are 2.3341, 2.2583, and 2.1056, which are the three most influential values among all factors, indicating that these three factors have the greatest influence on other factors. There are 8 result factors, including parking management (C11), urban greening layout (C15), urban traffic pollution (C14), financial cost (C4), management cost (C2), infrastructure construction cost (C3), convenient travel (C10), and urban space optimization (C9). They have a weaker impact on intelligent transportation under the blockchain technology, but are more susceptible to changes caused by other factors. Therefore, in actual management, proper attention and control should be given to help improve management effectiveness.

The degree of centrality reflects the importance of various influencing factors in the sustainable development system of blockchain-based intelligent transportation. Sorted by the degree of centrality, the factors in descending order are reliability (C5), reward and punishment system (C12), timeliness (C6), congestion management (C8), credit evaluation system (C13), Internet-based traffic management (C7), infrastructure construction cost (C3), transaction cost (C1), convenient travel (C10), urban space optimization (C9), management cost (C2), urban traffic pollution (C14), urban greening layout (C15), financial cost (C4), and parking management (C11). The degree of causality is positive and negative, the action direction is opposite, and the impact characteristics on intelligent transportation are

Table 3: The direct influence matrix of blockchain technology on intelligent transportation.

	C1	C2	C3	C4	C5	C6	C7	C8	C9	C10	C11	C12	C13	C14	C15
C1	0.0000	0.4302	0.4048	0.4048	0.1381	0.1508	0.0873	0.0111	0.2143	0.2524	0.2143	0.2143	0.1889	0.2016	0.2016
C2	0.1254	0.0000	0.2270	0.1381	0.1635	0.1000	0.1254	0.0111	0.1508	0.1762	0.1127	0.0111	0.1381	0.0111	0.0111
C3	0.1381	0.1254	0.0000	0.0238	0.1127	0.1762	0.1635	0.1762	0.1508	0.0111	0.1254	0.1127	0.1889	0.4302	0.4302
C4	0.1889	0.1508	0.1635	0.0000	0.1889	0.0111	0.0238	0.0111	0.0238	0.0111	0.1127	0.1762	0.1127	0.0111	0.0111
C5	0.4048	0.4302	0.1000	0.2778	0.0000	0.2651	0.4302	0.4302	0.3032	0.2524	0.2651	0.2524	0.4556	0.2524	0.1889
C6	0.4048	0.1889	0.1000	0.2397	0.2524	0.0000	0.4302	0.4556	0.2524	0.2651	0.4302	0.2397	0.4556	0.1762	0.2651
C7	0.1635	0.2524	0.4302	0.2524	0.2524	0.1254	0.0000	0.1635	0.0111	0.4048	0.2524	0.2778	0.2524	0.0365	0.0365
C8	0.1508	0.1381	0.4556	0.1635	0.1127	0.1635	0.4556	0.0000	0.4048	0.4048	0.1635	0.1000	0.2524	0.1635	0.2524
C9	0.1000	0.1762	0.1127	0.1762	0.0111	0.1000	0.1635	0.2397	0.0000	0.1000	0.4556	0.0111	0.0111	0.2524	0.4048
C10	0.1381	0.1254	0.1000	0.1508	0.1127	0.1889	0.1127	0.2524	0.1889	0.0000	0.0111	0.0238	0.0111	0.4556	0.4048
C11	0.1127	0.1381	0.1254	0.2397	0.0238	0.0111	0.0238	0.0238	0.2524	0.1127	0.0000	0.0111	0.0111	0.0111	0.0111
C12	0.2524	0.2524	0.1127	0.2524	0.2778	0.2778	0.4556	0.4556	0.1889	0.1889	0.1889	0.0000	0.4048	0.2397	0.2397
C13	0.1889	0.2651	0.4556	0.2270	0.1762	0.2016	0.1000	0.1635	0.0111	0.1889	0.1254	0.4556	0.0000	0.4302	0.2524
C14	0.0111	0.0111	0.1635	0.0111	0.0111	0.0111	0.1000	0.1127	0.1127	0.1127	0.1000	0.1254	0.2270	0.0000	0.0111
C15	0.0111	0.0111	0.1254	0.0111	0.0238	0.0111	0.0111	0.2524	0.1635	0.1127	0.1762	0.1000	0.0111	0.1000	0.0000

Table 4: The comprehensive impact matrix of blockchain technology on intelligent transportation.

	C1	C2	C3	C4	C5	C6	C7	C8	C9	C10	C11	C12	C13	C14	C15
C1	0.0580	0.1568	0.1610	0.1475	0.0764	0.0763	0.0781	0.0653	0.1038	0.1118	0.1103	0.0965	0.1031	0.1135	0.1111
C2	0.0601	0.0392	0.0911	0.0650	0.0613	0.0472	0.0607	0.0376	0.0647	0.0717	0.0610	0.0315	0.0647	0.0429	0.0417
C3	0.0714	0.0744	0.0632	0.0502	0.0579	0.0711	0.0846	0.0914	0.0802	0.0530	0.0804	0.0667	0.0923	0.1471	0.1450
C4	0.0700	0.0673	0.0715	0.0329	0.0643	0.0250	0.0354	0.0321	0.0328	0.0306	0.0543	0.0642	0.0570	0.0349	0.0329
C5	0.1733	0.1932	0.1452	0.1570	0.0726	0.1249	0.1885	0.1873	0.1540	0.1546	0.1563	0.1357	0.1955	0.1563	0.1396
C6	0.1703	0.1386	0.1411	0.1467	0.1220	0.0667	0.1848	0.1906	0.1420	0.1544	0.1883	0.1308	0.1908	0.1374	0.1537
C7	0.0979	0.1246	0.1727	0.1201	0.1055	0.0774	0.0690	0.1043	0.0648	0.1522	0.1183	0.1152	0.1235	0.0857	0.0816
C8	0.0953	0.1019	0.1875	0.1037	0.0760	0.0866	0.1679	0.0771	0.1533	0.1595	0.1118	0.0806	0.1239	0.1202	0.1386
C9	0.0555	0.0769	0.0765	0.0779	0.0294	0.0465	0.0731	0.0920	0.0450	0.0640	0.1440	0.0327	0.0397	0.0955	0.1297
C10	0.0682	0.0697	0.0779	0.0736	0.0549	0.0706	0.0707	0.1041	0.0870	0.0486	0.0522	0.0416	0.0492	0.1485	0.1372
C11	0.0438	0.0532	0.0529	0.0746	0.0203	0.0166	0.0238	0.0246	0.0756	0.0435	0.0261	0.0176	0.0207	0.0260	0.0273
C12	0.1339	0.1450	0.1366	0.1411	0.1250	0.1218	0.1879	0.1872	0.1216	0.1333	0.1309	0.0773	0.1785	0.1442	0.1412
C13	0.1046	0.1278	0.1824	0.1149	0.0912	0.0951	0.0959	0.1117	0.0691	0.1091	0.0971	0.1576	0.0791	0.1734	0.1304
C14	0.0251	0.0286	0.0698	0.0273	0.0214	0.0223	0.0487	0.0526	0.0486	0.0509	0.0482	0.0506	0.0761	0.0350	0.0335
C15	0.0220	0.0244	0.0567	0.0244	0.0202	0.0190	0.0284	0.0810	0.0624	0.0493	0.0643	0.0382	0.0247	0.0497	0.0308

Table 5: Comprehensive impact matrix analysis.

Factor	Influence degree	Affected degree	Centrality	Causality
C1	1.5695	1.2495	2.8190	0.3200
C2	0.8404	1.4213	2.2617	−0.5809
C3	1.2291	1.6862	2.9153	−0.4571
C4	0.7050	1.3570	2.0620	−0.6520
C5	2.3341	0.9985	3.3325	1.3356
C6	2.2583	0.9671	3.2254	1.2913
C7	1.6127	1.3977	3.0104	0.2150
C8	1.7838	1.4391	3.2228	0.3447
C9	1.0784	1.3048	2.3832	−0.2264
C10	1.1540	1.3866	2.5406	−0.2325
C11	0.5467	1.4436	1.9903	−0.8968
C12	2.1056	1.1369	3.2425	0.9688
C13	1.7395	1.4188	3.1584	0.3207
C14	0.6389	1.5104	2.1493	−0.8715
C15	0.5956	1.4744	2.0700	−0.8789

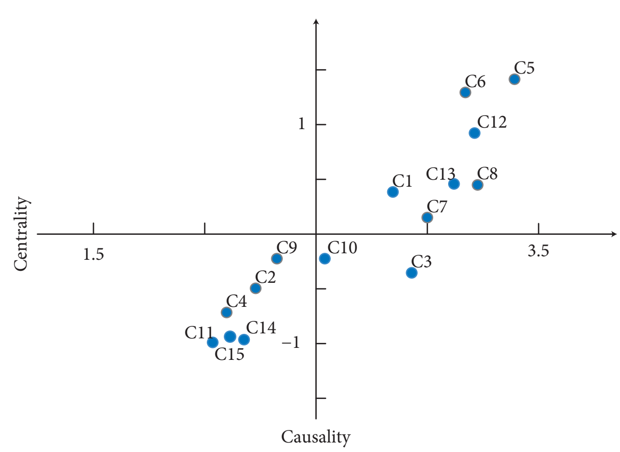

Figure 1: DEMATEL causal diagram.

also different. Figure 2 shows that factors according to the arrangement from big to small in turn are reliability (C5), timeliness (C6), reward and punishment system (C12), congestion management (C8), credit evaluation system (C13), transaction cost (C1), and Internet-based traffic management (C7). All these factors are active factors to promote intelligent transportation based on blockchain, which should be attached great importance.

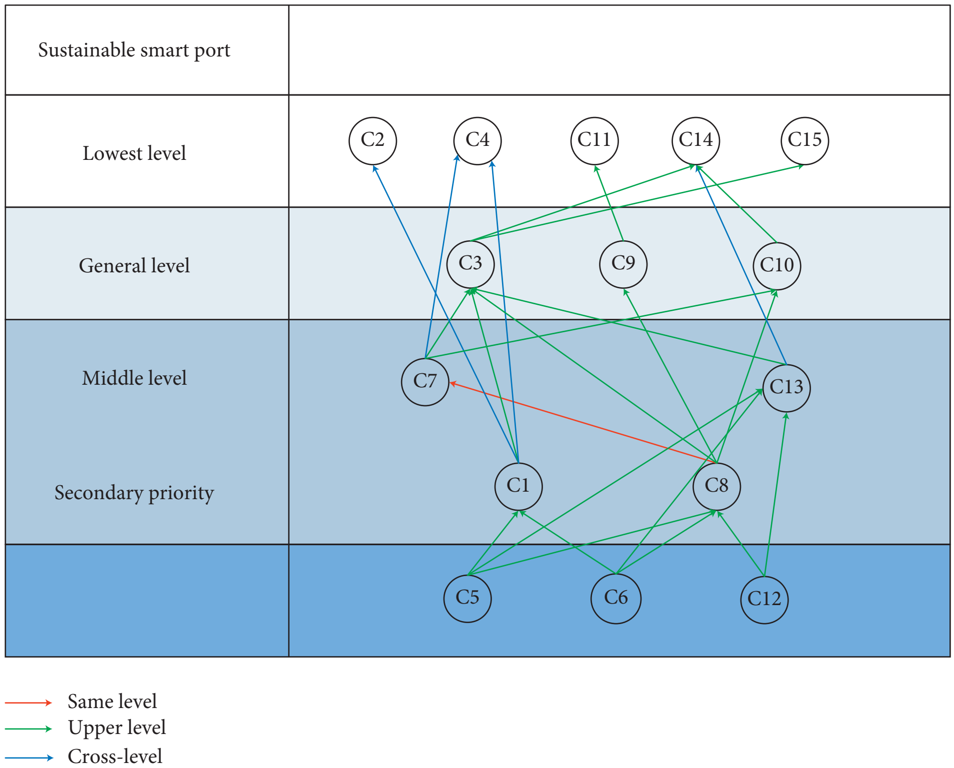

Figure 2: ISM structure model.

The overall influence matrix H obtained from formula (10) is shown in Table 6.

The reachable matrix M obtained from formula (11) is shown in Table 7.

The first-level decomposition structure is obtained from the reachable matrix and formula (12), as shown in Table 8.

Table 8 shows that the reachable set and common set intersect for factors C2, C4, C11, C14, and C15, so elements C2, C4, C11, C14, and C15 constitute the first-level influencing factors. The rows and columns of influencing factors C2, C4, C11, C14, and C15 in the matrix M are divided to obtain a higher-level decomposition matrix, and the above process is repeated. After multiple levels of division, the factor set Nq ($q = 1, 2, \ldots, 5$) of each layer is finally obtained as follows: first-level node $N1 = \{C2, C4, C11, C14, C15\}$; second-level node $N2 = \{C3, C9, C10\}$; third-level node $N3 = \{C7, C13\}$; fourth-level node $N4 = \{C1, C8\}$; and fifth-level node $N5 = \{C5, C6, C12\}$. The third-level node and the fourth-level node are merged, and the ISM model is established based on the above analysis, as shown in Figure 2.

According to the ISM analysis of the influencing factors, reliability (C5), timeliness (C6), and reward and punishment system (C12) compose the root of the influence of blockchain in intelligent transportation, and determining how to effectively track and control these factors is the key.

5. Discussions

This paper attempts to explore the sustainable development system of intelligent transportation based on blockchain technology. There are few studies on the application of blockchain technology in the field of intelligent transportation, and there is no comprehensive application system. This study systematically proposed a set of criteria about the development of intelligent transportation and constructed a hierarchical model.

In the index system, for the reward and punishment system, reliability and timeliness are at the first level and thus serve as the basis of the whole transportation consortium blockchain. The core of the entire blockchain-based intelligent transportation system lies in solving social problems, which depend on a complete top-level design. This paper proposes a top-level system design composed of a reward and punishment system and a credit evaluation system and rebuilds the social trust mechanism by encouraging users to participate in and conduct credit evaluations. The release of any information in the blockchain needs to be verified and can be traced by timestamp, ensuring the reliability of the information [42, 43], which is key to the stable operation of the system. Blockchain smart contract technology enables the free trade of access permits, allowing people to buy and sell as needed and adjust their travel strategies. Therefore, the improvement of social welfare brought about by solving and optimizing social problems highlights the characteristics of technology, which is consistent with the theory of social construction [44].

Transaction cost, congestion management, Internet-based traffic management, and the credit evaluation system are at the second level, which indicates that the development of blockchain-based intelligent transportation at the economic level mainly revolves around the intelligent contract

Table 6: Overall influence matrix.

	C1	C2	C3	C4	C5	C6	C7	C8	C9	C10	C11	C12	C13	C14	C15
C1	1.0580	0.1568	0.1610	0.1475	0.0764	0.0763	0.0781	0.0653	0.1038	0.1118	0.1103	0.0965	0.1031	0.1135	0.1111
C2	0.0601	1.0392	0.0911	0.0650	0.0613	0.0472	0.0607	0.0376	0.0647	0.0717	0.0610	0.0315	0.0647	0.0429	0.0417
C3	0.0714	0.0744	1.0632	0.0502	0.0579	0.0711	0.0846	0.0914	0.0802	0.0530	0.0804	0.0667	0.0923	0.1471	0.1450
C4	0.0700	0.0673	0.0715	1.0329	0.0643	0.0250	0.0354	0.0321	0.0328	0.0306	0.0543	0.0642	0.0570	0.0349	0.0329
C5	0.1733	0.1932	0.1452	0.1570	1.0726	0.1249	0.1885	0.1873	0.1540	0.1546	0.1563	0.1357	0.1955	0.1563	0.1396
C6	0.1703	0.1386	0.1411	0.1467	0.1220	1.0667	0.1848	0.1906	0.1420	0.1544	0.1883	0.1308	0.1908	0.1374	0.1537
C7	0.0979	0.1246	0.1727	0.1201	0.1055	0.0774	1.0690	0.1043	0.0648	0.1522	0.1183	0.1152	0.1235	0.0857	0.0816
C8	0.0953	0.1019	0.1875	0.1037	0.0760	0.0866	0.1679	1.0771	0.1533	0.1595	0.1118	0.0806	0.1239	0.1202	0.1386
C9	0.0555	0.0769	0.0765	0.0779	0.0294	0.0465	0.0731	0.0920	1.0450	0.0640	0.1440	0.0327	0.0397	0.0955	0.1297
C10	0.0682	0.0697	0.0779	0.0736	0.0549	0.0706	0.0707	0.1041	0.0870	1.0486	0.0522	0.0416	0.0492	0.1485	0.1372
C11	0.0438	0.0532	0.0529	0.0746	0.0203	0.0166	0.0238	0.0246	0.0756	0.0435	1.0261	0.0176	0.0207	0.0260	0.0273
C12	0.1339	0.1450	0.1366	0.1411	0.1250	0.1218	0.1879	0.1872	0.1216	0.1333	0.1309	1.0773	0.1785	0.1442	0.1412
C13	0.1046	0.1278	0.1824	0.1149	0.0912	0.0951	0.0959	0.1117	0.0691	0.1091	0.0971	0.1576	1.0791	0.1734	0.1304
C14	0.0251	0.0286	0.0698	0.0273	0.0214	0.0223	0.0487	0.0526	0.0486	0.0509	0.0482	0.0506	0.0761	1.0350	0.0335
C15	0.0220	0.0244	0.0567	0.0244	0.0202	0.0190	0.0284	0.0810	0.0624	0.0493	0.0643	0.0382	0.0247	0.0497	1.0308

Table 7: Reachable matrix.

M	C1	C2	C3	C4	C5	C6	C7	C8	C9	C10	C11	C12	C13	C14	C15
C1	1	1	1	1	0	0	0	0	0	0	0	0	0	0	0
C2	0	1	0	0	0	0	0	0	0	0	0	0	0	0	0
C3	0	0	1	0	0	0	0	0	0	0	0	0	0	1	1
C4	0	0	0	1	0	0	0	0	0	0	0	0	0	0	0
C5	1	1	1	1	1	0	1	1	1	1	1	0	1	1	1
C6	1	1	1	1	0	1	1	1	1	1	1	0	1	0	1
C7	0	0	1	0	0	0	1	0	0	1	0	0	0	0	0
C8	0	0	1	0	0	0	1	1	1	1	0	0	0	0	1
C9	0	0	0	0	0	0	0	0	1	0	1	0	0	0	0
C10	0	0	0	0	0	0	0	0	0	1	0	0	0	1	0
C11	0	0	0	0	0	0	0	0	0	0	1	0	0	0	0
C12	0	1	0	1	0	0	1	1	0	0	0	1	1	1	1
C13	0	0	1	0	0	0	0	0	0	0	0	1	1	1	0
C14	0	0	0	0	0	0	0	0	0	0	0	0	0	1	0
C15	0	0	0	0	0	0	0	0	0	0	0	0	0	0	1

Table 8: First-level decomposition structure.

i	$L(f_i)$	$P(f_i)$	$C(f_i) = L(f_i) \cap P(f_i)$
C1: transaction cost	1, 2, 3, 4	1, 5, 6	1
C2: management cost	2	1, 2, 5, 6, 12	2
C3: infrastructure construction cost	3, 14, 15	1, 3, 5, 6, 7, 8, 13	3
C4: financial cost	4	1, 4, 5, 6, 12	4
C5: reliability	1, 2, 3, 4, 5, 7, 8, 9, 10, 11, 13, 14, 15	5	5
C6: timeliness	1, 2, 3, 4, 6, 7, 8, 9, 10, 11, 13, 15	6	6
C7: Internet-based traffic management	3, 7, 10	5, 6, 7, 8, 12	7
C8: congestion management	3, 7, 8, 9, 10, 15	5, 6, 8, 12	8
C9: urban space optimization	9, 11	5, 6, 8, 9	9
C10: convenient travel	10, 14	5, 6, 7, 8, 10	10
C11: parking management	11	5, 6, 9, 11	11
C12: reward and punishment system	2, 4, 7, 8, 12, 13, 14, 15	12, 13	12, 13
C13: credit evaluation system	3, 12, 13, 14	5, 6, 12, 13	12, 13
C14: urban traffic pollution	14	3, 5, 10, 12, 13, 14	14
C15: urban greening layout	15	3, 5, 6, 8, 12, 15	15

and is affected by the social level. The combination of economic benefits and social benefits is the core of sustainable development [45]. The use of smart contracts eliminates some unnecessary steps in the current trade settlement process [46]; blockchain technology can establish a consensus mechanism without the participation of intermediaries, which will improve the efficiency and scope of the market and make transactions closer to the direct point-to-point ideal state [47], all of which reduce transaction costs. Congestion is an urgent problem to be solved in the field of transportation. Eliminating congestion is related to the sustainable development of cities, can promote the optimization of urban structure, and is the basis for giving full play to the potential of cities [48]. In terms of management costs, immutable distributed accounting reduces the labor costs of governments and enterprises. All these results prove that institutional construction is the premise of economic development, and the stable operation of the market requires institutional constraints and incentives.

Infrastructure construction cost, convenient travel, and urban space optimization are at the third level, which continues to reflect the complex relationship between economic benefits and social benefits, and development at the social level is also affected by the economic level. The analysis and processing of traffic information and the optimization of route selection are inseparable from infrastructure construction. Improved infrastructure can provide more accurate and abundant traffic information, which can effectively manage traffic via the Internet, reduce traffic congestion, make travel more convenient, and improve users' travel experience. In addition, instead of considering travel optimization at the user level, we should adopt a comprehensive view of the influence of urban traffic to more reasonably divide the functions of the city and promote the sustainable transformation of cities [49, 50]. All these indicate that economic construction and social construction are inextricably linked.

The continuous improvement of environmental issues requires a solution to social problems [51]. Urban traffic pollution and urban greening layout are at the last level; they are influenced by social factors and are important features of the sustainable development of blockchain-based intelligent transportation. The impact of social problems on environmental problems is mainly reflected in traffic congestion. Automobile exhaust contains a large amount of CO, which is harmful to the human body. Emissions from diesel trucks and vehicle exhaust are mixed with a large amount of inhalable particulate matter, which is an important factor leading to disease [52, 53]. Reducing traffic congestion by limiting driving, planning the most fuel-efficient route, and controlling speed can effectively control the emission of traffic-related air pollutants, reduce greenhouse effects, acid rain, and other environmental problems, create a livable urban environment, and improve the quality of life of citizens [54]. In addition, the overall planning of urban construction and plant sites and the layout of urban greening according to local conditions can also purify the environment. Therefore, with the combination of blockchain technology and intelligent transportation, the solution of social problems will promote urban development in the direction of green environmental protection and sustainability.

In addition, one innovation of this paper is its study of the related issues in the field of blockchain-based intelligent transportation from the perspective of finance and taxation. The application of blockchain will make the transaction information more real and transparent to companies and the financial and tax administration department. In the past, it was difficult for the transportation industry to collect taxes, and the input was chaotic. Enterprise transport capacity is difficult to calculate, and the affiliation phenomenon has serious implications. The tax rate of Internet transportation companies is ambiguous [55, 56], and there are many loopholes in tax administration. Through the combination of blockchain technology and Internet of Things technology, transaction information can be automatically uploaded to the blockchain by an Internet of Things device, which can realize reliable records for every transaction and facilitate the supervision of the tax administration department. The stability of tax sources will promote tax reform and establish specific tax rates for Internet transportation enterprises, realizing the standardized management of the Internet transportation industry [57]. According to the research results of this paper, financial cost, parking management, management cost, urban traffic pollution, and urban greening layout are at the fourth level, which shows that there is still a long way to go in the use of blockchain technology to carry out fiscal and tax reform in the transportation industry.

To better understand the theoretical system of this paper, we further developed a blockchain-based intelligent transportation sustainable GCU application system based on stakeholder theory, elaborating how stakeholders in intelligent transportation combine with blockchain, as shown in Figure 3. Blockchain plays the role of a large transaction information database in this system. The information in the blockchain includes public and private information, and the blockchain uses asymmetric encryption technology to encrypt information [58, 59], providing a higher security factor for private information.

The model can be divided into three levels: the government layer, the company layer, and the user layer. First, traffic management departments in the government layer can issue traffic licenses through the blockchain, and individuals can trade freely according to their needs. In addition, traffic management departments can also release road condition information, collect data statistics, and conduct traffic supervision through the blockchain. Urban construction departments can integrate traffic information to carry out more reasonable urban planning. Second, for the transportation company layer, including passenger transportation companies and Internet-based transportation companies, the credit rating of operating drivers can be obtained through the blockchain, and real-time monitoring of operating vehicles can be realized through the combination of the blockchain and the Internet of Things. Information on every transaction of an enterprise will be accurately recorded in the blockchain through asymmetric encryption technology. Companies and accounting and auditing institutions can conduct accounting according to the transaction information in the blockchain. The financial and tax administration departments can check the accounts of companies under authorization to facilitate tax administration. Insurance institutions, as third-party enterprises,

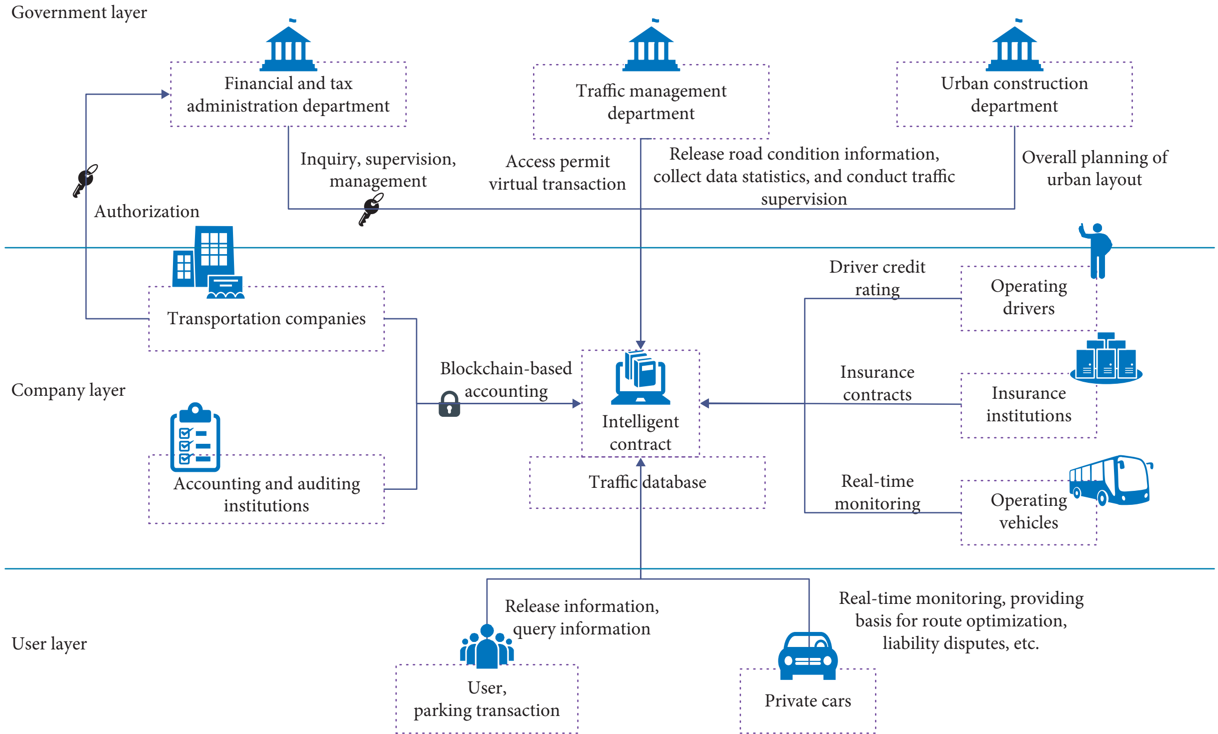

Figure 3: Blockchain-based intelligent transportation sustainable GCU application system.

can upload electronic insurance contracts and store them in the blockchain in the form of smart contracts [60, 61]. In the event of a traffic accident, the relevant authorization can be obtained to inquire about driving records and provide a basis for the settlement of accident disputes and insurance claims. Finally, at the user layer, the blockchain can be used to release or query traffic information, trade travel permits, or buy and sell parking that is not currently in use. Private cars can be monitored in real time through the combination of blockchain and Internet of Things devices, providing a basis for route optimization and liability disputes.

At this stage, the development of the blockchain is also facing some problems. For example, slower calculation speeds and large data volumes require more storage space, and low computing and storage capabilities of computer equipment may limit the use of blockchains [7, 62]. The basic blockchain processing that replicates all transaction history between all nodes is computationally expensive [63]. The immutability of the blockchain means that any modification to the smart contract, no matter how small, may be complicated in calculations, requiring the use of new blocks in the chain and increasing costs. Similarly, the combination of blockchain technology and intelligent transportation will also have corresponding problems. First, the blockchain uses public key encryption for transaction authentication and execution. Although this process is very secure, it requires the use of public and private keys. If one party loses or unwittingly publishes its private key, the system has no security mechanism to provide additional security. Secondly, the immutable append-only feature of the blockchain can ensure the integrity of the transaction, but may become an obstacle to use cases that require transaction changes [5]. Then, the principle that all nodes in the blockchain network store the complete transaction records of all information blocks can ensure network security credentials, but the addition of new blocks and subsequent transaction records is currently computationally expensive [22]. In addition, cultural, regulatory, legal, and logistical issues remain to be resolved to clear the way for further adoption of the technology [64]. Despite these uncertainties, the related research on the blockchain is still very hot, which will inevitably promote the development of related research on the blockchain.

6. Conclusions

At present, research on blockchain in the field of urban intelligent transportation is still in the exploratory stage. Most of the literature focuses on exploring the impact of the characteristics of blockchain on urban intelligent transportation. The development system for urban intelligent transportation under the blockchain is very vague. Few existing studies have explored the combination of blockchain and intelligent transportation from a sustainability perspective. Compared with previous studies, this paper considers the impact of blockchain technology on sustainable intelligent transportation development from the three aspects of the economy, society, and environment. The sustainable GCU application system of blockchain in intelligent transportation constructed in this paper is comprehensive and systematic. The comprehensive application of the fuzzy, DEMATEL, and ISM methods can not only screen out the unnecessary attributes, but also manage the complex interrelationships among the aspects and criteria.

However, there are still some limitations in this study. First, although the proposed criteria have been selected through the extensive literature review, it is still insufficient to cover all possible attributes. Second, the expert committee was consisted of the intelligent transportation management experts, and experts in other fields related to electronic technology, especially blockchain technology, should be included in the committee for increasing the scope and the applicable boundaries. Third, although the fuzzy set theory is used in this research to solve the problem of experts' subjective bias, there are still some errors that are difficult to eliminate completely that may have a certain impact on the research results. In addition, this study could also use other statistical tools, such as a structural equation model, to explore more influencing factors and carry out statistical verification of the model.

Data Availability

The data used to support the findings of this study are available from the corresponding author upon request.

Conflicts of Interest

The authors declare no conflicts of interest.

Acknowledgments

The authors would like to thank the China Natural Science Foundation (71501081), the China Postdoctoral Science Foundation (2019M651124), Yingkou Institute of Technology Excellent Scientific and Technological Talents Foundation (RC201904), Scientific Research Project of Yingkou Institute of Technology (QNW201719), and the Dalian University of Technology Fundamental Research Fund (DUT19RW107).

Supplementary Materials

Expert questionnaire results. (*Supplementary Materials*)

References

[1] G. Dimitrakopoulos and P. Demestichas, "Intelligent transportation systems," *IEEE Vehicular Technology Magazine*, vol. 5, no. 1, pp. 77–84, 2010.

[2] B. J. Kanninen, "Intelligent transportation systems: an economic and environmental policy assessment," *Transportation Research Part A: Policy and Practice*, vol. 30, no. 1, pp. 1–10, 1996.

[3] Z. Zeng, B. Song, X. Zheng, and H. Li, "Changes of traffic network and urban transformation: a case study of Xi'an city, China," *Land Use Policy*, vol. 88, Article ID 104195, 2019.

[4] D. Appelbaum and S. S. Smith, "Blockchain basics and hands-on guidance: taking the next step toward implementation and adoption," *The CPA Journal*, vol. 88, no. 6, pp. 28–37, 2018.

[5] F. Hawlitschek, B. Notheisen, and T. Teubner, "The limits of trust-free systems: a literature review on blockchain technology and trust in the sharing economy," *Electronic Commerce Research and Applications*, vol. 29, pp. 50–63, 2018.

[6] D. Andolfatto, "Blockchain: what it is, what it does, and why you probably don't need one," *Review*, vol. 100, no. 2, pp. 87–95, 2018.

[7] M. Holub and J. Johnson, "Bitcoin research across disciplines," *The Information Society*, vol. 34, no. 2, pp. 114–126, 2018.

[8] B. Shala, U. Trick, A. Lehmann, B. Ghita, and S. Shiaeles, "Novel trust consensus protocol and blockchain-based trust evaluation system for M2M application services," *Internet of Things*, vol. 7, Article ID 100058, 2019.

[9] S. Ahluwalia, R. V. Mahto, and M. Guerrero, "Blockchain technology and startup financing: a transaction cost economics perspective," *Technological Forecasting and Social Change*, vol. 151, Article ID 119854, 2020.

[10] C. G. Schmidt and S. M. Wagner, "Blockchain and supply chain relations: a transaction cost theory perspective," *Journal of Purchasing and Supply Management*, vol. 25, no. 4, Article ID 100552, 2019.

[11] A. Beirami, Y. Zhu, and K. Pu, "Trusted relational databases with blockchain: design and optimization," *Procedia Computer Science*, vol. 155, pp. 137–144, 2019.

[12] R. Chaudhary, A. Jindal, G. S. Aujla, S. Aggarwal, N. Kumar, and K.-K. R. Choo, "BEST: blockchain-based secure energy trading in SDN-enabled intelligent transportation system," *Computers & Security*, vol. 85, pp. 288–299, 2019.

[13] A. Jindal, G. S. Aujla, and N. Kumar, "SURVIVOR: a blockchain based edge-as-a-service framework for secure energy trading in SDN-enabled vehicle-to-grid environment," *Computer Networks*, vol. 153, pp. 36–48, 2019.

[14] S. A. Bagloee, M. Tavana, G. Withers, M. Patriksson, and M. Asadi, "Tradable mobility permit with bitcoin and ethereum–a blockchain application in transportation," *Internet of Things*, vol. 8, Article ID 100103, 2019.

[15] D. Bumblauskas, A. Mann, B. Dugan, and J. Rittmer, "A blockchain use case in food distribution: do you know where your food has been?" *International Journal of Information Management*, vol. 52, Article ID 102008, 2019.

[16] V. Gramoli, "On the danger of private blockchains," in *Proceedings of the Workshop on Distributed Cryptocurrencies and Consensus Ledgers (DCCL'16)*, Chicago, IL, USA, July 2016.

[17] V. J. Morkunas, J. Paschen, and E. Boon, "How blockchain technologies impact your business model," *Business Horizons*, vol. 62, no. 3, pp. 295–306, 2019.

[18] S. Davidson, P. De Filippi, and J. Potts, "Blockchains and the economic institutions of capitalism," *Journal of Institutional Economics*, vol. 14, no. 4, pp. 639–658, 2018.

[19] W. Li and V. Abiad, *Institutions, Institutional Change, and Economic Performance*, Cambridge University Press, Cambridge, UK, 1990.

[20] Z. Zheng, S. Xie, H.-N. Dai et al., "An overview on smart contracts: challenges, advances and platforms," *Future Generation Computer Systems*, vol. 105, pp. 475–491, 2020.

[21] S. Yadav and S. P. Singh, "Blockchain critical success factors for sustainable supply chain," *Resources, Conservation and Recycling*, vol. 152, Article ID 104505, 2020.

[22] J. G. Coyne and P. L. McMickle, "Can blockchains serve an accounting purpose?" *Journal of Emerging Technologies in Accounting*, vol. 14, no. 2, pp. 101–111, 2017.

[23] A. Wright and P. De Filippi, "Decentralized blockchain technology and the rise of lex cryptographia," *SSRN Electronic Journal*, vol. 15, 2015.

[24] D. Macrinici, C. Cartofeanu, and S. Gao, "Smart contract applications within blockchain technology: a systematic

mapping study," *Telematics and Informatics*, vol. 35, no. 8, pp. 2337–2354, 2018.

[25] L. Zhong, Q. Wu, J. Xie, Z. Guan, and B. Qin, "A secure large-scale instant payment system based on blockchain," *Computers & Security*, vol. 84, pp. 349–364, 2019.

[26] S. van de Hoef, K. H. Johansson, and D. V. Dimarogonas, "Efficient dynamic programming solution to a platoon coordination merge problem with stochastic travel times," *IFAC-PapersOnLine*, vol. 50, no. 1, pp. 4228–4233, 2017.

[27] C.-D. Chen, Y.-W. Fan, and C.-K. Farn, "Predicting electronic toll collection service adoption: an integration of the technology acceptance model and the theory of planned behavior," *Transportation Research Part C: Emerging Technologies*, vol. 15, no. 5, pp. 300–311, 2007.

[28] Q. Li, T. He, and G. Fu, "Judgment and optimization of video image recognition in obstacle detection in intelligent vehicle," *Mechanical Systems and Signal Processing*, vol. 136, Article ID 106406, 2020.

[29] L. Zhang, M. Luo, J. Li et al., "Blockchain based secure data sharing system for Internet of vehicles: a position paper," *Vehicular Communications*, vol. 16, pp. 85–93, 2019.

[30] Z. Yang, K. Yang, L. Lei, K. Zheng, and V. C. Leung, "Blockchain-based decentralized trust management in vehicular networks," *IEEE Internet of Things Journal*, vol. 6, no. 2, pp. 1495–1505, 2018.

[31] S. Grant-Muller and M. Usher, "Intelligent transport systems: the propensity for environmental and economic benefits," *Technological Forecasting and Social Change*, vol. 82, pp. 149–166, 2014.

[32] C.-Y. Hsu, C.-S. Yang, L.-C. Yu et al., "Development of a cloud-based service framework for energy conservation in a sustainable intelligent transportation system," *International Journal of Production Economics*, vol. 164, pp. 454–461, 2015.

[33] S. Chang, "An overview on an automated truck platoon within the energy ITS project," *IFAC Proceedings Volumes*, vol. 46, no. 21, pp. 41–46, 2013.

[34] R. Li, A. Kido, and S. Wang, "Evaluation index development for intelligent transportation system in smart community based on big data," *Advances in Mechanical Engineering*, vol. 7, no. 2, Article ID 541651, 2015.

[35] R.-J. Lin, "Using fuzzy DEMATEL to evaluate the green supply chain management practices," *Journal of Cleaner Production*, vol. 40, pp. 32–39, 2013.

[36] P. K. Singh and P. Sarkar, "A framework based on fuzzy Delphi and DEMATEL for sustainable product development: a case of Indian automotive industry," *Journal of Cleaner Production*, vol. 246, Article ID 118991, 2020.

[37] H. M. Chuang, C. K. Lin, D. R. Chen, and Y. S. Chen, "Evolving MCDM applications using hybrid expert-based ISM and DEMATEL models: an example of sustainable ecotourism," *The Scientific World Journal*, vol. 2013, Article ID 751728, 18 pages, 2013.

[38] S. Opricovic and G.-H. Tzeng, "Compromise solution by MCDM methods: a comparative analysis of VIKOR and TOPSIS," *European Journal of Operational Research*, vol. 156, no. 2, pp. 445–455, 2004.

[39] G. Büyüközkan and G. Çifçi, "A novel hybrid MCDM approach based on fuzzy DEMATEL, fuzzy ANP and fuzzy TOPSIS to evaluate green suppliers," *Expert Systems with Applications*, vol. 39, no. 3, pp. 3000–3011, 2012.

[40] W.-W. Wu and Y.-T. Lee, "Developing global managers' competencies using the fuzzy DEMATEL method," *Expert Systems with Applications*, vol. 32, no. 2, pp. 499–507, 2007.

[41] S. Altuntas, H. Selim, and T. Dereli, "A fuzzy DEMATEL-based solution approach for facility layout problem: a case study," *The International Journal of Advanced Manufacturing Technology*, vol. 73, no. 5–8, pp. 749–771, 2014.

[42] M. Pilkington, "Blockchain technology: principles and applications," in *Research Handbook on Digital Transformations*, Edward Elgar Publishing, Cheltenham, UK, 2016.

[43] M. Sharples and J. Domingue, "The blockchain and kudos: a distributed system for educational record, reputation and reward," in *Proceedings of the European Conference on Technology Enhanced Learning*, Springer, Lyon, France, pp. 490–496, September 2016.

[44] A. Schneider and M. Sidney, "What is next for policy design and social construction Theory?" *Policy Studies Journal*, vol. 37, no. 1, pp. 103–119, 2009.

[45] P. K. Agarwal, J. Gurjar, A. K. Agarwal, and R. Birla, "Application of artificial intelligence for development of intelligent transport system in smart cities," *Journal of Traffic and Transportation Engineering*, vol. 1, no. 1, pp. 20–30, 2015.

[46] K. Lauslahti, J. Mattila, and T. Seppala, "Smart contracts–How will blockchain technology affect contractual practices?" ETLA Report 68, The Research Institute of the Finnish Economy (ETLA), Helsinki, Finland, 2017.

[47] H. Treiblmaier, "The impact of the blockchain on the supply chain: a theory-based research framework and a call for action," *Supply Chain Management: An International Journal*, vol. 23, no. 6, pp. 545–559, 2018.

[48] Z. H. A. N. G. Taoxin, Y. A. N. G. Yin, and Y. U. Li, "Analysis of theory and practice for wisdom city," *Journal of Hunan University of Technology (Social Science Edition)*, vol. 1, 2012.

[49] M. M. Rathore, A. Paul, A. Ahmad, and G. Jeon, "IoT-based big data," *International Journal on Semantic Web and Information Systems*, vol. 13, no. 1, pp. 28–47, 2017.

[50] J. F. Sallis, F. Bull, R. Burdett et al., "Use of science to guide city planning policy and practice: how to achieve healthy and sustainable future cities," *The Lancet*, vol. 388, no. 10062, pp. 2936–2947, 2016.

[51] E. Deakin, *Sustainable Development and Sustainable Transportation: Strategies for Economic Prosperity, Environmental Quality, and Equity*, University of California, Berkeley, California, 2001.

[52] H. Khreis, C. Kelly, J. Tate, R. Parslow, K. Lucas, and M. Nieuwenhuijsen, "Exposure to traffic-related air pollution and risk of development of childhood asthma: a systematic review and meta-analysis," *Environment International*, vol. 100, pp. 1–31, 2017.

[53] C. Tonne, J. I. Halonen, S. D. Beevers et al., "Long-term traffic air and noise pollution in relation to mortality and hospital readmission among myocardial infarction survivors," *International Journal of Hygiene and Environmental Health*, vol. 219, no. 1, pp. 72–78, 2016.

[54] M. J. Anderson and L. T. Molina, "Megacities and atmospheric pollution," *Journal of the Air & Waste Management Association*, vol. 54, no. 6, pp. 644–680, 2004.

[55] J. P. Schwieterman and M. Pelon, "First zipcar, now uber: legal and policy issues facing the expanding shared mobility sector in US cities," *Belmont Law Review*, vol. 4, p. 109, 2017.

[56] Z. Yu and H. Bai, "Research on tax issues of shared economic business model," in *Proceedings of the International Conference on Education, Economics and Management Research (ICEEMR 2017)*, Atlantis Press, Singapore, May 2017.

[57] S. Quinton, *How Should Uber Be Regulated*, The PEW Charitable Trusts NGO, Philadelphia, PA, USA, 2015.

[58] L. Castaldo and V. Cinque, "Blockchain-based logging for the cross-border exchange of ehealth data in europe," in *International ISCIS Security Workshop*, pp. 46–56, Springer, Cham, Switzerland, 2018.

[59] D. Tse, K. Huang, B. Cai, and K. Liang, "Robust password-keeping system using block-chain technology," in *Proceedings of the 2018 IEEE International Conference on Industrial Engineering and Engineering Management (IEEM)*, IEEE, Bangkok, Thailand, pp. 1221–1225, December 2018.

[60] V. Gatteschi, F. Lamberti, C. Demartini, C. Pranteda, and V. Santamaría, "Blockchain and smart contracts for insurance: is the technology mature enough?" *Future Internet*, vol. 10, no. 2, p. 20, 2018.

[61] H. T. Vo, L. Mehedy, M. Mohania, and E. Abebe, "Blockchain-based data management and analytics for micro-insurance applications," in *Proceedings of the 2017 ACM on Conference on Information and Knowledge Management*, pp. 2539–2542, Singapore, November 2017.

[62] M. Staples, S. Chen, S. Falamaki et al., *Risks and Opportunities for Systems Using Blockchain and Smart Contracts*, Report number: EP175103, The Commonwealth Scientific and Industrial Research Organisation, Sydney, Australia, 2017.

[63] R. Böhme, N. Christin, B. Edelman, and T. Moore, "Bitcoin: economics, technology, and governance," *Journal of Economic Perspectives*, vol. 29, no. 2, pp. 213–238, 2015.

[64] L. Hughes, Y. K. Dwivedi, S. K. Misra, N. P. Rana, V. Raghavan, and V. Akella, "Blockchain research, practice and policy: applications, benefits, limitations, emerging research themes and research agenda," *International Journal of Information Management*, vol. 49, pp. 114–129, 2019.

Hindawi
Journal of Advanced Transportation
Volume 2020, Article ID 8829175, 9 pages
https://doi.org/10.1155/2020/8829175

Research Article

Social Welfare Analysis of China's High-Speed Rail Industry: Based on the Perspective of Enterprises' Entry in Upstream Market

Da Li and Xiaoyan Lin

School of Economics and Management, Beijing Jiaotong University, Beijing 100044, China

Correspondence should be addressed to Da Li; 18113009@bjtu.edu.cn

Received 26 March 2020; Revised 30 April 2020; Accepted 23 May 2020; Published 15 June 2020

Academic Editor: Wenqing Wu

Copyright © 2020 Da Li and Xiaoyan Lin. This is an open access article distributed under the Creative Commons Attribution License, which permits unrestricted use, distribution, and reproduction in any medium, provided the original work is properly cited.

Based on the analysis of the high-speed rail industry chain, first, this paper divides the high-speed rail industry chain into infrastructure construction market and manufacturing market of mobile equipment and, second, this paper uses the empirical method of new experience industry organization to measure the market power premium of the high-speed rail upstream market. The study shows that the market power premium of the high-speed rail upstream market is 0.551, and the scale elasticity is 0.314, indicating that there is no systematic market power in the high-speed rail upstream market and there is significant scale diseconomy. The vertical market structure where "private enterprises dominate the upstream competition market and state-owned enterprises dominate the downstream oligopoly market" is further established. Based on the perspective of enterprises' entry in upstream markets, the social welfare of the high-speed rail industry market structure is analyzed. It is found in the study that the upstream market of the high-speed rail industry has a tendency of insufficient enterprise entry, and the total social welfare increases with the increase in the number of upstream enterprises entry. What is more, the profit of enterprises in the upstream market of high-speed rail decreases with the increase in the number of enterprises in the upstream. This paper believes that policies such as stimulating upstream high-speed rail enterprises entry, providing subsidies to upstream enterprises, reducing upstream enterprises' entry barriers, and expanding international markets can effectively improve the overall social welfare of the high-speed railway industry.

1. Problem Presentation

Since the reform and opening up 40 years ago, with the deepening of the market-oriented reform of state-owned enterprises, China's downstream product market has basically achieved free competition, and the market mechanism has gradually played a decisive role in resource allocation. Ji and Guo estimated the upstream market of 122 sectors in China. The results showed that, in the industries of oil, natural gas, iron ore, heavy metal, and other raw materials supply and energy exploitation [1], state-owned enterprises dominated the upstream market, while in the industries of product service, operation, and sales, private enterprises dominated the downstream market [2]. According to the estimation of Wang and Shi, the average value of the Herfindahl index of China's upstream industries in 2007 was 0.21. According to the US Department of Justice's HHI measure of industrial concentration, the market structure corresponding to this value is an oligopoly structure [3]. To sum up, China's domestic market has basically formed a vertical structure in which "state-owned enterprises dominate the upstream market and private enterprises dominate the downstream market" (Liu [4], Li et al. [5], and Qian [6]).

The traditional railway transportation industry has public welfare attributes and aims to provide cheap transportation services [7]. China's railway transportation industry has many problems and phenomena that inhibit industrial development and reduce social welfare, such as high investment, high debt, low efficiency, and low profit [8]. China has successively implemented policies such as railway privatization reform, railway industry restructuring, and internal competition in the railway industry. The market-oriented reform of railway transportation enterprises has become a major trend. Different from the traditional railway transportation industry, the high-speed railway industry meets the higher-level needs of passengers, including the saving of travel time, the comfort of the journey, and the services of additional products. Therefore, the high-speed railway transportation service is not a traditional public welfare transportation service.

As a special railway transportation industry, does the market structure of the high-speed rail industry conform to the vertical structure of "state-owned enterprises dominating the upstream market monopoly and private enterprises dominating the downstream market competition" that has been formed in the domestic market? What are the constraints in the development of the high-speed rail industry? How to improve the overall social welfare through industrial or competition policies? Based on the analysis of the high-speed rail industry, this paper divides the high-speed rail industry into an upstream market focusing on the infrastructure construction and mobile equipment manufacturing, and a downstream market focusing on providing passenger transportation services adopts the empirical method of new experience industrial organization to measure the upstream market power of the high-speed rail and establishes an asymmetrically distributed vertical structure of the upstream and downstream markets in which "private enterprises dominate the upstream competition market and state-owned enterprises dominate the downstream oligopoly market." Based on the perspective of enterprises' entry in the upstream market, the social welfare situation of the market structure of the high-speed rail industry is analyzed, and the research results provide useful reference suggestions for improving the overall social welfare of the high-speed rail industry. The research framework of this paper is shown in Figure 1.

2. Literature Review

The purpose of high-speed rail development is to provide fast, comfortable, and safe passenger transport services with large volume, high speed, and low pollution. According to *the Medium- and Long-Term Railway Network Planning* of 2016, the high-speed railway network expanded from "four vertical and four horizontal planning" to "eight vertical and eight horizontal one." It is estimated that, by 2020, the high-speed railway operation mileage will reach 30000 kilometers and, by 2025, the mileage will reach 38000 kilometers. At that time, the high-speed rail network will connect almost all large- and medium-sized cities in China, and the time travel distance between adjacent cities will not exceed one hour. By 2018, China's high-speed rail has exceeded 29000 kilometers, ranking first in the world [9].

With the rapid expansion of China's high-speed rail network, the development of high-speed rail industry has been gradually valued and challenged. Most of the previous studies focused on the relationship between high-speed rail and national economy (Lin et al. [10], Zhao et al. [11], Wu et al. [12], and Chen and Haynes [13]), the relationship between high-speed rail and regional development (Lin et al. [14] and Hu et al. [15]), and the competition between high-speed rail and other modes of transportation (Wang et al. [16], D'Alfonso et al. [17], and Wang et al. [18]). For example, Tang Rong and Gu Naihua (2018) used the method of PSM-DID to empirically analyze the impact of high-speed rail development on the productive services and found that the appearance of high-speed rail reduced the revenue of productive services and there is regional heterogeneity [19]; Lin Xiaoyan (2015) used the yes-no method to analyze the impact of Wuhan-Guangzhou high-speed railway on talent attraction. The study found that the high-speed railway can effectively promote the flow of factors and increase the talent agglomeration effect of cities along the railway [10]; Hu Jing (2015) used the Herfindahl index to measure the industrial agglomeration of the tourism industry in Hubei Province. The study showed that the high-speed rail has increased the industrial agglomeration level of the tourism industry in Hubei Province, but there are significant regional differences [15]; D'Alfonso (2015) constructed a duopoly model of high-speed rail and civil aviation and analyzed the competition impact of high-speed rail and civil aviation. The study showed that even if the level of pollutants emitted by high-speed rail is much lower than that of civil aviation, because the substitution effect and the stimulation effect coexist simultaneously, the large-induced demand may make the high-speed rail have a net negative effect on the environment [17].

There are few researches regarding the high-speed rail as a complete industrial chain system. Jiang Mingyi (2019) analyzed the correlation effect of the high-speed rail industry on related industries from an industrial perspective. The study found that the backward correlation effect of the high-speed rail is mainly manifested in mechanical equipment manufacturing and metal product manufacturing. The forward correlation effect of the high-speed rail is mainly manifested in finance and education, services, and other tertiary industries [20]. In this paper, the high-speed railway is regarded as a complete industrial chain system, and the high-speed railway industry is divided into the upstream market mainly for infrastructure construction and mobile equipment manufacturing and the downstream market mainly for providing passenger transport services. The empirical method of new experience industrial organization is used to measure the upstream market power. Based on the analysis of the upstream and downstream markets of the high-speed railway industry, the asymmetrical vertical structure of the upstream and downstream markets in which "private enterprises dominate the upstream competition market and state-owned enterprises dominate the downstream oligopoly market" is constructed. And the social welfare of the high-speed rail industry market structure is analyzed based on the perspective of enterprises' entry in the upstream market.

3. Market Segmentation of High-Speed Rail Industry

3.1. Upstream Market of High-Speed Rail Industry. High-speed railway industry is a high-tech complex system including engineering design, infrastructure construction (high-speed railway network construction), mobile equipment manufacturing (high-speed railway EMU

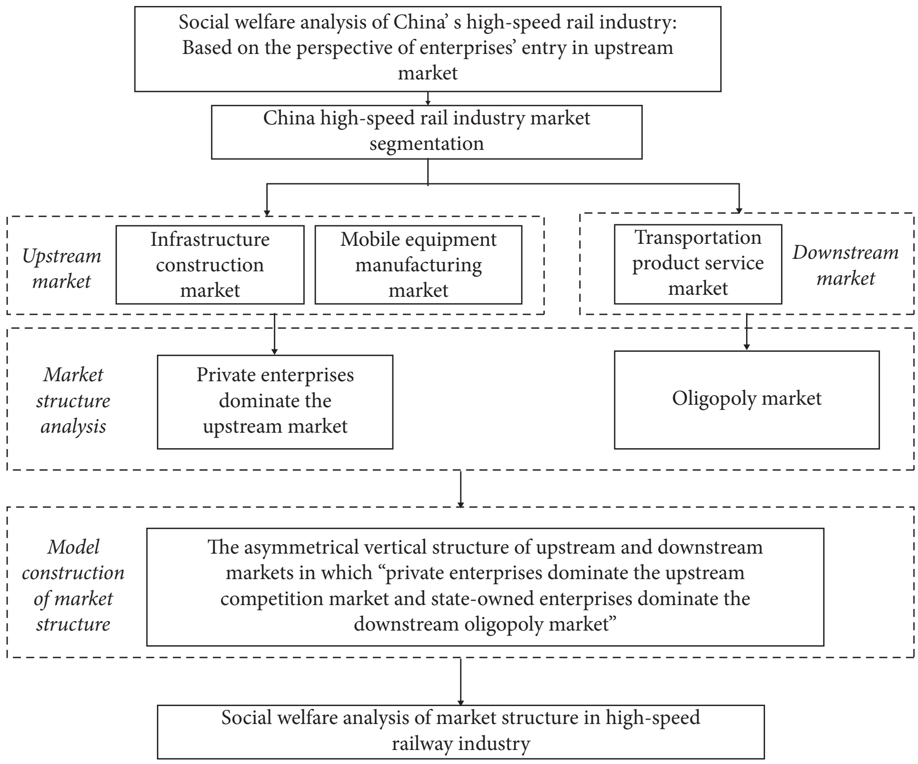

Figure 1: The research framework of this study.

manufacturing), communication signal and control system, operation and maintenance, and other subsystems (Lv and He [21]), in which the upstream industry chain of high-speed rail includes enterprises which engage in high-speed rail network infrastructure construction, mobile equipment manufacturing, and other enterprises [22]; the downstream industry chain of high-speed rail is the passenger transport service enterprises. This article used the empirical method of new experience industrial organization to measure the market power of the high-speed rail industry upstream market by drawing on the methods of Yu and Jiang [23] and Zhang and Zhang [24].

3.1.1. Regression Estimation Model. The empirical method of new experience industrial organization was first proposed by Bresnahan. This method uses the economic data of the industry to evaluate the market power of the monopoly market through the estimation model of Solow production function and does not need the accounting data which are difficult to obtain. Hall extended the traditional NEIO model, but his assumption of constant returns to scale is not in line with the actual situation. Kettle revised the assumption of constant returns to scale to improve the model [25]. This article uses Kettle's improved NEIO model to measure the premium situation of the upstream market power of the high-speed rail industry.

The production function that introduces technological changes and scale differences is shown in the following equation, where Q_{it} represents the output of company i in period t, X_{it} represents the factor input of company in period t, and A_{it} represents the technology progress:

$$Q_{it} = A_{it} * F_{it}(X_{it}). \quad (1)$$

Assuming a representative enterprise $Q_t = A_t * F_t(X_t)$, make the difference on the logarithm of the production function:

$$\ln Q_{it} - \ln Q_t = \ln A_{it} - \ln A_t + \ln F_{it}(X_{it}) - \ln F_t(X_t). \quad (2)$$

Assuming $q_{it}^* = \ln Q_{it} - \ln Q_t$, $a_{it}^* = a_{it}^* = \ln A_{it} - \ln A_t$, and $x_{it}^* = \ln X_{it} - \ln X_t$, from the transformation of differential mean value theorem, we can get the following result:

$$q_{it}^* = a_{it}^* + \sum_{j=1}^{m} \alpha_{it}^j x_{it}^{*j}. \quad (3)$$

According to the equilibrium condition MFC = VMP, the following result is obtained:

$$w_{it}^j = p * \left(1 - \frac{1}{\mu}\right) * A_{it} * \frac{\partial F_{it}}{\partial X_{it}^j}. \quad (4)$$

It can be obtained from $\lambda = P/\mathrm{MC} = 1/(1 - 1/\mu)$:

$$q_{it}^* = a_{it}^* + \lambda_{it} \sum_{j=1}^{m} \rho_{it}^j x_{it}^{*j}. \quad (5)$$

The elements of capital investment are needed to be separated, wherein η_{it} represents the scale elasticity and ρ_{it}^j represents the proportion of input of noncapital elements in total output, so it can be obtained:

$$q_{it}^{*} = a_{it}^{*} + \lambda_{it}\sum_{j\neq k}^{m}\rho_{it}^{j}\left(x_{it}^{*j} - x_{it}^{*k}\right) + \eta_{it}x_{it}^{*k}. \quad (6)$$

The fixed effect is removed by $a_{it}^{*} = a_i + \mu_{it}$, and the autocorrelation is eliminated by first-order difference:

$$\Delta q_{it}^{*} = \lambda * \Delta x_{it}^{*v} + \eta x_{it}^{*k} + \Delta \nu_{it}. \quad (7)$$

Then, the regression estimation equation is obtained:

$$q_{it}^{*} = \alpha + \lambda x_{it}^{*v} + \eta x_{it}^{*k} + \mu_{it}, \quad (8)$$

where in x_{it}^{*k} is the input of capital elements, x_{it}^{*j} is the investment of noncapital elements, $x_{it}^{*v} = \sum_{j\neq k} S_{ij}^{-j}(x_{it}^{*j} - x_{it}^{*k})$, and S_{ij}^{-j} is the proportion of input factor j in the total output of the enterprise. Because of the significant correlation between the error term μ_{it} and the explanatory variable x_{it}^{*v}, it is necessary to use the instrumental variable to solve the endogenous problem.

3.1.2. Major Listed Companies in the Upstream Market of High-Speed Rail Industry. According to the analysis of this paper, the upstream market of high-speed rail industry includes the infrastructure construction market and the market of mobile equipment, parts, and materials. Therefore, 15 major listed companies in the upstream market of high-speed rail industry are selected, and the situation of major listed companies is shown in Table 1.

3.1.3. Variable Selection. The output data select the operating income of the manufacturers in the upstream industry of high-speed rail transportation as the total value of the final products of the manufacturers' input factors. The input factors are capital input, labor input, and raw material input. Among them, the capital element is mainly in the depreciation of fixed assets, the labor element is the employee compensation and pay, and the raw material element is mainly the cash paid for the raw materials, energy, and auxiliary services purchased from outside [26].

This study selects 15 major listed companies related to the upstream market of the high-speed rail industry as a sample. The main businesses involved include infrastructure construction, mobile equipment manufacturing, production of parts and materials, etc.; the operating income, employee compensation level, depreciation of fixed assets, cash payment for purchase of goods and services, and other indicators from 2010 to 2018 of the 15 major listed companies are selected, and data sources are annual reports, audit reports, and Guotai'an databases of listed companies.

3.1.4. Estimation Results. λ is the market power premium of the upstream market of high-speed rail, η is the scale effect, and α is the intercept phase, reflecting the production efficiency difference between different upstream enterprises. The estimation results are shown in Table 2. The market power premium of the high-speed rail upstream market is 0.551, which is significant at 1%, indicating that there is no systematic market power in the high-speed rail upstream market, and the market power premium is less than 1. It can be seen that there is sufficient competition among enterprises in the upstream market; the elasticity of scale is 0.314, which indicates that there is significant scale diseconomy among enterprises in the upstream market, and there may be insufficient entry tendency of enterprises in the upstream market of high-speed rail.

3.1.5. Robustness Test. Considering the autocorrelation between the error term and the input factors, this paper selects the total capital and the number of employees as the instrumental variables to test the robustness. The results of the robustness test are shown in Table 3. The market power premium is significantly less than 1, and the scale elasticity is significantly less than 1, which indicates that there is no market power in the upstream market, and the upstream enterprises have significant scale diseconomy. The above model results are stable.

3.2. Downstream Market of High-Speed Rail Industry. The downstream market of the high-speed rail industry mainly refers to the passenger transport market that provides transportation products. The high-speed rail has an advantageous position in terms of speed, safety, comfort, and environmental protection. A significant phenomenon of the appearance of the high-speed rail is the impact on civil aviation. According to data from the World Bank Report (2018), the high-speed rail has reduced the service of Guangzhou to Wuhan by half, the service of the Guangzhou-Changsha flight has been reduced by two-thirds, and the Zhengzhou-Xi'an high-speed rail has forced the cancellation of this aviation route. The Nanjing-Wuhan high-speed rail has forced the aviation route to reduce 6 pairs of flights per day. Wei et al. found that the average ticket price of the Beijing-Shanghai aviation fell by about 29% after the appearance of high-speed railway between the Beijing-Shanghai but rebounded by about 20% after the Wenzhou high-speed rail accident [27]. This phenomenon not only takes place in China but also forces JAL to stop its flights from Tokyo to Osaka and Tokyo to Nagoya after the appearance of Shinkansen; the TGV high-speed rail project in France causes Air France to lose the market share of air from Paris to Lyon; the opening of high-speed rail in Britain causes BIM Airlines to stop some flights from London to Paris; after the construction of high-speed rail from Seoul to Busan in South Korea, the corresponding market share of civil aviation has declined dramatically [28].

The competition between high-speed rail and civil aviation is mainly reflected in the short-term and long-term impacts of ticket price, profit, frequency, seat capacity, network layout, and social welfare (Wan et al. [29], D'Alfonsoet al. [17], Ding et al. [30], Behrens and Pels [31], Jiang and Zhang [32], Xia and Zhang [33], and Yang and Zhang [34]). Yu et al. studied and analyzed the characteristics of the high-speed rail industry organization and its antitrust applicability. The study found that the high-speed rail industry does not generally belong to the natural monopoly industry. It further demonstrated that the high-speed

Table 1: Main listed companies in the upstream market of high-speed rail industry.

High-speed rail industry	Market segmentation	Name of the company	Main business
Upstream market of the high-speed rail industry chain	Infrastructure construction market	China Railway	Engineering infrastructure
		China Railway Construction	Engineering infrastructure
		China Railway Second Bureau	Engineering infrastructure
		China Communications Construction Co., Ltd.	Engineering infrastructure
		China Construction Group Co., Ltd.	Engineering infrastructure
		STEC	Engineering infrastructure
	Manufacturing market of mobile equipment, parts, and materials	CRRC	EMU manufacturing
		JXAC	Railway axle manufacturing
		Liyuan Refining	Transportation equipment
		Zhuzhou Times New Material Technology Co., Ltd	Equipment manufacturing
		Northern Entrepreneurship	Transportation materials
		Jinyi Industry	Transportation materials
		Oak Shares	Parts and materials
		AVIC Optoelectronics Technology Co., Ltd.	Parts and materials
		Daye Special Steel	Parts and materials

Source: annual reports, audit reports, and Guotai'an databases of listed companies.

Table 2: The estimation results of 2SLS model.

Estimated coefficient	Estimated value	Standard deviation
Market power premium (λ)	0.551***	0.039
Scale elasticity (η)	0.314***	0.045
Efficiency difference (α)	4.815***	0.668
R^2	0.9691***	

Note: ***, **, and * indicate that the estimated coefficients of the variable are significant at the level of 1%, 5%, and 10%, respectively. $^{*}p < 0.1$; $^{**}p < 0.05$; $^{***}p < 0.01$.

Table 3: The tool variable estimation results of 2SLS model.

Estimated coefficient	Estimated value	Standard deviation
Market power premium (λ)	0.1961***	0.067
Scale elasticity (η)	0.4071***	0.076
Efficiency difference (α)	10.9371***	1.174
R^2	0.88071***	

Note: ***, **, and * indicate that the estimated coefficients of the variable are significant at the level of 1%, 5%, and 10%, respectively. $^{*}p < 0.1$; $^{**}p < 0.05$; $^{***}p < 0.01$.

rail industry is also applicable to the antitrust law. And it is proposed that the upstream locomotive manufacturing and road network construction of high-speed rail industry are highly competitive market structures, and the downstream road network operation of high-speed rail industry is a competitive market (partial monopoly) [35]. Therefore, this study holds that the passenger transport market downstream of high-speed rail industry is an oligopoly market.

4. Construction of High-Speed Rail Industry Market Structure Model

Through analysis, it is shown that high-speed rail industry has formed a special vertical structure in China, that is, an asymmetrically distributed vertical structure of upstream and downstream markets in which "private enterprises dominate the upstream competition market and state-owned enterprises dominate the downstream oligopoly market." This study calls it the "$n+2$" vertical market structure.

The industry chain of high-speed rail is thought of as a closed economy, including infrastructure construction and mobile equipment manufacturing in the upstream market and transportation products and services in the downstream market. The model assumes that the upstream market is dominated by private enterprises, the market structure is set as monopoly competition, the downstream is dominated by state-owned enterprises, and the market structure is set as a duopoly market. It is assumed that the enterprises in the upstream competitive market are homogeneous, w is the price of the differentiated products provided by the upstream enterprises, c is the marginal cost of the upstream enterprises, d is the scale return coefficient of the upstream enterprises, d is the output of the upstream single enterprise, and f is private enterprise entry cost in the upstream; p is the price of state-owned enterprises in the downstream, f_0 is the fixed cost of oligarch 1 in the downstream market, c_0 is the intermediate product input cost of oligarch 2 in the downstream market, q_1 is the output of oligarch 1, and q_2 is the output of oligarch 2.

The counterdemand function of an individual enterprise in the upstream market is

$$w = m - \varepsilon d - \eta D. \tag{9}$$

That is,

$$w = m - \varepsilon d - \eta n d, \tag{10}$$

where ε represents the difference in producing homogeneous products and η represents the elasticity of substitution of differentiated products.

The profit of a single enterprise in the upstream market is

$$\pi = (w - c)d - f. \tag{11}$$

The equilibrium output of upstream enterprises is obtained based on profit maximization conditions:

$$d^* = \frac{m - c}{\varepsilon + n\eta}. \tag{12}$$

The counterdemand function of the downstream duopoly market is

$$p = a - \gamma(q_1 + q_2). \tag{13}$$

According to the profit maximization conditions, the response curve is

$$\begin{aligned} q_1 &= \frac{a - \gamma q_2 - w}{2\gamma}, \\ q_2 &= \frac{a - \gamma q_2 - c_0}{2\gamma}. \end{aligned} \tag{14}$$

According to the conditions of profit maximization, the equilibrium output q_1^* and the equilibrium price of the oligarch 1 are further obtained:

$$\begin{aligned} q_1^* &= \frac{a + c_0 - 2w}{3\gamma}, \\ p^* &= \frac{a + c_0 + w}{3}. \end{aligned} \tag{15}$$

According to the conditions of equal supply and demand in the upstream and downstream, we can get the following:

$$w^* = \frac{a + c_0}{2} - \frac{3bn\gamma(m - c)}{2(\varepsilon + n\eta)}. \tag{16}$$

5. Social Welfare Analysis of Market Structure of High-Speed Rail Industry

Based on the above model assumptions and model construction, the social welfare is further calculated as follows:

$$\begin{aligned} sw &= \pi_u + \pi_d + cs = n\left[(w - c)d^* - f\right] + (p^* - w)q_1^* - f_0 + \frac{(a + c_0 - 2p^*)}{2\gamma}\left(\frac{a + c_0}{2} - p^*\right) \\ &= \frac{(m - c)(nc_0 \mp an - 2nc)}{2(\varepsilon + n\eta)} - \frac{3n^2 b\gamma(m - c)^2}{2(\varepsilon + n\eta)^2} - nf + \frac{5[3nb\gamma(m - c)]^2}{36\gamma(\varepsilon + n\eta)^2} - f_0. \end{aligned} \tag{17}$$

Based on the conditions for maximizing social welfare, the following is obtained:

$$\frac{\partial s\,w}{\partial n} = \frac{\varepsilon(m - c)(a + c_0 - 2c)}{2(\varepsilon + n\eta)^2} + \frac{n\varepsilon b\gamma(m - c)^2(5b - 6)}{2(\varepsilon + n\eta)^3} - f > 0. \tag{18}$$

After calculation,

$$\begin{aligned} \frac{\partial sw/\partial n}{\partial n} &= -\varepsilon(m - c)(a + c_0 - 2c)\frac{\eta(\varepsilon + n\eta)}{\varepsilon + n\eta^4} \\ &\quad - \frac{b\gamma\varepsilon(m - c)^2(6 - 5b)}{2}\,\frac{(\varepsilon + n\eta)^2(\varepsilon - 2n\eta)}{(\varepsilon + n\eta)^6} < 0. \end{aligned} \tag{19}$$

According to the market equilibrium conditions, when n approaches 0, $\partial sw/\partial n$ approaches $(m - c)(a + c_0 - 2c)/2\varepsilon - f > 0$; when n approaches infinity, $\partial sw/\partial n$ approaches $-f < 0$. Therefore, when n is small, social welfare increases with the increase in the number of companies of the upstream market. When n approaches infinity, social welfare decreases with the increase in the number of companies in the upstream market, showing an inverted U-shaped structure. The diagram of the inverted U-shaped structure is shown in Figure 2.

The two parts of social welfare of consumer surplus and downstream market are further calculated:

$$\frac{\partial(\pi_d + cs)}{\partial n} = \frac{5n\varepsilon b^2\gamma(m - c)^2}{2(\varepsilon + n\eta)^3} > 0. \tag{20}$$

According to formula (20), the two parts of social welfare of consumer surplus and the downstream market increase with the increase in the number of companies entering upstream market.

The condition of profit maximization in the upstream market is

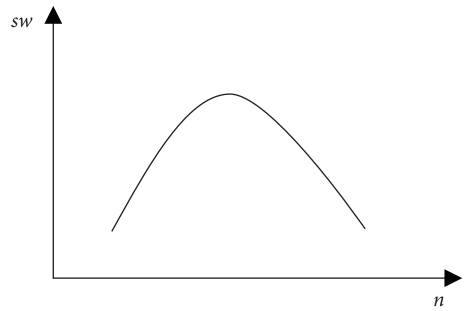

Figure 2: The diagram of the inverted U-shaped structure.

$$\frac{\partial \pi_u}{\partial n} = \frac{\varepsilon (m-c)(a+c_0-2c)}{2(\varepsilon + n\eta)^2} - \frac{3n\varepsilon b\gamma (m-c)^2}{(\varepsilon + n\eta)^3} - f < 0. \quad (21)$$

It can be known from $\partial \pi_u / \partial n < 0$ that, with the increase in the number of enterprises in the upstream market, the profit of enterprises in the upstream market decreases. There is a tendency of insufficient entry of enterprises in the upstream market.

It can be seen from the derivation and analysis of the above model that the profit of enterprises in the upstream market of high-speed rail decreases with the increase in the number of enterprises in the upstream. When the profit of enterprises in the upstream market is less or close to zero, the upstream enterprises will refuse to enter the upstream market, so there is a tendency of insufficient entry of enterprises in the upstream market, while the sum of the two parts of social welfare of the downstream market of high-speed rail and the consumer surplus will increase with the increase in the number of enterprises in the upstream market. It can be seen that private enterprises continue to enter the upstream market, although their profits are damaged, which can increase consumers' social welfare in the downstream oligopoly market.

6. Conclusions and Policy Suggestions

First of all, through the in-depth analysis of the high-speed rail industry, this paper divides the high-speed rail industry market into high-speed rail upstream market dominated by high-speed rail infrastructure construction and mobile equipment manufacturing enterprises and high-speed rail downstream market dominated by passenger transport service enterprises. The empirical method of new experience industrial organization is used to calculate the market power premium and scale elasticity of the upstream market of high-speed rail to be 0.551 and 0.314, respectively, which indicates that there is no systematic market power and significant scale diseconomy in the upstream market of high-speed rail. A special vertical market structure model of China's high-speed rail industry is constructed in this paper. Contrary to the market structure of other industrial sectors in China, the market structure of China's high-speed rail industry is an asymmetrically distributed vertical structure of upstream and downstream markets, in which private enterprises dominate the upstream competition market and state-owned enterprises dominate the downstream oligopoly market.

Secondly, based on the special vertical structure model of China's high-speed rail industry, the social welfare of the high-speed rail industry under this vertical structure is discussed from the perspective of the number of enterprises entering the upstream market. The study found that the number of enterprises in the upstream market is a key constraint on the total social welfare of the high-speed rail industry. The total social welfare of the high-speed rail industry has an inverted U-shaped relationship with the number of enterprises entering the upstream market. With the increase in number of companies of the upstream market, the profits of enterprises in the upstream market gradually decrease, while the sum of social welfare in the downstream market and consumer surplus gradually increases, which indicates that there is a tendency of insufficient enterprises entry in the upstream, and the number of upstream enterprises entry restricts the improvement of social welfare of high-speed rail industry.

Therefore, the following suggestions are put forward in this paper: first, the use of industrial policies. Encourage private enterprises to enter the upstream market of the high-speed rail industry through the government's policy means, that is, high-speed rail network infrastructure construction and mobile equipment manufacturing market. The policies may include tax relief, tax allowance and credit, and financial subsidies for enterprises related to the upstream market of high-speed rail; second, implement competition policies, deepen the reform of state-owned enterprises in the downstream market of high-speed rail, introduce competition within high-speed rail enterprises, and break the monopoly of the industrial chain. In December 2018, the China Railway Corporation was officially renamed as China National Railway Group Co., Ltd., which has completely realized the reform of the railway company system so far. At the same time, it is also a key step in transforming to a modern transportation business enterprise, which conforms to the reform thinking of the market-oriented economic system. Third, strengthen the "high-speed rail going out" strategy, expand the scope of the high-speed rail upstream market, and gradually open the international market for high-speed rail infrastructure construction and high-speed rail EMU manufacturing. In August 2019, CRRC Zhuzhou Locomotive Co., Ltd. acquired the locomotive business of the international railway giant German Vossloh. It can be seen that the international railway infrastructure construction and mobile equipment manufacturing are moving towards a direction of professional division of labor and higher efficiency.

Data Availability

Annual reports and audit reports of listed companies and Guotai'an databases were used to support this study.

Conflicts of Interest

The authors declare that there are no conflicts of interest.

Acknowledgments

This study was supported by the major project of the National Social Science Foundation of China (Research on the Analytical Framework and Evolution Path of China's High-Speed Rail Economy) (17ZDA084).

References

[1] Q. Ji and J.-F. Guo, "Oil price volatility and oil-related events: an internet concern study perspective," *Applied Energy*, vol. 137, no. 1, pp. 256–264, 2015.

[2] J. Ju and X. Yu, "Productivity, profitability, production and export structures along the value chain in China," *Journal of Comparative Economics*, vol. 43, no. 1, pp. 33–54, 2015.

[3] Y. Wang and B. Shi, "Upstream monopoly and product quality upgrade of Chinese enterprises," *Economic Research*, vol. 49, no. 4, pp. 116–129, 2014.

[4] R. Liu, "State-owned enterprises, implicit subsidies and market segmentation: theoretical and empirical evidence," *World of Management*, vol. 4, pp. 21–32, 2012.

[5] X. Li, X. Liu, and Y. Wang, "A model of china's state capitalism," in *Proceedings of the HKSTU Working Paper*, 2015.

[6] X. Qian, J. Zhang, and H. Mao, "Vertical structure, misplacement of resources and industrial policy," *Economic Research*, vol. 54, no. 2, pp. 54–67, 2019.

[7] M. Rizk, "Rizk-allah, aboul ella hassanien, mohamed elhoseny, A multi-objective transportation model under neutrosophic environment," *Computers and Electrical Engineering*, vol. 69, pp. 705–719, July 2018.

[8] J. Chen, X. Wang, and Z. Chu, "Capacity sharing, product differentiation and welfare," *Economic Research-Ekonomska Istraživanja*, vol. 33, no. 1, pp. 107–123, 2020.

[9] M. R. Reddy, K. G. Srinivasa, and B. E. Reddy, "Smart vehicular system based on the internet of things," *Journal of Organizational and End User Computing*, vol. 30, no. 3, pp. 45–62, 2018.

[10] X. Lin, Z. Shi, Y. Luo et al., "Analysis of the influence of high-speed railways on the attraction of urban talents," *Journal of Beijing Jiaotong University (Social Science Edition)*, vol. 14, no. 3, pp. 7–16, 2015.

[11] J. Zhao, Y. Zhao, and Y. Li, "The variation in the value of travel-time savings and the dilemma of high-speed rail in China," *Transportation Research Part A: Policy and Practice*, vol. 82, no. 82, pp. 130–140, 2015.

[12] J. Wu, C. Nash, and D. Wang, "Is high speed rail an appropriate solution to China's rail capacity problems?" *Journal of Transport Geography*, vol. 40, no. 40, pp. 100–111, 2014.

[13] Z. Chen and K. E. Haynes, "Impact of high speed rail on housing values: an observation from the Beijing-Shanghai line," *Journal of Transport Geography*, vol. 43, no. 43, pp. 91–100, 2015.

[14] X. Lin, X. Chen, Y. Bai et al., "Quantitative analysis of the impact of beijing-tianjin intercity high-speed railway on regional economy," *Railway Economic Research*, vol. 5, pp. 5–11, 2010.

[15] J. Hu, L. Cheng, and Mi Zhou, "Impact of high-speed rail on the agglomeration level of tourism industry in Hubei Province," *Journal of Chongqing Jiaotong University (Social Science Edition)*, vol. 15, no. 5, pp. 22–26, 2015.

[16] K. Wang, W. Xia, and A. Zhang, "Should China further expand its high-speed rail network? consider the low-cost carrier factor," *Transportation Research Part A: Policy and Practice*, vol. 100, no. 100, pp. 105–120, 2017.

[17] T. D'Alfonso, C. Jiang, and C. Jiang, "Would competition between air transport and high-speed rail benefit environment and social welfare?" *Transportation Research Part B:Methodological*, vol. 74, pp. 118–137, 2015.

[18] C. Wang, J. Yue, and H. Yang, "Measurement of substitution effect of high-speed railway on domestic civil passenger transport," *Journal of Natural Resources*, vol. 34, no. 9, pp. 1933–1944, 2019.

[19] R. Tang and N. Gu, "High-speed railway construction and the development of upstream productive service industry—an empirical test based on PSM-DID," *Economic and Management Research*, vol. 39, no. 7, pp. 58–68, 2018.

[20] M. Jiang, "*Research on High-Speed Rail Industry and its Related Effects—Based on the 2012 Input-Output Table*," M.S. Thesis, Beijing Jiaotong University, Beijing, China, 2019.

[21] T. Lv and J. He, "How effective the government intervention is: investigation and research on China's high-speed rail technology catch-up," *Management World*, vol. 35, no. 9, pp. 152–163, 2019.

[22] Z. Lv, B. Hu, and H. Lv, "Infrastructure monitoring and operation for smart cities based on IoT system," *IEEE Transactions on Industrial Informatics*, vol. 16, no. 3, pp. 1957–1962, 2019.

[23] L. Yu and Qi. Jiang, "Two-sided market power, asymmetric competition and reform path selection—on the dilemma and reform of China's railway transportation industry," *China Industrial Economy*, vol. 4, pp. 133–145, 2013.

[24] Z. Zhang and M. Zhang, "Market power, coal and electricity contradictions and potential welfare loss: empirical evidence from listed companies," *Research on Industrial Economy*, vol. 1, pp. 21–30, 2011.

[25] T. J. Klette, "Market power, scale economics and productivity: estimates from a panel of establishment data," *The Journal of Industrial Economics*, vol. 47, no. 4, pp. 451–476, 2003.

[26] N. Szumilo, "How do office buildings take advantage of energy efficiency? A study of the relationship between operating expenses and energy certification," *International Journal of Environmental Technology And Management*, vol. 18, no. 2, pp. 116–135, 2015.

[27] F. Wei, J. Chen, and L. Zhang, "Demand shocks, airline pricing, and high-speed rail substitution: evidence from the Chinese market," *Journal of Transport Economics and Policy*, vol. 51, no. 4, pp. 266–289, 2017.

[28] X. Jiang, "Analysis of competition between China's civil aviation and high-speed railway," *Shopping Mall Modernization*, vol. 8, pp. 68-69, 2010.

[29] Y. Wan, H.-K. Ha, Y. Yoshida, and A. Zhang, "Airlines' reaction to high-speed rail entries: empirical study of the Northeast Asian market," *Transportation Research Part A: Policy and Practice*, vol. 94, pp. 532–557, 2016.

[30] J. Ding, F. Jin, C. Wang et al., "Competitive game between high-speed rail and civil aviation and its spatial effect: a case study of beijing-shanghai high-speed rail," *Economic Geography*, vol. 33, no. 5, pp. 104–110, 2013.

[31] C. Behrens and E. Pels, "Intermodal competition in the London-Paris passenger market: high-speed rail and air transport," *Journal of Urban Economics*, vol. 71, no. 3, pp. 278–288, 2012.

[32] C. Jiang and A. Zhang, "Airline network choice and market coverage under high-speed rail competition," *Transportation Research Part A: Policy and Practice*, vol. 92, pp. 248–260, 2016.

[33] W. Xia and A. Zhang, "Effects of air and high-speed rail transport integration on profits and welfare: the case of air-rail

connecting time," *Journal of Air Transport Management, (Forthcoming)*, 2016.

[34] H. Yang and A. Zhang, "Effects of high-speed rail and air transport competition on prices, profits and welfare," *Transportation Research Part B: Methodological*, vol. 46, no. 10, pp. 1322–1333, 2012.

[35] Li Yu, Z. Xu, and H. Xu, "Analysis of China's high-speed railway industry and the applicability of antitrust law," *Sino-German Law Forum*, vol. 1, pp. 28–41, 2017.

Hindawi
Journal of Advanced Transportation
Volume 2020, Article ID 4380610, 13 pages
https://doi.org/10.1155/2020/4380610

Research Article

Analysis of Perceived Value and Travelers' Behavioral Intention to Adopt Ride-Hailing Services: Case of Nanjing, China

Ke Lu and Xuefen Wang

School of Management Science and Engineering, Nanjing University of Information Science & Technology, Nanjing 210044, China

Correspondence should be addressed to Ke Lu; k.lu1@outlook.com

Received 19 February 2020; Revised 22 April 2020; Accepted 15 May 2020; Published 30 May 2020

Academic Editor: Wenqing Wu

Copyright © 2020 Ke Lu and Xuefen Wang. This is an open access article distributed under the Creative Commons Attribution License, which permits unrestricted use, distribution, and reproduction in any medium, provided the original work is properly cited.

This study explored travelers' behavioral intention to adopt ride-hailing services. With regard to perceived value, several factors related to perceived benefit and perceived sacrifice were considered. Moreover, subjective norm and perceived policy support were further introduced into the concept model. After the construction of the concept model, an empirical analysis was put forward to test the hypotheses proposed. In addition, the effect of sociodemographic factors and usage frequency was further investigated. The empirical analysis was based on a survey that put forward in Nanjing, China. The results demonstrate that perceived value is positively related to behavioral intention. And factors of perceived benefit are related to perceived value positively, while factors of perceived sacrifice have a negative effect on perceived value.

1. Introduction

In 2017, DiDi announced that its number of orders is 7.43 billion, which shown that ride-hailing services have been one of the most important travel modes in China. The popularity of ride-hailing services is based on the rapid development of mobile Internet technology. What is more, ride-hailing services also related to the development of vehicle technology and energy consumption [1, 2]. Ride-hailing platforms have provided new travel options to urban residents, and the role in urban transport is becoming more and more critical [3, 4]. In China, the new travel options that ride-hailing platforms offer include fast-ride, tailored-ride, and carpool [5]. Among them, fast-ride is cheaper and the quality or brand of car is standard. As for tailored-ride, the quality or brand of car is better and the price is higher. For carpool, the quality or brand of car is similar to fast-ride, but the price level is cheaper than fast-ride. Moreover, the target consumers of these travel options vary a lot. For fast-ride, the target consumers are typical travelers who pursue similar travel experience as a taxi. And the target consumers of tailored-ride mainly are business travelers. The target consumers of carpool are travelers who willing to share a car with others. Similarly, Uber has also provided differentiated options that targeted on different traveler's groups, such as UberX, UberBlack, and UberVan.

People's travel behavior is gradually changing with the promotion of such new travel options facilitated by ride-hailing platforms. In assessing the potential of ride-hailing services for these travelers, behavioral intention toward ride-hailing provides a vital direction [6, 7]. What is more, methods of behavioral intention analysis have been introduced into the study of transportation services [8, 9]. And such purposes indicate future behavior and adoption rates of ride-hailing services. Also, it will be helpful for both ride-hailing platforms and government or transportation management organizations to understand travelers' behavioral intention of using ride-hailing services. For example, ride-hailing platforms may provide better service and yield more profit, while government or transportation management organizations can put forward more effective policies.

Most studies to date have focused on travelers' intention to adopt ride-hailing based on factors such as price, safety, convenience, and access, which have a significant effect on the travelers' choice behavior [3, 10–12]. What is more, feelings related to travel plays an important role on the adoption of specific travel services [13]. In addition, more specific factors have been investigated as well, for example, social norm [14], environmental concern [15], performance and effort expectancy on ride-hailing services [16], and trust [17]. Besides, social influence has a direct effect on users' behavioral intention [18]. It shows that behavior of ride-hailing travelers was studied with the consideration of various factors. However, to our best knowledge, little research has been done from viewpoint of perceived value and the attention of social influence and perceived policy support can be strengthened.

Unlike current studies, this research is mainly studied based on the research of perceived value to reflect travelers' behavior more accurately. The definition of perceived value is "consumer's overall assessment of the utility of a product based on the perception of what is received and what it is given" [19]. Perceived value mainly focuses on people's judgment on a specific product or service especially from the aspects of benefit and sacrifice, which has shown to be an effective method in the research of consumer behavior. Since perceived benefit and perceived sacrifice can embody travelers' perceived value comprehensively, it can be helpful to understand travelers' intention to adopt ride-hailing services by considering it from two aspects, i.e., perceived benefit and perceived sacrifice. Hence, it is important to study travelers' behavior intention of ride-hailing services based on perceived value. Further, the effect of social influence and perceived policy support can be considered more comprehensively. As a result of the rapid growth of social media in recent days, people are easier to be influenced by social factors than before. And their perception of policy support toward ride-hailing also plays a vital role in traveler's decision behavior. Moreover, the policy support discussed in this study is the measure taken by the government that intends to improve the development of ride-hailing industry. For example, in 2016, the Chinese government has promoted several policies to build healthier ride-hailing market and provide better services for travelers. Therefore, it is necessary to consider factors of social influence and perceived policy support into the study of ride-hailing.

This research aims to examine travelers' behavioral intention of ride-hailing services. (1) What is the effect of perceived value on the travelers' behavioral intention? (2) What are the factors included in perceived benefit or perceived sacrifice and their relationship with perceived value? (3) What is the relationship between social factors and perceived value, travelers' behavioral intention? (4) What is the effect of perceived policy support on travelers' behavioral intention?

The paper is organized as follows. The literature review is presented in the second section. In Section 3, the research model is constructed and hypotheses are proposed. Then data and research methods are described in Section 4. In Section 5, the empirical results are presented. Then, the discussion is put forward in Section 6. Finally, conclusion and future research directions are discussed in Section 7.

2. Literature Review

The literature related to this paper mainly consists of two parts, i.e., (1) behavior of ride-hailing travelers and (2) perceived value and behavioral intention.

2.1. Behavioral Intention of Ride-Hailing Services. With the expansion of ride-hailing services, the travel behavior of urban residents has changed. Currently, issues of ride-hailing services have been discussed in kinds of literature. Among them, travelers' behavioral intention of ride-hailing services was studied.

The effect of sociodemographic characteristic and attitude of ride-hailing users were explored. By referring to current research, the users tend to be younger, well-educated, and do not own a vehicle [3, 10–12]. Since ride-hailing is a new emerging service, some travelers may still not familiar and even not ever used them. Based on a survey of 15 metropolitan statistical areas in the United States, Dawes [10] showed that 28% of the respondents have never used Uber and the attitude toward ride-hailing services varies a lot among different groups. Nielsen [20] investigated users' negative and positive perceptions of ridesharing. Among them, availability, safety, and social awkwardness are negative perceptions, and positive perceptions include cost saving, flexibility, and social demand fulfillment. What is more, existing literature shows that both sociodemographic factors and attitudinal factors are also essential in the adoption of ride-hailing services.

The reasons for the adoption of ride-hailing services can further be illustrated from different sides. From the side of travel itself, less cost, shorter waiting time, parking problem, and car ownership are account for the adoption behavior [3, 12, 21]. From the side of nontravel reasons, avoid driving under the influence of alcohol may be one of the top reasons for ride-hailing adoption [3, 12]. Moreover, factors of environmental protection, energy consumption, and habit also contribute to the adoption of ride-hailing services [15, 16]. For example, travelers' acceptance of ride-hailing services is positively related to their habit [16].

The effect of latent variables was examined. Typically, it has shown that perceived ease of use and perceived usefulness related to behavioral intention or adoption of ride-hailing services positively [14, 17, 22]. But the effect of subjective norm varies in different research. In most research, the impact of subjective norm or social factors on consumers' behavioral intention is positive, which means usage behavior or positive opinion of friends, colleagues, and family members may increase consumers' behavioral intention [14, 16]. However, Septiani et al. [17] found that subjective norm plays a negative role in behavioral intention. Nevertheless, both results showed that people's behavior is influenced by social factors significantly and has been a critical factor of the study on consumer behavior.

As for the research methods in the current study, the model was built based on the combination of different theories to examine the relationship between behavioral intention of ride-hailing services and particular variables

[14, 16, 17, 21, 22]. For example, technology acceptance model, theory of planned behavior, diffusion of innovation theory, and unified theory of acceptance and use of technology 2. In these studies, the structural equation model and regression models were constructed and several latent variables were considered. In Table 1, the theory and variables in current studies are summarized.

In more detailed level, the research theories are introduced to reflect features of ride-hailing services from specific aspect. Ride-hailing is a new travel service based on advanced mobile Internet technology, which means the technology acceptance model or unified theory of acceptance and use of technology 2 can be considered to study travelers' adoption behavior. And it has shown that TAM and UTAUT2 are effective tools to explain ride-hailing adoption behavior [14, 17, 23, 24]. Further, travelers' adoption behavior of ride-hailing services may change as there are many other transportation modes, and hence the theory of planned behavior could be introduced [17]. Comparing with traditional travel modes, ride-hailing services are innovative modes, for example, advanced match technology and new economic style. Then, travelers' adoption behavior can be explained by diffusion of innovation theory as well. In summary, the theories considered in extant research are different and each of them focused on specific aspect of ride-hailing service adoption behavior.

Based on several theories of consumer behavior, travelers' behavioral intention on the adoption of ride-hailing services was studied. Then, the effect of factors related to travelers' behavior can be further investigated. Also, most of the factors considered in existing literature are the positive side of ride-hailing usage. To avoid this shortage, Wang et al. [23] extended technology acceptance model by introducing perceived risk to represent the negative aspect of ride-hailing services. However, in most studies, the negative effect of ride-hailing services was neglected.

Table 1: Summary of theories.

Theory	Key variables	Literature
TAM, TPB, DOI	Perceived ease of use Perceived usefulness Perceived enjoyment Subjective norm Trust	Septiani et al. [17]
TAM, TPB	Perceived usefulness Perceived ease of use Subjective norm Attitude Perceived behavior control	Giang et al. [14]
TAM	Perceived safety Perceived price Perceived convenience Perceived accessibility	Mohamad et al. [22]
UTAUT2	Perceived expectancy Effort expectancy Social influence Facilitating conditions Hedonic motivation Price value Habit	Chen et al. [16]
Extended TAM	Perceived ease of use Perceived usefulness Perceived risk Personal innovativeness Environmental awareness	Wang et al. [23]

2.2. Perceived Value and Behavioral Intention. It has added value to study travelers' behavioral intention of ride-hailing services with view of perceived value. The concept of perceived value has been introduced into plenty of research to reveal the mechanism of consumers' decision behavior. As mentioned above, a widely cited and more general definition was given by Zeithaml [19] from gain and loss. Generally, the study of perceived value is intended to explain the idea behind these factors and form a theoretical viewpoint.

The model construction of perceived value is the foundation for further research. In the current study, it can be concluded that perceived value contains various factors. And such factors can mainly be classified into the instrumental function, self-emotional function, and social function [25–27]. Based on the classification of perceived value, hypotheses on the relationship between perceived value and behavioral intention are carried out. And the utilitarian effect, hedonic effect, and social effect of perceived value are further examined.

In summary, consideration of dimensions in extant research can embody perceived value in a more detailed level, but the perceived value was mainly studied from positive side through this method. This may lead to the problem that some features of perceived value remain unexplored, and then factors which consumer cares and the process of decision-making may not be described well enough. To avoid this drawback, perceived value can further be studied from view of perceived benefit and perceived sacrifice. Then, the positive effect and negative effect of perceived value are introduced and their relationship with behavioral intention is further assumed [28–30].

Based on the construction of perceived value, the effect of perceived value on behavioral intention can be examined. Generally, perceived value has positive effect on behavioral intention, and this conclusion has been verified in different industries, for example, wearable device [29], mobile Internet technology [26, 28], tourism [25], shopping mall [27], and green products [30]. As for perceived benefit and perceived sacrifice, it can be concluded from extant studies that perceived benefit is positively related to perceived value and perceived sacrifice is negatively related to perceived value [28–30].

3. Research Model and Hypotheses

Based on the literature mentioned and characteristics of ride-hailing services, the research model is built as is shown in Figure 1. This concept model is built to investigate the effect of related factors on travelers' behavioral intention of ride-hailing services adoption. In particular, the perceived value consists of two parts, i.e., perceived benefit and

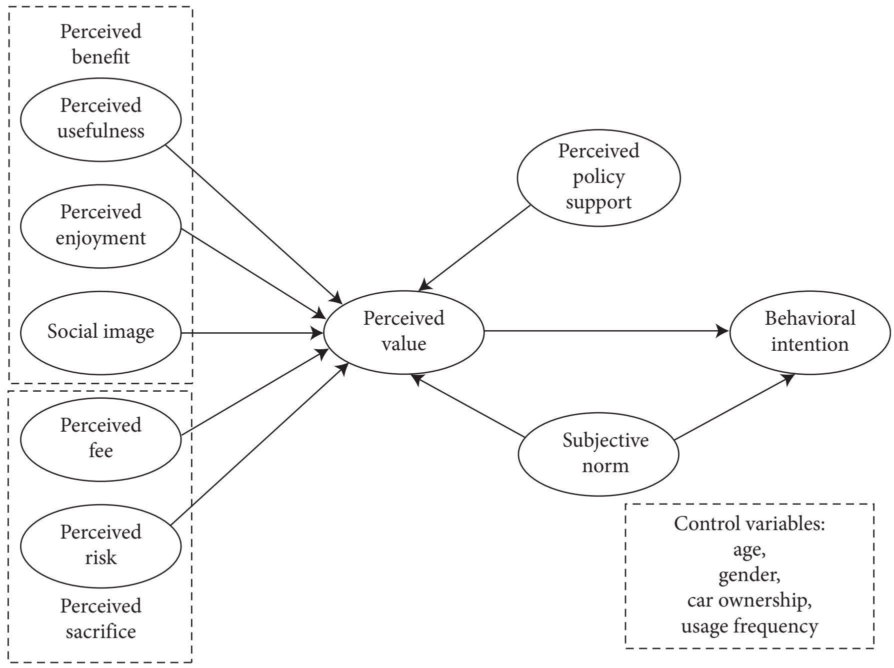

FIGURE 1: Research model.

perceived sacrifice. Moreover, perceived policy support and social norm are considered in this model as well. Besides, four control variables are further introduced, i.e., age, gender, car ownership, and usage frequency of ride-hailing services.

3.1. Perceived Value and Behavioral Intention. According to the definition of perceived value, travelers will evaluate both sides to form their behavioral intention to adopt ride-hailing services. Their perceived value is positive when evaluation value of the benefit is more excellent than sacrifice, and then the behavioral intention may form. As a result, travelers will choose whether to use ride-hailing services. Extant research has shown perceived value has a positive effect on behavioral intention [28, 29]. Therefore, the hypothesis can be depicted as follows.

H1. The perceived value of ride-hailing services will positively affect travelers' behavioral intention.

3.2. Perceived Benefit. According to extant research, the factors related to a customer's behavioral intention mainly consist of utilitarian, hedonic, and social effects. Utilitarian effect is the basic function the product or service provides. Also, hedonic effect is an internal effect which can reflect a customer's self-emotion or enjoyment. What is more, external factors may stem from the social network that customers belong, i.e., social effect. In this paper, perceived benefit is constituted by perceived usefulness, perceived enjoyment, and social image.

3.2.1. Perceived Usefulness. Perceived usefulness is defined as "the extent to which a person believes that using one specific product or service will enhance his or her job performance" [31]. Perceived usefulness has been introduced into many research studies that focus on IT or new product adoption. Venkatesh and Bala [32] found that perceived usefulness has a strong and positive effect. However, in most research, it implies that perceived usefulness has an indirect and positive impact on behavioral intention [28, 29, 33].

The usefulness or utilitarian effect is the primary function of ride-hailing services, and travelers' original purpose of adopting ride-hailing services is to fulfill their travel demands. If travelers can get better travel experience from ride-hailing services, they may tend to have a better perception of such services [14]. In this paper, perceived usefulness is defined as the extent to which an individual believes using ride-hailing services will enhance his or her travel quality or even job performance. The usefulness can be specified as shorter waiting time, faster way to the destination, and lower cost [3]. Then, the hypothesis is proposed.

H2. The perceived usefulness of ride-hailing services will positively affect travelers' perceived value.

3.2.2. Perceived Enjoyment. Besides fundamental functions, the feeling or enjoyment consumers experienced also plays a vital role in the evaluation of product or service. Perceived enjoyment is defined as suggested by Venkatesh and Davis [34]. And the effect of this factor has been examined, which indicates that perceived enjoyment has a positive effect on perceived value [28, 29, 35].

This paper defines perceived enjoyment as the extent to which the adoption of ride-hailing services is enjoyable aside any other performance. Ride-hailing can be more comfortable and independent besides of utilitarian functions [20, 36]. What is more, Septiani et al. [17] found that perceived enjoyment is one of the main factors that influence travelers' behavior. Therefore, the hypothesis can be described as follows.

H3. The perceived enjoyment of ride-hailing services will positively affect travelers' perceived value.

3.2.3. Social Image. Social image is defined as "the degree to which an individual perceives that use of innovation will enhance his or her status in his or her system" [37]. From many related pieces of research studies, it has shown that social image is a vital factor to consumers' decision behavior [38–42]. Nowadays, individuals tend to have more social interactions with their social network members. Moreover, the role of social image is further strengthened, especially on the behavioral intention of new emerged services.

In this paper, social image is the extent to which an individual thinks the adoption of ride-hailing services will enhance his or her social status. Social image has also been considered as one of the most important reasons for ride-hailing service adoption [10]. Sweeney and Soutar [43] identified the effect of social value (enhancement of social self-concept) on consumers' perceived value. Yang et al. [29] found that social image related to perceived value positively. Therefore, the hypothesis can be proposed as follows.

H4. The social image of ride-hailing services will positively affect travelers' perceived value.

3.3. Perceived Sacrifice. Perceived sacrifice includes not only monetary factors but also nonmonetary factors. On the monetary aspect, travelers need to pay a fee to have access to ride-hailing services, and their perception of the fee may vary with preference heterogeneity. On the nonmonetary aspect, there may be some potential risk of using ride-hailing services, such as accessibility risk, performance risk, and safety risk.

3.3.1. Perceived Fee. Travelers need to pay money to use ride-hailing services. The price charged by ride-hailing platforms includes two main forms, i.e., transaction fee and registration fee. On the context of ride-hailing services, perceived fee can be defined as the extent to which individual perceived on the fee he or she needs to pay for ride-hailing services. Besides, perceived fee can be studied as the monetary aspect of perceived sacrifice.

In many surveys, price or cost has been one of the most frequently mentioned factors [3, 12, 44]. It showed that travelers tend to make more travels using ride-hailing services if the price or cost is lower. Moreover, the relationship between perceived fee and perceived value has been examined in many research studies. It has been proposed that perceived fee has a negative effect on perceived value [28, 35, 45]. Therefore, the hypothesis can be proposed as follows.

H5. The perceived fee of ride-hailing services will affect travelers' perceived value negatively.

3.3.2. Perceived Risk. Accompany with adoption of ride-hailing services, travelers may experience risk related to such new transportation modes. Dowling and Staelin [46] defined perceived risk as customers' perception of uncertainty and adverse outcome of using the product or service. Moreover, perceived risk can be represented by various factors, such as risk being cheated, safety risk, social risk, and privacy risk [29, 35, 47, 48].

In the survey by Dawes [10], safety risk and performance risk (inconvenience, slow) are the main reasons against choosing ride-hailing services. Similarly, safety and performance were included in the research of Rayle et al. [3]. Moreover, availability, awkwardness, and social exclusion were considered as the negative reasons for nonadoption of ride-hailing services [20]. In this paper, the perceived risk of ride-hailing services consists of accessibility risk, performance risk, and safety risk. Therefore, the hypothesis can be given as follows.

H6. The perceived risk of ride-hailing services will negatively affect travelers' perceived value.

3.4. Subjective Norm. According to social influence theory, the process of people's attitude or behavioral change can be classified into three parts, i.e., compliance, identification, and internalization [38]. In the process of compliance, people's behavior will be affected by other members who belong to his or her social network. Usually, people have a demand to achieve a favorable reaction from others and suffer the pressure from his or her social network. This effect is also called subjective norm. Subjective norm is defined from the aspects of an individual's social network [34, 49].

The factor of subjective norm was considered in many research studies of consumer behavior. However, indirect effect of subjective norm has been rarely examined. This paper defines subjective norm as the extent to which a traveler perceived that most people who are important to him or her think he or she should or should not use ride-hailing services. Further, one of the reasons for ride-hailing service adoption is "my friends do it" [10]. On the one hand, the members of social network can influence the traveler's behavioral intention directly [32, 50, 51]. On another hand, the traveler's behavioral intention may be affected by subjective norm through perceived value indirectly. Therefore, two hypotheses can be given as follows.

H7. The subjective norm of ride-hailing services will positively affect travelers' perceived value.

H8. The subjective norm of ride-hailing services will positively affect travelers' behavioral intention.

3.5. Perceived Policy Support. As a new emerged transportation service, ride-hailing platforms have provided several cheaper and more convenient travel options to urban residents. But it has also generated some new problems worldwide, and then some political measures were put forward by governments [52–54]. However, little literature has studied the influence of perceived policy support on travelers' behavioral intention to adopt ride-hailing services.

According to a survey in the United States, it indicates that a significant proportion of urban residents hold the opinion that the government should regulate and form a partnership with Uber or Lyft [10]. If the government put forward policies to regulate the current ride-hailing market, then the price level may be more stable and fairer. In addition, more qualified drivers can provide better services if policies are taken. Finally, more travelers tend to adopt ride-hailing services. Therefore, the hypothesis can be described as follows.

H9. The perceived policy support of ride-hailing services will positively affect travelers' perceived value.

4. Data and Method

4.1. Data Collection. A survey was held from October to November 2017 in Nanjing City, China. Nanjing is a city located in the east of China and also the capital of Jiangsu Province. As one of the main cities in China, Nanjing has a square area of 6,587 km^2 and 8.27 million residents. The methods of stated preference surveys were applied into this study, which has shown an effective tool on study of emerging services [55]. The targeted respondents in this survey are the residents who live in Nanjing. Then, an online survey was designed for data collection. Moreover, a fraction of the data was collected offline to attract more respondents. With the development of Internet technology, online survey approach has become a popular method for data collection primarily when the product or service is operated based on Internet. In addition, current research has shown that the quality of online survey is similar to the offline survey [35, 56].

The survey includes sociodemographic information, daily travel information, and behavioral intention to adopt ride-hailing services. The items of the questionnaire were designed in English first and then be translated into the Chinese version. The questionnaires written in English and Chinese were compared and revised by authors and qualified translators. After then, the online survey was put forward and distributed through online forum and social media, for instance, WeChat, Weibo, QQ, etc. To attract more respondents, a bonus of 10 yuan with a probability of 20 percent was offered. Although most of the data were collected through an online method, part of data was also collected offline in the university campus and railway stations. Overall, a total of 503 samples are retained. Among them, 414 samples are valid for further analysis.

The detail information of items is presented in Table 2. The data were collected with a Likert 5-point scale that ranges from fully disagree (1) to fully agree (5).

4.2. Descriptive Analysis. Detailed information of descriptive statistics for sociodemographic characteristics of 414 valid respondents is listed in Table 3. Among the valid samples, 50.5% are men and 49.5% are women. Also, the slight skew toward male reflects the actual gender distribution in Nanjing. As for age distribution, the dominant part is 25–30 years old and the proportion is 53.4%. As regard to education, more than 57.7% have higher education experience. Approximately 63% of the respondents do not have a car, but the proportion of the group that plans to buy a car is 16.7%. Notably, 56.5% of the sample is unmarried. On the view of income, the sample is divided into five groups, viz. 1500 yuan and below (21.0%), 1501–3500 yuan (13.8%), 3501–5000 yuan (15.2%), 5001–8000 yuan (25.1%), and 8001 and above (24.9%).

5. Empirical Results

5.1. Reliability and Validity of Measurements. According to results, items of PE4, PF1, PF2, and PR1 were deleted. Then, the means, factor loading, reliability, and validity of all items are summarized in Table 4. To test reliability, Cronbach's α was conducted for given data. Then, the Kaiser-Meyer-Olkin (KMO) test and Bartlett's test were conducted to test the validity of related measurements. Moreover, factor loading and mean of each item were also examined.

In Table 4, the scales of Cronbach's α range from 0.806 to 0.927, and the total scale is 0.920, which significantly exceeds the threshold of 0.7 that is set for further analysis [58]. The KMO value of all items surpasses 0.5, which indicates that the sample data have a good validity [59]. In addition, combining with the factor loading value and significant results of Bartlett's test, it also established the convergent validity of the sample data [60].

5.2. Hypothesis Test. To examine the effect of control variables, age, gender, car ownership, and usage frequency of ride-hailing services are introduced and coded as dummy variables, as shown in Table 5.

The confirmatory factor analysis was performed based on the Amos 23 software, and results are presented in Table 6 and Figure 2. Before results analysis, the goodness of model fit should be examined first. The fit indices include absolute indices (chi-square, GFI, AGFI, RMSEA, and NCP), incremental indices (NFI, RFI, IFI, TLI and CFI), and parsimonious fit indices (PGFI, PNFI, and Chisq/df). According to the most frequently reported indices that summarized by Zainudin [61], the indices of Chisq/df, RMSEA, GFI, PGFI, IFI, and CFI are introduced. The indices' value of theoretical framework indicates that fitness of basic model is acceptable, and the results in Table 6 and Figure 2 can further be analyzed (Chisq/df = 2.696, GFI = 0.822, PGFI = 0.693, IFI = 0.905, CFI = 0.905, PCFI = 0.806, RMSEA = 0.064).

Regarding the empirical results, most of the relationships hypothesized are supported except for perceived risk and perceived value (−0.017 NS). As shown in Table 6 and Figure 2, perceived value has a positive effect on behavioral intention significantly (0.487^{***}). Perceived usefulness, perceived enjoyment, and social image all show a positive effect on perceived value. In addition, the effect of perceived usefulness (0.272^{***}) and social image (0.202^{***}) on perceived value is slightly stronger than perceived enjoyment (0.120^{*}). As for perceived sacrifice, perceived fee has a significant and negative effect on perceived value (-0.143^{**}),

Table 2: Appendix: list of items.

Construct	Item	Code
Perceived usefulness [31, 32]	Ride-hailing is very useful to my daily travel in general	PU1
	Ride-hailing can enhance the effectiveness of my travel	PU2
	Ride-hailing can improve the quality of my daily travel	PU3
	Ride-hailing can save my time and efforts during travel	PU4
	Ride-hailing can save my money during travel	PU5
Perceived enjoyment [28, 32]	I find using ride-hailing service can be enjoyable	PE1
	The actual process of using ride-hailing service is pleasant	PE2
	I have fun using ride-hailing service	PE3
	Using ride-hailing bores me	PE4
Behavioral intention [31, 32]	I intend to take ride-hailing as my usual travel mode in the future	BI1
	I intend to use ride-hailing more in the future	BI2
	I predict I would use ride-hailing in the future	BI3
	I am willing to recommend ride-hailing service to my family members/friends/colleagues	BI4
	Compared with traditional taxi, I would prefer to use ride-hailing service	BI5
Subjective norm [32]	My family members/friends/colleagues think that I should use ride-hailing service	SN1
	People who are important to me think that I should use ride-hailing service	SN2
	My family members/friends/colleagues who has the experience of using ride-hailing service think that I should use ride-hailing service	SN3
	In general, my social network has supported me to use ride-hailing service	SN4
Social image [29, 32]	People in my organization who use ride-hailing service have more prestige than those who do not	SI1
	Using ride-hailing service will makes me special in my organization	SI2
	Using ride-hailing improves my image within the organization	SI3
Perceived value [19]	Compared to the fee that I need to pay, the use of ride-hailing offers value for money	PV1
	Compared to the effort to put, using ride-hailing is beneficial to me	PV2
	Compared to the time to spend, using ride-hailing is worthwhile to me	PV3
	Overall, using ride-hailing delivers me good value	PV4
Perceived policy support [57]	If government encourage the development of ride-hailing industry, I would like to use ride-hailing service	PO1
	If government regulates the pricing mechanism of ride-hailing industry, I would like to use ride-hailing service	PO2
	If government regulates drivers' entry condition of ride-hailing industry, I would like to use ride-hailing service	PO3
Perceived fee [28]	The fee that I have to pay for the use of ride-hailing is too high	PF1
	The average fee level in ride-hailing market is unstable	PF2
	The fee that I have to pay for the use of ride-hailing is reasonable	PF3
	I am pleased with the fee that I have to pay for the use of ride-hailing	PF4
Performance risk [28, 29, 32]	Without the resources to use ride-hailing, it would not be easy for me to use ride-hailing service	PR1
	Using ride-hailing service makes me feel nervous	PR2
	It is uncertain that ride-hailing will work satisfactorily	PR3
	It is uncertain that ride-hailing will provide the level of benefits I expect	PR4
	It is uncertain that ride-hailing will work safely due to the reason from driver or car	PR5

while perceived risk has no significant effect (−0.017 NS). As one of the most critical factors, perceived policy support of ride-hailing is positively related to perceived value (0.545^{***}). Further, it is clear that subjective norm has a positive effect on both perceived value (0.184^{**}) and behavioral intention (0.599^{***}) significantly. Overall, from the results of SEM analysis, H1, H2, H3, H4, H5, H7, H8, and H9 are supported, while H6 is not supported.

To further investigate the moderate effect of control variables, the effect of age, gender, car ownership, and usage frequency of ride-hailing services was examined. However, most of the relationship between control variables and perceived value, and behavioral intention, is insignificant except for the effect of usage frequency of ride-hailing services on behavioral intention (0.098^{**}). This result implies that travelers' perceived value and behavioral intention will not be influenced by age or gender significantly. As regard of car ownership, its impact on perceived value and behavioral intention is insignificant. Further, although the relationship between usage frequency and perceived value is insignificant, but the significant effect of usage frequency of ride-hailing services on behavioral intention indicates that the usage frequency has an influence on travelers' behavioral intention significantly.

The indirect, direct, and cumulative effects are further examined, as presented in Table 7.

First, it is clear that both perceived benefit and perceived sacrifice can affect travelers' behavioral intention to adopt ride-hailing services indirectly. Among factors of perceived value, the strength of perceived usefulness, social image, and perceived fee are relatively stronger. Second, based on perceived benefit and perceived sacrifice, perceived value has a strong and direct effect on behavioral intention. Further, perceived policy support of ride-hailing has an indirect effect on behavioral intention. As for subjective norm, it affects travelers' behavioral intention of ride-hailing services both indirectly and directly. By the comparison between indirect and direct effect of subjective norm, it indicates that direct effect is much stronger than indirect effect.

Table 3: Descriptive analysis of sociodemographic information.

Value	Frequency	Percent
Gender		
Male	209	50.5
Female	205	49.5
Age (years)		
18 and below	8	1.9
19–24	90	21.7
25–30	221	53.4
31–35	58	14.0
35 and above	37	8.9
Education		
High school and below	8	1.9
Junior college	35	8.5
Bachelor	132	31.9
Master	184	44.4
PhD	55	13.3
Income (yuan)		
1500 and below	87	21.0
1501–3500	57	13.8
3501–5000	63	15.2
5001–8000	104	25.1
8001 and above	103	24.9
Car ownership		
No	198	47.8
No (but plan to buy a car)	69	16.7
Yes (only one car)	126	30.4
Yes (more than one car)	21	5.1
License		
Yes	316	76.3
No	98	23.7
Occupation		
Student	137	33.1
Corporation (state-owned)	48	11.6
Corporation (private)	111	26.8
Education	72	17.4
Government	30	7.2
Self-employed	13	3.1
Unemployed	3	0.7
Marital status		
Unmarried	234	56.5
Married (no child)	60	14.5
Married (have child)	116	28.0
Other	4	1.0

6. Discussion

This research found that perceived value has a positive and direct effect on travelers' behavioral intention to adopt ride-hailing services. This result also supports the conclusions in previous studies that focus on customer behavior [28, 29]. Based on consideration of perceived value, the formation of travelers' behavioral intention can be explained as a sequential process from a theoretical point. Travelers tend to evaluate and relate factors first and then form the behavioral intention. After then, their decision to adopt or not adopt ride-hailing services is made.

6.1. Perceived Benefit. Perceived benefit consists of perceived usefulness, perceived enjoyment, and social image. From empirical results, it indicates that all of them have a significant and positive effect on perceived value. Also, these factors affect travelers' behavioral intention to adopt ride-hailing services indirectly through perceived value. Moreover, these three factors can reflect perceived benefit from functional, hedonic, and social effects. As a new transportation service, ride-hailing not only provide cheaper and more convenient travel options but also with features of higher service level, more flexible, and customized travel time and route [62], which can reflect the functional and hedonic effects of ride-hailing services. To some extent, since ride-hailing is a new service and the behavior of early users may be special, travelers' social image may also be enhanced. Further, the difference between the effects of perceived benefit implies that travelers of ride-hailing services care more about functional effect and social effect than hedonic effect.

6.2. Perceived Sacrifice. Perceived fee and perceived risk were considered from views of monetary and nonmonetary. Based on the empirical results, perceived fee has a negative effect on perceived value. Similar to perceived benefit, perceived fee and perceived risk have an indirect influence on behavioral intention. However, the effect of perceived risk on perceived value is not significant and the effect of perceived fee is much stronger than the effect of perceived risk. This finding indicates that travelers care more on monetary cost than nonmonetary risk, and this result has been verified by Liu et al. [35]. As a result, perceived sacrifice will lead to a lower or even negative evaluation of ride-hailing services.

6.3. Social Effect. In this paper, subjective norm was introduced into the concept model. The empirical results indicate that subjective norm has a positive effect on both perceived value and behavioral intention significantly. The result of the direct effect verified many researches of consumer behavior that have considered social factors [17, 34, 63]. Moreover, the indirect effect of subjective norm was further examined in this paper. Usually, travelers' behavioral intention is affected by the social network to which he or she belongs. As defined above, subjective norm is the extent to which a traveler perceived that most people in his or her social network think he or she should or should not use ride-hailing services. Among travelers' group, when most members in his or her social network think he or she should or should not use ride-hailing services, the behavioral intention of him or her may change directly. On the other hand, the formation of behavioral intention to adopt ride-hailing services may be affected by others indirectly. On this context, subjective norm can influence travelers' behavioral intention to adopt ride-hailing services indirectly through perceived value, which means travelers would evaluate the opinion from his or her social network first and then form behavioral intention of ride-hailing services. According to the empirical results in this paper, the direct effect of subjective norm is much stronger than the indirect effect.

Table 4: Reliability and validity test.

Value	Item	KMO	Bartlett's test			Load	Cronbach's α	Mean
			Approx. chi-square	df	Sig.			
Perceived usefulness	PU1	0.846	1251.673	10	0.000	0.852	0.876	3.74
	PU2					0.897		3.90
	PU3					0.891		3.78
	PU4					0.869		3.89
	PU5					0.598		3.22
Perceived enjoyment	PE1	0.729	693.783	3	0.000	0.917	0.881	3.50
	PE2					0.914		3.67
	PE3					0.868		3.42
Behavioral intention	BI1	0.830	1034.513	10	0.000	0.794	0.869	2.90
	BI2					0.873		3.10
	BI3					0.817		3.57
	BI4					0.840		3.52
	BI5					0.741		3.63
Subjective norm	SN1	0.857	1314.681	6	0.000	0.901	0.927	3.18
	SN2					0.918		3.20
	SN3					0.928		3.30
	SN4					0.877		3.44
Social image	SI1	0.691	684.058	3	0.000	0.836	0.869	2.94
	SI2					0.903		2.67
	SI3					0.932		2.65
Perceived value	PV1	0.831	941.443	6	0.000	0.783	0.882	3.32
	PV2					0.900		3.57
	PV3					0.896		3.61
	PV4					0.869		3.63
Perceived policy support	PO1	0.728	750.069	3	0.000	0.875	0.891	3.71
	PO2					0.930		3.79
	PO3					0.914		3.84
Perceived fee	PF3	0.500	335.332	3	0.000	0.934	0.855	2.65
	PF4					0.934		2.66
Perceived risk	PR2	0.733	690.295	6	0.000	0.623	0.806	2.58
	PR3					0.880		3.00
	PR4					0.906		3.00
	PR5					0.767		3.19
Total							0.920	

Table 5: Control variables.

Variables	Definition
Gen	Male = 1 Female = 0
Age	18 years and below = 1 19–24 years = 2 25–30 years = 3 31–35 years = 4 36 years and more = 5
Car	Do not have a car = 1 Do not have a car, but plan to buy one = 2 Have only one car = 3 Have more than one car = 4
RHFre	I never do this = 1 I do this, but not in the past 30 days = 2 I did this 1–3 times in the past 30 days = 3 I did this 1 day per week = 4 I did this 2 or more times per week = 5

Table 6: Results of SEM analysis.

Path	Standardized regression weights	C.R.
PV < ---PU	0.272***	4.057
PV < ---PE	0.120*	1.774
PV < ---SI	0.202***	4.513
PV < ---PF	−0.143**	−3.086
PV < ---PR	−0.017	−0.471
PV < ---SN	0.184**	3.273
PV < ---PO	0.545***	8.591
BI < ---PV	0.487***	8.263
BI < ---SN	0.599***	8.922
PV < ---Gen	0.021	0.635
PV < ---Age	−0.008	−0.222
PV < ---Car	0.029	0.775
PV < ---RHFre	−0.002	−0.062
BI < ---Gen	0.021	0.630
BI < ---Age	0.034	0.875
BI < ---Car	−0.015	−0.381
BI < ---RHFre	0.098**	2.592

* $p < 0.1$; ** $p < 0.05$; and *** $p < 0.001$.

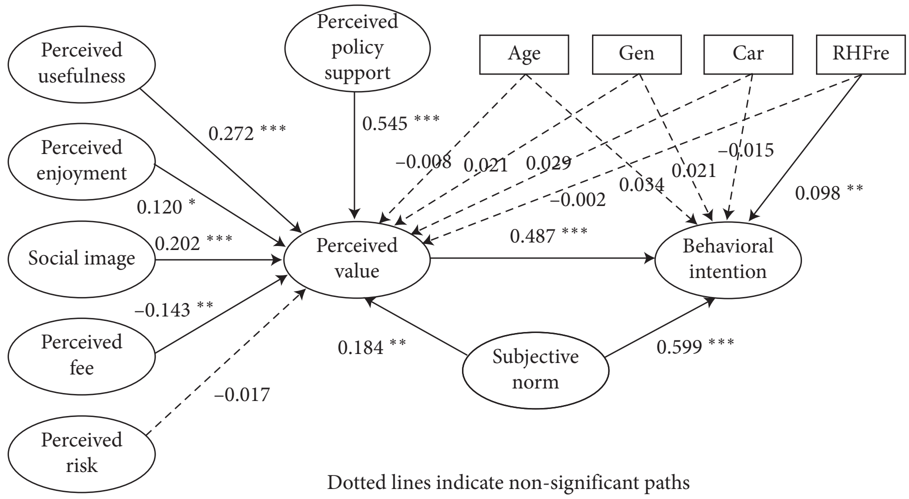

Figure 2: Results of SEM analysis. Note: $^{*}p < 0.1$; $^{**}p < 0.05$; and $^{***}p < 0.001$.

Table 7: Indirect effect, direct effect, and total effect.

Path	Indirect effect	Direct effect	Total effect
PO⟶BI	0.265	—	0.265
SN⟶BI	0.090	0.599	0.689
PR⟶BI	−0.008	—	−0.008
PF⟶BI	−0.069	—	−0.069
SI⟶BI	0.098	—	0.098
PE⟶BI	0.059	—	0.059
PU⟶BI	0.133	—	0.133
PV⟶BI	—	0.487	0.487

6.4. Policy Support. The policy of ride-hailing services has been widely discussed, and the effect of perceived policy support was examined in this paper. From the empirical study, it indicates that perceived policy support related to perceived value positively and has an indirect effect on behavioral intention. This further verified the pivotal role of perceived policy support in travelers' acceptance of ride-hailing services. In early stage, ride-hailing is a transportation service for travelers and most of them may not be familiar with such new travel modes. On the other hand, the legal status is ambiguous in some areas. Then, the price level and quality of drivers or cars vary a lot as a result of a lack of effective policy support. However, if some available measures and policies that intend to construct a better ride-hailing market put forward by the government, then more travelers will adopt such services.

6.5. Sociodemographic Factors. According to the results of sociodemographic factors and usage frequency related to ride-hailing services, age and gender will not affect perceived value and behavioral intention significantly. The insignificance of age and gender also exists in some studies of new emerged services or products [35, 64–66]. As for car ownership, the relationship is not significant. In a survey put forward by Clewlow [12], the adopters of ride-hailing services tend to have lower vehicle ownership rates than nonadopters of such services. Moreover, Dias et al. [11] demonstrate that car ownership plays a negative effect on travelers' underlying propensity of ride-sourcing. Further, previous studies showed that the usage frequency of Uber and Lyft is positively related to travelers' attitude toward Uber and Lyft [10]. In this study, the significant and positive relationship between usage frequency of ride-hailing services and behavioral intention verifies this result and indicates that if travelers use ride-hailing more frequently, then his or her behavioral intention to adopt ride-hailing services may further be strengthened with a satisfied performance of ride-hailing services.

7. Conclusions

7.1. Main Results. Ride-hailing service is becoming one of the most essential components of urban transportation. Some research studies were accomplished to reveal the regular pattern of consumer behavior related to ride-hailing services. However, little of them have considered both positive and negative aspects of ride-hailing services and the process of travelers' decision-making. Based on the research on perceived value, this paper analyzed the factors travelers concerned in order to construct a conceptual model. The factors can be classified into perceived benefit and perceived sacrifice. Moreover, factors of social influence and perceived policy support were introduced into this model as well. Based on a survey in Nanjing, China, an empirical analysis was put forward to investigate the relationships between related factors and travelers' behavioral intention to adopt ride-hailing services.

7.2. Limitations and Future Directions. There are still some limitations that should be noted. First, more factors that can reflect the characteristic of perceived value need to be considered. Hence, a more accurate and objective model should be established to reflect the actual behavior of ride-hailing service adoption better. Second, the size of sample data in this paper is still limited, and more surveys in different cities could be carried out to investigate the differences in travelers' adoption behavior of ride-hailing services in different cities or cultural background. Moreover, the differences in car ownership and public transport may be one of the reasons for the adoption of ride-hailing services, and then several surveys with a difference of car ownership and public transport could be put forward. Third, the consideration of policy purposes is still a limitation. In future, research on behavior of ride-hailing travelers can be studied by considering policy purposes.

Data Availability

The data used to support the findings of this study have not been made available because the data also form part of an ongoing study.

Conflicts of Interest

The authors declare no conflicts of interest.

Acknowledgments

This work was jointly supported by research grants from the Philosophy and Social Science Fund of Education Department of Jiangsu Province (2019SJA0155), the Natural Science Foundation of the Jiangsu Higher Education Institutions of China (19KJB580015), National Nature Science Foundation of China (Grant no. 71732003), the Startup Foundation for Introducing Talent of NUIST (Grant no. 2019r021), and China Scholarship Council (Grant no. 201706190073). The authors also would like to thank Prof. Dick Ettema for his kind suggestion.

References

[1] X. Sun, H. Zhang, W. Meng, R. Zhang, K. Li, and T. Peng, "Primary resonance analysis and vibration suppression for the harmonically excited nonlinear suspension system using a pair of symmetric viscoelastic buffers," *Nonlinear Dynamics*, vol. 94, no. 2, pp. 1243–1265, 2018.

[2] H. Xiong, X. Zhu, and R. Zhang, "Energy recovery strategy numerical simulation for dual axle drive pure electric vehicle based on motor loss model and big data calculation," *Complexity*, vol. 2018, Article ID 4071743, 14 pages, 2018.

[3] L. Rayle, D. Dai, N. Chan, R. Cervero, and S. Shaheen, "Just a better taxi? A survey-based comparison of taxis, transit, and ride-sourcing services in San Francisco," *Transport Policy*, vol. 45, pp. 168–178, 2016.

[4] X. Wang, M. Dessouky, and F. Ordonez, "A pickup and delivery problem for ridesharing considering congestion," *Transportation Letters*, vol. 8, no. 5, pp. 259–269, 2016.

[5] J. Y. Chen, "Thrown under the bus and outrunning it! the logic of DiDi and taxi drivers' labour and activism in the on-demand economy," *New Media & Society*, vol. 9, pp. 1–21, 2017.

[6] I. Ajzen, "From intentions to actions: a theory of planned behavior," in *Action-control: From Cognition to Behavior*, J. Kuhl and J. Beckmann, Eds., pp. 11–39, Springer, Heidelberg, Germany, 1985.

[7] I. Ajzen, "The theory of planned behavior," *Organizational Behavior and Human Decision Processes*, vol. 50, no. 2, pp. 179–211, 1991.

[8] S.-Y. Chen, "Eco-friendly value or others' environmental norms? Arguing the environmental using psychology of bike-sharing for the general public," *Transportation Letters*, vol. 11, no. 8, pp. 425–435, 2019.

[9] S.-Y. Chen and C.-C. Lu, "Investigating the psychology of green transportation via the green service profit chain," *Transportation Letters*, vol. 7, no. 3, pp. 143–153, 2015.

[10] M. Dawes, "Perspectives on the ride-sourcing revolution: surveying individual attitudes toward uber and lyft to inform urban transportation policy making," Thesis, Massachusetts Institute of Technology, Cambridge, MA, USA, 2016.

[11] F. F. Dias, P. S. Lavieri, V. M. Garikapati, S. Astroza, R. M. Pendyala, and C. R. Bhat, "A behavioral choice model of the use of car-sharing and ride-sourcing services," *Transportation*, vol. 44, no. 6, pp. 1307–1323, 2017.

[12] R. R. Clewlow and G. S. Mishra, "Disruptive transportation: the adoption, utilization, and impacts of ride-hailing in the United States," Research Report-UCD-ITS-RR-17-07, Institute of Transportation Studies, University of California, Cambridge, MA, USA, 2017.

[13] T. Gärling, "Travel-related feelings: review, theoretical framework, and numerical experiments," *Transportation Letters*, vol. 11, no. 1, pp. 54–62, 2019.

[14] P. T. Giang, P. T. Trang, and V. T. Yen, "An examination of factors influencing the intention to adopt ride-sharing applications: a case study in Vietnam," *Imperial Journal of Interdisciplinary Research*, vol. 3, no. 10, pp. 618–623, 2017.

[15] S. Malodia and H. Singla, "A study of carpooling behaviour using a stated preference web survey in selected cities of India," *Transportation Planning and Technology*, vol. 39, no. 5, pp. 538–550, 2016.

[16] Y. Chen, W. Salmanian, and A. Akram, "User acceptance in sharing economy-A study of transportation network companies in China," in *Proceedings of the 11th Mediterranean Conference on Information Systems*, pp. 1–17, Genoa, Italy, 2017.

[17] R. Septiani, P. W. Handayani, and F. Azzahro, "Factors that affecting behavioral intention in online transportation service: case study of GO-JEK," *Procedia Computer Science*, vol. 124, pp. 504–512, 2017.

[18] T. Grubljesic, P. S. Coelho, and J. Jaklic, "The shift to socio-organizational drivers of business intelligence and analytics acceptance," *Journal of Organizational and End User Computing*, vol. 31, no. 2, pp. 37–64, 2019.

[19] V. A. Zeithaml, "Consumer perceptions of price, quality, and value: a means-end model and synthesis of evidence," *Journal of Marketing*, vol. 52, no. 3, pp. 2–22, 1988.

[20] J. R. Nielsen, H. Hovmøller, P.-L. Blyth, and B. K. Sovacool, "Of "white crows" and "cash savers": a qualitative study of travel behavior and perceptions of ridesharing in Denmark,"

Transportation Research Part A: Policy and Practice, vol. 78, pp. 113–123, 2015.

[21] J. G. Neoh, M. Chipulu, and A. Marshall, "What encourages people to carpool? An evaluation of factors with meta-analysis," *Transportation*, vol. 44, no. 2, pp. 423–447, 2017.

[22] W. Mohamad, A. Fuad, N. Shahib, A. Azmi, S. Kamal, and D. Abdullah, "A framework of customer's intention to use Uber service in tourism destination," *International Academic Research Journal of Business and Technology*, vol. 2, no. 2, pp. 102–016, 2016.

[23] Y. Wang, S. Wang, J. Wang, J. Wei, and C. Wang, "An empirical study of consumers' intention to use ride-sharing services: using an extended technology acceptance model," *Transportation*, vol. 47, no. 1, pp. 397–415, 2020.

[24] A. M. Al-Momani, M. A. Mahmoud, and M. S. Ahmad, "Factors that influence the acceptance of Internet of things services by customers of telecommunication companies in Jordan," *Journal of Organizational and End User Computing*, vol. 30, no. 4, pp. 51–63, 2018.

[25] C.-K. Lee, Y.-S. Yoon, and S.-K. Lee, "Investigating the relationships among perceived value, satisfaction, and recommendations: the case of the Korean DMZ," *Tourism Management*, vol. 28, no. 1, pp. 204–214, 2007.

[26] Y. H. Kim, D. J. Kim, and K. Wachter, "A study of mobile user engagement (MoEN): engagement motivations, perceived value, satisfaction, and continued engagement intention," *Decision Support Systems*, vol. 56, pp. 361–370, 2013.

[27] M. I. El-Adly and R. Eid, "An empirical study of the relationship between shopping environment, customer perceived value, satisfaction, and loyalty in the UAE malls context," *Journal of Retailing and Consumer Services*, vol. 31, pp. 217–227, 2016.

[28] H.-W. Kim, H. C. Chan, and S. Gupta, "Value-based adoption of mobile Internet: an empirical investigation," *Decision Support Systems*, vol. 43, no. 1, pp. 111–126, 2007.

[29] H. Yang, J. Yu, H. Zo, and M. Choi, "User acceptance of wearable devices: an extended perspective of perceived value," *Telematics and Informatics*, vol. 33, no. 2, pp. 256–269, 2016.

[30] J. F. Medeiros, J. L. D. Ribeiro, and M. N. Cortimiglia, "Influence of perceived value on purchasing decisions of green products in Brazil," *Journal of Cleaner Production*, vol. 110, no. 1, pp. 158–169, 2016.

[31] F. D. Davis, R. P. Bagozzi, and P. R. Warshaw, "User acceptance of computer technology: a comparison of two theoretical models," *Management Science*, vol. 35, no. 8, pp. 982–1003, 1989.

[32] V. Venkatesh and H. Bala, "Technology acceptance model 3 and a research agenda on interventions," *Decision Sciences*, vol. 39, no. 2, pp. 273–315, 2008.

[33] M.-K. Kim, C. Joo, and J.-H. Park, "Investigating the determinants of low adoption of tablet PCs in Korean firms: effects of value perception and alternative attractiveness," *Telematics and Informatics*, vol. 34, no. 8, pp. 1557–1571, 2017.

[34] V. Venkatesh and F. D. Davis, "A theoretical extension of the technology acceptance model: four longitudinal field studies," *Management Science*, vol. 46, no. 2, pp. 186–204, 2000.

[35] F. Liu, X. Zhao, P. Y. K. Chau, and Q. Tang, "Roles of perceived value and individual differences in the acceptance of mobile coupon applications," *Internet Research*, vol. 25, no. 3, pp. 471–495, 2015.

[36] P. Delhomme and A. Gheorghiu, "Comparing French carpoolers and non-carpoolers: which factors contribute the most to carpooling?" *Transportation Research Part D: Transport and Environment*, vol. 42, pp. 1–15, 2016.

[37] G. C. Moore and I. Benbasat, "Development of an instrument to measure the perceptions of adopting an information technology innovation," *Information Systems Research*, vol. 2, no. 3, pp. 192–222, 1991.

[38] H. C. Kelman, "Compliance, identification, and internalization three processes of attitude change," *Journal of Conflict Resolution*, vol. 2, no. 1, pp. 51–60, 1958.

[39] N. Lacetera and M. Macis, "Social image concerns and prosocial behavior: field evidence from a nonlinear incentive scheme," *Journal of Economic Behavior & Organization*, vol. 76, no. 2, pp. 225–237, 2010.

[40] N. Gausel and C. W. Leach, "Concern for self-image and social image in the management of moral failure: rethinking shame," *European Journal of Social Psychology*, vol. 41, no. 4, pp. 468–478, 2011.

[41] L. Chassin, C. Tetzloff, and M. Hershey, "Self-image and social-image factors in adolescent alcohol use," *Journal of Studies on Alcohol*, vol. 46, no. 1, pp. 39–47, 1985.

[42] J. Andreoni and B. D. Bernheim, "Social image and the 50-50 norm: a theoretical and experimental analysis of audience effects," *Econometrica*, vol. 77, no. 5, pp. 1607–1636, 2009.

[43] J. C. Sweeney and G. N. Soutar, "Consumer perceived value: the development of a multiple item scale," *Journal of Retailing*, vol. 77, no. 2, pp. 203–220, 2001.

[44] S. A. Shaheen, N. D. Chan, and T. Gaynor, "Casual carpooling in the San Francisco bay area: understanding user characteristics, behaviors, and motivations," *Transport Policy*, vol. 51, pp. 165–173, 2016.

[45] J. L. M. Tam, "Customer satisfaction, service quality and perceived value: an integrative model," *Journal of Marketing Management*, vol. 20, no. 7-8, pp. 897–917, 2004.

[46] G. R. Dowling and R. Staelin, "A model of perceived risk and intended risk-handling activity," *Journal of Consumer Research*, vol. 21, no. 1, pp. 119–134, 1994.

[47] K. Jiang, S. T.-k. Luk, and S. Cardinali, "The role of preconsumption experience in perceived value of retailer brands: consumers' experience from emerging markets," *Journal of Business Research*, vol. 86, pp. 374–385, 2018.

[48] B. Snoj, A. Pisnik Korda, and D. Mumel, "The relationships among perceived quality, perceived risk and perceived product value," *Journal of Product & Brand Management*, vol. 13, no. 3, pp. 156–167, 2004.

[49] M. Fishbein and I. Ajzen, *Belief, Attitude, Intention and Behavior: An Introduction to Theory and Research*, Addison-Wesley, Reading, MA, USA, 1975.

[50] I. Arpaci, "Understanding and predicting students' intention to use mobile cloud storage services," *Computers in Human Behavior*, vol. 58, pp. 150–157, 2016.

[51] H. Han, "Travelers' pro-environmental behavior in a green lodging context: converging value-belief-norm theory and the theory of planned behavior," *Tourism Management*, vol. 47, pp. 164–177, 2015.

[52] G. Dudley, D. Banister, and T. Schwanen, "The Rise of Uber and regulating the disruptive innovator," *The Political Quarterly*, vol. 88, no. 3, pp. 492–499, 2017.

[53] C. Lee, "To Uberize or not to Uberize? Opportunities and challenges in Southeast Asia's sharing economy," *ISEAS Perspective*, vol. 33, pp. 2335–6677, 2016.

[54] B. G. Edelman and D. Geradin, "Efficiencies and regulatory shortcuts: how should we regulate companies like Airbnb and Uber?" *Stanford Technology Law Review*, vol. 19, pp. 293–328, 2016.

[55] O. Petrik, J. d. A. e. Silva, and F. Moura, "Stated preference surveys in transport demand modeling: disengagement of

respondents," *Transportation Letters*, vol. 8, no. 1, pp. 13–25, 2016.
[56] A. Dickinger and M. Kleijnen, "Coupons going wireless: determinants of consumer intentions to redeem mobile coupons," *Journal of Interactive Marketing*, vol. 22, no. 3, pp. 302–310, 2008.
[57] P. Ju, *A Study on Urban Residents' Usage Intention of Carsharing and Evolutionary Analysis of Choice Behavior*, Nanjing University, Nanjing, China, 2016.
[58] J. C. Nunnally and I. H. Bernstein, *Psychometric Theory*, McGraw-Hill, London, UK, 3rd edition, 1994.
[59] S. V. Budaev, "Using principal components and factor analysis in animal behaviour research: caveats and guidelines," *Ethology*, vol. 116, no. 5, pp. 472–480, 2010.
[60] J. C. Anderson and D. W. Gerbing, "Structural equation modeling in practice: a review and recommended two-step approach," *Psychological Bulletin*, vol. 103, no. 3, pp. 411–423, 1988.
[61] A. Zainudin, *SEM Made Simple*, MPWS Rich Publication, Selangor, Malaysia, 2015.
[62] L. Zha, Y. Yin, and Y. Du, "Surge pricing and labor supply in the ride-sourcing market," *Transportation Research Procedia*, vol. 23, pp. 2–21, 2017.
[63] S.-Y. Chen, "Using the sustainable modified TAM and TPB to analyze the effects of perceived green value on loyalty to a public bike system," *Transportation Research Part A: Policy and Practice*, vol. 88, pp. 58–72, 2016.
[64] K. M. S. Faqih and M.-I. R. M. Jaradat, "Assessing the moderating effect of gender differences and individualism-collectivism at individual-level on the adoption of mobile commerce technology: TAM3 perspective," *Journal of Retailing and Consumer Services*, vol. 22, pp. 37–52, 2015.
[65] J. K. Ayeh, N. Au, and R. Law, "Predicting the intention to use consumer-generated media for travel planning," *Tourism Management*, vol. 35, pp. 132–143, 2013.
[66] M. Leppäniemi, H. Karjaluoto, and H. Saarijärvi, "Customer perceived value, satisfaction, and loyalty: the role of willingness to share information," *The International Review of Retail, Distribution and Consumer Research*, vol. 27, no. 2, pp. 164–188, 2017.